

VIBRATIONAL AND THEORETICAL INVESTIGATIONS OF MOLECULAR  
CONFORMATIONS AND INTRAMOLECULAR  $\pi$ -TYPE HYDROGEN BONDING

A Dissertation

by

ESTHER JULIANA OCOLA

Submitted to the Office of Graduate Studies of  
Texas A&M University  
in partial fulfillment of the requirements for the degree of

DOCTOR OF PHILOSOPHY

December 2011

Major Subject: Chemistry

Vibrational and Theoretical Investigations of Molecular Conformations and  
Intramolecular  $\pi$ -Type Hydrogen Bonding

Copyright 2011 Esther Juliana Ocola

VIBRATIONAL AND THEORETICAL INVESTIGATIONS OF MOLECULAR  
CONFORMATIONS AND INTRAMOLECULAR  $\pi$ -TYPE HYDROGEN BONDING

A Dissertation

by

ESTHER JULIANA OCOLA

Submitted to the Office of Graduate Studies of  
Texas A&M University  
in partial fulfillment of the requirements for the degree of

DOCTOR OF PHILOSOPHY

Approved by:

Chair of Committee,	Jaan Laane
Committee Members,	Steven E. Wheeler
	Rand L. Watson
	George R. Welch
Head of Department,	David H. Russell

December 2011

Major Subject: Chemistry

## ABSTRACT

Vibrational and Theoretical Investigations of Molecular Conformations and  
Intramolecular  $\pi$ -Type Hydrogen Bonding. (December 2011)

Esther Juliana Ocola, B.S., Universidad Nacional de Ingeniería, Perú;

M.S., Cornell University

Chair of Advisory Committee: Dr. Jaan Laane

The molecular conformations, potential energy functions and vibrational spectra of several cyclic molecules have been investigated by ab initio and density functional theory calculations and by infrared and Raman spectroscopy. The ab initio computations of 3-cyclopenten-1-ol predict that its lowest energy conformer has a weak  $\pi$ -type intramolecular hydrogen bonding. The three other conformers lie 301 to 411  $\text{cm}^{-1}$  higher in energy. The infrared and Raman spectra of this molecule confirm the presence of the four conformers. The energy difference between the two conformers of lowest energy was also determined from the experimental spectroscopic data and was found to be  $435 \pm 160 \text{ cm}^{-1}$ , in reasonable agreement with the ab initio computations results.

Ab initio calculations for cyclopentane and  $\text{d}_1$ , 1,1- $\text{d}_2$ , 1,1,2,2,3,3- $\text{d}_6$ , and  $\text{d}_{10}$  isotopomers confirm cyclopentane confirmed that has twist and bent structures and that these differ in energy by less than 10  $\text{cm}^{-1}$ . The bending angle is  $41.5^\circ$  and the twisting angle is  $43.2^\circ$ . A complete vibrational assignment for each of the isotopomers was achieved.

Ab initio calculations were also carried out for methylcyclopropane, cyclopropylsilane, cyclopropylgermane, cyclopropylamine, cyclopropanethiol and cyclopropanol. The structure and the potential energy function for internal rotation was calculated for each and compared to available experimental results determined from infrared and Raman spectra. The calculated barriers to internal rotation agree very well with the experimental data.

The structures, relative energies, and frequencies for the lowest energy vibrations of the twisted, bent, and planar forms of cyclohexene and four of its oxygen analogs were calculated and compared to experimental results. The calculated structural data agree very well with that from the microwave work, but the computed barriers are somewhat lower than those based on far-infrared data.

4-Silaspiro-(3,3)-heptane possesses two four-membered rings, each puckered with an angle of  $34^\circ$ . The molecule possesses a two-dimensional ring-puckering potential energy surface with four equivalent minima. The ab initio calculations predict a barrier to planarity of each ring of  $582\text{ cm}^{-1}$  while the energy of the structure with both rings planar is  $1220\text{ cm}^{-1}$  higher. The calculated infrared and Raman spectra were compared to those previously published, and the agreement is excellent.

## DEDICATION

To my loved parents, family and friends

## ACKNOWLEDGEMENTS

I would like to thank my advisor, Dr. Jaan Laane, for giving me an opportunity to do research in his group, his advice, support, and patience with me all the years I have worked with him. I would also like to thank Dr. Rand L. Watson, Dr. George Welch and Dr. Wheeler for being members of my Ph.D. committee, and to Dr. Goodman for his support during my first semesters at Texas A&M University and for being a member of my initial Ph.D. Committee.

I would also like to give special thanks to Dr. Lisa Pérez, manager of the Laboratory for Molecular Simulation at Texas A&M University who taught me how to do the quantum mechanical calculations using the Gaussian program and helped me with many input problems at the beginning of my research.

Thanks to Mrs. Linda Redd for her time in typing manuscripts and her friendship, and to my family and friends who have supported me during my life and career.

## NOMENCLATURE

3CPOL	3-Cyclopentenol
CYH	Cyclohexene
23DHP	2,3-Dihdropyran
36DHP	3,6-Dihydro-2H-pyran
14DOX	1,4-Dioxene
13DOX	1,3-Dioxene
SSH	4-Silaspiro-(3,3)-heptane



## TABLE OF CONTENTS

	Page
ABSTRACT.....	iii
DEDICATION.....	v
ACKNOWLEDGEMENTS.....	vi
NOMENCLATURE.....	vii
TABLE OF CONTENTS.....	viii
LIST OF FIGURES.....	xi
LIST OF TABLES.....	xvi
CHAPTER	
I INTRODUCTION .....	1
Intramolecular $\pi$ -type hydrogen bonding.....	1
Cyclopentane and its deuterated isotopomers... ..	2
Methylcyclopropane and related molecules.....	3
Cyclohexene and its oxygen analogs.....	3
4-Silaspiro-(3,3)-heptane.....	4
II THEORETICAL AND COMPUTATIONAL METHODS.....	5
Introduction.....	5
Ab initio methods.....	6
Density functional theory methods.....	11
Basis sets.....	14
III EXPERIMENTAL METHODS.....	17
Introduction.....	17
Infrared spectra .....	17
Raman spectra.....	18

	Page
IV	FACTORS AND TYPES OF FORCES AFFECTING CONFORMATIONS OF CYCLIC MOLECULES..... 21
	Introduction..... 21
	Different types of strain..... 21
	Non-planar cyclic conformations..... 23
	The intramolecular $\pi$ -type hydrogen bonding interaction..... 24
V	INTRAMOLECULAR $\pi$ -TYPE HYDROGEN BONDING OF 3-CYCLOPENTEN-1-OL..... 28
	Introduction..... 28
	Computations..... 29
	Experimental..... 31
	Results and discussion..... 32
	Energy difference between conformers..... 51
	Conclusions..... 53
VI	INTRAMOLECULAR $\pi$ -TYPE HYDROGEN BONDING OF OTHER CYCLIC ALCOHOLS AND AMINES..... 55
	Introduction..... 55
	3-Cyclopenten-1-amine..... 56
	2-Aminoindan..... 61
	2-Cyclopenten-1-ol..... 67
	2-Cyclopenten-1-amine..... 72
	1-Aminoindan..... 78
	2-Cyclohexen-1-ol..... 84
	2-Hydroxytetralin..... 90
	Conclusions..... 95
VII	CYCLOPENTANE AND ITS DEUTERATED ISOTOPOMERS... 97
	Introduction..... 97
	Experimental..... 103
	Computations..... 104
	Results and discussion..... 105
	Conclusions..... 135

	Page
VIII	METHYLCYCLOPROPANE AND RELATED MOLECULES..... 136
	Introduction..... 136
	Results and discussion..... 136
IX	CYCLOHEXENE AND ITS OXYGEN ANALOGS..... 146
	Introduction..... 146
	Computations..... 147
	Results and discussion..... 148
X	4-SILASPIRO-(3,3)-HEPTANE..... 157
	Introduction..... 157
	Results and discussion..... 158
XI	CONCLUSIONS..... 167
	REFERENCES..... 172
	VITA..... 181

## LIST OF FIGURES

FIGURE		Page
1	Diagram of a long-path multi-reflection cell.....	18
2	Raman vapor cell.....	20
3	Definition of puckering angle, PA, and puckering coordinate, x.....	23
4	Conformers of 3-cyclopenten-1-ol.....	28
5	Calculated potential energy surface of 3-cyclopenten-1-ol in terms of the puckering angle and internal rotation angle of the -OH group.....	30
6	Contour of the potential energy map of 3-cyclopenten-1-ol.....	30
7	Calculated structures for the four conformers of 3-cyclopenten-1-ol.....	33
8	The ring-puckering potential energy function for the interconversion of conformers A and D of 3-cyclopenten-1-ol.....	35
9	Comparison between the experimental and computed infrared spectra of conformer A of 3-cyclopenten-1-ol.....	41
10	Comparison between the experimental and computed Raman spectra of conformer A of 3-cyclopenten-1-ol.....	42
11	Infrared and Raman spectra of 3-cyclopenten-1-ol vapor.....	43
12	Infrared and Raman spectra of vapor-phase 3-cyclopenten-1-ol in the O-H stretching region.....	48
13	Infrared and Raman spectra of vapor-phase 3-cyclopenten-1-ol in the C=C stretching region.....	49
14	Infrared and Raman spectra of vapor-phase 3-cyclopenten-1-ol for $\nu_{18}$ , CH out-of-plane bending.....	50
15	Vapor-phase infrared and Raman spectra of 3-cyclopenten-1-ol in the 600-1200 $\text{cm}^{-1}$ region.....	51

FIGURE		Page
16	Cyclic alcohols and amines with intramolecular $\pi$ -type hydrogen bonding.....	55
17	Conformers of 3-cyclopenten-1-amine.....	57
18	Internal rotation potential energy function of 3-cyclopenten-1-amine with the ring puckered "up".....	58
19	Internal rotation potential energy function of 3-cyclopenten-1-amine with the ring puckered "down".....	59
20	Conformers of 2-aminoindan.....	62
21	Two-dimensional potential energy surface of 2-aminoindan in terms of the puckering coordinate and the $-\text{NH}_2$ torsion angle.....	63
22	Ring-puckering potential energy function for the interconversion of the conformers A and B of 2-aminoindan.....	65
23	Conformers of 2-cyclopenten-1-ol.....	68
24	Internal rotation potential energy function of 2-cyclopenten-1-ol with the ring puckered "down".....	69
25	Internal rotation potential energy function of 2-cyclopenten-1-ol with the ring puckered "up".....	70
26	Conformers of 2-cyclopenten-1-amine.....	73
27	Internal rotation potential energy function of 2-cyclopenten-1-ol with the ring puckered "up".....	74
28	Internal rotation potential energy function of 2-cyclopenten-1-amine with the ring puckered "down".....	75
29	Conformers of 1-aminoindan.....	79
30	Internal rotation potential energy function of 1-aminoindan with the five-membered ring puckered "up".....	80

FIGURE	Page
31	Internal rotation potential energy function of 1-aminoindan with the five-membered ring puckered "down"..... 81
32	Conformers of 2-cyclohexen-1-ol..... 85
33	Internal rotation potential energy function of 2-cyclohexen-1-ol with a "negative" twist angle..... 86
34	Internal rotation potential energy function of 2-cyclohexen-1-ol with a "positive" twist angle..... 87
35	Experimental infrared and Raman spectra of 2-cyclohexen-1-ol in the O-H stretching region..... 89
36	Conformers of 2-hydroxytetralin..... 91
37	Internal rotation potential energy function of 2-hydroxytetralin with a "positive" twist angle..... 92
38	Internal rotation potential energy function of 2-hydroxytetralin with a "negative" twist angle..... 93
39	Laser-induced fluorescence spectrum of 2-hydroxytetralin..... 95
40	Pseudorotational pathways for cyclopentane in terms of the phase angle $\phi$ given as fractions of $2\pi$ radians..... 98
41	Two-dimensional potential energy surface for the pseudorotation of cyclopentane in terms of ring-bending and ring-twisting coordinates..... 101
42	One-dimensional potential energy function for Eq. (1) for the pseudorotation of cyclopentane in terms of the pseudorotational angle $\phi$ ..... 102
43	Calculated bond distances and angles for the twist ( $C_2$ ) and bent ( $C_s$ ) forms of cyclopentane..... 106
44	Observed and calculated infrared spectra of cyclopentane..... 109
45	Observed and calculated Raman spectra of cyclopentane..... 110
46	Observed and calculated infrared spectra of cyclopentane- $d_1$ ..... 111

FIGURE		Page
47	Observed and calculated Raman spectra of cyclopentane-d <sub>1</sub> .....	112
48	Observed and calculated infrared spectra of cyclopentane-1,1-d <sub>2</sub> .....	113
49	Observed and calculated Raman spectra of cyclopentane-1,1-d <sub>2</sub> .....	114
50	Observed and calculated infrared spectra of cyclopentane-1,1,2,2,3,3-d <sub>6</sub> .	115
51	Observed and calculated Raman spectra of cyclopentane-1,1,2,2,3,3-d <sub>6</sub> ..	116
52	Observed and calculated infrared spectra of cyclopentane-d <sub>10</sub> .....	117
53	Observed and calculated Raman spectra of cyclopentane-d <sub>10</sub> .....	118
54	Internal rotation potential energy function of cyclopropylamine .....	138
55	Internal rotation potential energy function of cyclopropanethiol.....	139
56	Internal rotation potential energy function of cyclopropanol .....	140
57	Experimental and theoretical potential energy functions of methyl- propane.....	142
58	Experimental and theoretical potential energy functions of propylene oxide.....	143
59	Experimental potential energy functions for propylene sulfide and propylene oxide.....	145
60	Calculated structures for cyclohexene, 2,3-dihydropyran, 3,6-dihydropyran, 1,4-dioxene, and 1,3-dioxene.....	149
61	Out of plane coordinates for the ring vibrations of cyclohexene.....	152
62	Comparison of the experimental and calculated Raman spectra of 2,3-dihydropyran .....	155
63	Comparison of the experimental and calculated Raman spectra of 1,4-dioxene.....	156
64	Puckering angle and puckering coordinate of 4-silaspiro-(3,3)-heptane..	159

FIGURE		Page
65	Calculated structure of 4-silaspiro-(3,3)-heptane.....	159
66	Ring-puckering potential energy surface of 4-silaspiro-(3,3)-heptane.....	160
67	Topographic view of the ring-puckering potential surface of 4-silaspiro-(3,3)-heptane.....	161
68	Observed and calculated infrared spectra of 4-silaspiro-(3,3)-heptane.....	163
69	Observed and calculated Raman spectra of 4-silaspiro-(3,3)-heptane.....	164



## LIST OF TABLES

TABLE		Page
1	Relative energies ( $\Delta E$ ) and puckering angles ( $\Phi$ ) of the conformers and the planar structure (P) of 3-cyclopenten-1-ol.....	34
2	Calculated vibrational frequencies ( $\text{cm}^{-1}$ ) of the $-\text{OH}$ stretching and the lowest three large-amplitude motions for 3-cyclopenten-1-ol and 2-indanol .....	37
3	Calculated abundance (%) of 3-cyclopenten-1-ol conformers at different temperatures.....	39
4	Observed and calculated vibrational frequencies ( $\text{cm}^{-1}$ ) for the four conformers of 3-cyclopenten-1-ol.....	44
5	Observed and calculated frequency ( $\text{cm}^{-1}$ ) shifts between the conformers of 3-cyclopenten-1-ol.....	47
6	Calculated potential energy, relative abundance, structural parameters and vibrational frequencies of 3-cyclopenten-1-amine.....	60
7	Calculated potential energy, relative abundance, structural parameters and vibrational frequencies of 2-aminoindan.....	66
8	Calculated potential energy, relative abundance, structural parameters and vibrational frequencies of 2-cyclopenten-1-ol.....	71
9	Calculated potential energy, relative abundance, structural parameters and vibrational frequencies of 2-cyclopenten-1-amine.....	77
10	Calculated potential energy, relative abundance, structural parameters and vibrational frequencies of 1-aminoindan.....	83
11	Calculated potential energy, relative abundance, structural parameters and vibrational frequencies of 2-cyclohexen-1-ol.....	88
12	Calculated potential energy, relative abundance, structural parameters and vibrational frequencies of 2-hydroxytetralin.....	94
13	Correlation of $D_{5h}$ symmetry species with $C_2$ and $C_s$ point groups.....	107

TABLE	Page
14	Observed and calculated wavenumbers ( $\text{cm}^{-1}$ ) for cyclopentane..... 120
15	Observed and calculated wavenumbers ( $\text{cm}^{-1}$ ) for cyclopentane- $\text{d}_{10}$ ..... 121
16	Observed and calculated wavenumbers ( $\text{cm}^{-1}$ ) for cyclopentane- $\text{d}_2$ and cyclopentane - $\text{d}_6$ ..... 122
17	Wavenumbers ( $\text{cm}^{-1}$ ) for the vibrations of cyclopentane and cyclopentane- $\text{d}_1$ ..... 124
18	Calculated vibrational frequencies ( $\text{cm}^{-1}$ ) for conformers of cyclopentane-1,1- $\text{d}_2$ ..... 125
19	Calculated vibrational frequencies ( $\text{cm}^{-1}$ ) for conformers of cyclopentane-1, 1, 2, 2, 3, 3 - $\text{d}_6$ ..... 127
20	Calculated vibrational frequencies ( $\text{cm}^{-1}$ ) for conformers of cyclopentane- $\text{d}_1$ ..... 130
21	Ring vibrations ( $\text{cm}^{-1}$ ) of cyclopentane and its isotopomers..... 134
22	Potential energy values and calculated geometrical parameters of the minimum energy conformations and barriers of methylcyclopropane, cyclopropylsilane and cyclopropylgermane ..... 137
23	Potential energy values and calculated geometrical parameters of the minimum energy conformations and barriers of cyclopropylamine..... 138
24	Potential energy values and calculated geometrical parameters of the minimum energy conformations and barriers of cyclopropanethiol..... 139
25	Potential energy values and calculated geometrical parameters of the minimum energy conformations and barriers of of cyclopropanol..... 140
26	Potential energy values and calculated geometrical parameters of the minimum energy conformations and barriers of propylene sulfide and propylene oxide..... 144
27	Experimental and calculated structural parameters for cyclohexene and its oxygen analogs..... 150

TABLE		Page
28	Low-frequency vibrations of cyclohexene and its oxygen analogs.....	151
29	Rotational constants of cyclohexene and its oxygen analogs.....	151
30	Bending and twisting angles of cyclohexene and oxygen analogs.....	152
31	Twisting barriers and barrier to interconversion.....	154
32	Calculated potential energy, puckering angles and puckering coordinates of 4-silaspiro-(3,9)-heptane.....	162
33	Vibrational assignments of 4-silaspiro-(3,9)-heptane.....	165

## CHAPTER I

### INTRODUCTION

Several different types of molecules have been studied to better understand their structures and conformations as well as their spectroscopic properties. Infrared and Raman spectra were collected to provide the experimental data and these were complemented by theoretical calculations. Ab initio (CCSD/cc-pVTZ and MP2/cc-pVTZ) were used to determine the structures and energy of the molecular conformations and density functional theory (B3LYP/cc-pVTZ) was applied to compute the vibrational frequencies.

#### **Intramolecular $\pi$ -type hydrogen bonding**

##### *3-Cyclopenten-1-ol*

3-Cyclopenten-1-ol (3CPOL) has four conformations, one of which has an unusual weak intramolecular  $\pi$ -type hydrogen bond between the hydroxyl hydrogen and the carbon-carbon double bond. The four 3CPOL conformers can interconvert through the ring-puckering vibration and the internal rotation of the -OH group on the five-membered ring. Previous infrared measurements of 3CPOL in dilute solutions showed two bands in the O-H stretching region [1]. This indicated the presence of molecules without hydrogen bonding and others with intramolecularly bonded -OH groups.

---

This dissertation follows the style of Journal of Molecular Structure.

Al-Saadi in the Laane's research group [2] performed initial ab initio computations that concluded that the lowest energy 3CPOL conformer is the one which possesses the weak intramolecular  $\pi$ -type hydrogen bond. In the present work the vapor-phase infrared and Raman spectra of 3CPOL have been collected over a range of temperatures. The experimental spectra were compared with the theoretical spectra obtained by using density functional theory (DFT) calculations. Additional ab initio calculations for the structure and energy determinations of the conformers were also performed.

#### *Other cyclic alcohols and amines*

The presence of the intramolecular  $\pi$ -type hydrogen bonding in other cyclic alcohols and amines, in addition to 3CPOL has also been studied experimentally by infrared and Raman techniques and theoretically by ab initio and DFT computations. For the molecules studied, 3-cyclopenten-1-amine, 2-aminoindan, 2-cyclopenten-1-ol, 2-cyclopenten-1-amine, 1-aminoindan, 2-cyclohexen-1-ol, and 2-hydroxytetralin the relative energies between the molecules with and without a  $\pi$ -type hydrogen bonding were investigated.

#### **Cyclopentane and its deuterated isotopomers**

Cyclopentane is a molecule with ten equivalent bent and ten equivalent twisted structures with very small energy differences, thus resulting in twenty conformations with very nearly the same energy. These conformations can readily interconvert into

one another. This process is known as pseudorotation and it was first proposed by Kilpatrick, Pitzer, and Spitzer [3]. The infrared and Raman spectra of vapor, liquid, and solid state cyclopentane and four of its deuterated isotopomers were previously recorded and analyzed by Bauman [4] in the Laane's research group. In the present work ab initio and DFT computations were carried out to provide the structures of the cyclopentane conformers, their relative energies, and vibrational frequencies and intensities.

### **Methylcyclopropane and related molecules**

Methylcyclopropane is a cyclic molecule for which the interconversion between conformers results from the internal rotation of the methyl group. CCSD/cc-pVTZ and MP2/cc-pVTZ calculations have been performed for the different configurations of methylcyclopropane and related molecules, the energy barriers were compared to experimental results, and the torsional potential energy function were compared to the theoretical potential function.

### **Cyclohexene and its oxygen analogs**

The low-frequency vibrations and conformational dynamics of cyclohexene (CYH) and its oxygen analogs 2,3-dihydropyran (23DHP), 3,6-dihydro-2H-pyran (36DHP), 1,4-dioxene (14DOX), and 1,3-dioxene (13DOX) have been previously studied using far-infrared spectroscopy by Rivera-Gaines, Leibowitz and Tecklenburg in Laane's research group [5,6]. CYH, 23DHP, 36DHP, 14DOX and 13DOX possess twisted structures while the bent forms represent saddle points in two-dimensional surfaces. Each of the molecules was found to be twisted with a high barrier to planarity.

Raman and microwave spectra and electron diffraction studies relative to these molecules have also been reported [7-14]. In the present work ab initio and DFT calculations have been carried out for these same molecules. The structures, relative energies, and frequencies for the lowest energy vibrations of the twisted, bent, and planar forms were calculated and compared to experimental results.

#### **4-Silaspiro-(3,3)-heptane**

4-Silaspiro(3,3)-heptane is a bicyclic molecule formed where two four-membered rings are joined at a single silicon atom. Ab initio MP2/cc-pVTZ calculations have been carried out to determine the degree of non-planarity of the rings. A two-dimensional potential surface was calculated for this molecule in terms of its ring-puckering coordinates. In addition, the experimental vapor-phase infrared spectrum recorded by Cooke in Laane's group [15] has been compared to the calculated B3LYP/cc-pVTZ spectrum of this molecule, and vibrational assignments have been made.

## CHAPTER II

### THEORETICAL AND COMPUTATIONAL METHODS

#### **Introduction**

This chapter discusses the different methods of calculations of energy of molecules that have been used in this work. The concept of basis sets is also included. Two ab initio methods have been applied in this work: (1) MP2 ab initio method, which is an application of the Møller-plesset perturbation theory (MPPT), and (2) coupled cluster theory with single and double excitations (CCSD) method, which is an application of the coupled-cluster (CC) methods.

In order to aid the understanding of the Møller-plesset perturbation theory (MPPT), a brief introduction to perturbation theory is presented at the end of this introduction section. In addition to the ab initio methods of calculation, density functional theory (DFT) methods were also applied in this work.

#### *Perturbation theory*

In perturbation theory, there is a breakup of a Hamiltonian into a part  $\mathbf{H}^0$ , whose eigenfunctions are known, and an additional term  $\mathbf{H}'$ . The approximate eigenstates of the total Hamiltonian  $\mathbf{H}$  are to be determined. In Eq. (1),  $\mathbf{H}$  is the Hamiltonian for the system being studied,  $\mathbf{H}^0$  is an approximate Hamiltonian for which exact solutions can be found, called the unperturbed Hamiltonian, while  $\mathbf{H}'$  is called the perturbation Hamiltonian [16,17].



$$\mathbf{H} = \mathbf{H}^0 + \mathbf{H}' \quad (1)$$

It is assumed that the perturbation Hamiltonian,  $\mathbf{H}'$ , is small compared to the unperturbed Hamiltonian,  $\mathbf{H}^0$ . Another underlying assumption in perturbation theory is that the eigenstates and eigenenergies of the total Hamiltonian  $\mathbf{H}$  do not differ appreciably from those of the unperturbed Hamiltonian,  $\mathbf{H}^0$ .

Because  $\mathbf{H}'$  is small, it can be written as  $\lambda\mathbf{H}'$ , where  $\lambda$  is  $\ll 1$ . This way the equation to seek a solution becomes

$$\mathbf{H} \phi_n = (\mathbf{H}^0 + \lambda\mathbf{H}') \phi_n = E_n \phi_n \quad (2)$$

The eigenstates and eigenenergies of  $\mathbf{H}^0$  are assumed to be known. Since  $\phi_n \rightarrow \phi_n^{(0)}$  as  $\lambda \rightarrow 0$ , it is consistent to search for a solution to  $(\mathbf{H}^0 + \lambda\mathbf{H}') \phi_n = E_n \phi_n$  in the form of a series with  $\phi_n^{(0)}$  as the leading term (Eq.3). In a similar manner,  $E_n$  is expanded, with  $E_n^{(0)}$  as the leading term of Eq. 4 [17].

$$\phi_n = \phi_n^{(0)} + \lambda\phi_n^{(1)} + \lambda^2\phi_n^{(2)} + \dots \quad (3)$$

$$E_n = E_n^{(0)} + \lambda E_n^{(1)} + \lambda^2 E_n^{(2)} + \dots \quad (4)$$

## Ab initio methods

### *Møller-plesset perturbation theory (MPPT)*

This procedure is also referred to as the many-body perturbation theory (MBPT) method. The two names arose because two different schools of physics and chemistry

developed them for somewhat different applications [18]. In 1934 Møller and Plesset, proposed a perturbation treatment of atoms and molecules, in which the unperturbed Hamiltonian,  $\mathbf{H}^0$ , is taken as a sum of one-particle Fock operators; this form of MBPT is called Møller-Plesset (MP) perturbation theory [19].

The Møller-Plesset perturbation MP2 method treats a system of N electrons in which the Hartree-Fock solution appears as the zero-order approximation. As shown by Møller and Plesset, the first order correction for the energy and the charge density of the system is zero. The development of the higher approximation involves only calculations based on a definite one-body problem [19]. The Møller-Plesset perturbation MP2 method performs a restricted Hartree-Fock calculation for singlets and an unrestricted Hartree-Fock calculation for higher multiplicities followed by a Møller-Plesset correlation energy correction, truncated at the second order. The expression for the second-order correction for the energy greatly simplifies because of the special property of the zero-order solution. The MP2 method is a relatively simple method which incorporates electron correlation, and it provides size-extensive energy corrections at low cost [20,21].

The MP2 method uses first the single-configuration self consistent field (SCF) process to determine a set of the linear-combination-of-atomic-orbital-molecular-orbital (LCAO-MO) coefficients and hence a set of orbitals that obey

$$\mathbf{F}\phi_i = E_i \phi_i . \quad (5)$$

Where  $\mathbf{F}$  is a Fock operator. Then, using an unperturbed Hamiltonian equal to the sum of these Fock operators for each of the  $N$  electrons

$$\mathbf{H}^0 = \sum_{i=1, N} \mathbf{F}(i) \quad (6)$$

perturbation theory is used to determine the  $C_l$  amplitude of the configuration state functions,  $\Phi_l$ , where  $\Phi_l$  is a spin- and space-symmetry adapted configuration state function (CSF) such that  $\Psi = \sum_l C_l \Phi_l$ .

The amplitude for the so-called reference CSF used in the SCF process is taken as unity and the other CSFs' amplitudes are determined, relative to this one, by perturbation theory using the full  $N$ -electron Hamiltonian minus the sum of Fock operators  $\mathbf{H} - \mathbf{H}^0$  as the perturbation. The Slater-Condon rules are used for evaluating matrix elements of  $(\mathbf{H} - \mathbf{H}^0)$  among these CSFs [18].

#### *Coupled-cluster (cc) methods*

The coupled-cluster (CC) method was introduced into molecular electronic structure theory in 1966 by Čížek [22] and further developed by several researchers [18,21]. The coupled-cluster (CC) method represents a higher-level treatment of electron correlation beyond MP4, usually providing greater accuracy [23]. The coupled-cluster (CC) method expresses the configuration interaction part of the wavefunction in the following manner:

$$\Psi = \exp(\mathbf{T}) \Phi_0 \quad (7)$$

where  $\Psi$  is the correlated molecular electronic wave and  $\Phi_0$  is a single configuration state function (CSF) which has been used to independently determine a set of spin-orbitals and linear-combination-of-atomic-orbital-molecular-orbital coefficients via the self consistent field process [18,21]. The operator  $\mathbf{T}$  generates, when acting on  $\Phi_0$ , single, double, etc., excitations (i.e., CSFs in which one, two, etc., of the occupied spin-orbitals in  $\Phi_0$  have been replaced by virtual spin-orbitals).  $\mathbf{T}$  is expressed in terms of operators that affect such spin-orbital removals and additions as follows:

$$\mathbf{T} = \sum_{i,m} t_i^m m^+ i + \sum_{i,j,m,n} t_{i,j}^{m,n} m^+ n^+ j i + \dots \quad (8)$$

where the operator  $m^+$  is used to denote creation of an electron in the virtual spin-orbital  $\phi_m$  and the operator  $j$  is used to denote removal of an electron from the occupied spin-orbital  $\phi_j$ . The  $t_i^m$ ,  $t_{i,j}^{m,n}$  etc., amplitudes, which play the role of the configuration interaction (CI) coefficients in the CC theory, are determined through the set of equations generated by projecting the Schrödinger equation in the form

$$\exp(-\mathbf{T}) \mathbf{H} \exp(\mathbf{T}) \Phi = E \Phi \quad (9)$$

against CSFs, which are single, double, etc., excitations relative to  $\Phi_0$ . For example, for double excitations  $\Phi_{i,j}^{m,n}$  the equations read:

$$\langle \Phi_{i,j}^{m,n} | \exp(-\mathbf{T}) \mathbf{H} \exp(\mathbf{T}) | \Phi_0 \rangle = E \langle \Phi_{i,j}^{m,n} | \Phi_0 \rangle = 0 \quad (10)$$

Zero is obtained on the right hand side because the excited CSFs  $|\Phi_{i,j}^{m,n}\rangle$  are orthogonal to the reference function  $|\Phi_0\rangle$ . The elements on the left hand side of the CC equations can be expressed, as described below, in terms of one- and two-electron integrals over the spin-orbitals used in forming the reference and excited CSFs [18].

The  $\exp(\mathbf{T})$  operator is defined by its usual Taylor-series expansion as shown in Eq. (11)

$$\exp(\mathbf{T}) = 1 + \mathbf{T} + \mathbf{T}^2/2! + \dots = \sum_{k=0}^{\infty} \mathbf{T}^k/k! \quad (11)$$

where the global cluster excitation operator  $\mathbf{T}$  is defined as the sum of n-tuple excitation operators  $\mathbf{T}_n$ , *i.e.*

$$\mathbf{T} = \mathbf{T}_1 + \mathbf{T}_2 + \dots + \mathbf{T}_n \quad (12)$$

in which the maximum value of n equals the number of electrons. The aim of a CC calculation is to solve nonlinear equations for the CC amplitudes in each  $\mathbf{T}_n$ . Once these are determined, the multideterminantal, many-electron wave function is known.

Some highlights of CC theory are as follows: (a) at any given level of excitation/truncation, CC methods are size-extensive; (b) the exponential form of  $|\Phi_0\rangle$  ensures that all higher excitations are included in the wave function, although they may be restricted to be simple products of lower excitations; (c) the starting point of the CC calculations are almost always based on determinants rather than configuration state functions (CSFs) because spin adaptation is not straightforward; and (d) CC wave functions are not variational. An important practical consequence of (d) is that

calculation of energy derivatives of CC wave functions is somewhat costly and requires the setup and solution of additional linear response equations, known as lambda equations [21].

In the usual applications of CC theory, only certain excitation operators are included in the cluster operator. Inclusion of  $T_1$  and  $T_2$  gives the widely employed CC singles and doubles (CCSD) method that involves a coupled cluster calculation using both single and double substitutions, as shown by Purvis and Barlett in 1982 [20,24].

The CCSD method is capable of recovering typically 95% or more of the correlation energy for molecules in the vicinity of their equilibrium structures. In this method, linearization can be understood as changing CC coefficients to CI ones and neglecting higher excitations [21].

### **Density functional theory methods**

Density functional theory (DFT) methods include the effects of electron correlation in which electrons of a molecular system react to another's motion and attempt to keep out of the other's way. DFT methods compute electron correlation via general functionals of the electron density [23].

The basic idea behind DFT is that energy of an electronic system can be written in terms of the electron probability density,  $\rho$ . For a system of  $N$  electrons,  $\rho(r)$  denotes the total electron density at a particular point in space  $r$ . The electronic energy  $E$  is said to be a functional of the electron density,  $E[\rho(r)]$ . Several different schemes have been

developed for obtaining approximate forms for the functional of the exchange-correlation energy [25].

DFT functionals partition the electronic energy into several components which are computed separately: the kinetic energy, the electron-nuclear interaction, the Coulomb repulsion, and an exchange-correlation term accounting for the remainder of the electron-electron interaction, which is also usually divided into separate exchange and correlation components [23].

In DFT, approximate forms for energy terms, as a function of the electron density, are adopted and parametrized, with no explicit reference to the wave function. Most DFT methods employed today, especially the most accurate ones, are not really ab initio techniques, as they contain empirical parameters [21].

B3LYP is a hybrid functional suggested by Stephens, Devlin, Chabalowski and Frish in 1994, where they also named it Becke3LYP [26]. This hybrid is very similar to the three parameter ( $a_0$ ,  $a_x$  and  $a_c$ ) exchange-correlation approximation B3 proposed by Becke in 1993 [27], which includes the Lee, Yang and Parr (LYP) correlation functional and some additional modifications.

In the proposed hybrid functional B3 (Eq. 13), the amount of exact exchange is determined through  $a_0$ , while  $a_x$  and  $a_c$  control the contributions of exchange and correlation gradient corrections to the local density approximation [28]. In this equation,  $\Delta E_x^{\text{B88}}$  is the gradient correction to the local spin density approximation (LSDA) for exchange proposed by Becke in 1988 [29], and  $\Delta E_c^{\text{PW91}}$  is the 1991 gradient correction for correlation of Perdew and Wang (PW91) [30].

$$E_{xc} = E_{xc}^{LSDA} + a_0(E_x^{exact} - E_x^{LSDA}) + a_x \Delta E_x^{B88} + a_c \Delta E_c^{PW91} \quad (13)$$

The second term is the exact exchange energy calculated at the limit  $\lambda=0$  of the exchange-correlation energy  $E_{xc}$  of Kohn-Sham density theory. This energy term is given by a rigorous ab initio formula known as the adiabatic connection formula, corresponding to the Kohn-Sham reference system. Here, the exchange-correlation potential energy is the pure exchange energy of Slater determinant of the Kohn-Sham orbitals, with no dynamical correlation. It is essentially but not exactly equal in value to the conventional Hartree-Fock exchange-energy [27,31].

The semiempirical coefficients of Eq. 13 were determined by Becke in 1993 [27] by a linear least-squares fit to the 56 atomization energies, 42 ionization potentials, 8 proton affinities, and the 10 first-row total atomic energies of Ref. [32]. The optimum values resulted to be  $a_0 = 0.20$ ,  $a_x = 0.72$  and  $a_c = 0.81$ .

Stephens et al. [26] replaced the PW91 term by both the Lee, Yang and Parr (LYP) [33] non-local correlation functional and a local correlation expression VWN. VWN stands for Vosko, Wilk and Nusair functional [34]. Both terms were included since the LYP approximations do not have an easily separable local component, while the VWN is a local correlation expression useful in attaining the different coefficients of local and gradient correlation functionals.

$$E_{xc}^{B3LYP} = (1 - a_0) E_x^{LSDA} + a_0 E_x^{HF} + a_x \Delta E_x^{B88} + a_c E_c^{LYP} + (1 - a_c) E_c^{VWN} \quad (14)$$



DFT calculations can be applied satisfactorily to the prediction of vibrational spectra. With the most accurate density functionals in use, DFT predicts harmonic vibrational frequencies more accurately than MP2 calculations. Since DFT calculations are substantially less demanding computationally than MP2 calculations, it is clear that DFT offers significant advantages in predicting harmonic vibrational force fields, frequencies, and spectra [28].

### **Basis sets**

A basis set is the mathematical description of the orbitals within a system, which in turn, combine to approximate the total electronic wavefunction used to perform the theoretical calculation [23].

The molecular orbitals can be described as linear combinations of atomic orbitals as follows

$$\Psi = \sum_r c_r \phi_r \quad (15)$$

where the atomic orbitals used in this expansion constitute the basis set for the calculation [25]. Larger basis sets more accurately approximate the orbitals by imposing fewer restrictions on the locations of the electrons in space [23].

Much effort has been devoted to developing sets of STO or GTO basis orbitals for main-group elements and the lighter transition metals. This ongoing effort is aimed at providing basis sets which:

1. Yield reasonable chemical accuracy in the computed wavefunctions and energies.
2. Are cost effective in that their use in practical calculations is feasible.

3. Are relatively transferrable in the sense that the basis for a given atom is flexible enough to be used for that atom in a variety of bonding environments, where the atom's hybridization and local polarity may vary [18].

Examples of basis sets, are the known minimal basis sets STO-nG that are Slater-type orbitals that use n primitive Gaussian functions, such as STO-3G, STO-4G, STO-6G, and other basis sets such as MidiX basis set; the split valences basis sets, which have two or more sizes of basis functions for each valence orbital that increase the size of the basis sets such as the Pople basis sets 3-21G, 6-21G, 4-31G, 6-31G, 6-31G<sup>†</sup>, 6-31G<sup>††</sup>, 6-311G; the correlation-consistent basis sets cc-pDTZ, cc-pVTZ, cc-pVQZ, cc-pV5Z, cc-pV6Z, which may be augmented with diffuse functions by adding the aug-prefix, and other split valences basis sets such as D95, SV, SVP, TZV, TZVP.

Other existent basis sets are the polarized basis sets 6-31G(d), 6-31G(d,p), 6-31G(d'), 6-31G(d',p), 6-31H(d'f), 6-31G(d), that change the shape of the orbitals, adding orbitals with angular momentum beyond what is required for the ground state to the description of each atom; basis sets with diffuse functions 6-311+G, 6-31++G(d), which have large-size versions of s- and p-type functions and allow orbitals to occupy larger regions of space, which are important for systems where electrons are relatively far from the nucleus; and high angular momentum basis sets 6-32G(2d), 6-31++G(3df, 3pd), 6-311+(3df,2df,p), which add multiple polarization functions. In addition to the basis sets mentioned above, LanL2DZ is a basis set for post-third row atoms; other basis sets are D95V, SHC, CEP-4G, CEP-31G, CEP-121G,

LanL2MB, SDD, SHF, SDF, MHF, MDF, MWB, SDDAII, EPR-II, EPR-III, UGBS, UGBS1P, UGBS2P, UBG3P, MTSmall, DGDZVP, DGDZVP2, and DGTZVP [20,23].

The correlation-consistent basis set cc-pVTZ was proposed by Dunning Jr. in 1988 [35], along with the other basis sets cc-pVDZ and cc-pVQZ. These correlation consistent sets were proposed by Dunning, for all the first row atoms from boron through neon. The basis set used in this work has been the cc-pVTZ basis set, which actually includes the valence polarization functions 3s, 2p and 1d for hydrogen; 4s, 3p, 2d and 1f for boron-neon; 5s, 4p, 2d, and 1f for aluminum-argon; and 6s, 5p, 3d and 1f for gallium-krypton.

## CHAPTER III

### EXPERIMENTAL METHODS

#### **Introduction**

A general description of the procedures followed for obtaining the infrared and Raman spectra of the molecules with interest will be described here. More specific conditions used for individual molecules will be discussed in the individual chapters.

#### **Infrared spectra**

The infrared spectra were recorded using a Bruker Vertex 70 instrument which was purged by a stream of nitrogen gas. Once obtained, the spectrum of the sample was then subtracted from the spectrum of the background. The infrared spectra of the vapor-samples at 25°C were obtained using a 4.2 meter Infrared Industries long-path, multi-reflection cell with KBr windows with a resolution of 0.2  $\text{cm}^{-1}$ . The vapor of the sample was introduced at its saturated vapor pressure at room temperature into the long path multi-reflection cell with the aid of a vacuum line. Fig. 1 shows a diagram of this kind of cell. In this cell the laser beam passes four times through the vapor sample thereby increasing the absorption of the light by the vapor sample. The cell possesses concave gold mirrors that collect and focus the laser beam after exciting the sample to a planar mirror that finally directs it to the detector. The infrared spectra collected at higher temperatures were obtained in a heatable metal 10 cm cell (Specac Storm 10 with Model 4000 temperature controller) with KBr windows. In this case, an appropriate amount of

liquid sample was placed into the stainless steel cylindrical cell using a micro-syringe. The windows were then replaced and the cell was evacuated. Infrared liquid-phase spectra were collected by placing a drop of the sample between two KBr discs in order to form a capillary film. The liquid-phase spectra were recorded with a resolution of  $0.5\text{ cm}^{-1}$ .

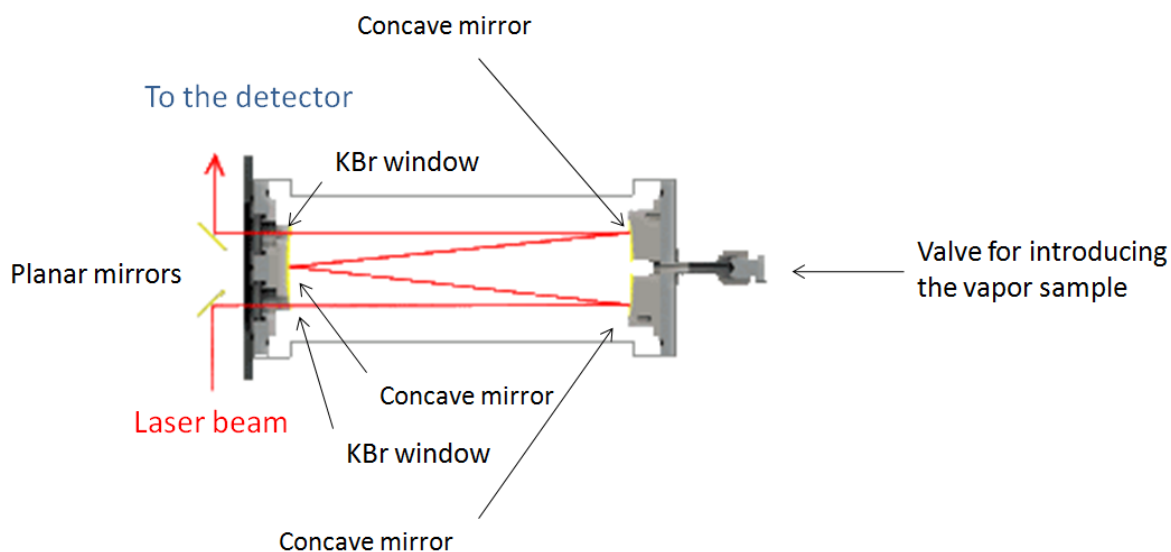


**Fig. 1.** Diagram of a long-path multi-reflection cell.

### Raman spectra

The Raman spectra were recorded with a resolution of  $0.7\text{ cm}^{-1}$  using a Jobin-Yvon U-1000 spectrometer. This specific equipment has a double monochromator and is equipped with 1800 mm holographic gratings. A Coherent Verdi V10 laser operating at

532 nm with a power of 5 W was used as the excitation source. The vapor samples were contained in heatable glass Raman cells, 8 cm long by 2 cm in diameter described by Laane et al. in Refs. [36,37]. Liquid samples were transferred into the Raman vapor cell using a syringe. The samples were frozen with liquid nitrogen and the air of the container was evacuated using a vacuum line. The containers were sealed by glass blowing. As described before [36,37] the cells were wrapped with heating tape, leaving a 1 x 2 cm opening so that the Raman scattering could be collected. The cell windows were left uncovered to permit laser excitation of the samples. The cell extensions beyond the windows were also wrapped with the heating tape to maintain the window temperature close to that of the cell body. This is done to avoid the condensation of the sample on the windows which can distort the input laser beam. The amount of sample used was calculated to have a vapor pressure of one atmosphere in the container at its boiling point. The Raman vapor cell was heated by the heating tape which was connected to a variable autotransformer. A liquid-nitrogen-cooled charge-coupled device (CCD) detector was used to collect the signal. Fig. 2 illustrates briefly the process described above.

A sample with one Torr of vapor pressure has approximately  $10^4$  times less molecules than the corresponding volume of liquid. This makes the vapor-phase Raman spectra much more difficult to be collected than for the liquid phase. Heating the Raman cell containing a measured amount of the sample in its liquid sample increases the vapor pressure of the sample and provides a stronger Raman signal. For example, an organic molecule with a boiling point of 220°C or higher only has a vapor pressure of about

0.1 Torr. The Raman spectra of the liquid samples were recorded utilizing a cuvette as the sample container. A laser power of 0.8 W was typically used.

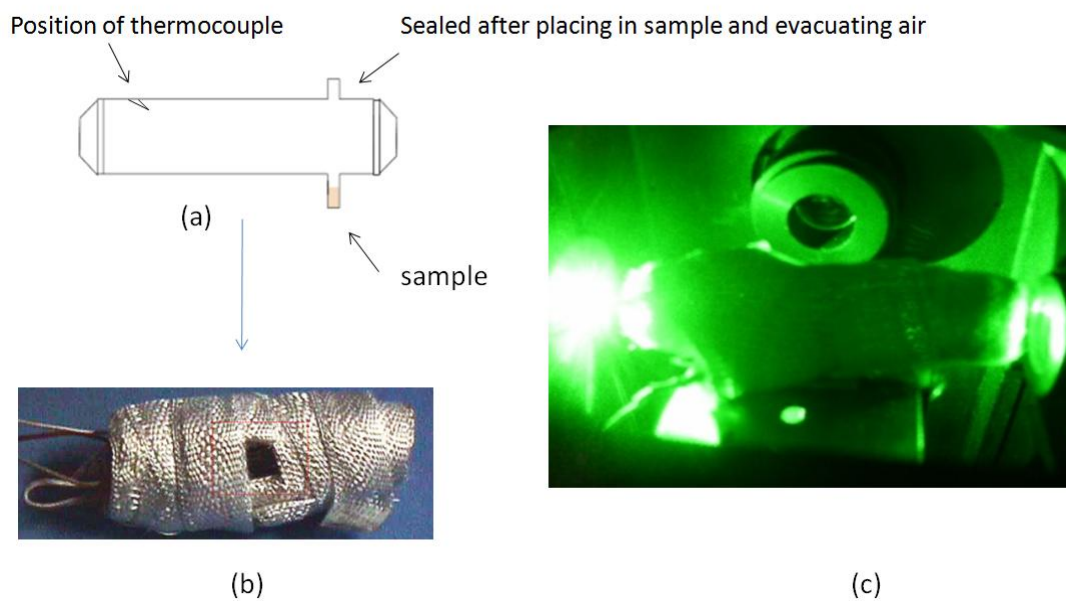


**Fig. 2.** Raman vapor cell. (a) Basis scheme. (b) Raman cell covered with a heating tape. (c) Vapor sample in heating cell wrapped with a heating tape interacting with the laser light. The scattered light is directed to the detector.

CHAPTER IV  
FACTORS AND TYPES OF FORCES AFFECTING CONFORMATIONS  
OF CYCLIC MOLECULES

**Introduction**

Different conformations of a molecule can have different conformational energies which result from various intramolecular forces. Angle strain, torsional strain and steric strain increase the energy of molecules [38,39]. However, the intramolecular  $\pi$ -hydrogen bonding lowers the energy of the molecular conformations. A molecule minimizes its energy by rotations about single bonds and adjustment of bond angles and bond lengths [38]. In this way, a cyclic molecule with more than three carbons generally prefers to adopt a non-planar structure.

**Different types of strain**

*Angle strain*

Angle strain is the energy involved in forcing a molecule to have its angle different from the ideal tetrahedral angle [39]. Baeyer in 1885 discussed the variation in ease of formation and stability of cycloalkanes with ring-size. He assumed that all the ring molecules are planar, and that greater deviations in the bond angles from the tetrahedral angle ( $109.47^\circ$ ) would result in a greater strain. Baeyer suggested that if a carbon atom prefers to have tetrahedral geometry, molecules other than five-membered rings and six-membered rings may be too strained to exist. Baeyer was incorrect in his



belief that small and large rings are too strained to exist. Nowadays, cyclic molecules ranging from three to more than thirty molecules are known [39,40].

### *Torsional strain*

Torsional strain is described as the resistance to bond rotation. This type of strain refers to the component of total molecular energy that results from non-optimal arrangements of vicinal bonds, such as appears in the eclipsed conformations of ethane. Open-chain alkanes have a lower energy for a staggered conformation than for an eclipsed conformation. Cycloalkanes present torsional strain unless all the bonds have staggered arrangements. This can only occur if the molecules are non-planar [38,39].

Most chemists now believe that torsional strain is due to the slight repulsion between electron clouds in the carbon-hydrogen bonds as they pass by each other at close quarters in the eclipsed conformer [40]. Calculations indicate that the internuclear hydrogen-hydrogen distance in the staggered conformer of ethane is 2.55 Å, but this distance decreases to about 2.29 Å in the eclipsed conformer.

### *Steric strain*

Steric strain is the repulsive interaction that occurs when two atoms of a molecule are forced to be closer to each other than their atomic radii allow. Mainly, it is the result of trying to force two atoms to occupy the same space [40].

Small cyclic rings such as cyclopropane and cyclobutane are dominated by angle strain and torsional strain. Cyclopentane, cyclohexane and cycloheptane, instead, are relatively unstrained, and their conformations are most influenced by torsional factors.

Rings such as cyclooctane through cycloundecane, exhibit conformational equilibria and chemical properties that indicate that cross-ring van der Waals interactions play an important role in the stability of these molecules. Large rings such as cyclododecane and higher numbered cyclic molecules become increasingly flexible and possess a large number of low-energy conformations [38].

### Non-planar cyclic conformations

Cyclobutane (I) and cyclopentene (II) molecules have puckered structures. Cyclopentene is considered as a pseudo-four-membered ring since the atoms connected by double bonds behave as single units during the puckering vibrations for this molecule [41]. Cyclobutane and pseudo-four membered rings present angle strain and pucker to minimize the energy. Fig. 3 illustrates the definition of the puckering angle (PA) and the puckering coordinate ( $x$ ) of four-membered rings and pseudo-four-membered rings. The puckering angle is the external angle between the two planes of a four-membered ring or a pseudo-four-membered ring.

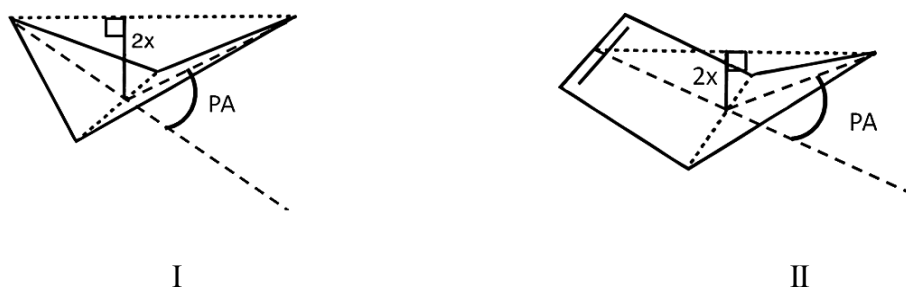


**Fig. 3.** Definition of puckering angle, PA, and puckering coordinate,  $x$ .

The cyclopentane and cyclohexene twist and bent to minimize the eclipsing of bonds on adjacent atoms. The twist ( $C_2$ ) and bent ( $C_s$ ) conformations of these molecules will be described in the respective chapters in this work.

### **The intramolecular $\pi$ -type hydrogen bonding interaction**

The hydrogen bond is a composite interaction that involves wide ranges of geometry and energy. This is due to the great chemical variation that exists among the hydrogen bond donor and acceptor groups [42,43]. In the case of the presence of a  $\pi$ -acceptor, a donor X-H can interact with the electrons in the bonding orbital, assuming that it is sterically accessible. This interaction could be considered electrostatic between the donor H and the "negative" charge of the electron  $\pi$ -cloud. Though these bonds are electrostatic, this characteristic is modified by variable dispersive and charge transfer components that depend on the nature of the donor and acceptor. One of the strongest bonds of this type is considered to be OH $\cdots$ Ph. The intramolecular  $\pi$ -type hydrogen bonding is considered to be a weak hydrogen bond, since the energy involved is less than  $1400\text{ cm}^{-1}$  (17 kJ/mol). X-H  $\cdots$   $\pi$  hydrogen bonds are usually longer than 2.4 Å. In general, weak hydrogen bonds of this type are considered to be between 2 and 3 Å [42].

The relative strength of an intramolecular  $\pi$ -hydrogen bonding cannot be determined independently based on either energetic criteria, bond distances or on infrared wavenumber shifts [42]. The existence of an intramolecular  $\pi$ -hydrogen bond lowers the energy of a conformer whereas torsional, angle and steric strain are

factors that increase the energy. For this reason, the conformer of a molecule with an intramolecular  $\pi$ -hydrogen bond would not necessarily be the conformer of lowest energy.

The existence of an intramolecular  $\pi$ -type hydrogen bonding in a cyclic molecule lowers its energy. Twisting, bending, or puckering of a molecule can help to shorten the distance between the hydrogen atom and a  $\pi$  cloud of a  $X-H \cdots \pi$  bond. The shortening of this distance permits an intramolecular  $\pi$ -type hydrogen bonding to become stronger, and a stabilization of the molecule is attained. Another factor that increases the strength of an intramolecular  $\pi$ -type hydrogen bonding is an adequate orientation of a  $X-H$  bond towards an electron  $\pi$ -cloud.

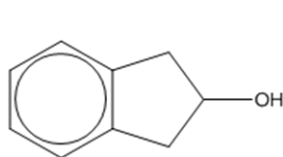
A relatively short distance from the hydrogen of an  $X-H$  bond to a  $\pi$  cloud is expected to increase the  $X-H$  bond length and the  $C=C$  bond length involved. If these bonds lengths are increased, a decrease of the stretching vibration frequencies of the  $X-H$  bond and  $C=C$  bond is also expected.

Hydrogen bonding plays an important role in determining the stability and structures for many chemical and biochemical molecules. Weak intramolecular hydrogen bonding has been reported in alcohols, amines, carboxylic acids, aromatic rings and  $C=C$  double bonds. Hydrogen bonding has been extensively studied and has been shown to play an important role in conformational equilibria, chemical reactions, supramolecular structures, life processes and molecular assemblies [42-45].

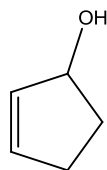
Pejov and co-workers [46] have previously carried out theoretical calculations on weak intramolecular  $\pi$ -type hydrogen bonding present in the phenol-acetylene dimer. They reported that DFT calculations overestimated the decrease in the O-H stretching frequency due to  $\pi$ -type hydrogen bonding, while MP2 calculations did a better job. Karaminkov and co-workers [47] investigated 2-(*p*-fluorophenyl) ethanol with high-resolution UV spectroscopy and ab initio calculations. They determined that the gauche conformer is stabilized by an OH intramolecular  $\pi$ -type hydrogen bond. In earlier work Honkawa and co-workers [48] studied aniline-furan and aniline-phenol using infrared spectroscopy and DFT calculations. Two structural isomers were identified in each case with one of them possessing the  $\pi$ -type hydrogen bond.

The weak intramolecular hydrogen bonding in 3-buten-1-ol has been the subject of several previous infrared spectroscopic investigations [1,49-51]. The O-H stretching region of 3-buten-1-ol in solution shows two bands which are approximately  $40\text{ cm}^{-1}$  apart, corresponding to structures with and without a weak O-H... $\pi$ -electron interaction. Other infrared investigations have also been carried out for similar cyclic molecules, including 2-cyclopenten-1-ol [52] (2CPOL) and 3-cyclopenten-1-ol (3CPOL) [1,53], which is being reinvestigated in this present work. For 3CPOL in solution, two bands in the infrared O-H stretching region were observed about  $25\text{ cm}^{-1}$  apart. This result was reported by Professor J. D. Lewis of St. Edwards University in Austin, and he initially provided a small amount of the sample. The presence of more than one isomer for 3CPOL was also confirmed by  $^1\text{H}$  NMR spectroscopy [1]. From the  $^1\text{H}$  NMR

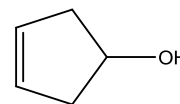
experiment it was found that the puckering angle of the conformer with the bonding between the alcoholic hydrogen and the  $\pi$ -electrons of the C=C double bond was  $40^\circ$ .



2INOL



2CPOL



3CPOL

In recent work [54], detailed computational and laser induced fluorescence spectroscopic studies of vapor-phase 2-indanol (2INOL) in its electronic ground and excited states were presented. These studies showed that 2INOL can exist in four different conformers, with the conformer having the intramolecular hydrogen bonding between the -OH group and the benzene ring possessing the lowest energy. The three non-hydrogen-bonded conformers exist 400 to 700  $\text{cm}^{-1}$  higher in energy.

CHAPTER V  
INTRAMOLECULAR  $\pi$ -TYPE HYDROGEN BONDING OF  
3-CYCLOPENTEN-1-OL

**Introduction**

3-Cyclopenten-1-ol (3CPOL) in the vapor phase is ideally suited for studying weak  $\pi$ -type hydrogen bonding since only intramolecular hydrogen bonding is possible and there is no interference from intermolecular interactions. Al-Saadi et al. [55] recently reported initial theoretical ab initio, density functional theory, and potential energy surface computations for the four 3CPOL conformers and examined the role of ring-puckering and internal rotation in the interconversions of the conformers. The 3CPOL conformers are shown in Fig. 4.

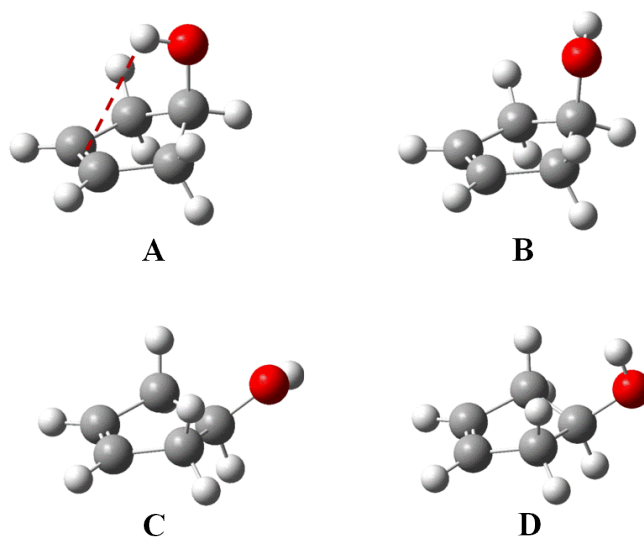


**Fig. 4.** Conformers of 3-cyclopenten-1-ol.

Al-Saadi [2] used MP2/6-31+G(d,p) calculations to produce a set of optimized energies for 3CPOL by varying the ring-puckering angle from  $-50^\circ$  to  $50^\circ$  and the hydroxyl group internal rotation angle from  $0^\circ$  to  $180^\circ$ . These energies were compared to the energy of the conformer of lowest energy. The values can be found elsewhere [2]. A total of 227 calculations were carried out. MATLAB software of MathWorks was then used to construct two-dimensional potential energy maps (Figs. 5 and 6) in terms of the puckering angle and -OH internal rotation. The calculated potential surface provides insight into the energetics of the conformational processes [55].

In the present work, the vapor-phase infrared and Raman spectra of 3CPOL have been collected in the vapor phase at temperatures ranging from  $25^\circ$  to  $257^\circ\text{C}$ , and also in the liquid phase at room temperature. These results were compared to the density functional theory calculations, and were recently published [56]. Additional ab initio (CCSD/cc-pVTZ) and density functional theory (B3LYP/cc-pVTZ) calculations for 3CPOL were also performed. The results confirm the presence of the four predicted conformers.

### **Computations**

Computations for 3CPOL were performed using the coupled cluster theory with single and double excitations (CCSD) level of theory with the cc-pVTZ (triple- $\zeta$ ) basis set in order to calculate the energies and geometries for each of its four conformers using the Gaussian 09 program [57].



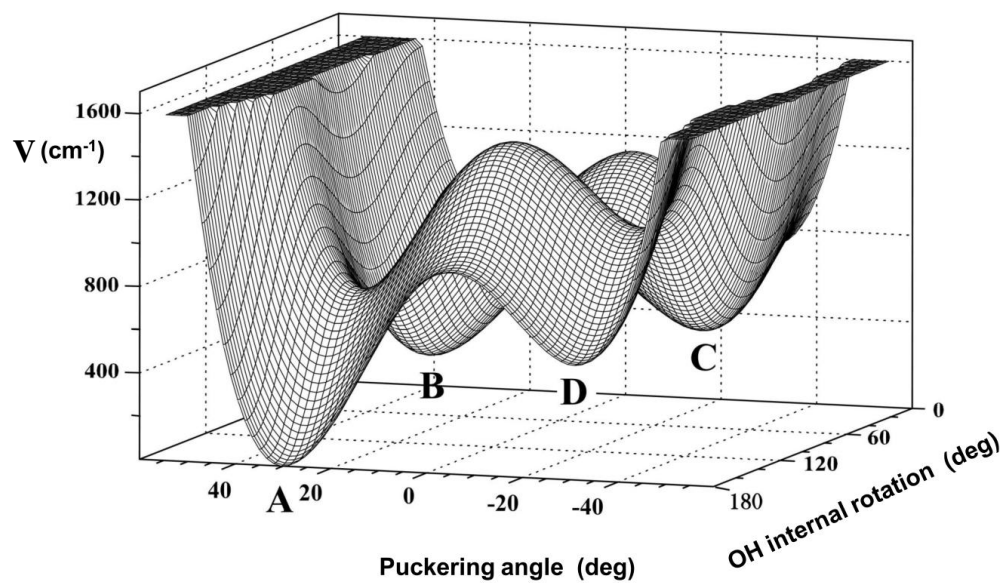


**Fig. 5.** Calculated potential energy surface of 3-cyclopenten-1-ol in terms of the ring-puckering angle and internal rotation angle of the  $\text{-OH}$  group. MP2/6-31+G(d,p) computations.

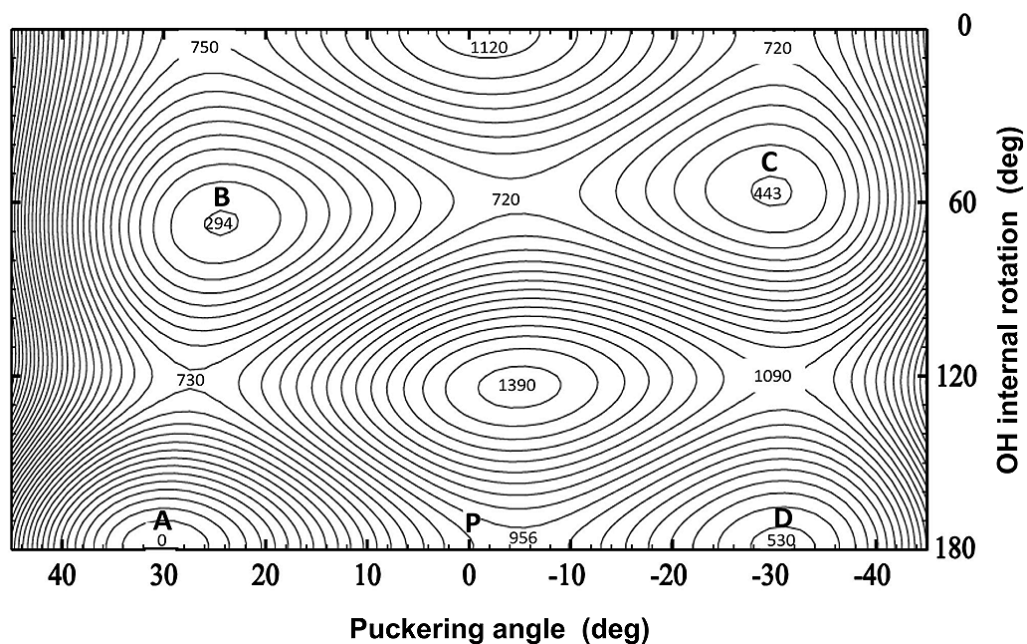


**Fig. 6.** Contour of the potential energy map of 3-cyclopenten-1-ol. Contour lines are  $50 \text{ cm}^{-1}$  apart.

The vibrational frequencies for the four conformations were computed using the density functional theory B3LYP hybrid functional and the cc-pVTZ basis set. These frequencies were scaled using a scaling factor of 0.961 for the spectral region above  $1800\text{ cm}^{-1}$ , and 0.985 for the region below  $1800\text{ cm}^{-1}$  and compared to experimental results. The scaling factors were selected based on previous work on related molecules [58-62]. The frequency shifts were calculated for each conformer in order to aid the confirmation of the coexistence of the four conformers of 3CPOL.

## **Experimental**

The sample of 3CPOL was prepared in the Henning Hopf laboratory in Germany. The procedure involved three steps. 1,3-Cyclopentadiene was initially obtained by the thermal cracking of its dimer [63], and this was then monoepoxidized to 3,4-epoxycyclopentene as described by Crandall and co-workers [64]. The 3CPOL (b.p.  $136^\circ$ ) then was obtained by  $\text{LiAlH}_4$  reduction [53] and purified by Kugelrohr distillation at  $50^\circ\text{C}$  and 30 Torr pressure. Better than 98% purity was verified by NMR.

The infrared spectra of vapor-phase 3CPOL were recorded using a Bruker Vertex 70 instrument which was purged by a stream of nitrogen gas. Samples at  $25^\circ\text{C}$  (vapor pressure of  $\sim 3$  Torr) were obtained using a 4.2 meter Infrared Industries long path multi-reflection cell with KBr windows. Infrared spectra at temperatures up to  $90^\circ$  were obtained in a heatable metal 10 cm cell (Specac Storm 10 with Model 4000 temperature controller) with KBr windows. At  $90^\circ$  the vapor pressure was estimated to be  $\sim 90$  Torr. Infrared spectra of a capillary film of the neat liquid between two KBr discs were

recorded on the same infrared instrument. Raman spectra of 3CPOL vapor were obtained using a Jobin-Yvon U-1000 spectrometer and a Coherent Verdi V10 laser operating at 532 nm with a power of 5 W. Samples were contained in special heatable Raman cells which as described in Refs. [36,37]. Temperatures up to 257°C with ~600 Torr of vapor pressure were used. Raman spectra of the neat liquid contained in a cuvette were recorded using the same instrumentation.

## Results and discussion

The calculated structure parameters of the four conformations for 3CPOL using the CCSD level of theory and cc-pVTZ basis set are shown in Fig. 7. Conformer **A** is the only conformer that can undergo the intramolecular  $\pi$ -type hydrogen bonding. **A** can interconvert to **B** by internal rotation of the -OH group or to **D** by ring-puckering. **D** can interconvert to **C** by internal rotation while a puckering can transform **B** to **C**. Both conformers **A** and **D** have  $C_s$  symmetry with the plane of symmetry bisecting the molecule through the C-O-H bond. The bond distances and angles of the molecule do not vary much with or without the presence of the hydrogen bonding, although the O-H and C=C bond distances are at their largest values for the hydrogen-bonded conformer. The distance from the hydroxyl hydrogen to the center of the C=C bond in conformer **A** is 2.74 Å according to the CCSD/cc-pVTZ calculations.

The relative stabilities and puckering angles of the four conformers were also computed at the CCSD level of theory using the cc-pVTZ basis set and the results are compared to the ones previously calculated [55] and given in Table 1. These

calculations all confirm that there exist four conformers for 3CPOL and that the conformer with the  $\pi$ -type intramolecular hydrogen bonding is the one with the lowest energy.

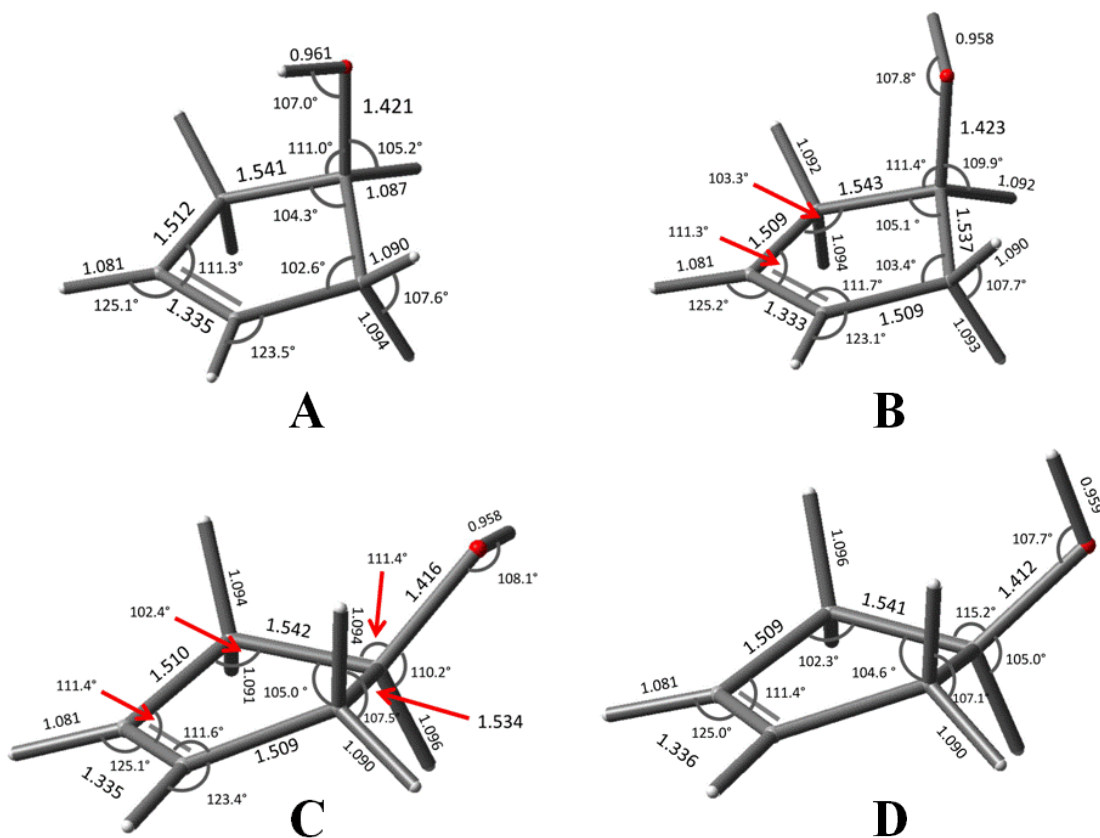


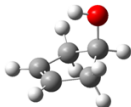
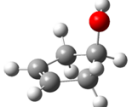
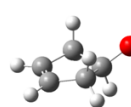
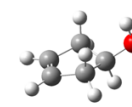
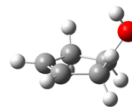
**Fig. 7.** Calculated structures for the four conformers of 3-cyclopenten-1-ol. CCSD/cc-pVTZ calculations.

Based on previous reported work [65-74] it is expected that the ab initio calculated structures to be more reliable than the ones calculated by density functional theory methods and give reasonably good agreement with experiment. CCSD is the

highest level of theory and the cc-pVTZ basis set is the largest basis set used for the calculations reported on Table 1 and for instance the most trustable values reported on this table. The high-level computational results of the puckering angle of **A** listed in Table 1 are significantly lower than the previously reported experimental value of 40° from the proton NMR experiment [1]. Moreover, the computed energies for conformers **A** and **B** with the alcoholic group in the axial position are lower than for the other two conformers.

**Table 1**

Relative energies<sup>a</sup> ( $\Delta E$ ) and puckering angles ( $\phi$ ) of the conformers and the planar structure (**P**) of 3-cyclopenten-1-ol.

									
	<b>A</b>		<b>B</b>		<b>C</b>		<b>D</b>		<b>P</b>
	$\Delta E$	$\phi$	$\Delta E$	$\phi$	$\Delta E$	$\phi$	$\Delta E$	$\phi$	$\Delta E$
	(cm <sup>-1</sup> )	(deg.)	(cm <sup>-1</sup> )	(deg.)	(cm <sup>-1</sup> )	(deg.)	(cm <sup>-1</sup> )	(deg.)	(cm <sup>-1</sup> )
HF/cc-pVTZ <sup>a</sup>	0	24.9	180	19	147	-24.4	200	-25.1	401
B3LYP/cc-pTVZ <sup>a</sup>	0	24.3	226	17.2	325	-20.6	353	-23.5	388
B3LYP/6-311++G(2d,2pd) <sup>a</sup>	0	23.8	146	17	284	-19.7	337	-22.8	348
MP2/6-31+G(d,p) <sup>a</sup>	0	30.1	294	24.5	443	-29.8	530	-31.0	896
MP2/cc-pVTZ <sup>a</sup>	0	30.2	401	24.3	560	-29.5	564	-30.6	871
CCSD/6-311++G(d,p) <sup>a</sup>	0	28.5	274	23.5	409	-27.9	420	-29.0	693
CCSD/cc-pVTZ <sup>b</sup>	0	28.0	301	22.1	402	-26.8	411	-28.0	631

<sup>a</sup> Ref. [55].

<sup>b</sup> This work.

The potential energy function for the interconversion between conformers **A** and **D** in terms of the ring-puckering coordinate based on CCSD/cc-pVTZ calculations is shown in Fig. 8. These calculations estimate an energy difference of 411 cm<sup>-1</sup> between

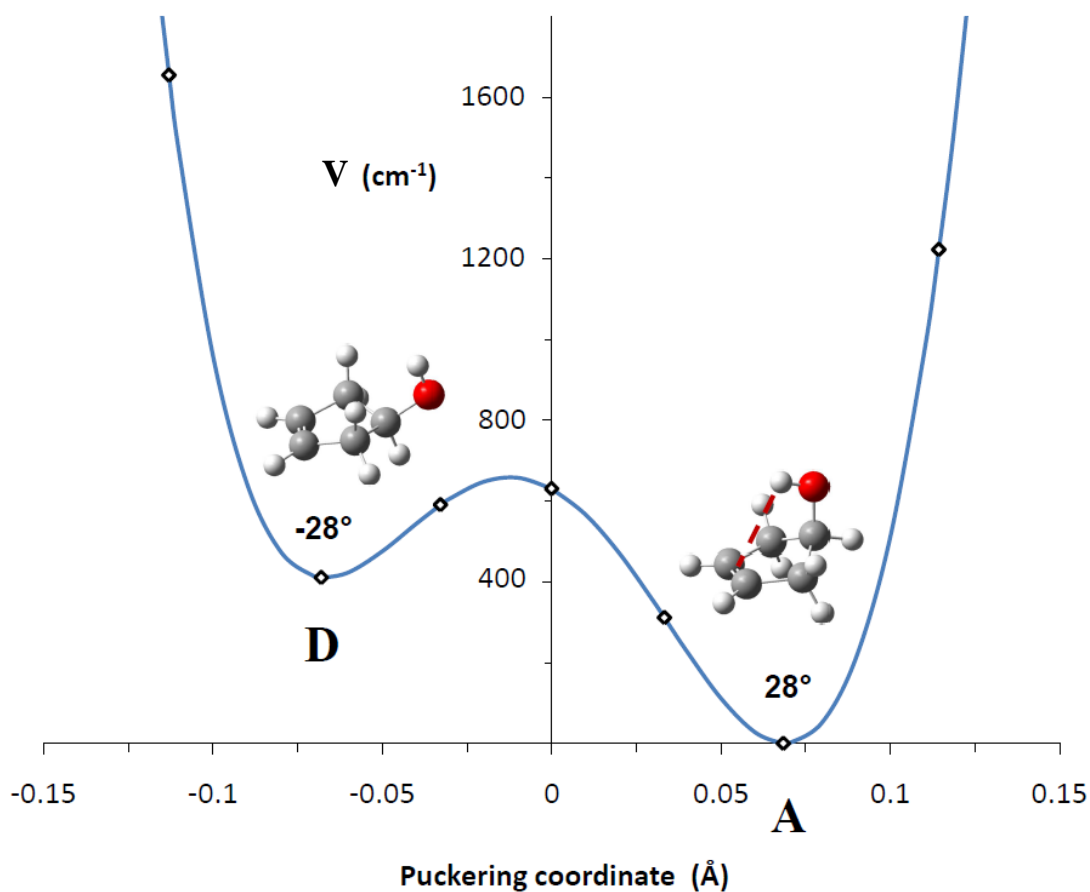


**Fig. 8.** The ring-puckering potential energy function for the interconversion of conformers **A** and **D** of 3-cyclopenten-1-ol. The calculated conversion barrier is  $659\text{ cm}^{-1}$ . CCSD/cc-pVTZ computations.

conformers **A** and **D** and a puckering barrier of  $659\text{ cm}^{-1}$ . Fig. 8 shows that the transition structure located along the ring-puckering pathway between conformers **A** and **D** (with the internal rotation angle of the -OH group equal to  $180^\circ$  measured respect to the center of the C=C double bond) is not completely planar (approximately  $30\text{ cm}^{-1}$  higher in energy than the planar structure), but is slightly puckered towards the direction of the **D** isomer. This suggests that the molecule retains some of the weak interaction between the hydroxyl hydrogen and the C=C double bond at the planar geometry and thereby

slightly lowers the energy. Another interesting result is that for conformer **A** the puckering angle was calculated to be about  $6^\circ$  greater than that for conformer **B**. This indicates that the intramolecular hydrogen bonding in **A** causes an increase in the puckering angle so that the  $-OH$  group can move closer to the  $C=C$  double bond.

The two-dimensional surface described by Figs. 5 and 6 [55] depicts the conformational dynamics of the molecule. Conformation **A** with the intramolecular  $\pi$ -type hydrogen bonding lies significantly lower in energy from the other three conformations. According to the CCSD/cc-pVTZ calculations done in the present work this structure is puckered by  $28^\circ$  and has the hydrogen of the  $-OH$  group pointing directly at the  $C=C$  double bond (internal rotation angle of  $180^\circ$ ). **A** can interconvert to **B** through the  $-OH$  internal rotation. With the loss of the hydrogen bonding the ring has less tendency to be as puckered and the puckering angle drops to  $22^\circ$ . **A** can also interconvert to **D** this time by puckering in the opposite direction thereby eliminating the hydrogen bonding. Either **B** or **D** can interconvert to **C** by puckering or internal rotation respectively. It has been customary to visualize four conformers such as these as separate molecules, but this potential energy surface (Figs. 5 and 6) shows is that it is really the same molecule just sitting at different coordinate values of these two large amplitude vibrations.

The vibrational frequencies for the four conformers in the  $S_0$  electronic ground state have been calculated using B3LYP/cc-pVTZ calculations and compared to B3LYP/6-311++G(2d,2pd) calculations [56]. Only the frequencies of the lowest three large-amplitude motions and the O-H stretching vibration are shown in Table 2. These

values are compared to the ones observed for 2-indanol [54]. The O–H stretching frequency for **A** was calculated to be  $25\text{ cm}^{-1}$  lower than those for **B** and **C**, in excellent agreement with experimental values [1,53,56]. Ab initio and density functional theory results (Tables 1 and 2) suggest that the two O–H stretching bands previously observed in the infrared experiments are due to the two conformers of lowest energy (**A** and **B**) with minor contributions from the other conformers. The ring-puckering frequencies in 3CPOL were predicted from B3LYP/cc-pVTZ calculations to spread over a relatively wide spectral region (from 66 to  $119\text{ cm}^{-1}$ ). This indicates that the puckering vibrations could be experimentally resolved from one conformer to another and be analyzed independently.

**Table 2**

Calculated vibrational frequencies<sup>a</sup> ( $\text{cm}^{-1}$ ) of the –OH stretching and the lowest three large-amplitude motions for 3-cyclopenten-1-ol and 2-indanol. B3LYP/cc-pVTZ computations.

	3-Cyclopenten-1-ol <sup>b</sup>				2-Indanol <sup>c</sup>			
	<b>A</b>	<b>B</b>	<b>C</b>	<b>D</b>	<b>A</b>	<b>B</b>	<b>C</b>	<b>D</b>
-OH stretching	5 <i>3661</i>	3663 <i>3682</i>	3670 <i>3688</i>	3646 <i>3666</i>	3637	3646	3665	3672
-OH torsion	322 <i>307</i>	282 <i>273</i>	275 <i>271</i>	255 <i>250</i>	302 (296) <sup>DF</sup>	251	273	255
Ring twisting	376 <i>371</i>	360 <i>359</i>	391 <i>388</i>	395 <i>392</i>	155 (156) <sup>R</sup>	184 (192) <sup>R</sup>	155	183
Ring puckering	119 <i>115</i>	96 <i>99</i>	71 <i>66</i>	93 <i>87</i>	87 (92) <sup>DF</sup>	87	80 (86) <sup>DF</sup>	84 (90) <sup>DF</sup>

<sup>a</sup> Scaling factor 0.961 for the spectral region above  $1800\text{ cm}^{-1}$  and 0.985 for the region below  $1800\text{ cm}^{-1}$ .

<sup>b</sup> Frequencies in italics are calculated using the 6-311++G(2d,2pd) basis set [2].

<sup>c</sup> Ref. [2]. Frequencies in parentheses are from liquid-phase Raman (R) or dispersed fluorescence (DF) experiments.



In this work the infrared and Raman spectra of both liquid and vapor-phase 3CPOL were analyzed. In the vapor phase all four of the predicted conformers were clearly present and the experimental spectra agree very well with the predicted vibrational frequencies. Conformer **A** with the intramolecular  $\pi$ -type hydrogen bond produces strong spectra but the lower-abundance conformers **B**, **C**, and **D** can also be clearly seen. In the liquid phase the much stronger intermolecular hydrogen bonding between hydroxyl groups on neighboring molecules is present so that little or no intramolecular hydrogen bonding is retained. Thus, the theoretical calculations performed in this research work are not applicable to the molecule in condensed phases.

The vapor spectra of 3CPOL to be described result from the combination of the individual spectra of the four conformers. Table 3 lists the calculated abundance of the conformers at the different temperatures at which the spectra were recorded. The hydrogen-bonded conformer is calculated to be more than 34% abundant at the temperatures used.

In addition to the overlap of the spectra from different conformers the spectra also show a large number of hot bands arising from the vibrational excited states of the low-frequency vibrations, notably the ring-puckering vibrations with frequencies below  $120\text{ cm}^{-1}$ . The  $\text{-OH}$  torsional vibrations near  $300\text{ cm}^{-1}$  are also expected to produce a number of observed hot bands.

**Table 3**Calculated abundance (%) of 3-cyclopenten-1-ol conformers at different temperatures.<sup>a</sup>

Temp (°C)	A (0 cm <sup>-1</sup> )	B (301 cm <sup>-1</sup> )	C (402 cm <sup>-1</sup> )	D (411 cm <sup>-1</sup> )
25	53	25	15	7
90	45	27	18	9
186	38	30	22	10
257	35	31	23	11

<sup>a</sup> Based on CCSD/cc-pVTZ energy calculations.

Figs. 9 and 10 show the liquid- and vapor-phase infrared (90°C) and Raman spectra (186°C) of the sample and compare these to the calculated spectra for conformer **A** based on B3LYP/cc-pVTZ computations. Since most of the bands from the other conformers are only shifted by a few wavenumbers, it is only necessary to show the calculated spectrum for **A** in these broad general views. Fig. 11 compares the vapor-phase infrared and Raman spectra and illustrates how very different the infrared and Raman intensities are from each other. Table 4 presents a listing of the vibrational assignments of the spectra for all four conformers and compares these to the scaled values from the B3LYP/cc-pVTZ computation. The vibrational descriptions were verified utilizing the Semichem APAC/AGUI 9.2 program [75]. The agreement between the experimental and calculated values is remarkably good, especially for the predicted wavenumber shifts between the different conformations. The wavenumber shifts in the table are listed as  $\Delta\nu$ . All of the calculated values are listed in italics below the experimental ones. The vibrations have been numbered according to C<sub>s</sub> symmetry for the **A** conformer. In some cases the numbering would change for the **D** conformer

which also has  $C_s$  symmetry since the frequency order may change. Conformations **B** and **C** have  $C_1$  symmetry and their usual vibration numbering would not be according to  $A'$  and  $A''$  symmetry species. For comparison's sake, Table 4 also lists the vibrational frequencies for cyclopentene [61] along with their symmetry species according to the  $C_{2v}$  symmetry group. As expected, many of the 3CPOL vibrations are very similar to cyclopentene in both description and frequency. Whereas the wavenumber agreement is very good between experimental and computed values, the intensities agree more poorly. This can be seen in Figures 9 and 10 and also is evident in Table 4.

The majority of vibrations, as shown in Table 4, show wavenumber differences of only a few  $\text{cm}^{-1}$  for the different conformers reflecting that the vibrations themselves are little changed. Those vibrations that do show changes, however, are of greatest interest as they provide insight into the bonding differences between the four conformers. Fig. 12 shows the O-H stretching region for 3CPOL vapor. All four conformers are clearly observed in both infrared and Raman spectra although conformer **C** appears as a shoulder in both spectra. Conformer **A**, as expected, with its intramolecular hydrogen bond has the lowest O-H stretching frequency and the strongest infrared band. The frequencies for **B**, **C**, and **D** are 32, 36, and 14  $\text{cm}^{-1}$  higher, respectively. Table 5 summarizes the frequency shifts for the seven vibrational modes of greatest significance, including  $\nu_1$ , and compares these to the calculated shifts. Figs. 13 and 14 show the infrared and Raman spectra in the regions for two of the other modes, the C=C stretching region and CH out-of-plane bending region, respectively.

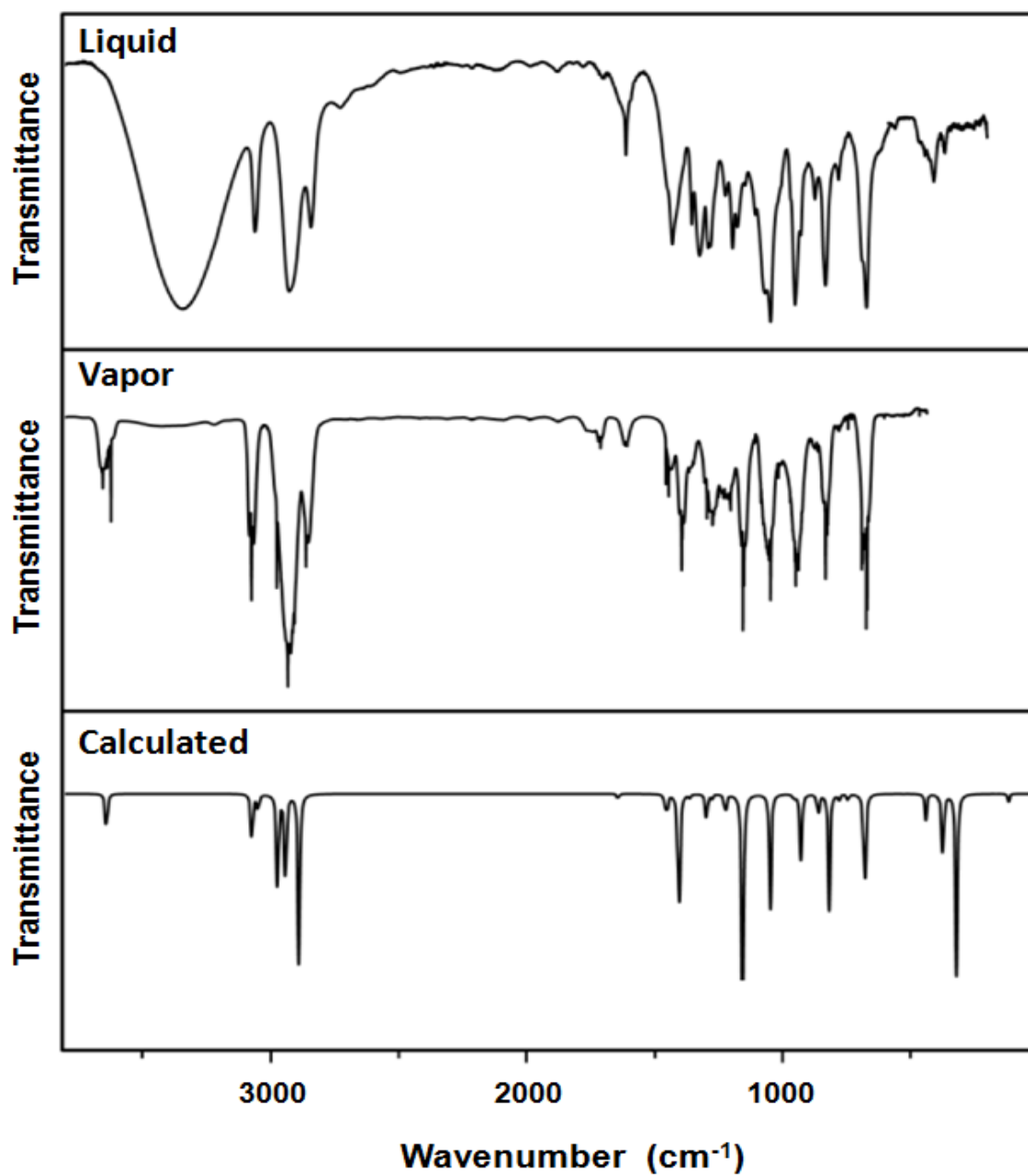


Fig. 9. Comparison between the experimental and computed infrared spectra of conformer A of 3-cyclopenten-1-ol.

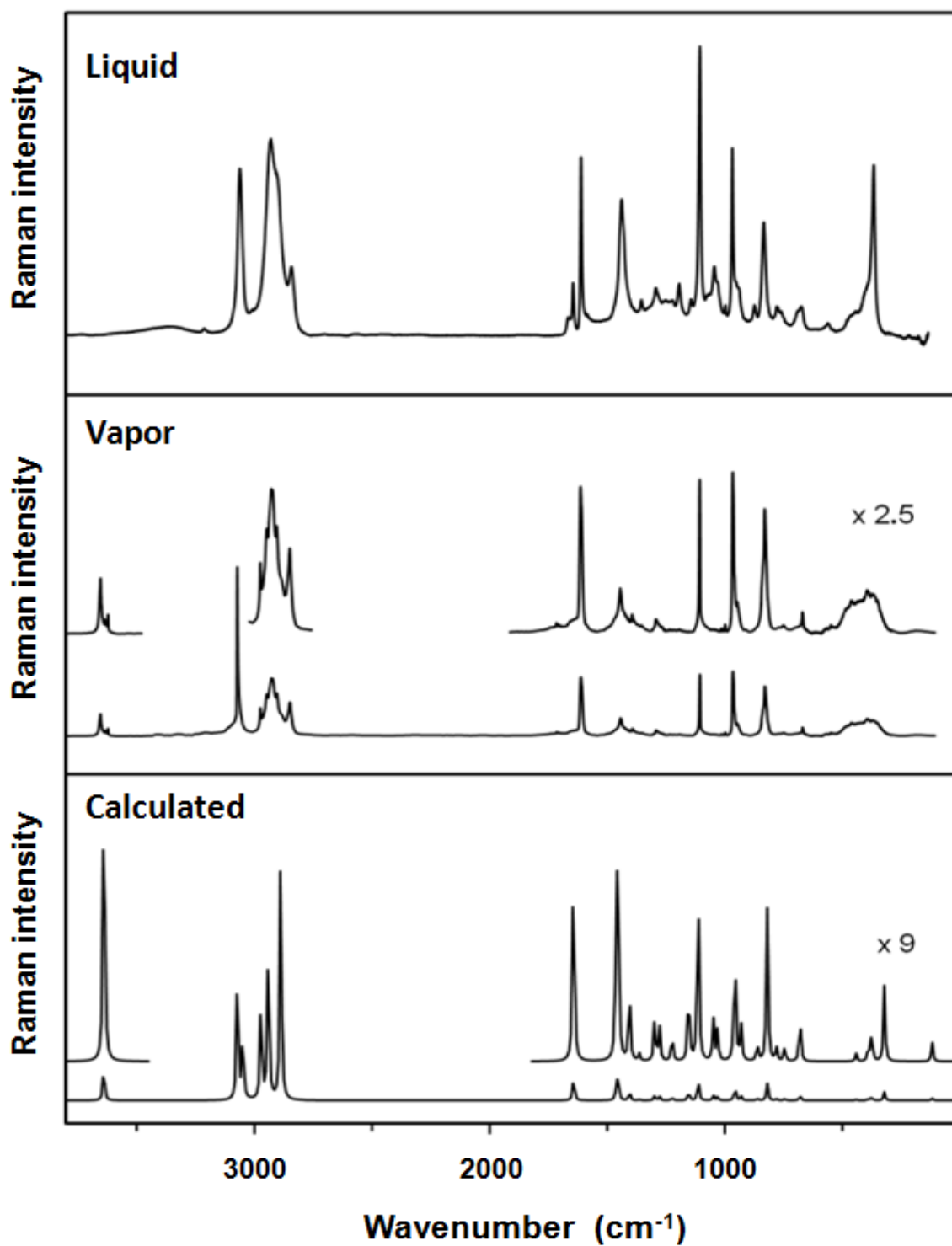


Fig. 10. Comparison between the experimental and computed Raman spectra of conformer A of 3-cyclopenten-1-ol.

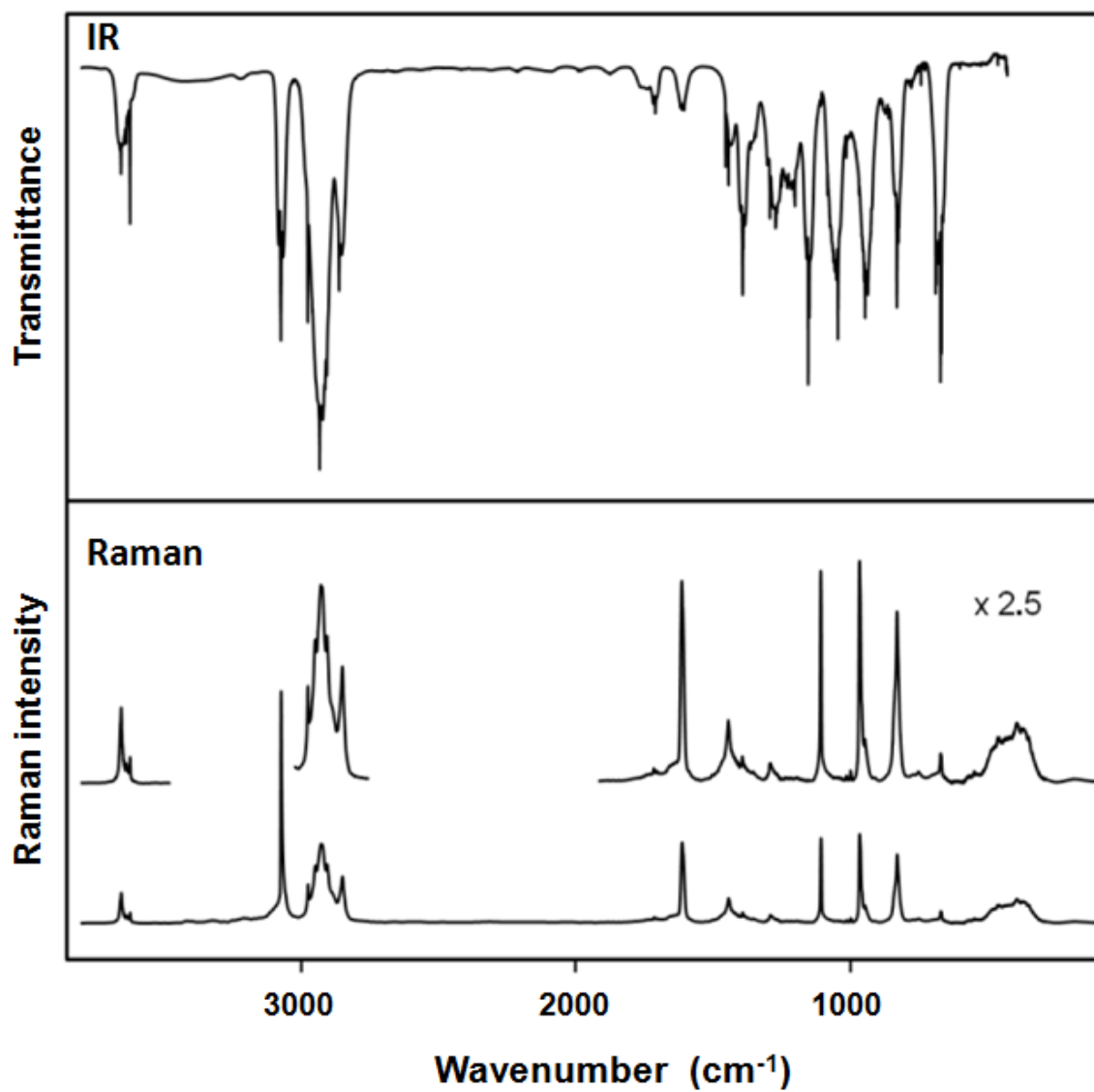


Fig. 11. Infrared and Raman spectra of 3-cyclopenten-1-ol vapor.

**Table 4**Observed and calculated vibrational frequencies ( $\text{cm}^{-1}$ ) for the four conformers of 3-cyclopenten-1-ol<sup>a</sup>.

Assignments			3-Cyclopenten-1-ol										Cyclopentene		
			$\nu(\text{A})$	Int.(IR, R)	$\nu(\text{B})$	$\Delta\nu$	Int.(IR, R)	$\nu(\text{C})$	$\Delta\nu$	Int.(IR, R)	$\nu(\text{D})$	$\Delta\nu$	Int.(IR, R)	$\nu$	Sym.
A'	$\nu_1$	O-H stretch	3623.4	41, 9	3655.4	32.0	10, 31	3659	36	3, 22	3637.6	14.2	7, 3		
			3640.9	19, 554	3663.5	22.6	26, 1078	3670.1	29.2	33, 1144	3645.9	5.0	18, 720		
	$\nu_2$	=C-H sym. stretch	3074.4	85, 194	3075.7	1.3	58, 26	3073.5	-0.9	43, 232	~ 3073	-1	27, 28	3078	A <sub>1</sub>
			3072.3	25, 1939	3072.5	0.2	28, 2014	3070.3	-2.0	30, 2027	3069.2	-3.1	30, 2044		
	$\nu_3$	C-H stretch	2976.7	62, 23	2949	-28	3, 20	2940	-37	5, 22	2949	-28	3, 20	2963/2903	B <sub>2</sub> /A <sub>2</sub>
			2972.7	50, 1376	2946.0	-26.7	18, 1026	2941.4	-31.3	45, 1224	2951.9	-20.8	59, 1686		
	$\nu_4$	$\alpha$ -CH <sub>2</sub> antisym. str. i.p.	2933.0	202, 43	2921.3	-11.7	54, 45	2929	-4	1, 46	2939	6	---, 23	2933	B <sub>2</sub>
			2942.1	23, 1177	2918.0	-24.1	44, 987	2926.2	-15.9	49, 1210	2939.6	-2.5	45, 1071		
	$\nu_5$	$\alpha$ -CH <sub>2</sub> sym. str. i.p.	2862.6	25, 10	2861.5	-1.1	21, 10	2849.1	-13.5	---, 39	2845.8	-16.8	---, 24	2860	A <sub>1</sub>
			2888.9	33, 2365	2892.0	3.1	14, 804	2888.3	-0.6	41, 1166	2865.3	-23.6	58, 2369		
	$\nu_6$	C=C stretch	1607.3	2, 46	1620.7	13.4	1, 25	1615.3	8.0	2, 86	1609.4	2.1	1, 75	1623	A <sub>1</sub>
			1644.0	2, 220	1657.0	13.0	3, 222	1654.8	10.8	3, 219	1650.5	6.5	2, 237		
	$\nu_7$	$\alpha$ -CH <sub>2</sub> def. i.p.	1445.6	17, 19	1443.8	-1.8	12, 18	1457	11.4	19, 7	1457	11	19, 7	1445	A <sub>1</sub>
			1460.4	3, 163	1457.2	-3.2	1, 180	1470.9	10.5	2, 197	1469.7	9.3	2, 204		
	$\nu_8$	$\beta$ -CH bend/COH bend	1394.5	38, 13	1392.0	-2.5	14, 2	1392.7	-1.8	6, 4	1394.1	-0.4	36, 4	-----	
			1405.6	64, 72	1394.0	-11.6	5, 45	1403.0	-2.6	3, 55	1404.1	-1.5	74, 54		
	$\nu_9$	$\alpha$ -CH <sub>2</sub> wag i.p.	1295.1	18, 8	1303.5	8.4	4, 2	1305.3	10.2	3, ---	1303.9	8.8	3, 2	1290	A <sub>1</sub>
			1299.2	8, 32	1311.2	12.0	9, 21	1318.7	19.5	12, 10	1312.3	13.1	1, 27		
	$\nu_{10}$	COH bend / $\beta$ -CH bend	1274.6	9, 3	1273.8	-0.8	8, 3	1273.4	-1.2	7, 3	1272.8	-1.8	3, 3	-----	-----
			1278.0	2, 32	1270.5	-7.5	59, 19	1273.3	-4.7	10, 15	1276.2	-1.8	16, 37		
	$\nu_{11}$	$\alpha$ -CH <sub>2</sub> twist i.p.	1155.5	100, 0.7	1195	39.5	~1, ~1	1178.8	23.3	1, ---	1134.4 ?	-21.1	~1, ---	1211	B <sub>2</sub>
			1157.3	100, 34	1193.7	36.4	5, 47	1181.5	24.2	3, 16	1139.8	-17.5	17, 76		
	$\nu_{12}$	=CH wag o.p in plane	1108.0	4, 95	1110.5	2.5	3, 95	1111.4	3.4	2, ---	-----	-----	---, ---	1101	A <sub>1</sub>
			1113.8	0.01, 168	1114.6	0.8	1, 174	1117.9	4.1	1.3, 173	1117.8	4.0	7, 155		
	$\nu_{13}$	$\alpha$ -CH <sub>2</sub> rock	1047.5	54, 0.7	1053.3	5.8	10, 0.4	1076.0	28.5	4, 3	1085.0	37.5	9, 4	-----	B <sub>2</sub>
			1049.3	49, 36	1056.9	7.6	17, 44	1069.8	20.5	72, 55	1074.4	25.1	161, 48		
	$\nu_{14}$	ring stretch	967.9	2, 100	970.2	2.3	5, 75	970.8	2.9	3, 56	968.8	0.9	1, ---	962	A <sub>1</sub>
			956.6	2, 100	965.6	9.0	0.4, 11	963.9	7.3	1, 12	961.6	5.0	0.7, 11		
	$\nu_{15}$	C-O stretch	948.3	29, 17	951.8	3.5	11, 13	1016.7	68.4	8, 3	1011.3	63.0	1, 1	1047	B <sub>2</sub>
			931.0	18, 29	944.2	13.2	72, 62	1011.8	80.8	0.2, 96	1009.8	78.8	1, 93		

Table 4 continued.

Assignments		3-Cyclopenten-1-ol											Cyclopentene	
		$\nu(\text{A})$	Int.(IR, R)	$\nu(\text{B})$	$\Delta\nu$	Int.(IR, R)	$\nu(\text{C})$	$\Delta\nu$	Int.(IR, R)	$\nu(\text{D})$	$\Delta\nu$	Int.(IR, R)	$\nu$	Sym.
$\nu_{16}$	ring stretch	832.4	51, 77	834.1	0.6	5, 61	839.8	7.4	3, 45	833.0	0.6	-10, ---	900	$A_1$
		819.9	45, 116	823.9	4.0	22, 116	829.3	9.4	0.6, 90	823.0	3.1	2, 76		
$\nu_{17}$	ring deformation	744.6	5, 3	729.9	-14.7	1, 0.7	571.2	-173.4	---, 3	551.6	-193	---, 4	593	$A_1$
		746.3	3, 12	736.4	-9.9	1, 15	572.3	-174.0	53, 46	561.9	-184.4	63, 40		
$\nu_{18}$	CH i.p. bend out of plane	673.5	97, 12	669.7	-3.8	75, 10	690.1	16.6	42, 1	688.1	14.6	26, 1	695	$B_2$
		680.7	51, 37	676.3	-4.4	39, 36	700.6	19.9	4, 27	695.6	14.9	5, 37		
$\nu_{19}$	CO rock	397.4	---, 8	-----	-----	---, ---	464.8	67.4	2, 5	-----	-----	---, ---	-----	-----
		390.1	0.6, 10	408.5	18.4	11, 5	467.5	77.4	1.2, 23	455.7	65.6	1, 25		
$\nu_{20}$	ring puckering	-----	---, ---	-----	-----	---, ---	-----	-----	---, ---	-----	-----	---, ---	127	$B_2$
A'' $\nu_{21}$	=CH antisym. stretch	3057 sh	2, 30	-----	-----	---, ---	-----	-----	---, ---	-----	-----	---, ---	3068	$B_1$
		3049.14	8, 912	3049.13	-0.01	9, 944	3047.2	-1.9	10, 950	3046.4	-2.7	9, 933		
$\nu_{22}$	$\alpha$ -CH <sub>2</sub> antisym. str. o.p.	2933.0	202, 43	2913.8	-19.2	54, 18	2906.9	-26.1	27, 20	2918.9	-14.1	23, 28	2955	$A_2$
		2941.2	23, 1068	2905.2	-36.0	88, 3108	2898.2	-43.0	32, 1532	2930.0	-11.2	3, 748		
$\nu_{23}$	$\alpha$ -CH <sub>2</sub> sym. stretch o.p.	2862.4	28, 10	-----	-----	---, ---	-----	-----	---, ---	2844.6	-17.8	28, ---	2873	$B_1$
		2889.3	43, 738	2879.8	-9.5	67, 744	2868.2	-21.1	46, 1321	2864.7	-24.6	37, 690		
$\nu_{24}$	$\alpha$ -CH <sub>2</sub> deformation o.p.	1446.4	3, 19	-----	-----	---, ---	-----	-----	---, ---	-----	-----	---, ---	1438	$B_1$
		1453.0	8, 130	1448.1	-4.9	8, 108	1462.1	9.1	4, 104	1461.3	8.3	5, 107		
$\nu_{25}$	=CH wag i.p. in plane	1356	---, 3	-----	~ 0	---, ---	-----	~ 0	---, ---	-----	~ 0	---, ---	1353	$B_1$
		1363.8	1, 6	1365.2	1.4	8, 24	1366.8	3.0	12, 29	1363.9	0.1	0.1, 11		
$\nu_{26}$	$\alpha$ -CH <sub>2</sub> wag o.p.	1283.2	1, 4	1294.9	11.7	4, 7	1286.1	2.9	3, 6	-----	-----	---, ---	1297	$B_1$
		1294.4	3, 5	1305.5	11.1	5, 20	1295.0	0.6	9, 33	1307.5	13.1	1.1, 12		
$\nu_{27}$	$\beta$ -CH wag	1230.8	5, ---	~ 1217.3	-14.0	2, ---	1251.8	21.0	6, ---	-----	-----	---, ---	-----	$B_1$
		1224.9	10, 25	1215.6	-9.3	48, 54	1252.3	27.4	74, 47	1271.4	46.5	7, 16		
$\nu_{28}$	$\alpha$ -CH <sub>2</sub> twist o.p.	1151.3	33, 0.4	1152.7	1.4	23, 0.4	1134.4 ?	-16.9	1, 0.4	1134.4 ?	16.9	1, 0.4	1268	$A_2$
		1150.3	2, 26	1152.0	1.7	7, 11	1137.9	-12.4	3, 8	1131.5	-18.8	2, 7		
$\nu_{29}$	ring stretch	1034	---, 0.7	1022.5	-11.5	1, 0.4	1046.6	12.6	35, 0.4	1063.0	29	3, ---	1047	$B_2$
		1030.9	0.02, 27	1019.4	-11.5	5, 29	1043.2	12.3	1, 23	1066.1	35.2	5, 11		
$\nu_{30}$	=CH wag o.p out of plane	-----	---, ---	-----	-----	---, ---	-----	-----	---, ---	-----	-----	---, ---	933	$A_2$
		965.7	0.001, 5	962.8	-2.9	3, 57	968.3	2.6	69, 34	969.8	4.1	12, 13		
$\nu_{31}$	ring stretch	926.1	5, 2	927.5	1.4	3, 2	937.6	11.5	10, 2	939.5	13.4	6, 2	1037	$B_1$
		927.2	13, 1.2	930.2	3.0	23, 5	939.6	12.4	19, 1	940.6	13.4	18, 1		



**Table 4** continued.

Assignments		3-Cyclopenten-1-ol										Cyclopentene		
		$\nu$ (A)	Int.(IR, R)	$\nu$ (B)	$\Delta\nu$	Int.(IR, R)	$\nu$ (C)	$\Delta\nu$	Int.(IR, R)	$\nu$ (D)	$\Delta\nu$	Int.(IR, R)	$\nu$	Sym.
$\nu_{16}$	ring stretch	832.4	51, 77	834.1	0.6	5, 61	839.8	7.4	3, 45	833.0	0.6	~10, ---	900	A <sub>1</sub>
		<i>819.9</i>	<i>45, 116</i>	<i>823.9</i>	<i>4.0</i>	<i>22, 116</i>	<i>829.3</i>	<i>9.4</i>	<i>0.6, 90</i>	<i>823.0</i>	<i>3.1</i>	<i>2, 76</i>		
$\nu_{17}$	ring deformation	744.6	5, 3	729.9	-14.7	1, 0.7	571.2	-173.4	---, 3	551.6	-193	---, 4	593	A <sub>1</sub>
		<i>746.3</i>	<i>3, 12</i>	<i>736.4</i>	<i>-9.9</i>	<i>1, 15</i>	<i>572.3</i>	<i>-174.0</i>	<i>53, 46</i>	<i>561.9</i>	<i>-184.4</i>	<i>63, 40</i>		
$\nu_{18}$	CH i.p. bend out of plane	673.5	97, 12	669.7	-3.8	75, 10	690.1	16.6	42, 1	688.1	14.6	26, 1	695	B <sub>2</sub>
		<i>680.7</i>	<i>51, 37</i>	<i>676.3</i>	<i>-4.4</i>	<i>39, 36</i>	<i>700.6</i>	<i>19.9</i>	<i>4, 27</i>	<i>695.6</i>	<i>14.9</i>	<i>5, 37</i>		
$\nu_{19}$	CO rock	397.4	---, 8	-----	-----	---,---	464.8	67.4	2,5	-----	-----	---,---	-----	-----
		<i>390.1</i>	<i>0.6, 10</i>	<i>408.5</i>	<i>18.4</i>	<i>11, 5</i>	<i>467.5</i>	<i>77.4</i>	<i>1.2, 23</i>	<i>455.7</i>	<i>65.6</i>	<i>1, 25</i>		
$\nu_{20}$	ring puckering	-----	---,---	-----	-----	---,---	-----	-----	---,---	-----	-----	---,---	127	B <sub>2</sub>
		<i>119.0</i>	<i>3, 13</i>	<i>96.1</i>	<i>-22.9</i>	<i>0.1, 16</i>	<i>71.4</i>	<i>-47.6</i>	<i>0.7, 7</i>	<i>92.7</i>	<i>-26.3</i>	<i>2, 12</i>		

<sup>a</sup>The first line for each vibration presents experimental data. The second line in italics presents calculated values using the B3LYP/cc-pVTZ basis set. The scaling factors for the wavenumbers are 0.985 for numbers below 1800 cm<sup>-1</sup> and 0.961 for those above 1800 cm<sup>-1</sup>.

As shown in Table 5, the experimentally observed trend in frequency shifts is confirmed for each of these vibrations, and the actual calculated shift agrees to within a few  $\text{cm}^{-1}$ . The poorest agreements are for the  $\nu_{15}$  shifts of conformer **D** (78.8 vs. 63.0  $\text{cm}^{-1}$ ) and  $\nu_1$  for conformer **B** (22.6 vs. 32.0  $\text{cm}^{-1}$ ). Nonetheless, the computed shifts result to be remarkably accurate. It is noteworthy that upon examination of Table 4, the **A** and **B** conformations have similar vibrational frequencies for all of the vibrations. This is also true for **B** and **C**. However, vibrations  $\nu_{15}$ ,  $\nu_{17}$ , and  $\nu_{19}$  show big differences between the two pairs reflecting strong vibrational coupling between these modes. The  $\nu_{17}$  ring-deformation shifts dramatically, -173.4  $\text{cm}^{-1}$  for **C** and -193  $\text{cm}^{-1}$  for **D** as compared to **A** while  $\nu_{15}$ , the C-O stretching, increases 68.4 and 63.0  $\text{cm}^{-1}$  for **C** and **D**, respectively. At the same time  $\nu_{19}$ , the C-O rock, increases 67  $\text{cm}^{-1}$  for **C** and 65.6 (calculated) for **D**. Both the experimental spectra and the calculations confirm these large changes.

**Table 5**Observed and calculated<sup>a</sup> frequency ( $\text{cm}^{-1}$ ) shifts between the conformers of 3-cyclopenten-1-ol.

Vibration	$\Delta\nu_A$		$\Delta\nu_B$		$\Delta\nu_C$		$\Delta\nu_D$	
	Obs.	Calc.	Obs.	Calc.	Obs.	Calc.	Obs.	Calc.
$\nu_1$ O-H stretch	3623.4	3640.9	32.0	22.6	36	29.2	14.2	5.0
$\nu_6$ C=C stretch	1607.3	1644.0	13.4	13.0	8.0	10.8	2.1	6.5
$\nu_{15}$ C-O stretch	948.3	931.0	3.5	13.2	68.4	80.8	63.0	78.8
$\nu_{17}$ Ring deformation	744.6	746.3	-14.7	-9.9	-173.4	-174.0	-193	-184.4
$\nu_{18}$ CH i.p. bend out of plane	673.5	680.7	-3.8	-4.4	16.6	19.9	14.6	14.9
$\nu_{27}$ $\beta$ -CH wag	1230.8	1224.9	-14.0	-9.3	21.0	27.4	-----	46.5
$\nu_{29}$ Ring stretch	1034	1030.9	-11.5	-11.5	12.6	12.3	29	35.2

<sup>a</sup> B3LYP/cc-pVTZ calculations. Scaling factor: 0.985 for numbers below 1800  $\text{cm}^{-1}$  and 0.961 for those above.

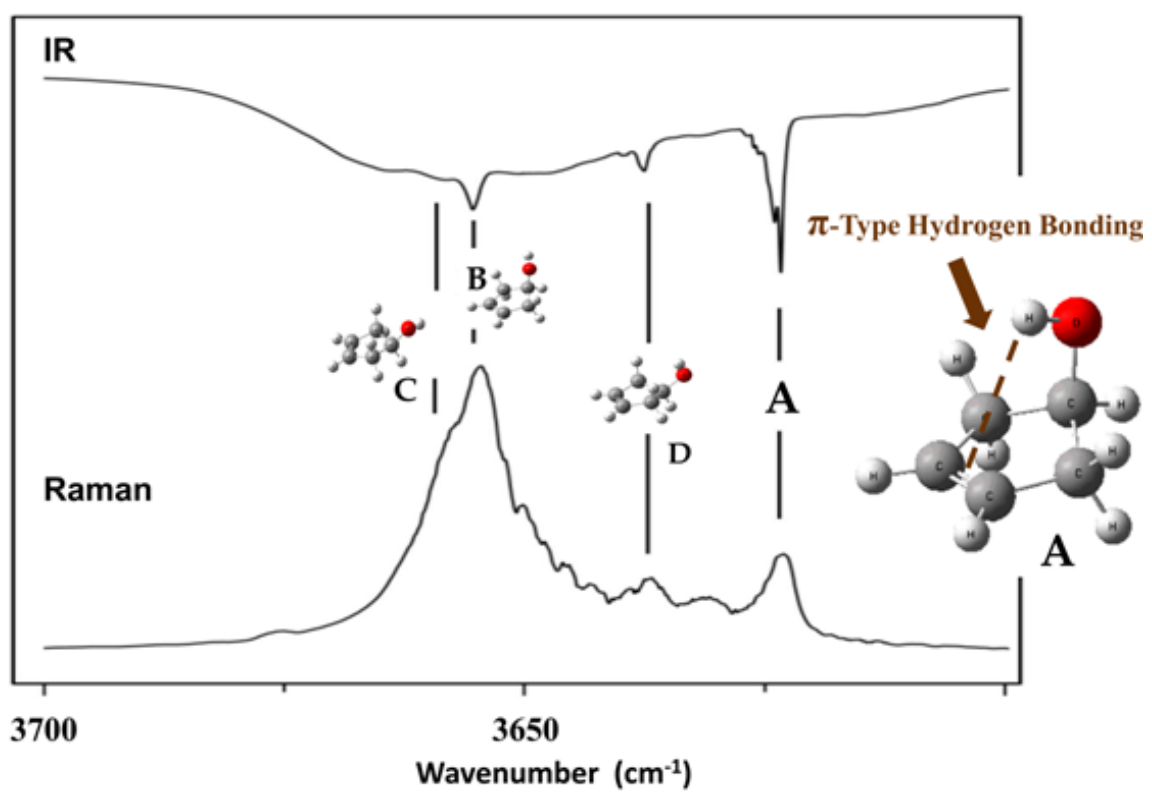
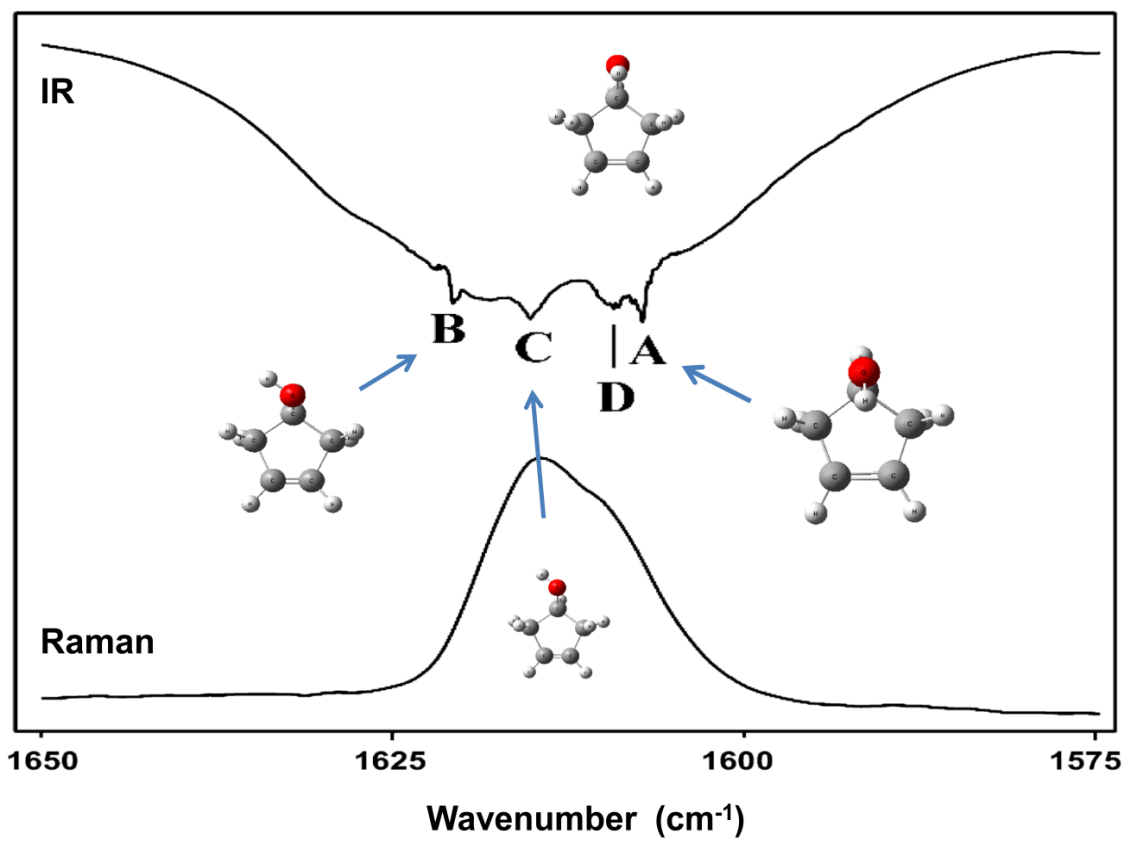
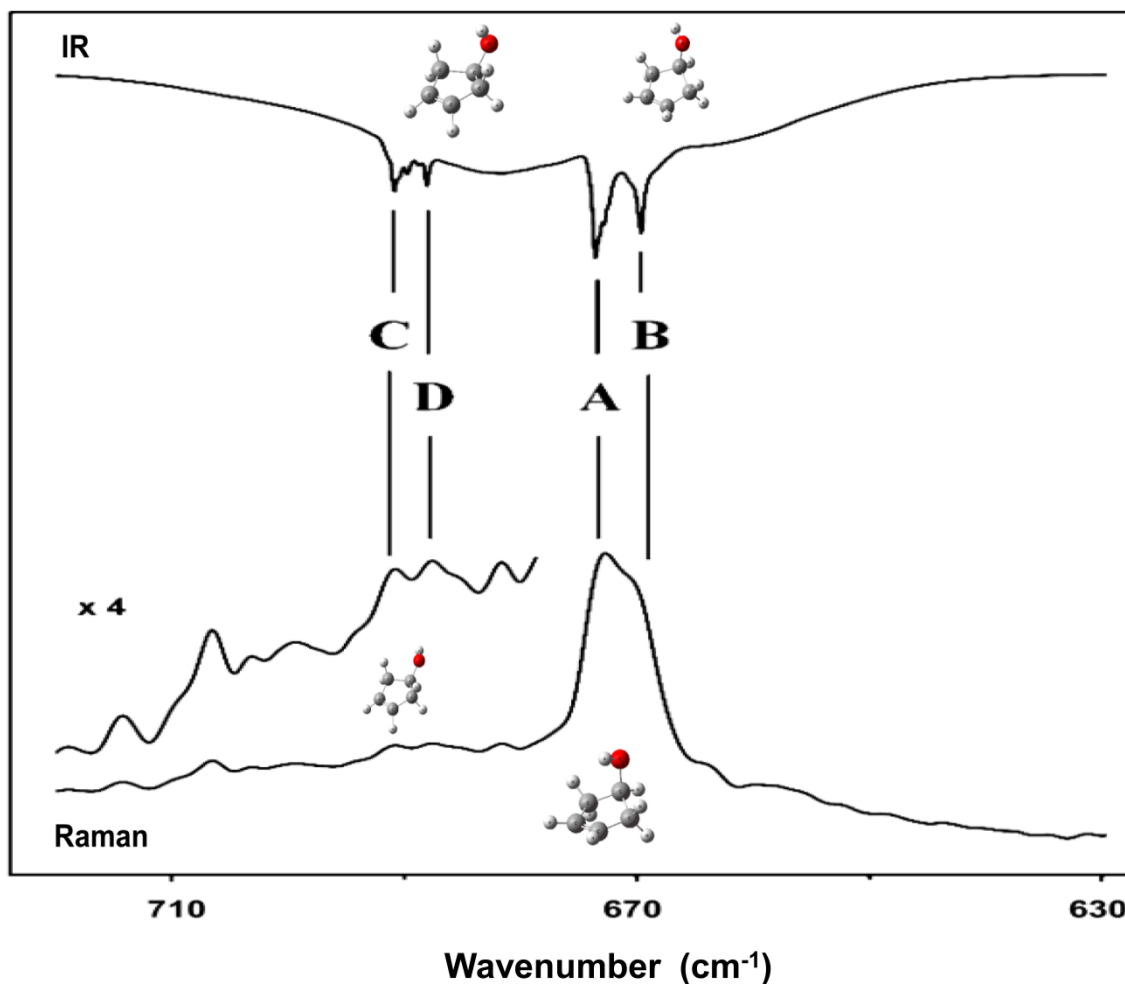


Fig. 12. Infrared and Raman spectra of vapor-phase 3-cyclopenten-1-ol in the O-H stretching region.



**Fig. 13.** Infrared and Raman spectra of vapor-phase 3-cyclopenten-1-ol in the C=C stretching region.



**Fig. 14.** Infrared and Raman spectra of vapor-phase 3-cyclopenten-1-ol for  $\nu_{18}$ , CH out-of-plane bending.

To provide additional perspective on the spectra, Fig. 15 shows the vapor-phase infrared and Raman spectra in the 600 to 1220  $\text{cm}^{-1}$  region. The many Q branches in the infrared spectra arise both from the presence of the four conformers as well as from hot bands originating mostly from the vibrational excited states of the ring-puckering.

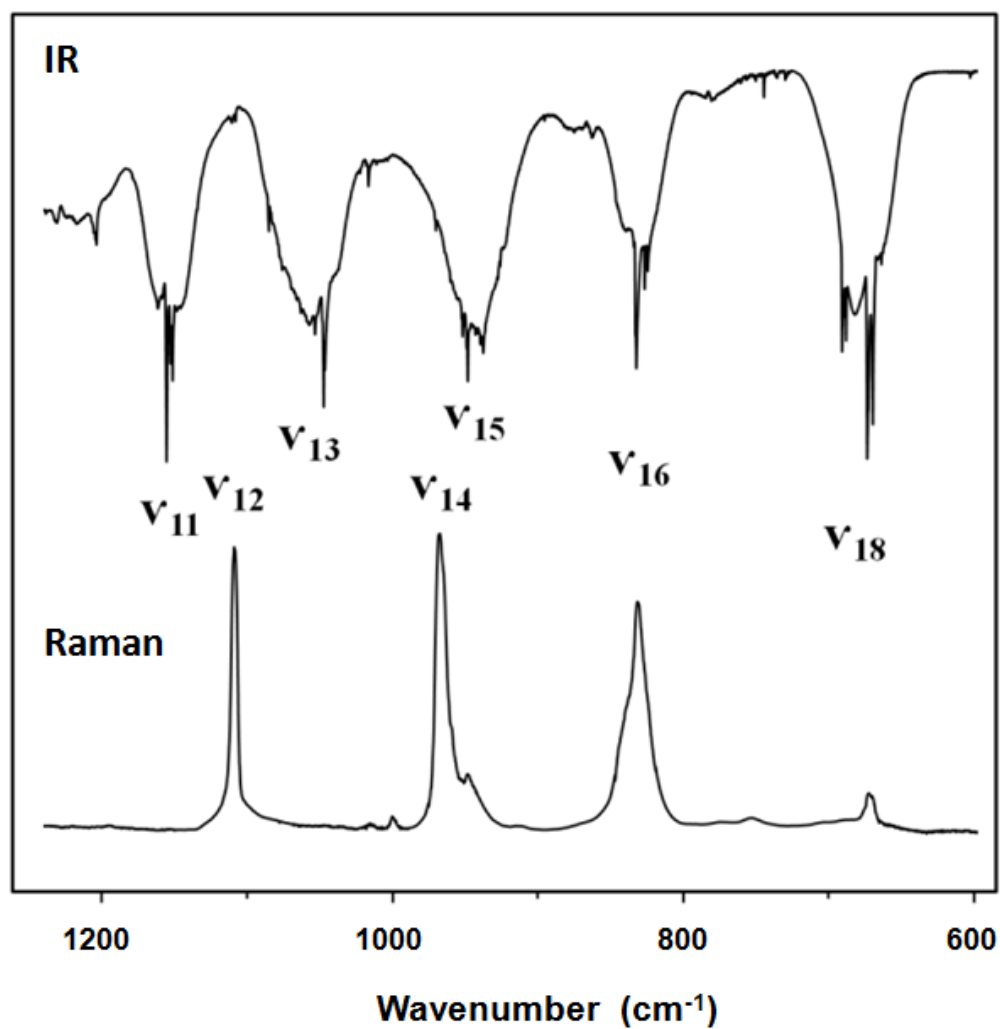


**Fig. 15.** Vapor-phase infrared and Raman spectra of 3-cyclopenten-1-ol in the 600-1200 cm<sup>-1</sup> region.

### **Energy difference between conformers**

Since both the Raman and infrared vapor-phase spectra were recorded at different temperatures, it is possible to estimate the energy difference between conformers from the observed intensity changes. As the temperature is increased the

populations of the higher energy conformers are increased as shown in Table 1 which assumed calculated energy difference values. For the calculations the intensity  $I$  (infrared absorbance or Raman intensity) is given by

$$I = \alpha \cdot P \quad (16)$$

where  $\alpha$  is a proportionality constant based on the Raman cross section or infrared absorption constant as well as instrumental and / or sampling methods, and  $P$  is the molecular population. The relative intensity of bands from conformers **A** and **B** can then be written as

$$(I_B / I_A) = (\alpha_B / \alpha_A) \cdot (P_B / P_A) \quad (17)$$

If it is assumed that **A** is the lowest energy  $\pi$ -bonded conformer, the population ratio is given by

$$(P_B / P_A) = g_B \exp[-(E_B - E_A) / kT] = 2 \exp(-\Delta E_{AB} / kT) \quad (18)$$

where  $E_A$  and  $E_B$  are the molecular energies of the two conformers and where the degeneracy  $g_B = 2$  for the two equivalent **B** conformations. Then

$$(I_B / I_A) = 2 (\alpha_B / \alpha_A) \exp(-\Delta E_{AB} / kT) \quad (19)$$

and

$$\ln(I_B / I_A) = \ln(2 \alpha_B / \alpha_A) - \Delta E_{AB} / kT \quad (20)$$

Thus, having in this work the data for  $I_B / I_A$  for different vibrations as a function of temperature,  $\ln ( I_B / I_A )$  vs.  $( kT )^{-1}$  can be graphed to obtain the slope which is  $\Delta E_{AB}$ , the energy difference between conformers **A** and **B**. This has been done only for these two conformers since the intensity data for the higher energy **C** and **D** conformers is not as reliable. Even for the **A** and **B** data there are fairly large uncertainties in measuring  $I_B / I_A$  (typically about 10%) and temperature (up to  $\pm 5^\circ\text{C}$ ) so that the calculated  $E_{AB}$  value will be somewhat approximate. The Raman and infrared data for  $\nu_1$  and the infrared data for  $\nu_{18}$  have been used for these calculations. Only two data points were available for each of the infrared calculations while the Raman data were collected at three different temperatures. The calculations gave the energy difference  $E_{AB}$  between conformers **A** and **B** to be  $435 \pm 160 \text{ cm}^{-1}$  where the uncertainty is given as twice the standard deviation ( $2\sigma$ ). This value is not very accurate due to the uncertainties in the intensity measurements but it is not inconsistent with the highest level of theory and largest basis set calculation result shown in Table 2 and which is  $301 \text{ cm}^{-1}$  according to the CCSD/cc-pVTZ calculations.

## Conclusions

The conformational energies of 3CPOL were studied using several different levels of ab initio and density functional theory calculations. The calculated potential surface calculated by Al-Saadi [2] is consistent with the experimental data shown in this work. Conformer **A** with the intramolecular hydrogen bonding between the hydroxyl hydrogen and the  $\pi$ -electron density of the C=C double bond is of lowest energy.



CCSD/cc-pVTZ calculations define the energies of the four conformers in the order **A** < **B** < **C** ~ **D**, with the planar structure being  $631\text{ cm}^{-1}$  higher in energy than **A** with its hydrogen bonding.

The infrared and Raman spectral data recorded at four different temperatures agree remarkably well with the B3LYP/cc-pVTZ computed values for all four conformers. This is especially true for the frequency shifts between the conformers for the same vibrational modes. The O-H stretching band for conformer **A** with the weak intramolecular  $\pi$ -type hydrogen bond was observed at  $3623.4\text{ cm}^{-1}$  whereas the conformers without hydrogen bonding have higher frequency bands at  $3655.4$  (**B**),  $3659$  (**C**), and  $3637.6$  (**D**)  $\text{cm}^{-1}$ . The wavenumber difference between conformers **A** and **B** implies that the O-H stretching force constant is reduced by about 2% due to the hydrogen bonding. The C=C stretching frequencies for **A** and **B** are  $1607.3$  and  $1620.7\text{ cm}^{-1}$ , respectively, implying that this stretching force constant is reduced by about 2% due to the hydrogen bonds. Thus the effects on the O-H and C=C bonds are not great. Nonetheless, the intramolecular hydrogen bonding is large enough to give conformer **A** sufficiently lower energy to make it the dominant species.

## CHAPTER VI

INTRAMOLECULAR  $\pi$ -TYPE HYDROGEN BONDING OF  
OTHER CYCLIC ALCOHOLS AND AMINES**Introduction**

The purpose of this work has been to find evidence of the unusual intramolecular  $\pi$ -type hydrogen bonding in several other cyclic alcohols and amines, in addition to 3-cyclopenten-1-ol (3CPOL) previously studied. Potential energy functions have been determined for all the molecules shown in Fig. 16, based on MP2/cc-pVTZ computations. The relative energy of the molecules conformers and the value of the conformational interconversion barriers have been determined. Moreover, infrared and Raman spectra have been recorded for 2-cyclohexen-1-ol (VI), and the laser-induced fluorescence spectrum (LIF) of 2-hydroxytetralin (VII) is presented. The calculations have been carried out using *ab initio* (MP2/cc-pVTZ) and density functional theory (B3LYP/cc-pVTZ) computations.

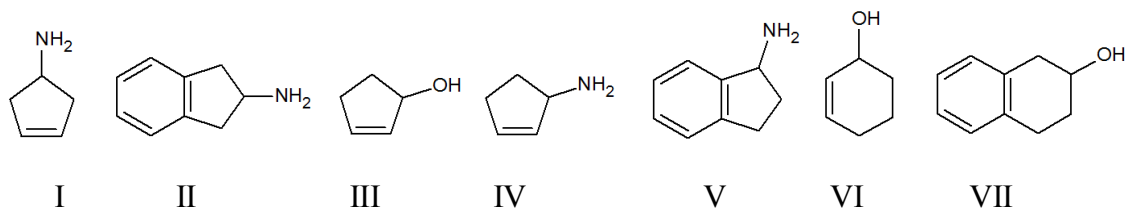


**Fig. 16.** Cyclic alcohols and amines with intramolecular  $\pi$ -type hydrogen bonding.

Previous theoretical and experimental studies have been carried out for 2-aminoindan (II), 2-cyclopenten-1-ol (III) and 1-aminoindan (V) by other researchers [76-79]. However, not all the predicted conformers were distinguished.

### 3-Cyclopenten-1-amine

3-Cyclopenten-1-amine (I) is analogous in structure to 3CPOL discussed previously but the -OH group has been replaced by -NH<sub>2</sub>. Fig. 17 shows the conformers of 3-cyclopenten-1-amine determined from MP2/cc-pVTZ computations labeled in increasing order of their relative energy. Conformer **A** possesses an intramolecular  $\pi$ -type hydrogen bonding illustrated by dotted lines.

The top part of Fig. 17 shows the interconversion of the conformers **A** and **B** by the internal rotation of the -NH<sub>2</sub> group where the five-membered ring of the molecule is puckered "up". Fig. 18 illustrates graphically how the potential energy changes during this process, and shows the calculated internal rotation energy barriers (cm<sup>-1</sup>). The two conformations of **A** shown are mirror images of one another. The bottom part of Fig. 17 shows the interconversion of the conformers **C** and **D** by the internal rotation of the -NH<sub>2</sub> group where the five-membered ring of the molecule is puckered "down". Fig. 19 presents the potential energy function for this process. The illustrated conformations **C** are also mirror images of one another. Conformers **A** and **C** are also mirror images of one another. Conformers **A** and **C** can interconvert through the ring puckering motion. **A** has the ring puckered "up" and **C** has the ring puckered "down". The calculated interconversion barrier is 661 cm<sup>-1</sup> as shown in Fig. 17.

**B** and **D** can also interconvert one to another by puckering motion with a calculated barrier of  $581\text{ cm}^{-1}$ .

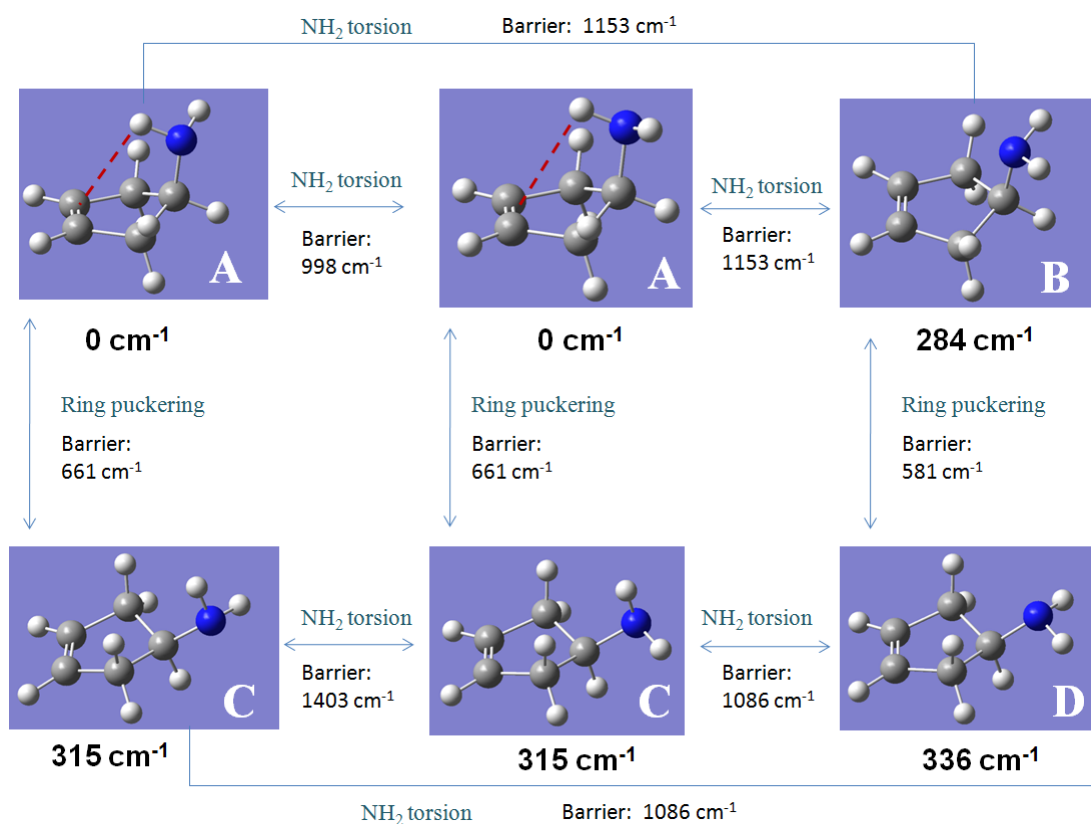


**Fig. 17.** Conformers of 3-cyclopenten-1-amine. MP2/cc-pVTZ calculated energies.

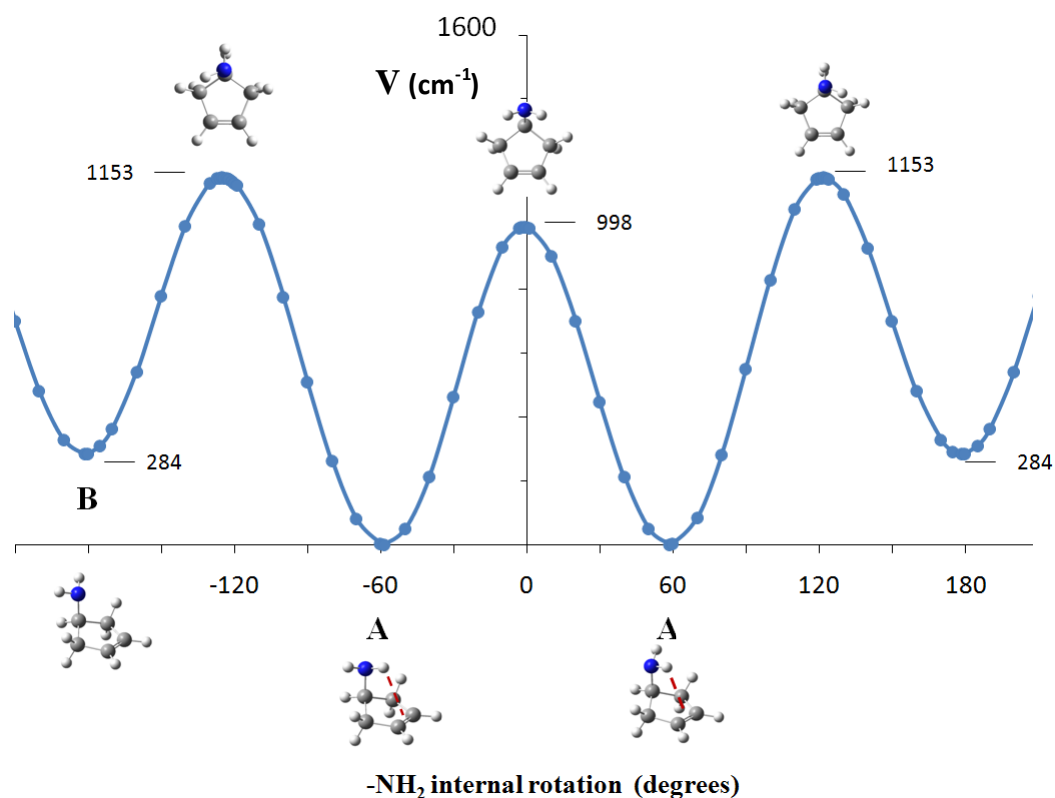


**Fig. 18.** Internal rotation potential energy function of 3-cyclopenten-1-amine with the ring puckered "up". MP2/cc-pVTZ calculated energies.

Table 6 shows the calculated energy, relative abundance, structural parameters and vibrational frequencies of 3-cyclopenten-1-amine. The two N-H bond lengths of Conformer **A** are different since only one of the hydrogens is participating in the hydrogen bonding with the C=C double bond. Table 6 shows that the conformer with the lowest vibrational frequency of the C=C stretch is **A** and the calculated distance of the hydrogen involved in the  $\pi$ -type hydrogen bonding -NH<sub>2</sub> group to the center of the C=C bond is 2.8 Å.

The presence of an intramolecular  $\pi$ -type hydrogen bond in conformer **A** is evidenced by the different lengths of the two N-H bonds that belong to a same -NH<sub>2</sub> group, the relative weakness of the C=C bond reflected by the lower frequency of the C=C vibration, the relative nearness of the amine hydrogen to the double bond, and the relative low energy of this conformer.

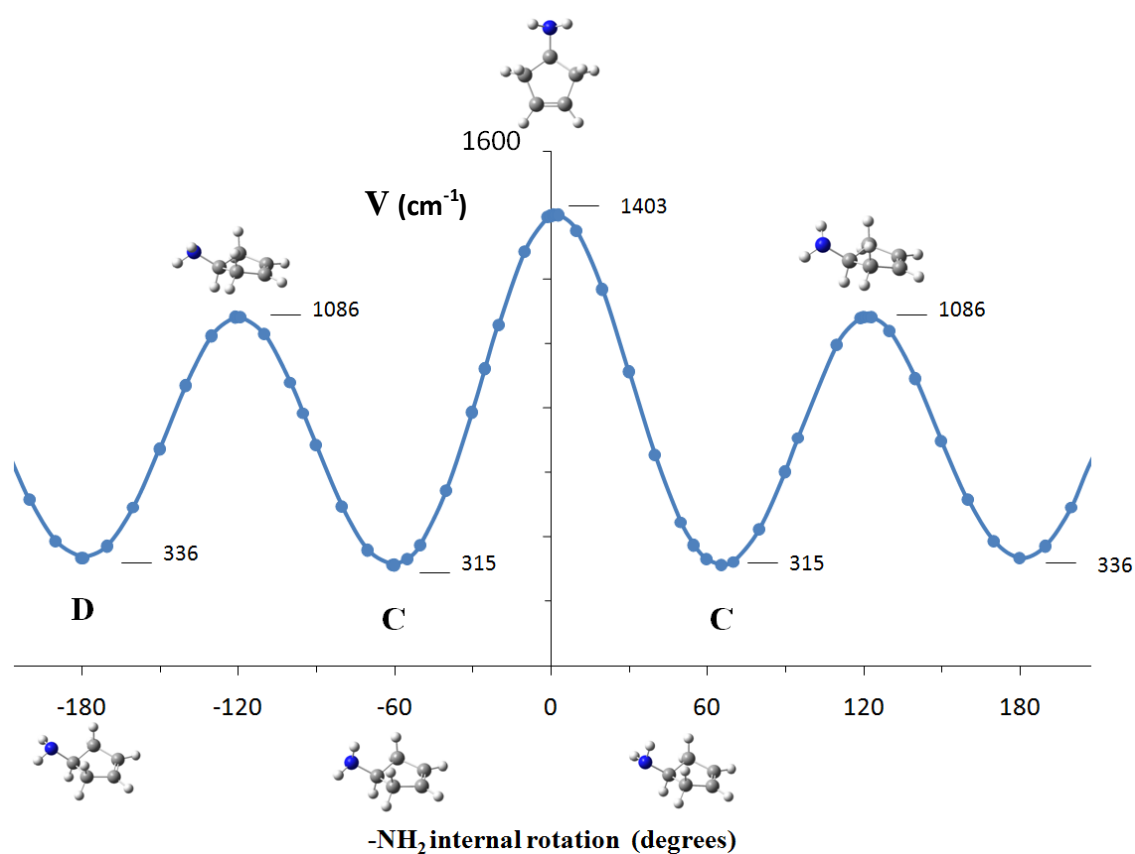


**Fig. 19.** Internal rotation potential energy function of 3-cyclopenten-1-amine with the ring puckered "down". MP2/cc-pVTZ calculated energies.

**Table 6**

Calculated potential energy, relative abundance, structural parameters and vibrational frequencies of 3-cyclopenten-1-amine.

	A	B	C	D
Energy (cm <sup>-1</sup> ) <sup>a</sup>	0	284	315	336
Relative abundance (%)	69	9	15	7
Population factor	2	1	2	1
<b>Angles (degrees)<sup>a</sup></b>				
Puckering angle	28.7	23.0	-29.3	-28.5
-NH <sub>2</sub> torsion angle	58.7 (-58.7, 58.7)	-181.3	63.1 (-63.1, 63.1)	-179.1
<b>Distances (Å)<sup>a</sup></b>				
Puckering coordinate	0.140	0.112	-0.143	-0.139
R(C=C)	1.339	1.336	1.340	1.339
R(N-H <sub>1</sub> )	1.014	1.014	1.013	1.014
R(N-H <sub>2</sub> )	1.016	1.014	1.014	1.014
R(NH <sub>1</sub> ...C=C)	2.773	3.750	4.217	4.168
R(NH <sub>2</sub> ...C=C)	3.715	3.750	3.793	4.168
<b>Vibrational frequencies (cm<sup>-1</sup>)<sup>b</sup></b>				
N-H antisymmetric stretch	3409	3412	3417	3412
N-H symmetric stretch	3333	3339	3339	3341
C=C stretch	1610	1622	1611	1616

<sup>a</sup> MP2/cc-pVTZ calculation.

<sup>b</sup> B3LYP/cc-pVTZ calculation.

## 2-Aminoindan

2-Aminoindan (II) is analogous in structure to 3-cyclopenten-1-amine but the benzene ring has been attached to the five-membered ring molecule. Fig. 20 shows the conformers of 2-aminoindan determined from MP2/cc-pVTZ computations. **A** is the conformer calculated to have the lowest energy and it possesses an intramolecular  $\pi$ -type hydrogen bonding. In 2007 Iga et al. [76] carried out MP2/6-311+G(d,p) and B3LYP/cc-pVTZ calculations to study 2-aminoindan and determined the same structures **A**, **B**, **C** and **D**. Their laser-induced fluorescence excitation results proved the existence of the conformers **A**, **B** and **C**, which are the conformers of lowest energy of this molecule.

The top part of Fig. 20 shows the interconversion of the conformers **A** and **D** by the internal rotation of the  $-\text{NH}_2$  group where the five-membered ring of the molecule is puckered "up". The two illustrated conformations of **A** are mirror images of one another. Similarly, the bottom part of Fig. 20 shows the interconversion of the conformers **B** and **C** by the internal rotation of the  $-\text{NH}_2$  group where the five-membered ring of the molecule is puckered "down". The two conformations of **B** shown are also mirror images of one another.



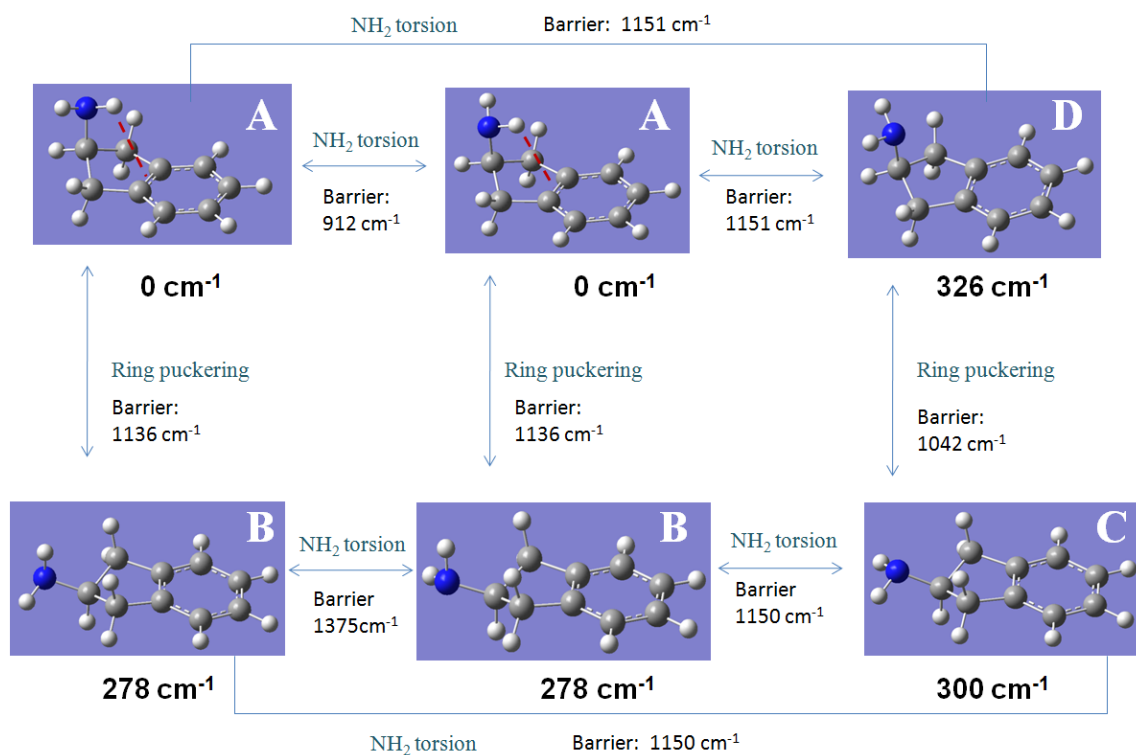


**Fig. 20.** Conformers of 2-aminoindan. MP2/cc-pVTZ calculated energies.

Fig. 21 shows the calculated energy surface of 2-aminoindan in terms of the puckering coordinate and the -NH<sub>2</sub> internal rotation. The calculated potential surface provides insight into the energetics of the conformational process. The values of the calculated energy barriers ( $\text{cm}^{-1}$ ) for the interconversion of the conformers are indicated on both Figs. 20 and 21.

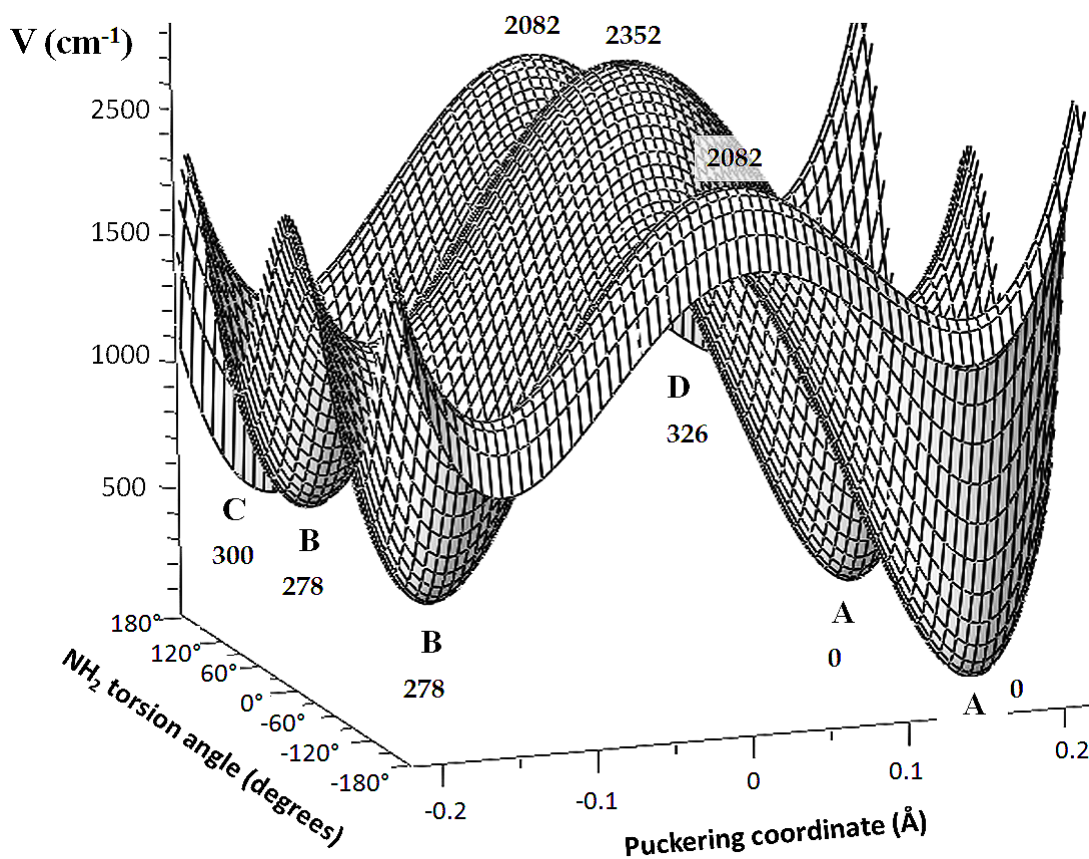


**Fig. 21.** Two-dimensional potential energy surface of 2-aminoindan in terms of the puckering coordinate and the  $\text{-NH}_2$  torsion angle. MP2/cc-pVTZ calculated energies.

Conformers **A** and **B** can interconvert by the ring puckering motion. **A** has the five-membered ring puckered "up" and **B** has the five-membered ring puckered "down". The calculated MP2/cc-pVTZ interconversion barrier is  $1136 \text{ cm}^{-1}$  as shown in Fig. 20. **D** and **C** can interconvert one to another by the puckering motion and the calculated barrier is  $1042 \text{ cm}^{-1}$ .

Fig. 22 illustrates graphically how the potential energy changes during the interconversion between conformers **A** and **B** through puckering motion. The MP2/cc-pVTZ calculations estimate an energy difference of  $278\text{ cm}^{-1}$  between conformers **A** and **B** and a puckering barrier of  $1136\text{ cm}^{-1}$ . Fig. 22 shows that the transition structure located along the ring-puckering pathway between conformers **A** and **B** is not completely planar (approximately  $1\text{ cm}^{-1}$  higher in energy than the planar structure), and is slightly puckered towards the direction of the **B** conformer. This suggests that the molecule retains some of the weak interaction between an amine hydrogen and the C=C double bond at the planar geometry and thereby slightly lowers the energy. In addition, for conformer **A** the puckering angle was calculated to be about  $0.6^\circ$  greater than that for conformer **B**. Nonetheless, this difference is not big, it indicates that the intramolecular hydrogen bonding in **A** causes an increase in the puckering angle so that the  $-\text{NH}_2$  group can move closer to the C=C double bond.

Table 7 shows the calculated energy, relative abundance, structural parameters and vibrational frequencies of 2-aminoindan. Conformer **A** has different N-H bond lengths for the  $-\text{NH}_2$  group with one bond being longer than the other due to the interaction with the C=C double bond. The calculated distance of the hydrogen involved in the  $\pi$ -type hydrogen bonding  $-\text{NH}_2$  group to the center of the C=C bond is  $2.8\text{ \AA}$ . Table 7 also shows that conformer **A** has the lowest frequency of vibration for the C=C stretching. The presence of an intramolecular  $\pi$ -type hydrogen bond in conformer **A** is evidenced by the different lengths of the two N-H bonds that belong to a same  $-\text{NH}_2$  group, the relative weakness of the C=C bond reflected by the lower frequency of the

C=C vibration, the relative nearness of the amine hydrogen to the double bond, and the relative low energy of this conformer.

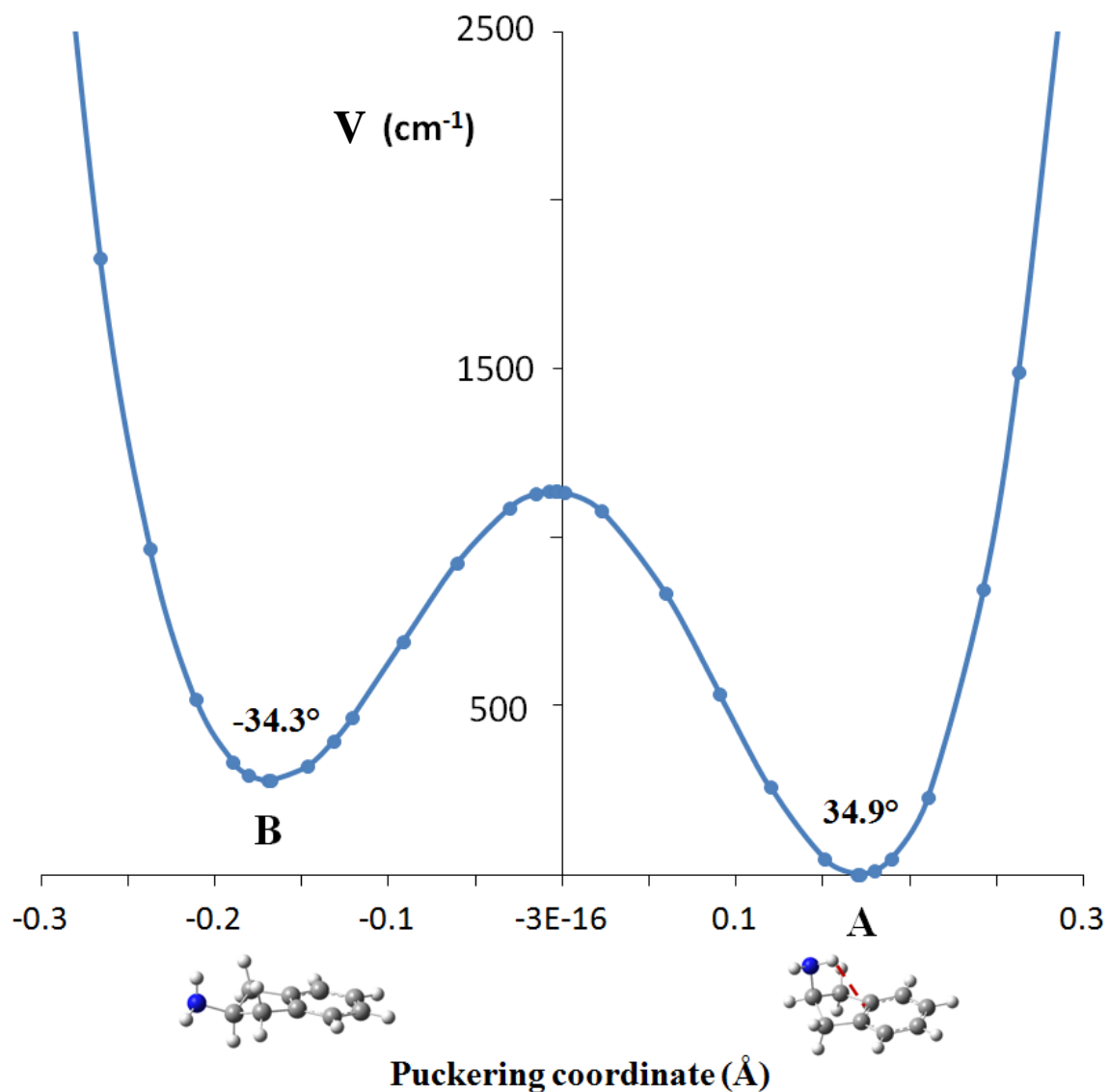


**Fig. 22.** Ring-puckering potential energy function for the interconversion of the conformers A and B of 2-aminoindan. MP2/cc-pVTZ calculated energies.

**Table 7**

Calculated potential energy, relative abundance, structural parameters and vibrational frequencies of 2-aminoindan.

	A	B	C	D
Energy (cm <sup>-1</sup> ) <sup>a</sup>	0	278	300	326
Relative abundance (%)	67	18	8	7
Population factor	2	2	1	1
Angles (degrees) <sup>a</sup>				
Puckering angle	34.9	-34.3	-34.4	30.9
NH <sub>2</sub> torsion angle	58.2	63.4	-179.6	-182.1
	(-58.2, 58.2)	(-63.4, 63.4)		
Distances (Å) <sup>a</sup>				
Puckering coordinate	0.171	-0.168	-0.168	0.151
R(C=C)	1.400	1.401	1.400	1.397
R(N-H <sub>1</sub> )	1.014	1.013	1.014	1.014
R(N-H <sub>2</sub> )	1.016	1.014	1.014	1.014
R(NH <sub>1</sub> ...C=C)	3.628	3.828	4.173	3.642
R(NH <sub>2</sub> ...C=C)	2.654	4.219	4.173	3.642
R(NH <sub>1</sub> ...C <sub>2</sub> )	3.551	3.882	4.363	3.858
R(NH <sub>2</sub> ...C <sub>2</sub> )	2.774	3.361	4.096	3.552
Vibrational frequencies (cm <sup>-1</sup> ) <sup>b</sup>				
N-H antisymmetric stretc	3412	3419	3413	3420
N-H symmetric stretch	3335	3341	3343	3345
C=C stretch	1561	1562	1563	1565

<sup>a</sup> MP2/cc-pVTZ calculation.

<sup>b</sup> B3LYP/cc-pVTZ calculation.

## 2-Cyclopenten-1-ol

2-Cyclopenten-1-ol (III) has its -OH group attached to the carbon adjacent to the C=C bond of a five-membered ring. This molecule has been studied previously by Bakke et al. in 1986 [78] using NMR and infrared spectroscopy in dilute solution. They proposed the existence of the conformers **A** and **B** (Fig. 23) with a shift of  $19\text{ cm}^{-1}$  of the O-H stretching frequency. Fig. 23 shows the six conformers of 2-cyclopenten-1-ol determined by MP2/cc-pVTZ computations. **A** and **B** are the conformers with the lowest calculated energy and both possess an intramolecular  $\pi$ -type hydrogen bonding.

The top part of Fig. 23 shows the interconversion of the conformers **A**, **C** and **F** by the internal rotation of the -OH group where the five-membered ring of the molecule is puckered "down". Fig. 24 illustrates graphically how the potential energy changes during this process, and shows the calculated internal rotation energy barriers ( $\text{cm}^{-1}$ ). The bottom row of Fig. 23. shows the interconversion of the conformers **B**, **E** and **D** by the internal rotation of the -OH group where the five-membered ring of the molecule is puckered "up". Fig. 25 shows the potential energy function for this process.

Conformers **A** and **B** can interconvert by the ring puckering motion. **A** has the ring puckered "down" and **B** has the ring puckered "up". The calculated MP2/cc-pVTZ interconversion barrier is  $281\text{ cm}^{-1}$ , as shown in Fig. 23. Similarly, **C** and **E** can interconvert by the puckering motion with a calculated barrier of  $622\text{ cm}^{-1}$ , and **F** and **D** can interconvert one to another by puckering motion with a calculated barrier of  $674\text{ cm}^{-1}$ .

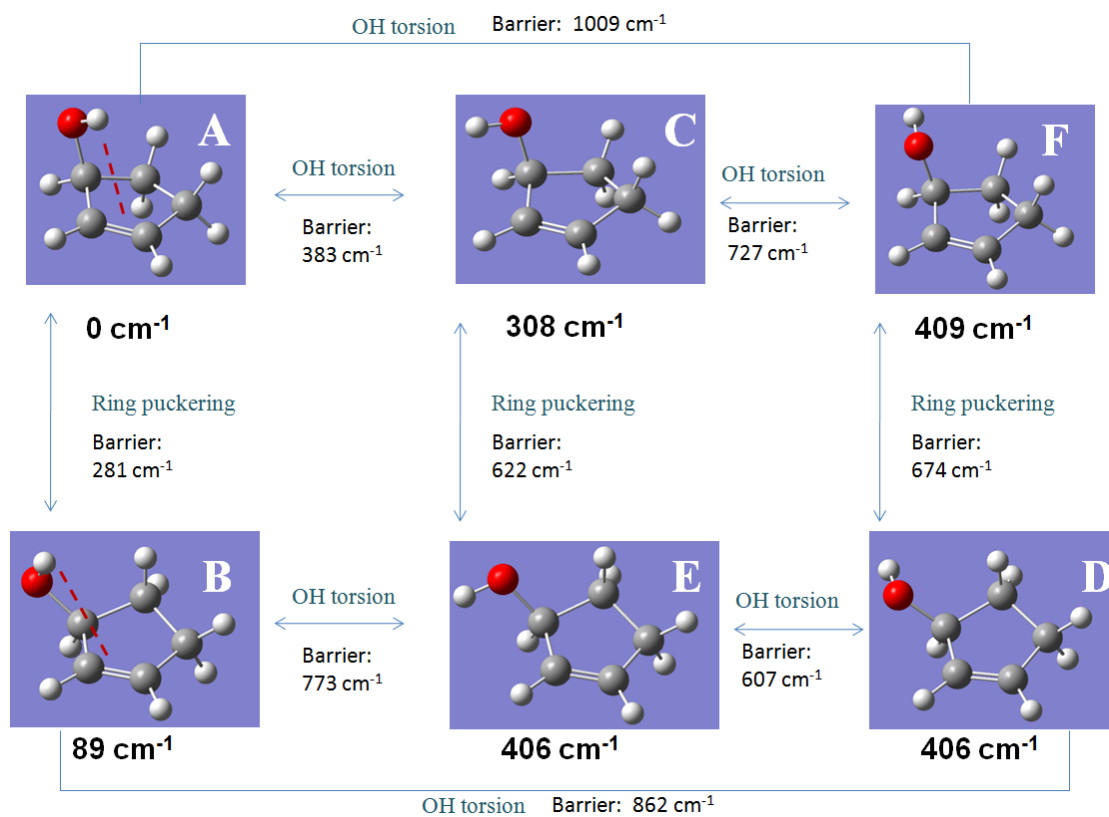


**Fig. 23.** Conformers of 2-cyclopenten-1-ol. MP2/cc-pVTZ calculated energies.

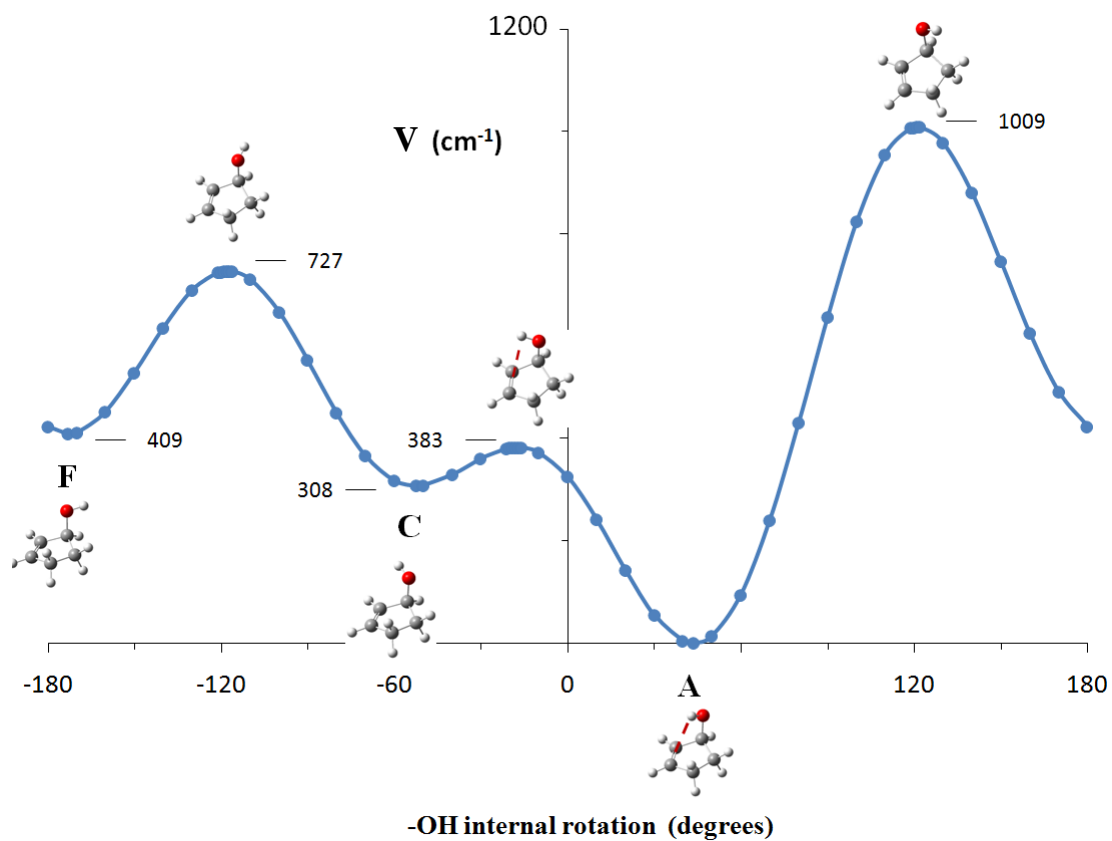


**Fig. 24.** Internal rotation potential energy function of 2-cyclopenten-1-ol with the ring puckered "down". MP2/cc-pVTZ calculated energies.



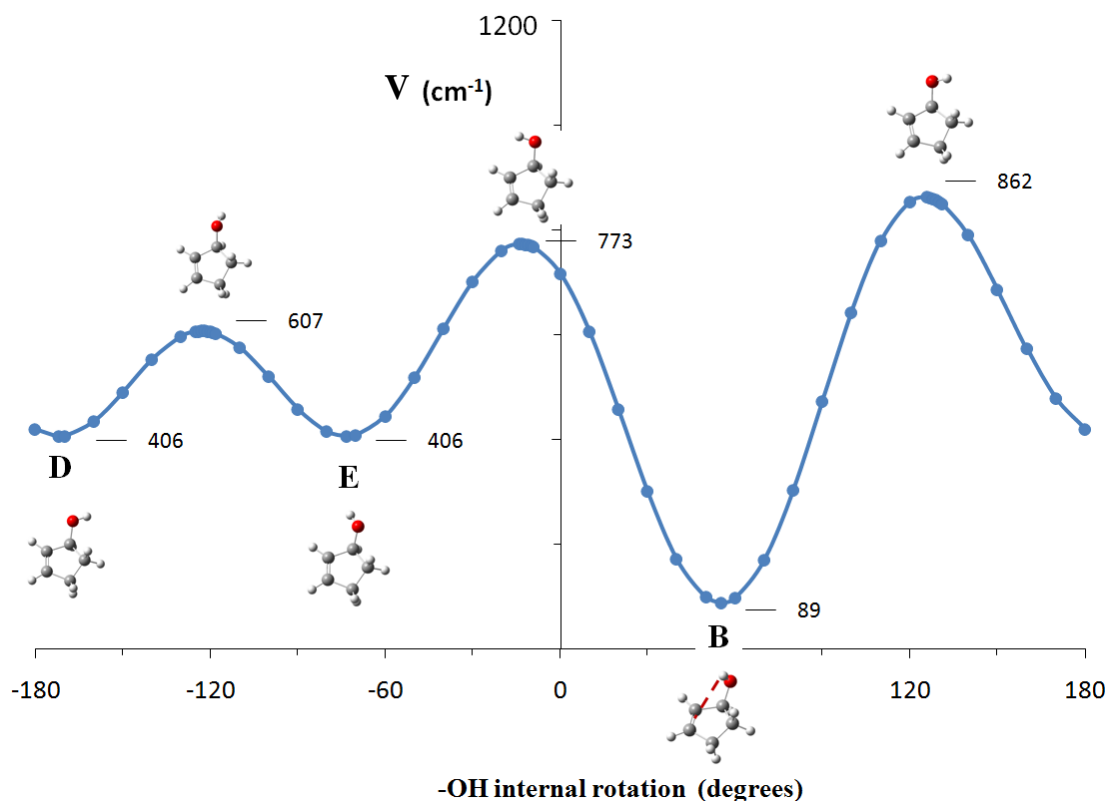


**Fig. 25.** Internal rotation potential energy function of 2-cyclopenten-1-ol with the ring puckered "up". MP2/cc-pVTZ calculated energies.

Table 8 shows the calculated energy, relative abundance, structural parameters and vibrational frequencies of 2-cyclopenten-1-ol. This table shows that the conformer with the longest C=C bond is conformer **A**. The calculated distance of the hydrogen involved in the  $\pi$ -type hydrogen bonding -OH group to the center of the C=C bond is  $1.3 \text{ \AA}$ . Table 8 shows that the conformers with lowest frequency of vibration of the C=C stretch are **A** and **B**.

The presence of an intramolecular  $\pi$ -type hydrogen bond in conformers **A** and **B** of 2-cyclopenteno-1-ol is evidenced by the relative weakness of the C=C bond reflected by the lower frequency of the C=C vibration, the relative nearness of the hydroxyl hydrogen to the double bond, and the relative low energy of both of these conformers.

**Table 8**

Calculated potential energy, relative abundance, structural parameters and vibrational frequencies of 2-cyclopenten-1-ol.

	A	B	C	D	E	F
Energy (cm <sup>-1</sup> ) <sup>a</sup>	0	89	308	406	406	409
Relative abundance (%)	44	28	10	6	6	6
Angles (degrees) <sup>a</sup>						
Puckering angle	-23.7	24.4	-25.8	25.6	24.4	-25.3
-OH torsion angle	43.5	55.1	-52.3	-171.9	-73.4	172.9
Distances (Å) <sup>a</sup>						
Puckering coordinate	-0.114	0.118	-0.124	0.124	0.118	-0.122
R(C <sub>1</sub> =C <sub>2</sub> )	1.339	1.338	1.338	1.337	1.337	1.337
R(O-H)	0.963	0.963	0.962	0.962	0.962	0.963
R(OH....C <sub>1</sub> =C <sub>2</sub> )	2.631	2.997	2.972	3.678	3.337	3.534
Vibrational frequencies (cm <sup>-1</sup> ) <sup>b</sup>						
O-H stretch	3646	3641	3661	3670	3670	3663
C <sub>1</sub> =C <sub>2</sub> stretch	1608	1610	1613	1617	1615	1618

<sup>a</sup> MP2/cc-pVTZ calculation.

<sup>b</sup> B3LYP/cc-pVTZ calculation.

## 2-Cyclopenten-1-amine

2-Cyclopenten-1-amine (IV) is analogous in structure to 2-cyclopenten-1-ol but with the -OH group replaced by -NH<sub>2</sub>. Fig. 26 shows the six conformers of 2-cyclopenten-1-amine determined by MP2/cc-pVTZ computations. **A** is the calculated conformer with the lowest energy and possesses an intramolecular  $\pi$ -type hydrogen bonding. In this case, however, **B**, **C** and **D** also possess this type of bonding. All these conformers have a N-H bond directed towards the middle of the C=C bond of the ring.

The top part of Fig. 26 shows the interconversion of the conformers **A**, **B** and **F** by the internal rotation of the -NH<sub>2</sub> group where the five-membered ring of the molecule is puckered "up". Fig. 27 illustrates graphically how the potential energy changes during this process, and shows the calculated internal rotation energy barriers (cm<sup>-1</sup>). The bottom part of Fig. 26. shows the interconversion of the conformers **D**, **C** and **E** by the internal rotation of the -NH<sub>2</sub> group where the five-membered ring of the molecule is puckered "down". Fig. 28 presents the potential energy curve for this process .

Conformers **A** and **D** can interconvert by the ring puckering motion. **A** has the ring puckered "up" and **D** has the ring puckered "down". The calculated MP2/cc-pVTZ interconversion barrier is 280 cm<sup>-1</sup> as shown in Fig. 26. Similarly, **B** and **C** can interconvert by the puckering motion with a calculated 332 cm<sup>-1</sup> barrier, and finally **F** and **E** can interconvert one to another by puckering motion with a calculated barrier of 719 cm<sup>-1</sup>.

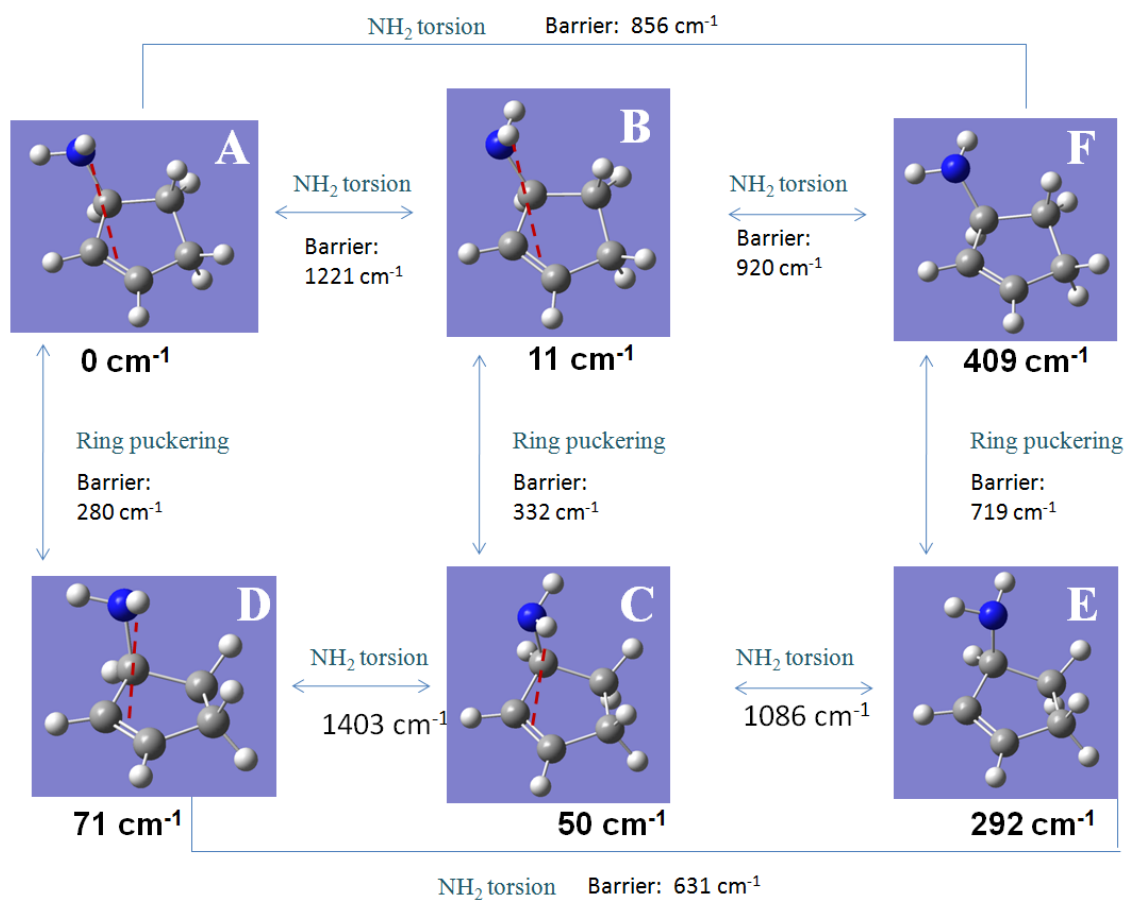


**Fig. 26.** Conformers of 2-cyclopenten-1-amine. MP2/cc-pVTZ calculated energies.

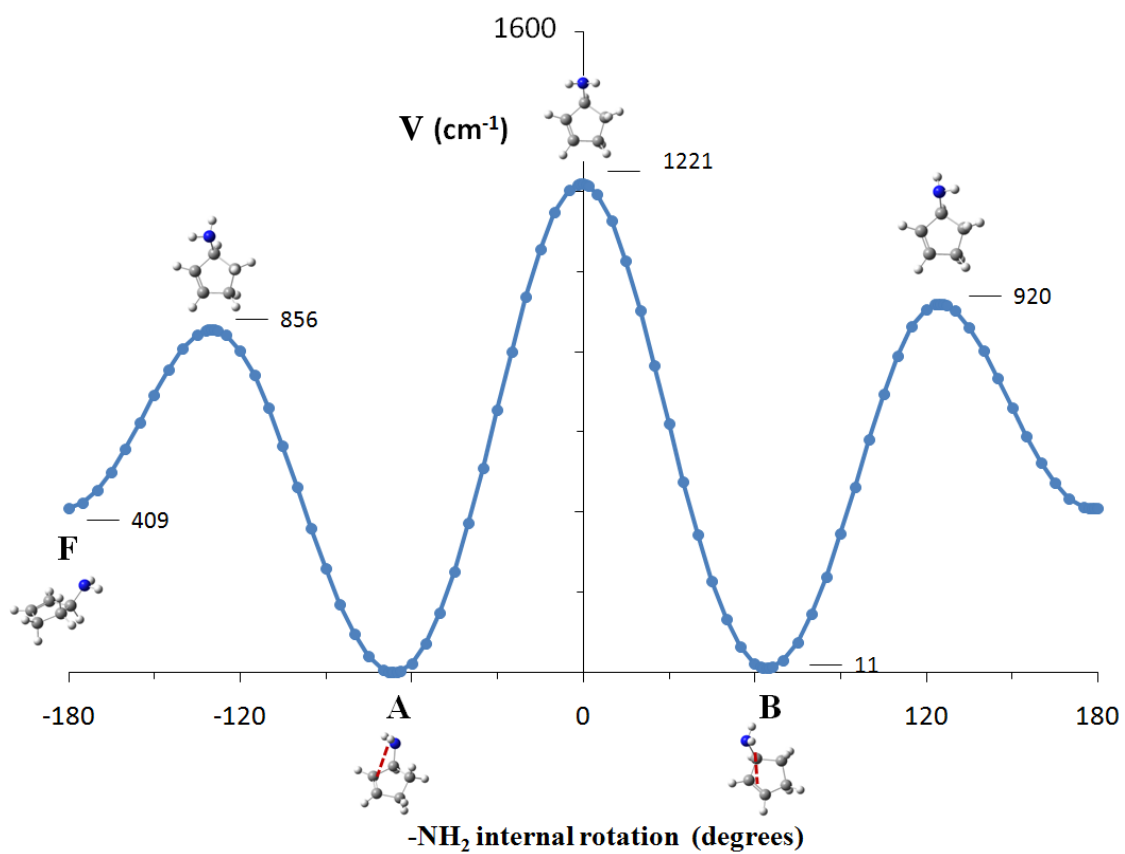


**Fig. 27.** Internal rotation potential energy function of 2-cyclopenten-1-amine with the ring puckered "up". MP2/cc-pVTZ calculated energies.

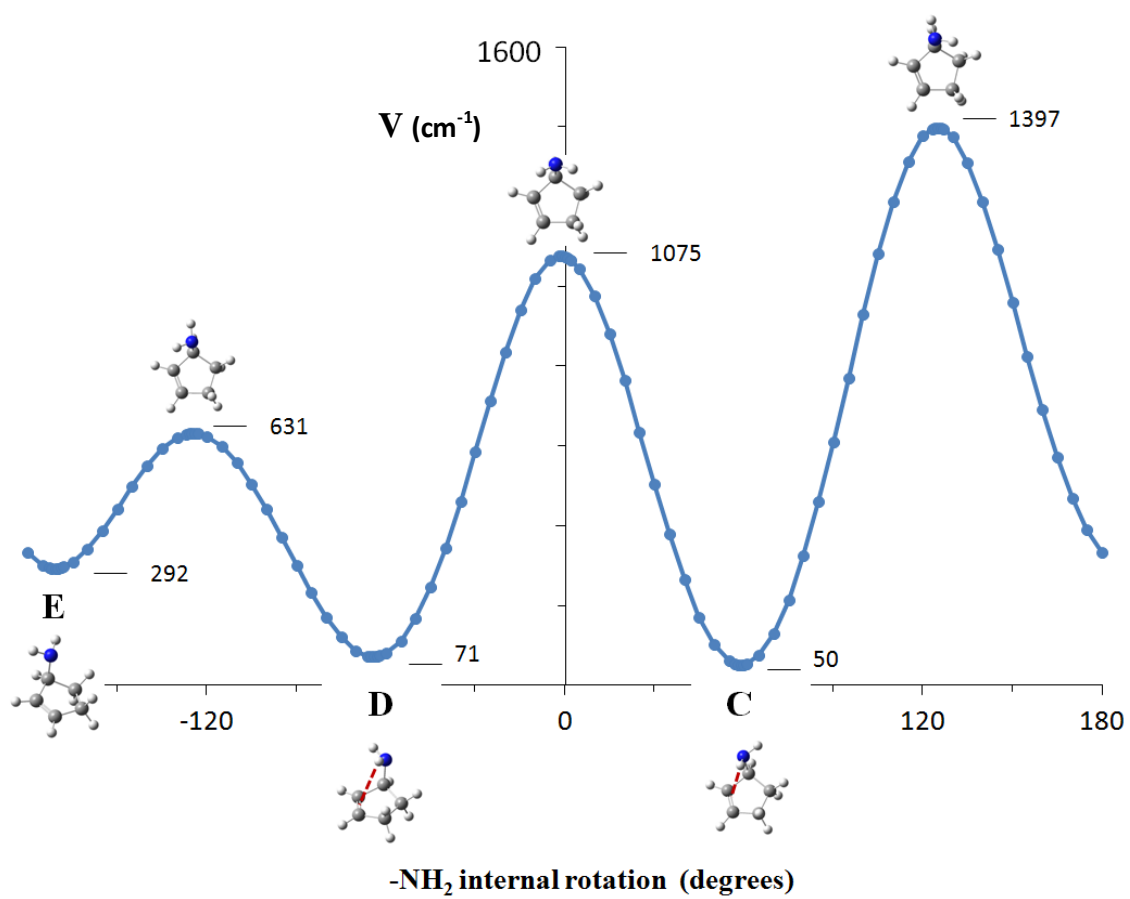


**Fig. 28.** Internal rotation potential energy function of 2-cyclopenten-1-amine with the ring puckered "down". MP2/cc-pVTZ calculated energies.

Table 9 shows the calculated energy, relative abundance, structural parameters and vibrational frequencies of 2-cyclopenten-1-amine. Conformers **A**, **B**, **D** and **E** have different N-H bond lengths in the -NH<sub>2</sub> group, one bond being larger than the other. Table 9 shows that the conformers with lowest frequency of vibration of the C=C stretching are **A**, **B** and **D**. Moreover, conformers **C** and **D** have the shortest calculated distance between a hydrogen of the -NH<sub>2</sub> group to the center of the C=C bond.

The presence of an intramolecular  $\pi$ -type hydrogen bonding in all the conformers of 2-cyclopenten-1-amine with the exception of the conformers **E** and **F** is evidenced by the different lengths of N-H bonds belonging to a same -NH<sub>2</sub> group of conformers **A**, **B**, **C** and **D**, the relative weakness of the C=C bond reflected by the lower frequency of the C=C vibration of conformers **A**, **B** and **D**, the relative nearness of the amine hydrogen to the double bond in conformers **C** and **D**, and the relative low energy of conformers **A**, **B**, **C** and **D**. The conformers **E** and **F** do not have the N-H adequately directed towards the C=C bond as to facilitate the formation of an intramolecular  $\pi$ -type hydrogen bond. If there is any intramolecular  $\pi$ -type hydrogen bonding in the conformer **E**, which has a tiny difference between the N-H bond lengths in the -NH<sub>2</sub> group, it would be very weak.

**Table 9**

Calculated potential energy, relative abundance, structural parameters and vibrational frequencies of 2-cyclopenten-1-amine.

	A	B	C	D	E	F
Energy (cm <sup>-1</sup> ) <sup>a</sup>	0	11	50	71	292	409
Relative abundance (%)	26	25	21	19	6	4
<b>Angles (degrees)<sup>a</sup></b>						
Puckering angle	24.9	26.2	-25.4	-24.0	-27.9	26.9
NH <sub>2</sub> torsion angle	-66.4	64.4	59.0	-64.1	-170.8	-181.4
Twisting angle	-1.1	-0.5	-2.9	-3.0	-1.9	0.5
<b>Distances (Å)<sup>a</sup></b>						
Puckering coordinate	0.120	0.127	-0.123	-0.116	-0.135	0.130
R(C=C)	1.338	1.338	1.338	1.339	1.338	1.337
R(N-H <sub>1</sub> )	1.013	1.014	1.014	1.015	1.015	1.014
R(N-H <sub>2</sub> )	1.015	1.013	1.014	1.016	1.014	1.014
R(NH <sub>1</sub> ....C=C)	3.424	3.110	2.755	3.223	3.636	3.773
R(NH <sub>2</sub> ....C=C)	3.088	3.792	3.632	2.780	3.028	3.339
<b>Vibrational frequencies (cm<sup>-1</sup>)<sup>b</sup></b>						
N-H antisymmetric stretch	3415	3419	3420	3407	3411	3408
N-H symmetric stretch	3336	3339	3339	3331	3336	3337
C=C stretch	1609	1613	1617	1611	1618	1618

<sup>a</sup> MP2/cc-pVTZ calculation.

<sup>b</sup> B3LYP/cc-pVTZ calculation.



## 1-Aminoindan

1-Aminoindan (**V**) is analogous in structure to 2-cyclopenten-1-amine but the benzene ring has been attached to the five-membered ring molecule. In 2005 Le Barbus et al. [78] carried out B3LYP/6-31G\*\* calculations and determined six conformers of 1-aminoindan. Their laser-induced excitation results proved the existence of the conformers **A** and **B** shown in Fig. 29, which are the conformers of lowest energy. In 2007 Isozaki et al. [79] determined the six structures using B3LYP/cc-pVTZ calculations and proved the existence of **A** and **B** by UV-UV hole burning spectroscopy. Fig. 29 shows the six conformers of 1-aminoindan determined by MP2/cc-pVTZ calculations. **A** is the calculated conformer with the lowest energy and possesses the intramolecular  $\pi$ -type hydrogen bonding. Conformers **B**, **C**, **D** and **E** also show evidence of possessing an intramolecular  $\pi$ -type hydrogen bonding.

The top part of Fig. 29 shows the interconversion of the conformers **A**, **B** and **F** by the internal rotation of the -NH<sub>2</sub> group where the five-membered ring of the molecule is puckered "up". Fig. 30 illustrates graphically how the potential energy changes during this process, and shows the internal rotation energy barriers (cm<sup>-1</sup>). The bottom part of Fig. 29 shows the interconversion of the conformers **E**, **D** and **C** by the internal rotation of the -NH<sub>2</sub> group where the five-membered ring of the molecule is puckered "down". Fig. 31 presents the potential function for this process.

Conformers **A** and **E** can interconvert by the ring puckering motion. **A** has the ring puckered "up" and **E** has the ring puckered "down". The calculated MP2/cc-pVTZ interconversion barrier is 881 cm<sup>-1</sup> as shown in Fig. 29. **B** and **D** can interconvert by the

puckering motion with a calculated barrier of  $899\text{ cm}^{-1}$ , and **F** and **C** can also interconvert by puckering motion with a calculated barrier of  $1266\text{ cm}^{-1}$ .

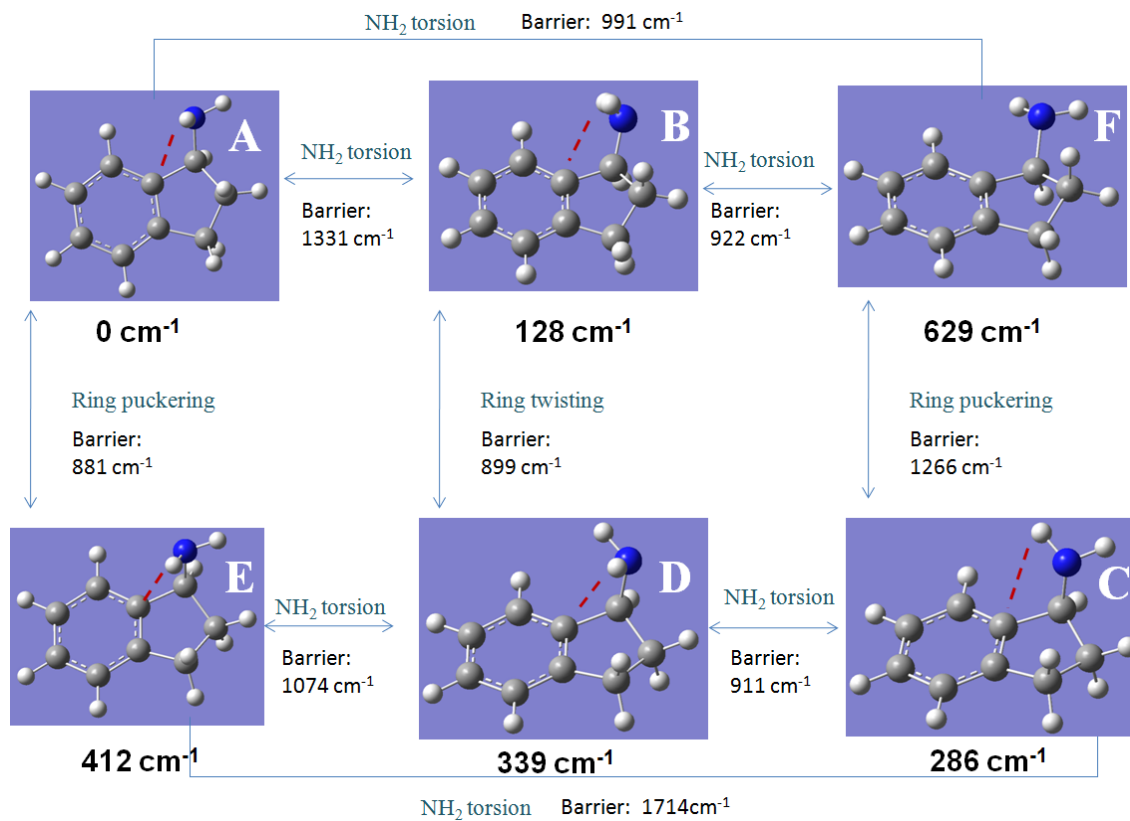


**Fig. 29.** Conformers of 1-aminoindan. MP2/cc-pVTZ calculated energies.

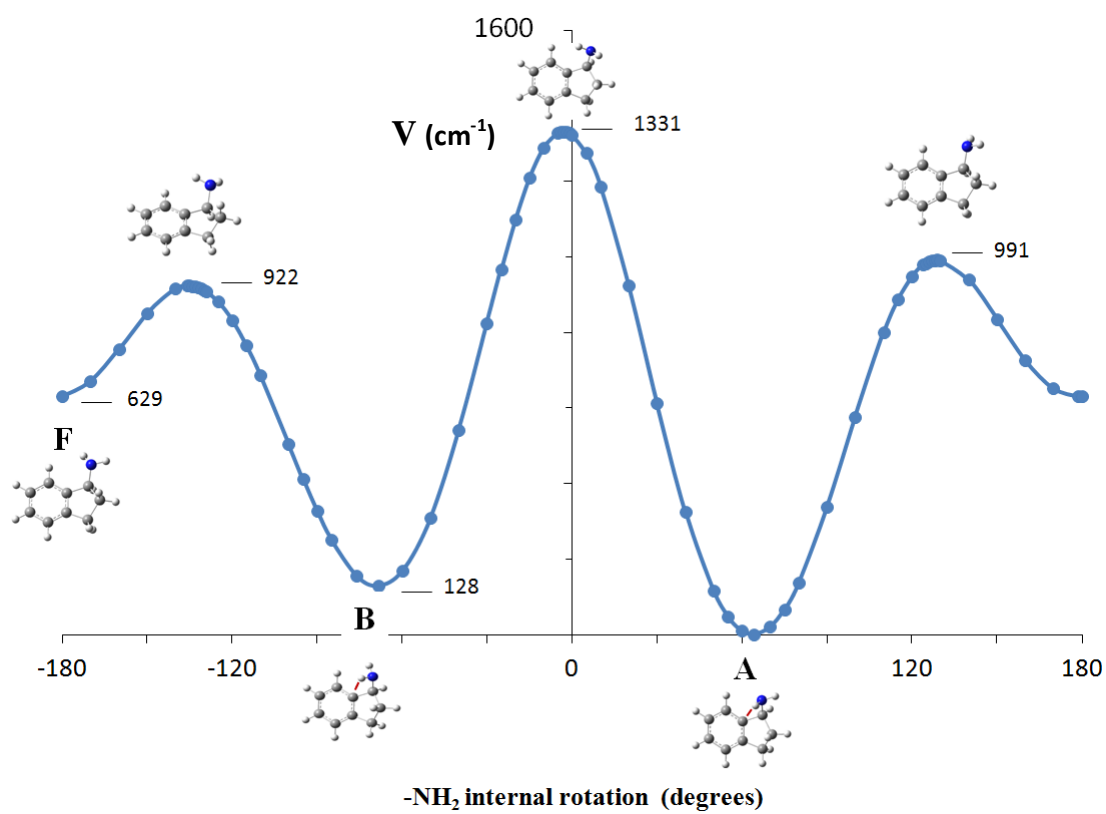


**Fig. 30.** Internal rotation potential energy function of 1-aminoindan with the five-membered ring puckered "up". MP2/cc-pVTZ calculated energies.

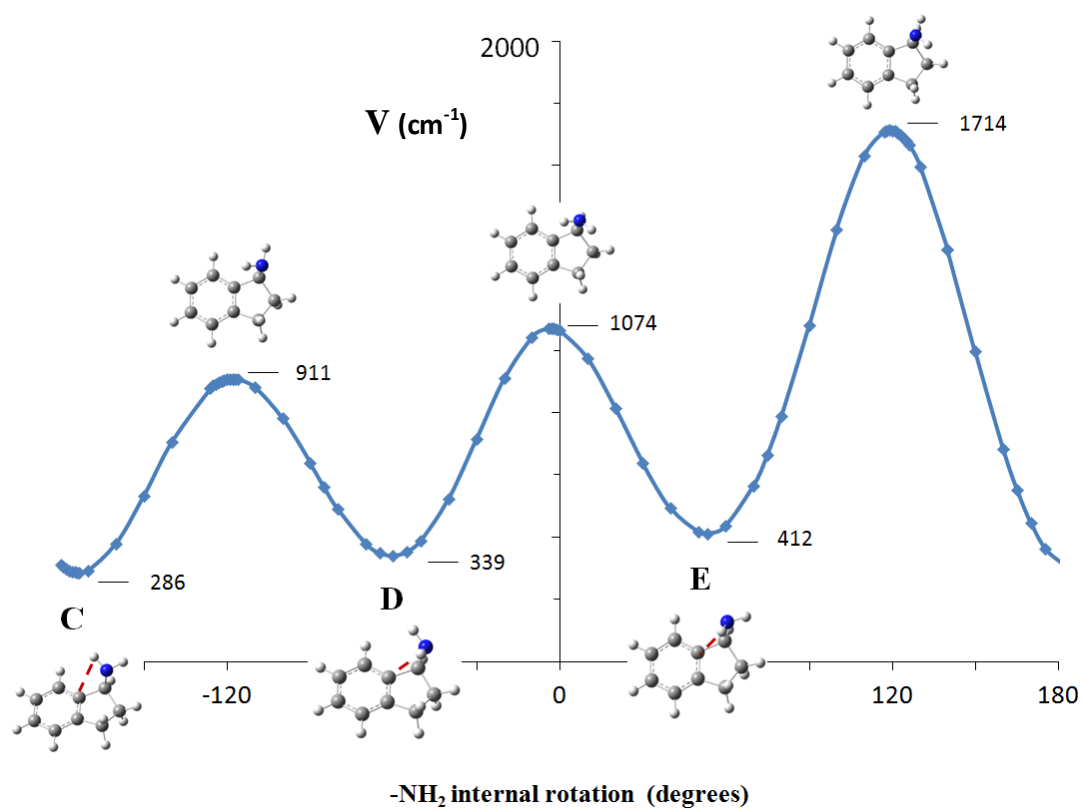


**Fig. 31.** Internal rotation potential energy function of 1-aminoindan with the five-membered ring puckered "down". MP2/cc-pVTZ calculated energies.

Table 10 shows the calculated energy, relative abundance, structural parameters and vibrational frequencies of 1-aminoindan. Conformers **A**, **B**, **D** and **F** have different N-H bond lengths in the -NH<sub>2</sub> group, one bond being larger than the other. Table 10 also shows that the conformers with lowest frequency of vibration of the C=C stretch are **B**, **D** and **E**. Conformers **A**, **B**, **C**, **D** and **E** have the shortest calculated distances between a hydrogen of the -NH<sub>2</sub> group to the closest carbon of the aromatic ring, which range from 2.6 to 2.8 Å.

The presence of an intramolecular  $\pi$ -type hydrogen bonding in 1-aminoindan with the exception of conformer **F**, is reflected by the different lengths of N-H bonds belonging to a same -NH<sub>2</sub> group of conformers **A**, **B**, and **D**, the relative weakness of the C=C bond reflected by the lower frequency of the C=C vibration of conformers **B** and **D**, the relative nearness of the amine hydrogen to the double bond in conformers **A**, **B**, **C**, **D** and **E**, and the relative low energy of conformers **A**, **B**, **C**, **D** and **E**. Conformer **F** does not have the N-H adequately directed towards the C=C bond to facilitate the formation of an intramolecular  $\pi$ -type hydrogen bond. If there is any intramolecular  $\pi$ -type hydrogen bonding in conformer **F**, which has a tiny difference between the N-H bond lengths in the -NH<sub>2</sub> group, is very weak.

**Table 10**

Calculated potential energy, relative abundance, structural parameters and vibrational frequencies of 1-aminoindan.

	A	B	C	D	E	F
Energy (cm <sup>-1</sup> ) <sup>a</sup>	0	128	286	339	412	629
Relative abundance (%)	46	25	12	9	6	2
<b>Angles (degrees)<sup>a</sup></b>						
Puckering angle	33.0	32.3	-33.5	-31.2	-31.2	33.4
-NH <sub>2</sub> torsion angle	64.0	-68.4	-173.4	-60.4	53.2	-182.5
Twisting angle	0.0	-0.2	-1.9	-2.8	-1.6	0.9
<b>Distances (Å)<sup>a</sup></b>						
Puckering coordinate	0.160	0.156	-0.163	-0.151	-0.151	0.162
R(C <sub>1</sub> =C <sub>2</sub> )	1.397	1.397	1.398	1.399	1.398	1.398
R(C <sub>2</sub> =C <sub>3</sub> )	1.390	1.390	1.390	1.392	1.391	1.390
R(N-H <sub>1</sub> )	1.014	1.013	1.014	1.015	1.014	1.015
R(N-H <sub>2</sub> )	1.013	1.015	1.014	1.016	1.014	1.014
R(NH <sub>1</sub> ....C <sub>1</sub> =C <sub>2</sub> )	3.160	3.481	3.610	3.174	2.711	3.798
R(NH <sub>2</sub> ....C <sub>1</sub> =C <sub>2</sub> )	3.818	3.152	3.015	2.762	3.610	3.382
R(NH <sub>1</sub> ....C <sub>2</sub> =C <sub>3</sub> )	2.853	2.879	3.700	2.846	2.922	3.648
R(NH <sub>2</sub> ....C <sub>2</sub> =C <sub>3</sub> )	3.614	2.852	2.733	3.066	3.697	2.737
R(NH <sub>1</sub> ....C <sub>2</sub> )	2.692	2.847	3.298	2.704	2.554	3.341
R(NH <sub>2</sub> ....C <sub>2</sub> )	3.338	2.687	2.582	2.675	3.298	2.736
<b>Vibrational frequencies (cm<sup>-1</sup>)<sup>b</sup></b>						
N-H antisymmetric stretch	3425	3426	3459	3407	3420	3413
N-H symmetric stretch	3344	3346	3381	3332	3339	3339
C=C stretch	1564	1563	1564	1562	1563	1564

<sup>a</sup> MP2/cc-pVTZ calculation.

<sup>b</sup> B3LYP/cc-pVTZ calculation.

## 2-Cyclohexen-1-ol

2-Cyclohexen-1-ol (VI) has the -OH group attached to the carbon one carbon away from the C=C bond of a six-membered ring. Fig. 32 shows the six conformers of 2-cyclohexen-1-ol determined by MP2/cc-pVTZ calculations. **A**, **B** and **C** are the calculated conformers with the lowest energy and possess  $\pi$ -type intramolecular hydrogen bonding.

The top part of Fig. 32 shows the interconversion of the conformers **A**, **C** and **D** by the internal rotation of the -OH group where the molecule has a "negative" twist angle between the C-C bond opposite to the C=C bond. Fig. 33 illustrates graphically how the potential energy changes during this process, and shows the calculated internal rotation barriers ( $\text{cm}^{-1}$ ). The bottom part of Fig. 32 shows the interconversion of the conformers **B**, **E** and **F** by the internal rotation of the -OH group where the molecule has a "positive" twist angle between the C-C bond opposite to the C=C bond. Fig. 34 presents the potential energy function for this process.

Conformers **A** and **B** can interconvert by ring twisting motion. **A** has a "negative" twist angle and **B** has a "positive" twist angle. The calculated MP2/cc-pVTZ interconversion barrier is  $4258 \text{ cm}^{-1}$  as shown in Fig. 32. **C** and **F** can interconvert by twisting motion with a calculated barrier of  $4499 \text{ cm}^{-1}$ , and **D** and **E** can interconvert one to another by twisting motion with a calculated barrier of  $4642 \text{ cm}^{-1}$ .

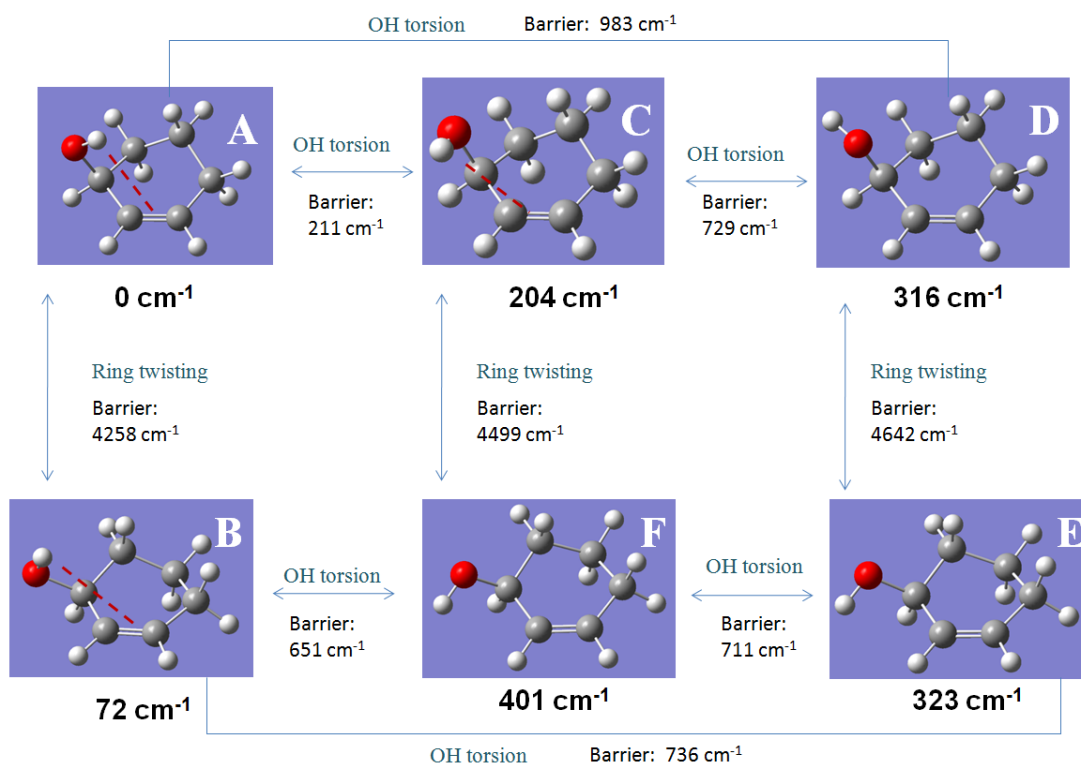


**Fig. 32.** Conformers of 2-cyclohexen-1-ol. MP2/cc-pVTZ calculated energies.



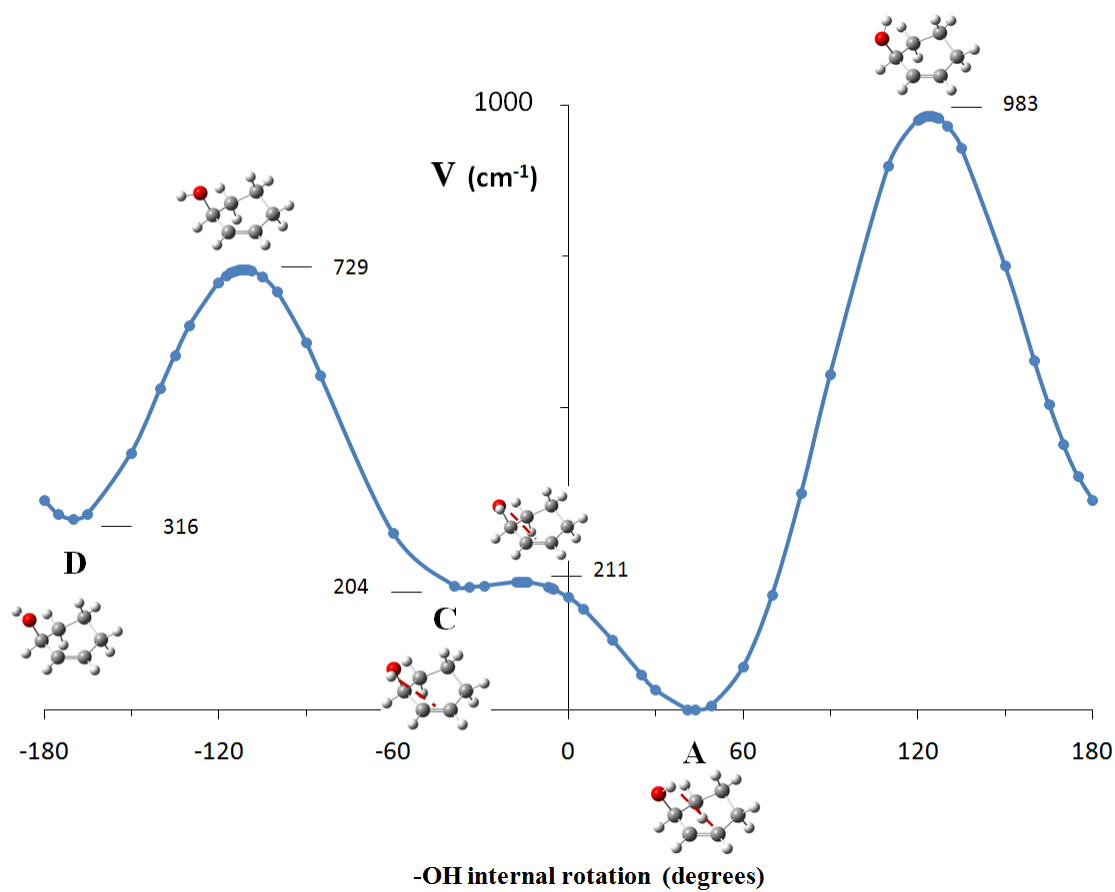


**Fig. 33.** Internal rotation potential energy function of 2-cyclohexen-1-ol with a "negative" twist angle. MP2/cc-pVTZ calculated energies.

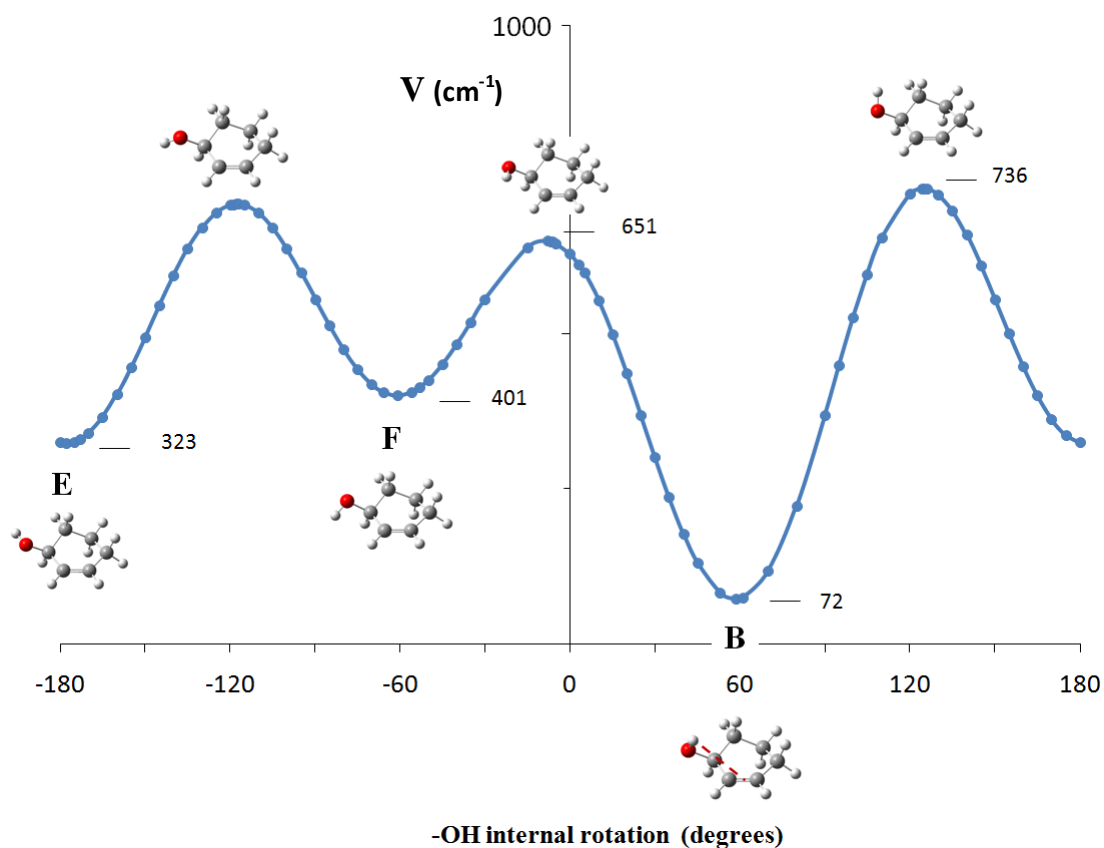


**Fig. 34.** Internal rotation potential energy function of 2-cyclohexen-1-ol with a "positive" twist angle. MP2/cc-pVTZ calculated energies.

Table 11 shows the calculated energy, relative abundance, structural parameters and vibrational frequencies of 2-cyclohexen-1-ol. This table indicates that the conformer with the longest C=C bond is conformer **A**. Table 11 also shows that the conformers with lowest frequency of vibration of the C=C stretch are **A**, **B** and **C**. The calculated distance of the hydrogen involved in the  $\pi$ -type hydrogen bonding -OH group of conformer **A** to the center of the C=C bond is 2.7 Å.

The evidence of the presence of an intramolecular  $\pi$ -type hydrogen bonding in conformers **A**, **B** and **C** of 2-cyclohexen-1-ol is reflected by the relative weakness of the C=C bond reflected by the lower frequency of the C=C vibration of conformers **A**, **B** and **C**, the relative nearness of the hydroxyl hydrogen to the double bond of conformer **A**, and the relative low energy of the conformers **A**, **B** and **C**.

**Table 11**

Calculated potential energy, relative abundance, structural parameters and vibrational frequencies of 2-cyclohexen-1-ol.

	A	B	C	D	E	F
Energy (cm <sup>-1</sup> ) <sup>a</sup>	0	72	204	316	323	401
Relative abundance (%)	38	27	14	8	8	5
Angles (degrees) <sup>a</sup>						
-OH torsion angle	43.6	58.4	-33.9	-169.9	-177.8	-60.8
Twisting angle	-29.8	31.6	-30.6	-31.5	31.0	31.0
Distances (Å) <sup>a</sup>						
R(C <sub>1</sub> =C <sub>2</sub> )	1.340	1.339	1.339	1.338	1.338	1.338
R(O-H)	0.963	0.963	0.962	0.963	0.963	0.962
R(OH...C <sub>1</sub> =C <sub>2</sub> )	2.737	3.015	2.906	3.651	3.725	3.227
Vibrational frequencies (cm <sup>-1</sup> ) <sup>b</sup>						
O-H stretch	3660	3644	3670	3655	3664	3665
C <sub>1</sub> =C <sub>2</sub> stretch	1638	1641	1642	1648	1651	1646

<sup>a</sup> MP2/cc-pVTZ calculation.

<sup>b</sup> B3LYP/cc-pVTZ calculation.

Fig. 35 illustrates the vapor-phase infrared spectrum 2-cyclohexen-1-ol and its vapor-phase Raman spectrum in the O-H stretching region. The vapor-phase infrared spectrum was collected at 100°C in a heating cell, and the vapor-phase Raman spectrum was obtained at 174°C in a vapor Raman cell. A relatively sharp peak is observed indicating the presence of an intramolecular hydrogen bonding, and other small peaks indicate the existence of other conformers to be identified in a future work.

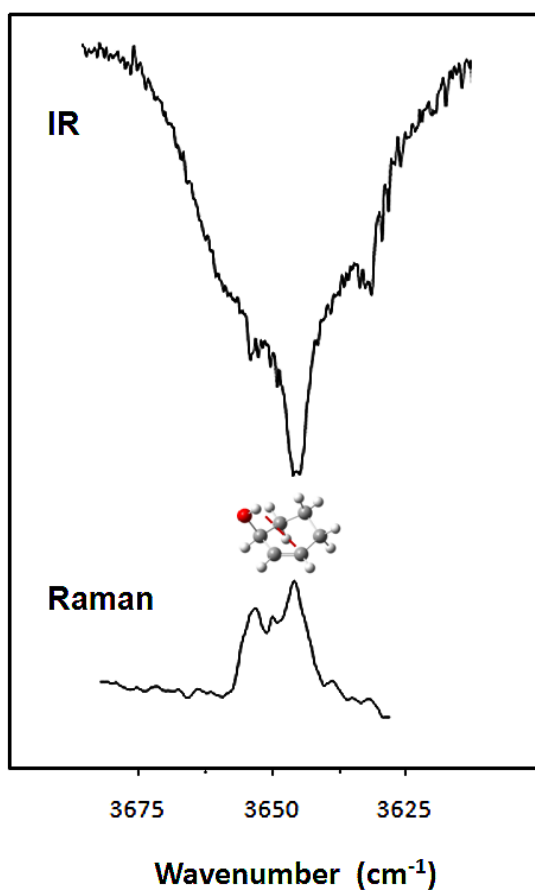


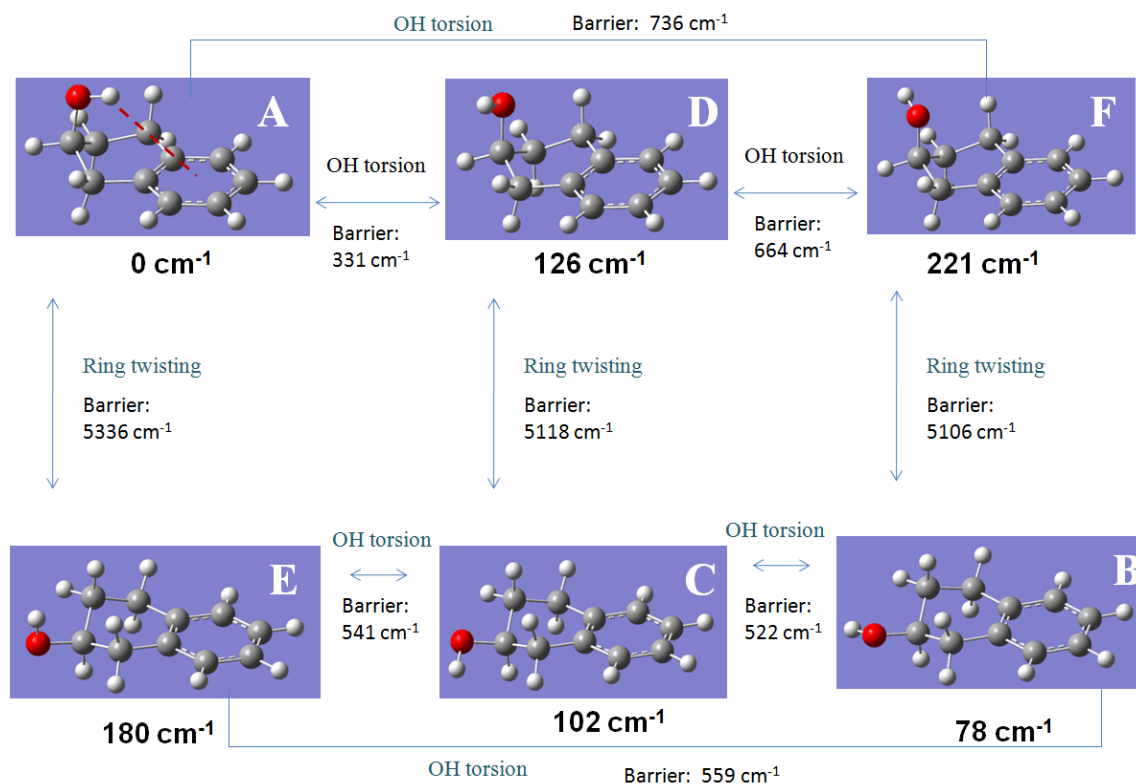
**Fig. 35.** Experimental infrared and Raman spectra of 2-cyclohexen-1-ol in the O-H stretching region.

## 2-Hydroxytetralin

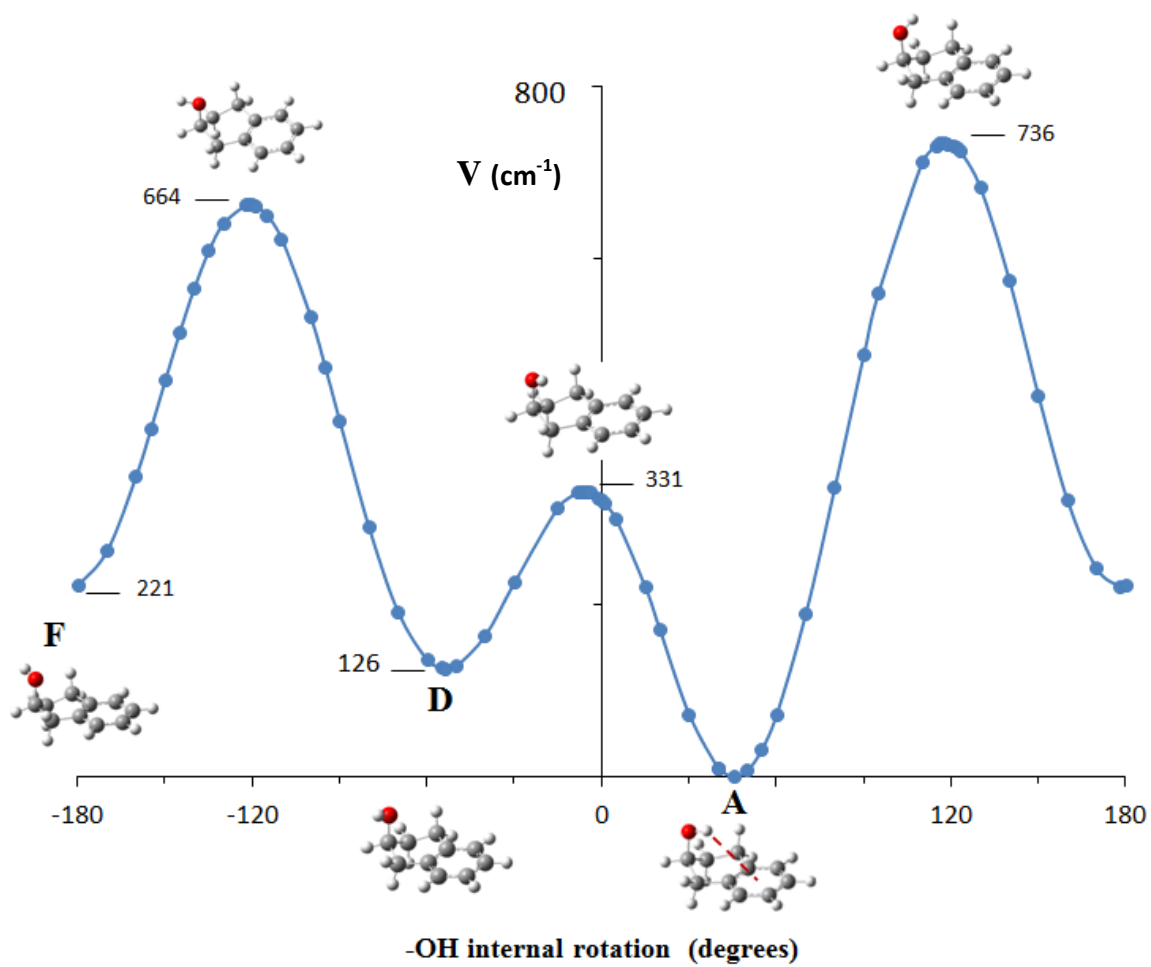
2-Hydroxytetralin (VII) has the -OH group attached to the carbon two carbons away from the C=C bond of a six-membered ring attached to a benzene ring. In 2010 Isozaki et al. [80] reported that they could only distinguish the existence of two conformers of 1-hydroxytetralin utilizing laser-induced fluorescence excitation spectra and of single vibronic level fluorescence. However, there are six calculated conformations of 1-hydroxytetralin according to B3LYP/aug-cc-pVTZ computations. This molecule is similar to 2-hydroxytetralin but with the -OH group attached to a carbon next to the C=C bond of a six-membered ring attached to a benzene ring.

Fig. 36 shows the six conformers of 2-hydroxytetralin determined by MP2/cc-pVTZ computations. Conformer **A** is the calculated conformer with the lowest energy and possesses an intramolecular  $\pi$ -type hydrogen bonding. The top part of Fig. 36 shows the interconversion of the conformers **A**, **D** and **F** by the internal rotation of the -OH group where the molecule has a "positive" twist angle between the C-C bond opposite to the C=C bond. Fig. 37 illustrates how the potential energy changes during this process, and shows the calculated energy barriers ( $\text{cm}^{-1}$ ). The bottom part of Fig. 36 shows the interconversion of the conformers **E**, **C** and **B** by the internal rotation of the -OH group where the molecule has a "negative" twist angle between the C-C bond opposite to the C=C bond. Fig. 38 presents the potential energy function for this process. Conformers **A** and **E** can interconvert by the ring twisting motion. **A** has "positive" twist angle and **E** has a "negative" twist angle. The calculated MP2/cc-pVTZ

interconversion barrier is  $5336\text{ cm}^{-1}$  as shown in Fig. 36. **D** and **C** can interconvert by twisting motion with a calculated barrier of  $5118\text{ cm}^{-1}$ , and **F** and **B** can interconvert one to another by twisting motion with a calculated barrier of  $5106\text{ cm}^{-1}$ .



**Fig. 36.** Conformers of 2-hydroxytetralin. MP2/cc-pVTZ calculated energies.



**Fig. 37.** Internal rotation potential energy function of 2-hydroxytetralin with a "positive" twist angle. MP2/cc-pVTZ calculated energies.

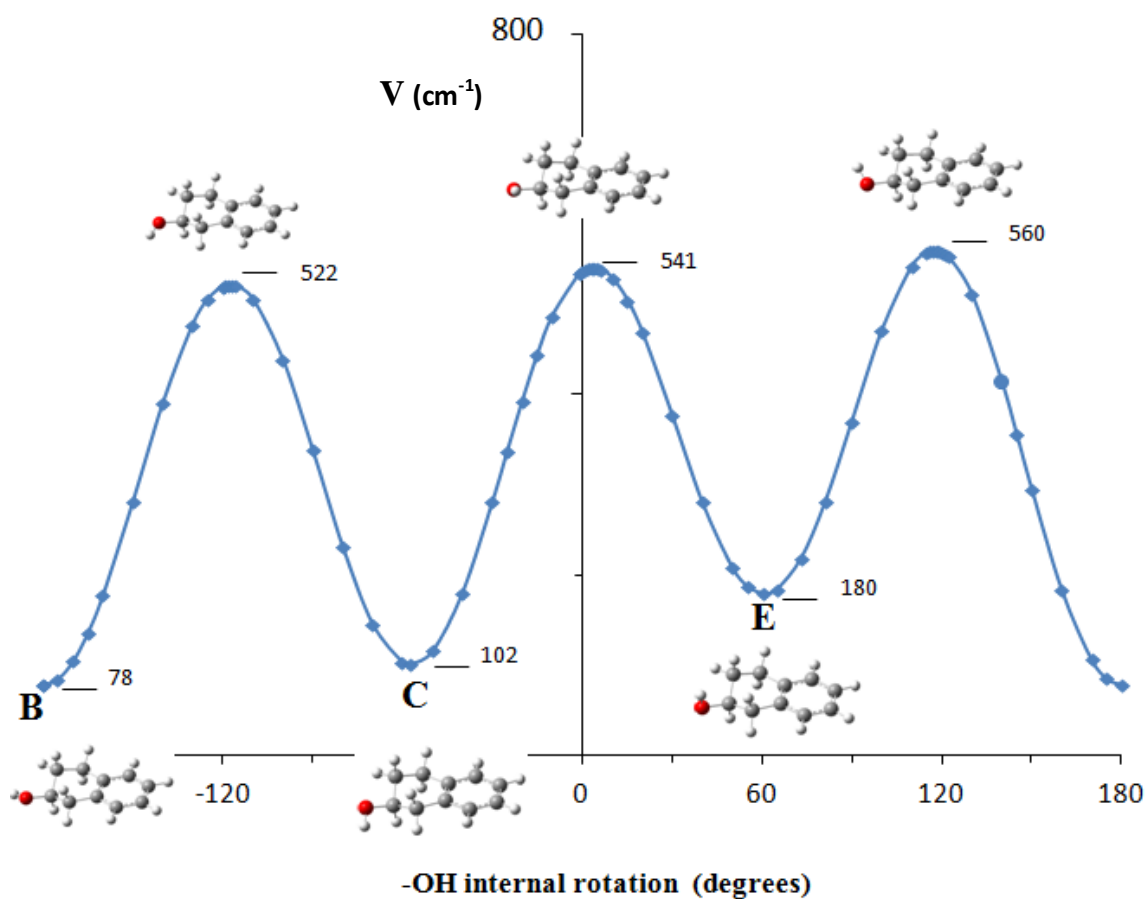


**Fig. 38.** Internal rotation potential energy function of 2-hydroxytetralin with a "negative" twist angle. MP2/cc-pVTZ calculated energies.

Table 12 shows the calculated energy, relative abundance, structural parameters and vibrational frequencies of 2-hydroxytetralin. This table shows that the conformer with the longest C=C bond is conformer **A**. Table 12 also shows that the conformers with lowest frequency of vibration of the C=C stretch are **A**, **B**, **C** and **E**. The calculated distance of the hydrogen involved in the  $\pi$ -type hydrogen bonding -OH group of conformer **A** to the center of the C=C bond is 2.6 Å. Conformers **B**, **C** and **E** although they have a relative low frequency of vibration of the C=C stretch, they do not have the



hydrogen of the hydroxyl group adequately directed towards the benzene ring. The presence of an intramolecular  $\pi$ -type hydrogen bonding in conformer **A** of 2-hydroxytetralin is evidenced by the relative weakness of the C=C bond reflected by the lower frequency of the C=C vibration, the relative nearness of the hydroxyl hydrogen to the double bond, and the relative low energy.

**Table 12**

Calculated potential energy, relative abundance, structural parameters and vibrational frequencies of 2-hydroxytetralin.

	A	B	C	D	E	F
Energy (cm <sup>-1</sup> ) <sup>a</sup>	0	78	102	126	180	221
Relative abundance (%)	28	19	17	15	12	10
Angles (degrees) <sup>a</sup>						
-OH torsion angle	45.3	-179.9	-57.2	-53.6	60.7	-181.8
Twisting angle	29.3	29.8	-29.9	28.7	-29.5	28.2
Distances (Å) <sup>a</sup>						
R(C <sub>1</sub> =C <sub>2</sub> )	1.404	1.402	1.402	1.402	1.402	1.401
R(O-H)	0.964	0.962	0.963	0.962	0.963	0.963
R(OH....C <sub>1</sub> =C <sub>2</sub> )	2.546	4.525	4.319	3.494	4.167	3.809
R(OH....C <sub>2</sub> )	2.585	4.430	4.013	3.323	3.949	3.878
Vibrational frequencies (cm <sup>-1</sup> ) <sup>b</sup>						
O-H stretch	3652	3663	3663	3670	3644	3644
C <sub>1</sub> =C <sub>2</sub> stretch	1556	1556	1556	1558	1556	1559

<sup>a</sup> MP2/cc-pVTZ calculation.

<sup>b</sup> B3LYP/cc-pVTZ calculation.

Fig. 39 shows the laser-induced fluorescence spectrum of 2-hydroxytetralin obtained by H-W. Shin in Laane's research group. This spectrum shows the co-existence of more than one conformer of 2-hydroxytetralin. Two pairs of peaks, most likely from overlapping pairs of band from conformers **C** and **D** and conformers **E** and **F** appear were observed.

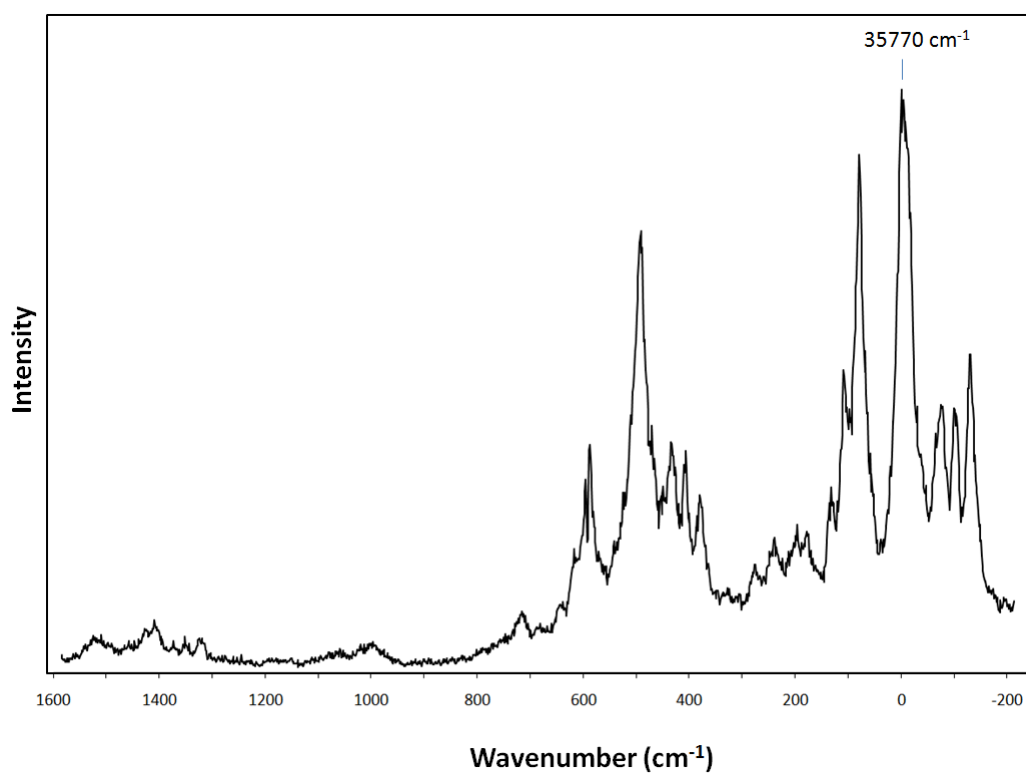


**Fig. 39.** Laser-induced fluorescence spectrum of 2-hydroxytetralin.

## Conclusions

The conformers with the lowest energy of the three cyclic alcohols 2-cyclopenten-1-ol, 2-cyclohexen-1-ol and 2-hydroxytetralin studied in this chapter,

are the ones with the strongest intramolecular  $\pi$ -type hydrogen bonding. The conformers of lowest energy of these molecules have the hydroxyl group directed towards the middle of the electron  $\pi$ -cloud and the ring puckers or twists to shorten the interaction.

2-Cyclopenten-1-ol has an hydroxyl group attached to the carbon next to the double bond C=C. It puckers "down" to get the -OH closer to the double bond increasing the strength of the intramolecular  $\pi$ -type hydrogen bonding. 2-Cyclohexen-1-ol and 2-hydroxytetralin are six-membered rings with an -OH group attached next to and two carbons away from the double bond C=C. These molecules twist to attain the highest stability with the formation of an intramolecular  $\pi$ -type hydrogen bonding.

The conformers of lowest energy for 3-cyclopenten-1-amine, 2-aminoindan, 2-cyclopenten-1-amine and 1-aminoindan, are not necessarily the ones with the strongest intramolecular  $\pi$ -type hydrogen bonding. This is because the amines have an -NH<sub>2</sub> group where while one N-H bond may be oriented to the double bond of the ring, the hydrogen of the other N-H bond could be undergoing repulsion due to steric strain increasing the total energy of the molecule.

As seen in the results for 2-cyclopenten-1-amine and 2-cyclohexenol, if the an -NH<sub>2</sub> group or an -OH group is attached to a carbon next to a double bond in a cyclic ring, more than one conformer with an intramolecular  $\pi$ -type hydrogen bonding can be expected.

## CHAPTER VII

## CYCLOPENTANE AND ITS DEUTERATED ISOTOPOMERS

**Introduction**

In many ways cyclopentane is a truly remarkable molecule, and its structure and vibrations are among the most unusual. The molecule has ten equivalent bent structures of  $C_s$  symmetry and ten equivalent twisted structures of  $C_2$  symmetry. Moreover, all experimental evidence indicates that the bent and twisted structures have very small energy differences thus resulting in twenty conformations with very nearly the same energy. Fig. 40 shows these conformations and how they can readily interconvert into one another. This process is known as pseudorotation and it was first proposed by Kilpatrick, Pitzer, and Spitzer [3] in 1947 to explain the unusual thermodynamic properties of this molecule. These workers showed that the out-of-plane ring vibrations of cyclopentane, which would be doubly degenerate of  $E_2''$  symmetry for a  $D_{5h}$  planar ring molecule, would be better represented by pseudorotational and radial motions. The pseudorotational phase angle would characterize the interconversion between the different conformations as shown in Fig. 40, and the radial coordinate would be a measure of out-of-plane motion of the carbon atoms. For one-dimensional free pseudorotation (without a barrier), which was postulated for cyclopentane, the transitions were predicted to be  $2B$  apart where  $B$  is the pseudorotational constant of magnitude less than  $3\text{ cm}^{-1}$ . The radial vibration was expected to be much higher in to

include substituted five-membered rings. frequency. In 1959 Pitzer and Donath [81] extended their theoretical model to include substituted five-membered rings.

In 1965 Lafferty and co-workers obtained the first spectroscopic evidence for pseudorotation by observing the far-infrared spectrum of tetrahydrofuran [82]. These workers postulated free pseudorotation with a pseudorotational constant of  $B = 3.2 \text{ cm}^{-1}$ .

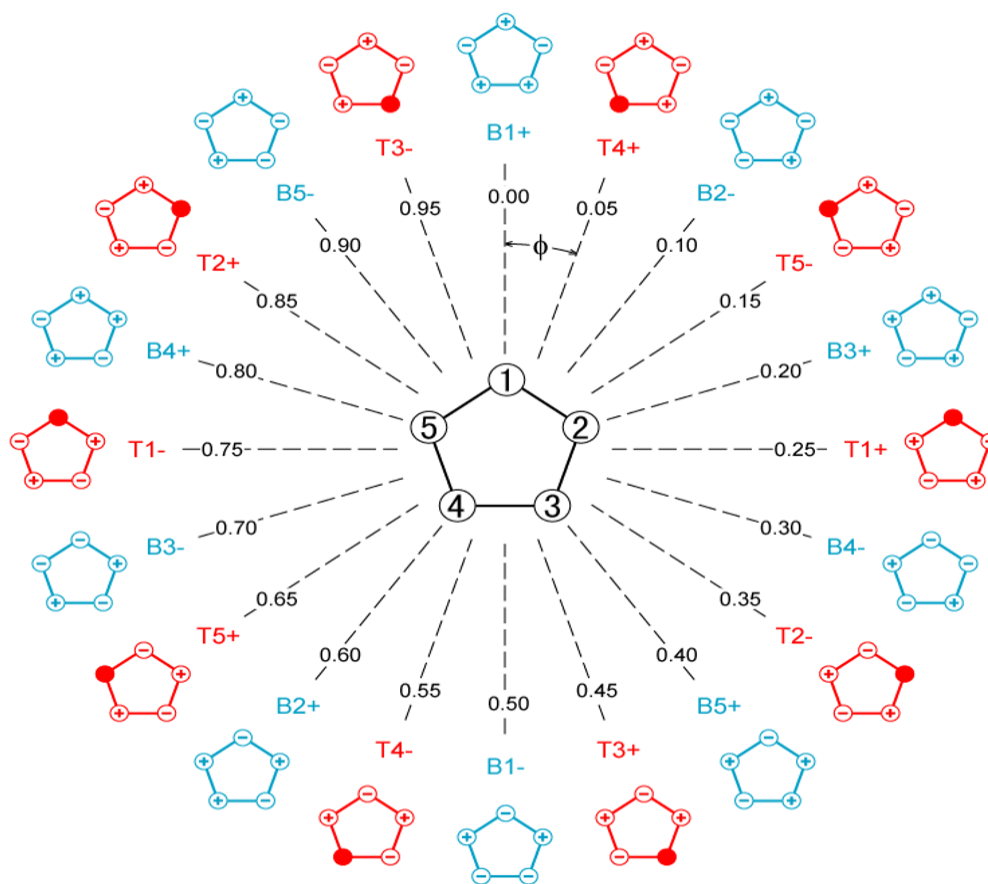


**Fig. 40.** Pseudorotational pathways for cyclopentane in terms of the phase angle  $\phi$  given as fractions of  $2\pi$  radians. B = bent and T = twist forms. The numbers identify the unique atoms and the + and - indicate opposite orientations.

Later work [83,84] showed the presence of small two-fold and four-fold barriers to pseudorotation, but the initial interpretation is understandable since all but the lowest levels are unperturbed by the barriers. 1,3-Dioxolone [84] is similar with nearly free pseudorotation. The pure pseudorotational spectrum for cyclopentane has not been observed, but infrared combination bands with a CH<sub>2</sub> deformation were reported in 1968 by Durig and Wertz [85] under low resolution. These were separated by approximately 5 cm<sup>-1</sup> and were analyzed assuming a pseudorotational constant of 2.54 cm<sup>-1</sup>. Three Q branches near 272 cm<sup>-1</sup> for the radial band were observed directly in the vapor-phase Raman spectrum by Carreira and co-workers [86] and these were used for a two-dimensional calculation to estimate a barrier to planarity of 1824 cm<sup>-1</sup>.

In addition to studies of cyclopentane, tetrahydrofuran, and 1,3-dioxolone, all of which have nearly free pseudorotation, the far-infrared spectra of a number of substituted five-membered rings were investigated and these showed significant barriers to pseudorotation. Among these were silacyclopentane [87], thiacyclopentane [88], selenacyclopentane [89], cyclopentanone [90], and germacyclopentane [91]. Each of these was analyzed using the computer programs which previously developed [92] for periodic potential functions containing cos(2φ) terms (φ = pseudorotational phase angle). Somewhat later, two-dimensional calculations were carried out for a number of molecules including silacyclopentane [93] cyclopentanone [94] and 1,3-oxathiolone [95]. Reviews published in 1972 and 1983 present more details of some of the earlier work [96,97].

In 1988 an extensive study of the pseudorotation of cyclopentane and four of its deuterated isotopomers was completed by Bauman in Laane's research group [98]. A much higher resolution spectrum of the combination bands was presented for the parent compound, and additional combination bands were reported for the deuterated species. Pseudorotational fine structure was also observed in the overtone region of the radial band for the different isotopomers, and Raman spectra of the radial band series were also recorded. All this data was utilized to calculate a two-dimensional potential energy surface with a barrier to planarity of  $1808 \text{ cm}^{-1}$ . There was insufficient data to determine the energy difference between bent and twisted conformations, but in earlier work Chao in Laane's research group [99] had shown that this had to be less than  $25 \text{ cm}^{-1}$  based on the spectroscopic data. Fig. 41 shows this two-dimensional surface previously calculated but with improved graphics. This surface assumes that the bent and twisted forms have the same energy. However, a tiny difference is anticipated and this would result in an energy function for the pseudorotation in terms of its phase angle  $\phi$  with ten-fold and twenty-fold terms:

$$V = \frac{1}{2} V_{10} [1 - \cos(10\phi)] + \frac{1}{2} V_{20} [1 - \cos(20\phi)] \quad (21)$$

This potential function is shown in Fig. 42 where the twist structure is taken to be slightly lower in energy. Based on available data [98] both  $V_{10}$  and  $V_{20}$  terms are expected to be less than about  $20 \text{ cm}^{-1}$ .

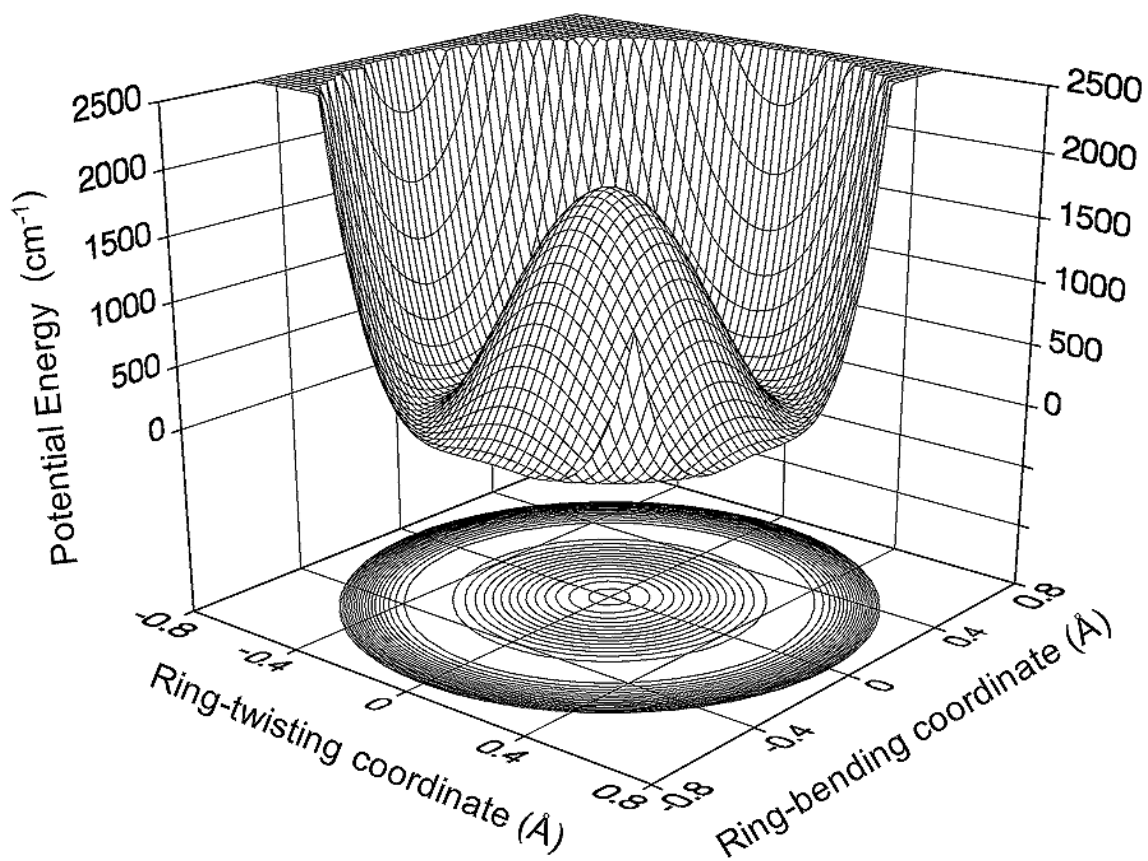


**Fig. 41.** Two-dimensional potential energy surface for the pseudorotation of cyclopentane in terms of ring-bending and ring-twisting coordinates.



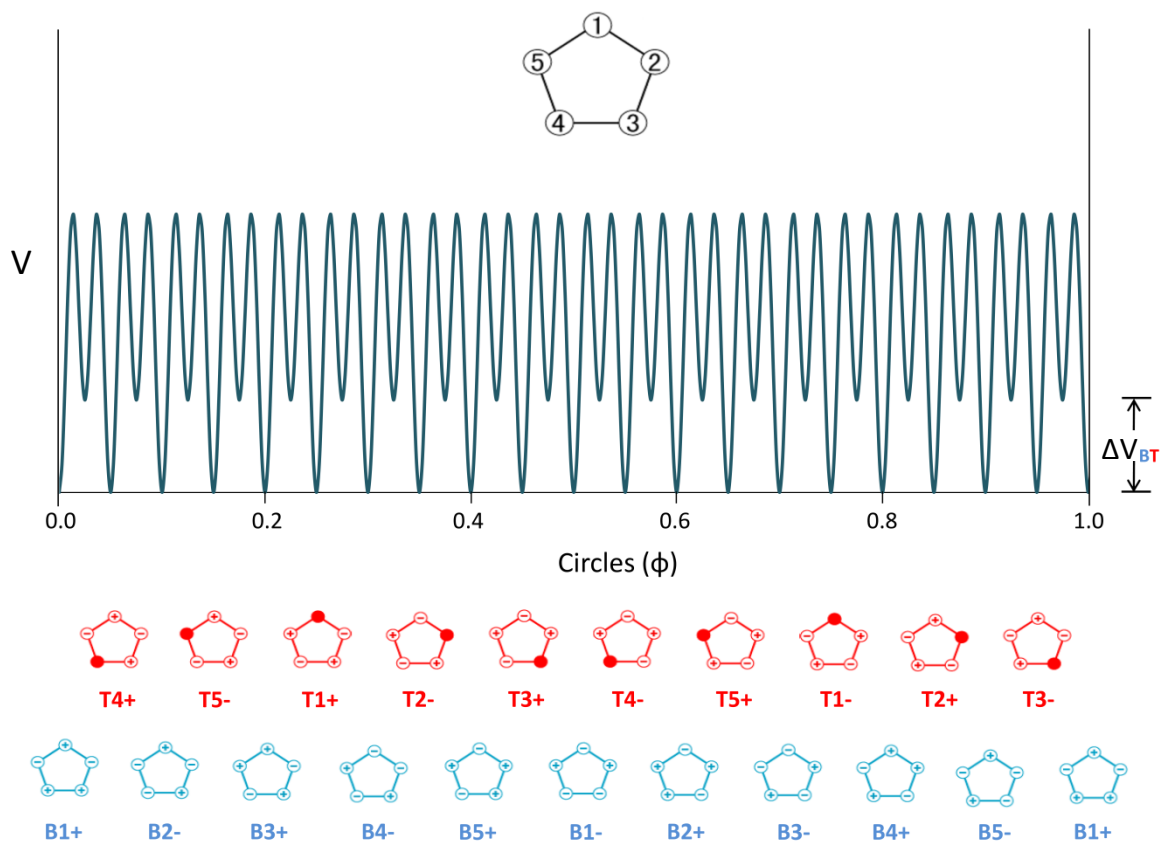


**Fig. 42.** One-dimensional potential energy function for Eq. (1) for the pseudorotation of cyclopentane in terms of the pseudorotational angle  $\phi$ . Magnitudes are arbitrary but  $\Delta V_{BT}$  is expected to be less than  $10 \text{ cm}^{-1}$ .

While carrying out the analysis of the pseudorotational and radial vibrations for all these isotopomers, the infrared and Raman spectra of the molecules in their vapor, liquid, and solid phases were also recorded [4]. Complete assignments were made and force constant calculations were completed, but the work was never published until 2011 [100]. This was in part due to the fact that vibrations for a planar cyclopentane molecule

would follow  $D_{5h}$  symmetry, but many of these split into doublets when the degeneracies are lifted for bent ( $C_s$ ) or twisted ( $C_2$ ) conformations. The extent of the splittings was difficult to predict before the availability of reliable ab initio calculations. Hence, a number of uncertainties in the assignments remained.

A vibrational assignment for cyclopentane was published by Miller and Inskeep [101] in 1950. Bauman in Laane's research group [98] already had showed previously that many of the assignments needed revision. Remarkably, there has apparently been no attempt in the literature to present a modern and complete assignment of the vibrational modes of this important molecule till 2011 [100]. However, in 1969 and 1972 Schettino and Marzocchi [102,103] did present infrared and Raman data and analyses for cyclopentane  $d_0$  and  $d_{10}$  crystals .

In this work a complete analysis of cyclopentane and four of its deuterated isotopomers is provided with the aid of ab initio and density functional theory calculations. In addition, the results of these calculations will be used to examine how well the determination of the two-dimensional potential energy surface of this molecule was done previously.

## **Experimental**

The preparation of the deuterated isotopomers has been previously described as have the experimental details for collecting the infrared and Raman spectra [4,98]. In brief, the infrared spectra were recorded with a Digilab FTS-20 interferometer and the Raman spectra were recorded with a Cary 82 spectrometer using a Coherent Radiation

Model 53 argon ion laser operating at 5145 Å and with powers of 100 mW to 3 W. Resolutions of 0.1 to 0.5 cm<sup>-1</sup> were used for the vapor-phase infrared spectra which were recorded of samples in 10 cm glass cells with KBr or CsI windows with vapor pressures ranging from 10 to 400 Torr. Multiple reflection optics were used to record the Raman spectra of 400 Torr of vapor samples in glass cells with quartz windows set at Brewster angles. Infrared and Raman spectra were recorded of solid samples frozen onto salt windows (for infrared) or a copper surface (for Raman) which was cooled by liquid nitrogen.

### **Computations**

The ab initio and density functional theory calculations were performed using the Gaussian 09, Revision A.02 program [57]. The Semichem APAC/AGUI 9.2 program [75] was used to visualize the vibrational motions. The CCSD level of theory with the cc-pVTZ basis set was used to determine the energy barrier and the geometry of the cyclopentane conformers. The frequency calculations were carried out using B3LYP/cc-pVTZ. Frequencies below the 1450 cm<sup>-1</sup> region were scaled with a factor of 0.985, frequencies within the 1450 cm<sup>-1</sup> and 2000 cm<sup>-1</sup> region were scaled by a factor of 0.975 and the C-H and C-D stretching frequencies by 0.961.

For the deuterated isotopomers the calculated frequencies for all of the possible positions for the isotopic substitution for the twist and bent conformers were carried out. The individual results are given in supplementary tables while the averaged values are

presented in the main text. The relative intensity data for the vibrational frequencies is presented separately for the C-H vibrations and all of the other vibrations.

## **Results and discussion**

### *Structure and conformational energy differences*

Fig. 43 shows the bond distances and angles calculated for the twist and bent forms of cyclopentane using the CCSD level of theory and cc-pVTZ basis set. The twist angle was computed to be  $43.2^\circ$  for the  $C_2$  form while the bending angle for the  $C_s$  conformation was calculated to be  $41.5^\circ$ . Because the energy difference between the two conformations and the barrier between them is very small, the molecule is rapidly interconverting between the many possible twist and bent forms. The energy difference between the two conformations was calculated to be only  $0.6 \text{ cm}^{-1}$  with the  $C_2$  form being of lower energy. This value is so small that it is difficult to know which conformation is of lower energy, but it does support the notion that the energy difference is tiny. In previous work [91,94] it was found that the experimental data showed the energy difference to be less than  $25 \text{ cm}^{-1}$ , and that it was likely less than  $10 \text{ cm}^{-1}$ . This notion is supported by the present calculations. The energy difference and the barrier between the twist and bent conformations are so small that the molecule is virtually freely pseudorotating between the conformations shown in Fig. 40 in accord with the original Pitzer [3,81] model. In the present work the planar form of cyclopentane was calculated with the CCSD/cc-pVTZ basis set to be  $1887 \text{ cm}^{-1}$  higher in energy, in excellent agreement with the experimental value of  $1808 \text{ cm}^{-1}$ . The MP4/cc-pVTZ

calculation, which took several months to complete, gave a barrier of  $1944\text{ cm}^{-1}$ . The B3LYP/cc-pVTZ calculations, which is expected to be somewhat poorer for the energy differences, predicted the bent form to be  $4.0\text{ cm}^{-1}$  higher in energy and the barrier to planarity to be  $1511\text{ cm}^{-1}$ .

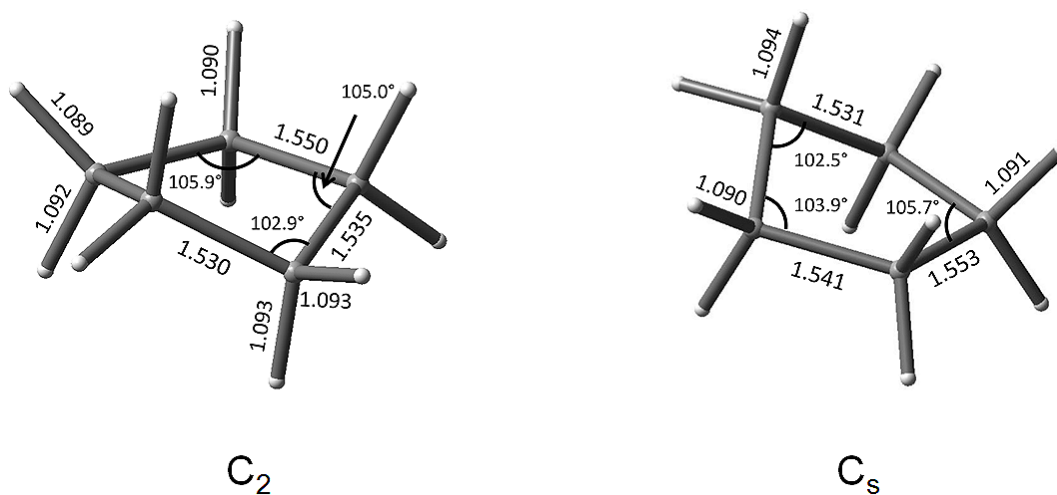


**Fig. 43.** Calculated bond distances and angles for the twist ( $C_2$ ) and bent ( $C_s$ ) forms of cyclopentane.

### *Symmetry considerations*

A planar cyclopentane molecule would have  $D_{5h}$  symmetry and its vibrational description would be

$$\Gamma(D_{5h}) = 3A_1' + A_2' + 4E_1' + 5E_2' + A_1'' + 2A_2'' + 3E_1'' + 4E_2'' \quad (22)$$

The  $E_1'$  and  $A_2''$  would be infrared active while  $A_1'$ ,  $E_2'$ , and  $E_1''$  would be Raman active with the  $A_1'$  bands being Raman polarized. As discussed, however, the cyclopentane

molecule is free to flop back and forth between the many twisted and bent structures of  $C_2$  and  $C_s$  symmetry shown in Fig. 43. For these symmetry point groups the distributions of vibrations over the symmetry species are

$$\Gamma(C_2) = 20A + 19B \quad (23)$$

and

$$\Gamma(C_s) = 21A' + 18A'' \quad (24)$$

For both cases all of the vibrations would be infrared and Raman active. However, as it will be seen, the molecule does follow the  $D_{5h}$  selection rules to some extent in that forbidden vibrations for  $D_{5h}$  produce relatively weak intensities for the actual molecule with  $C_2$  or  $C_s$  symmetry. Table 13 presents the correlation table between  $D_{5h}$  and  $C_2$  and  $C_s$  symmetry species.

**Table 13**

Correlation of  $D_{5h}$  symmetry species with  $C_2$  and  $C_s$  point groups.

$D_{5h}$	$C_2$	$C_s$
$A_1'$	A	$A'$
$A_2'$	B	$A'$
$E_1'$	A + B	$A' + A''$
$E_2'$	A + B	$A' + A''$
$A_1''$	A	$A''$
$A_2''$	B	$A''$
$E_1''$	A + B	$A' + A''$
$E_2''$	A + B	$A' + A''$

The vibrations of cyclopentane-d<sub>10</sub> follow exactly the same principles as the d<sub>0</sub> molecule so that the vibrations can be described as those from D<sub>5h</sub> symmetry being perturbed to those of either a C<sub>2</sub> or C<sub>s</sub> structure. For the 1,1-d<sub>2</sub> and 1,1,2,2,3,3-d<sub>6</sub> isotopomers, if the deuterium substitution is done most symmetrically, the planar structures would result in C<sub>2v</sub> symmetry and the vibrations would be distributed as

$$\Gamma(C_{2v}) = 12A_1 + 8A_2 + 10B_1 + 9B_2 \quad (25)$$

The A<sub>1</sub>, B<sub>1</sub>, and B<sub>2</sub> modes are infrared active while all, including the Raman polarized A<sub>1</sub> modes, are Raman active. In the twisted and bent forms of the d<sub>2</sub> and d<sub>6</sub> isotopomers of C<sub>2</sub> and C<sub>s</sub> symmetry, respectively, the vibrational description is the same as that given in eqs. (23) and (24). This assumes that the deuterium substitution is at the carbon atoms which will preserve the C<sub>2</sub> or C<sub>s</sub> symmetry. If the deuterium substitution is done asymmetrically, the symmetry groups become C<sub>1</sub> (no symmetry) and, as it shall be seen, this affects the computed vibrational frequencies for the deuterated isotopomers to a small extent. For cyclopentane-d<sub>1</sub> both the planar and bent forms have C<sub>s</sub> symmetry with Eq. (24) applicable if the deuterium substitution is on the unique carbon atom.

### *Infrared and Raman spectra*

Figs. 44-53 show the observed infrared and Raman spectra of solid, liquid, and vapor cyclopentane and its four deuterated isotopomers and compare these to the calculated spectra. Spectra calculated for C<sub>2</sub> and C<sub>s</sub> structures are very similar and only

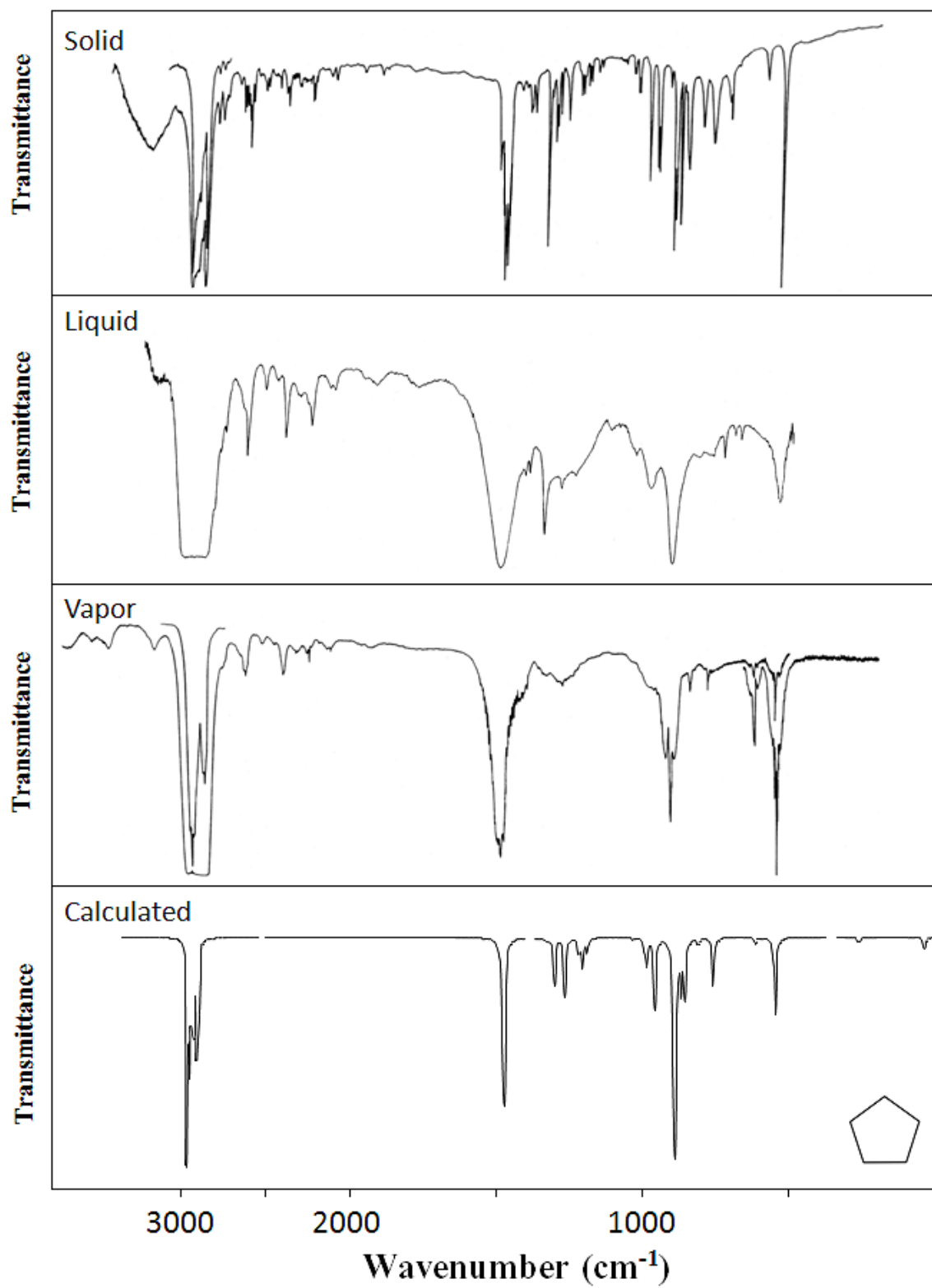


Fig. 44. Observed and calculated infrared spectra of cyclopentane.



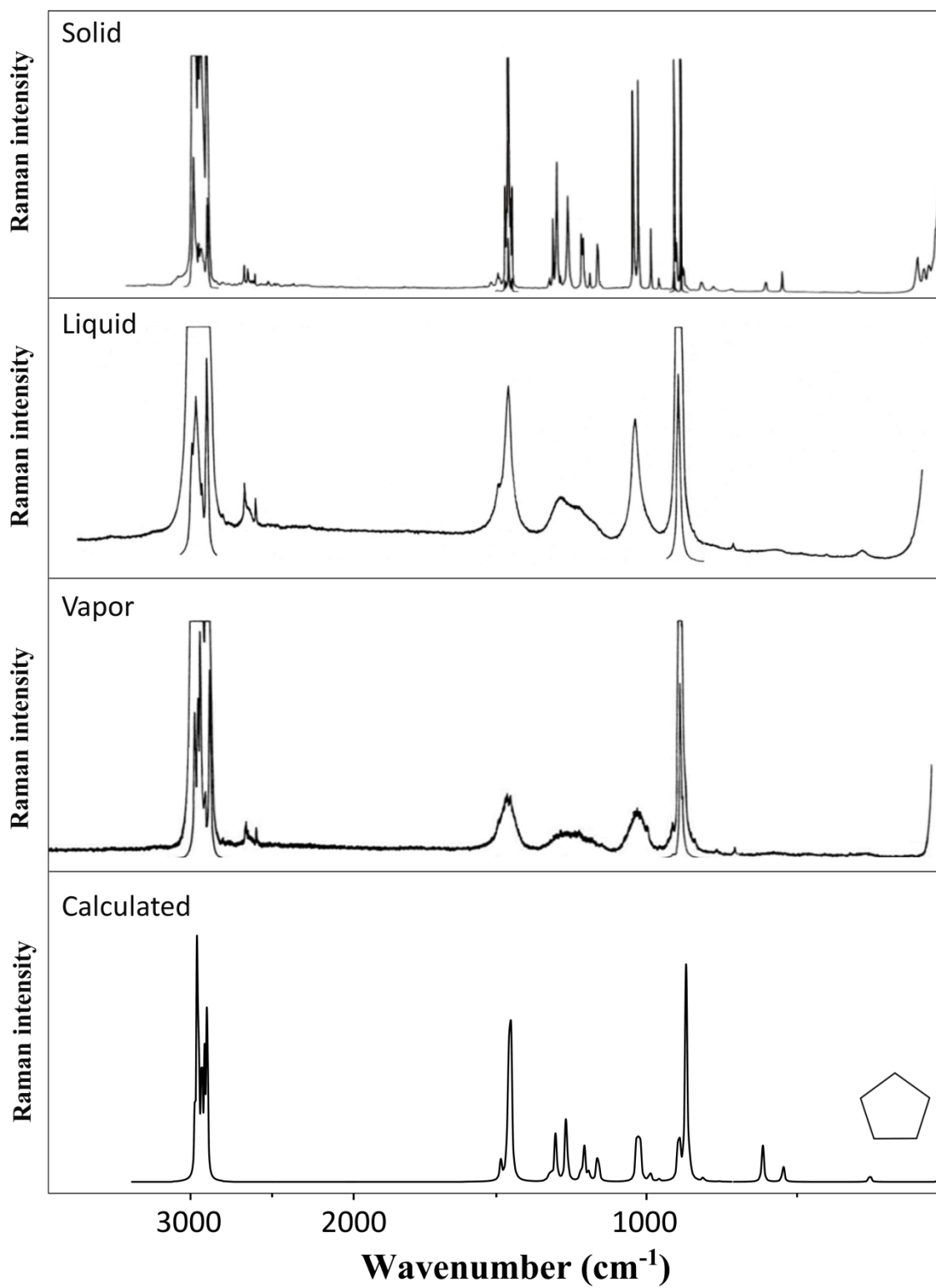


Fig. 45. Observed and calculated Raman spectra of cyclopentane.

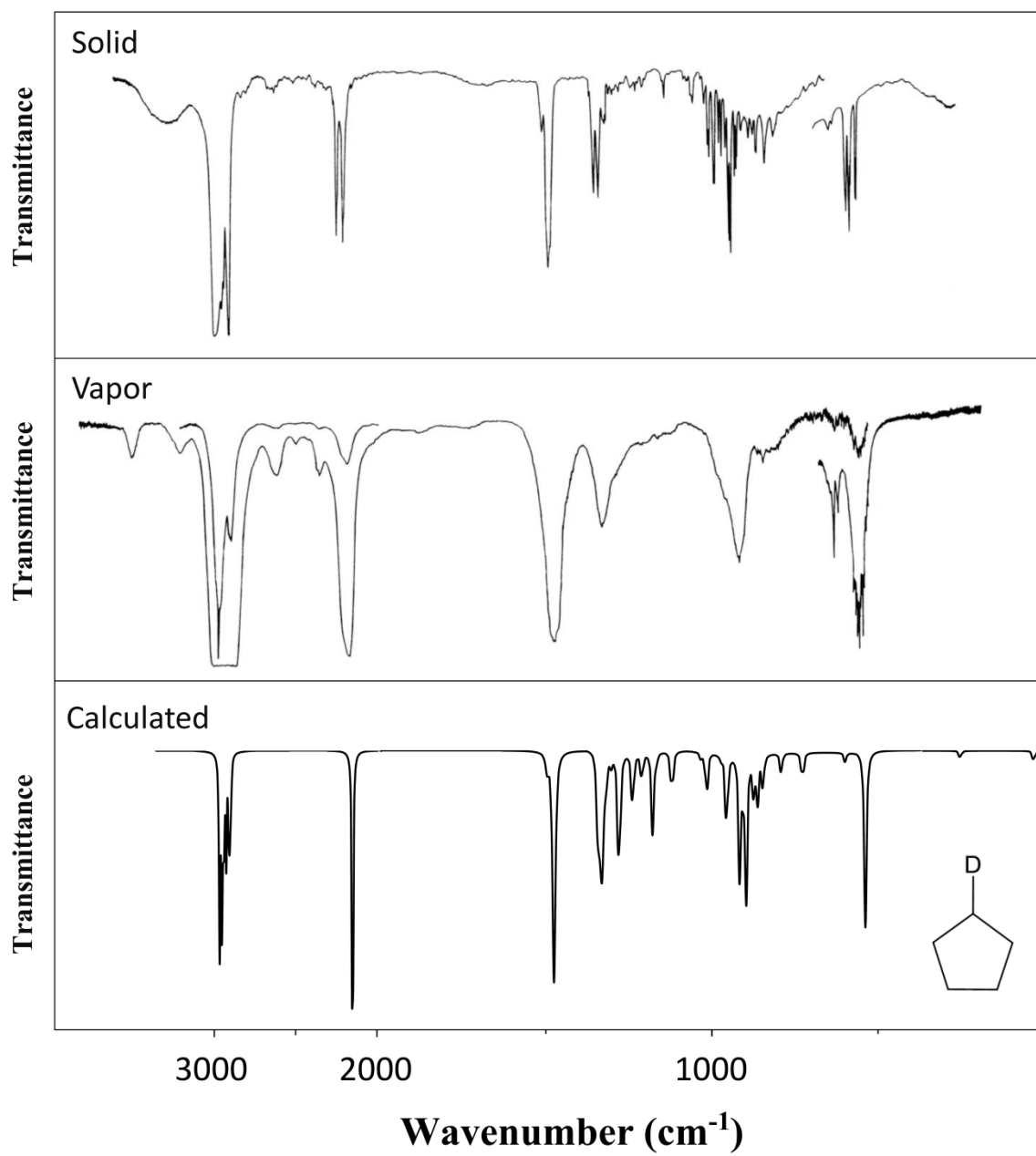


Fig. 46. Observed and calculated infrared spectra of cyclopentane-d<sub>1</sub>.

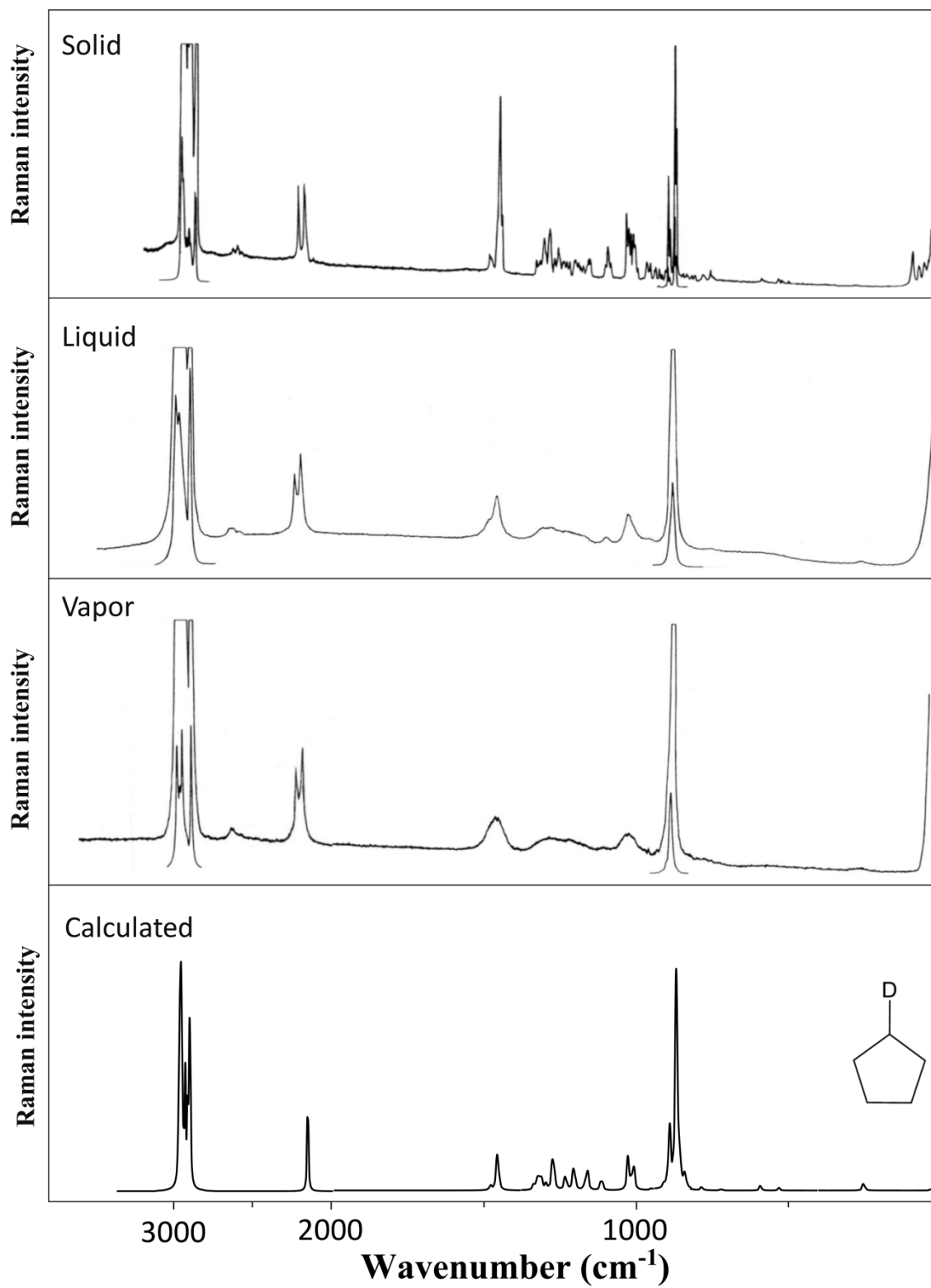
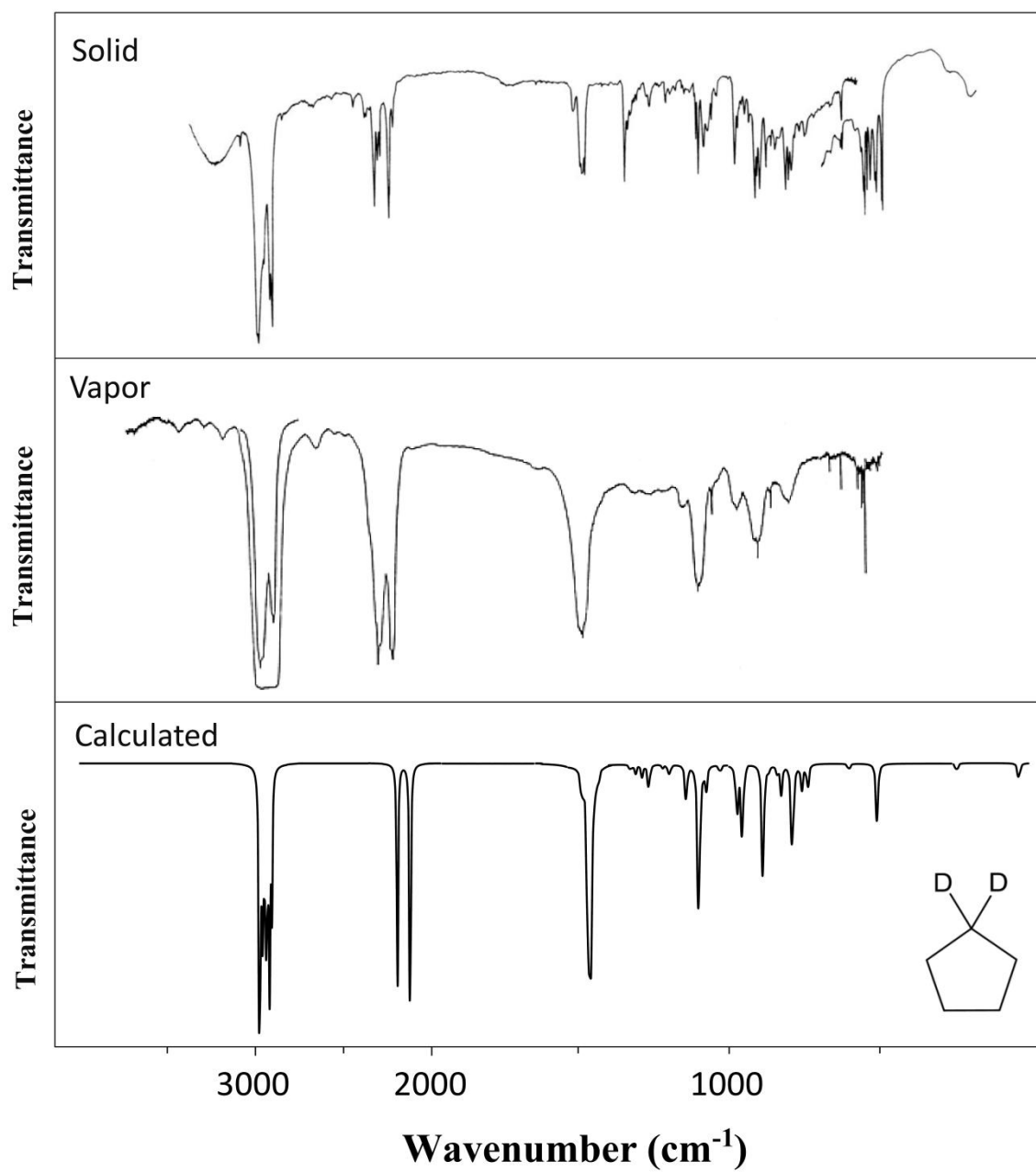


Fig. 47. Observed and calculated Raman spectra of cyclopentane-d<sub>1</sub>.



**Fig. 48.** Observed and calculated infrared spectra of cyclopentane-1,1-d<sub>2</sub>.

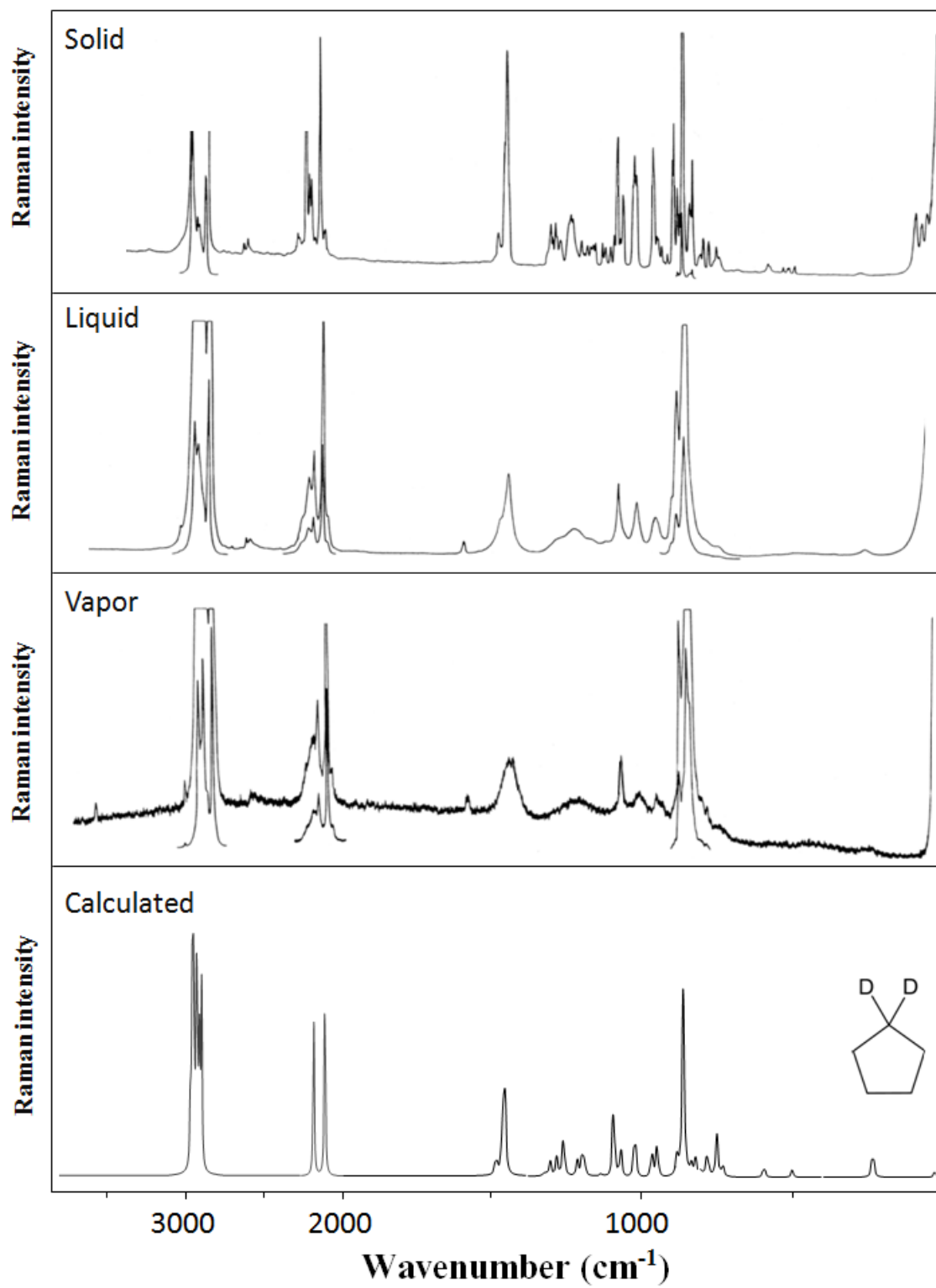
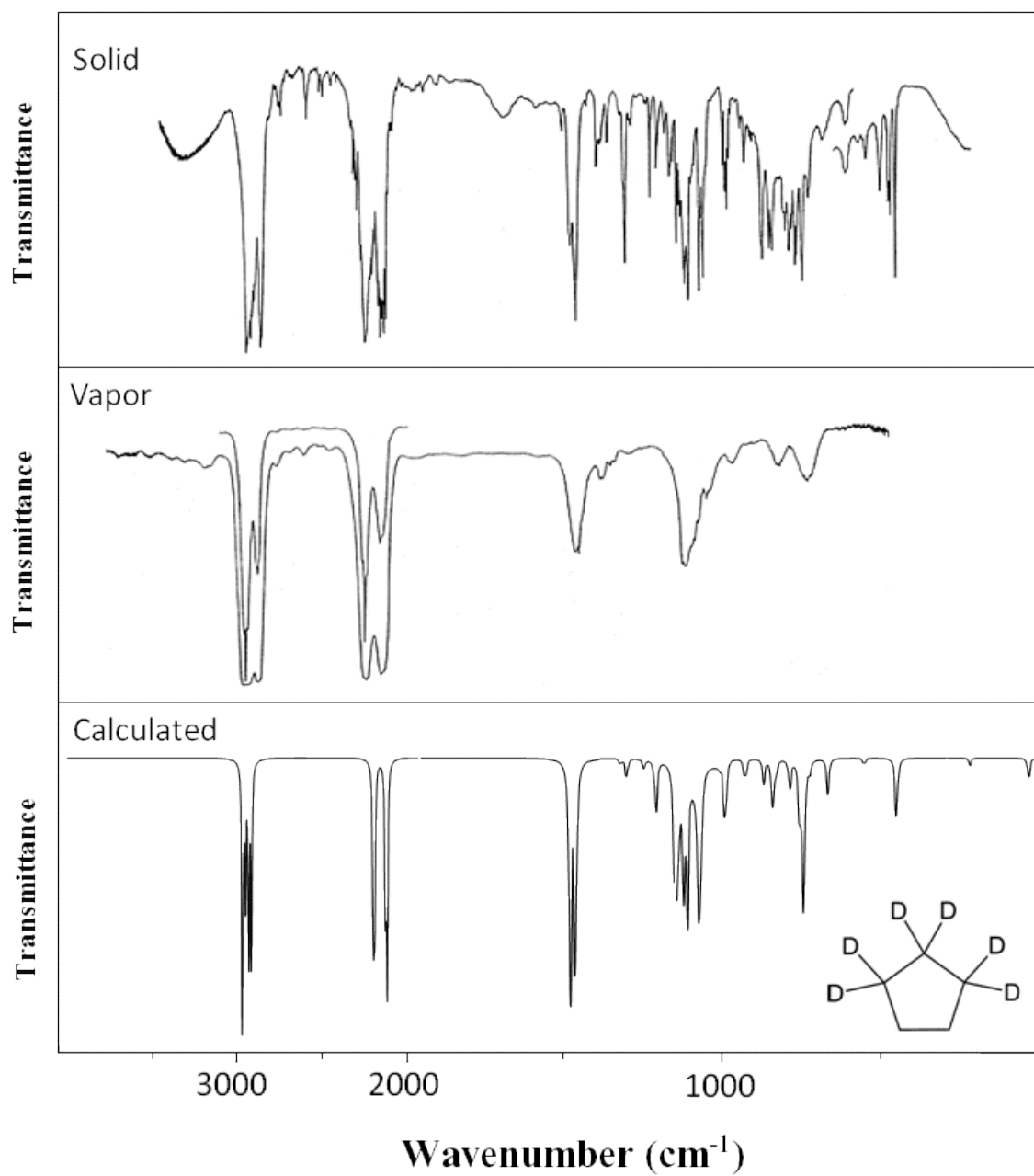


Fig. 49. Observed and calculated Raman spectra of cyclopentane-1,1-d<sub>2</sub>.



**Fig. 50.** Observed and calculated infrared spectra of cyclopentane-1,1,2,2,3,3-d<sub>6</sub>.

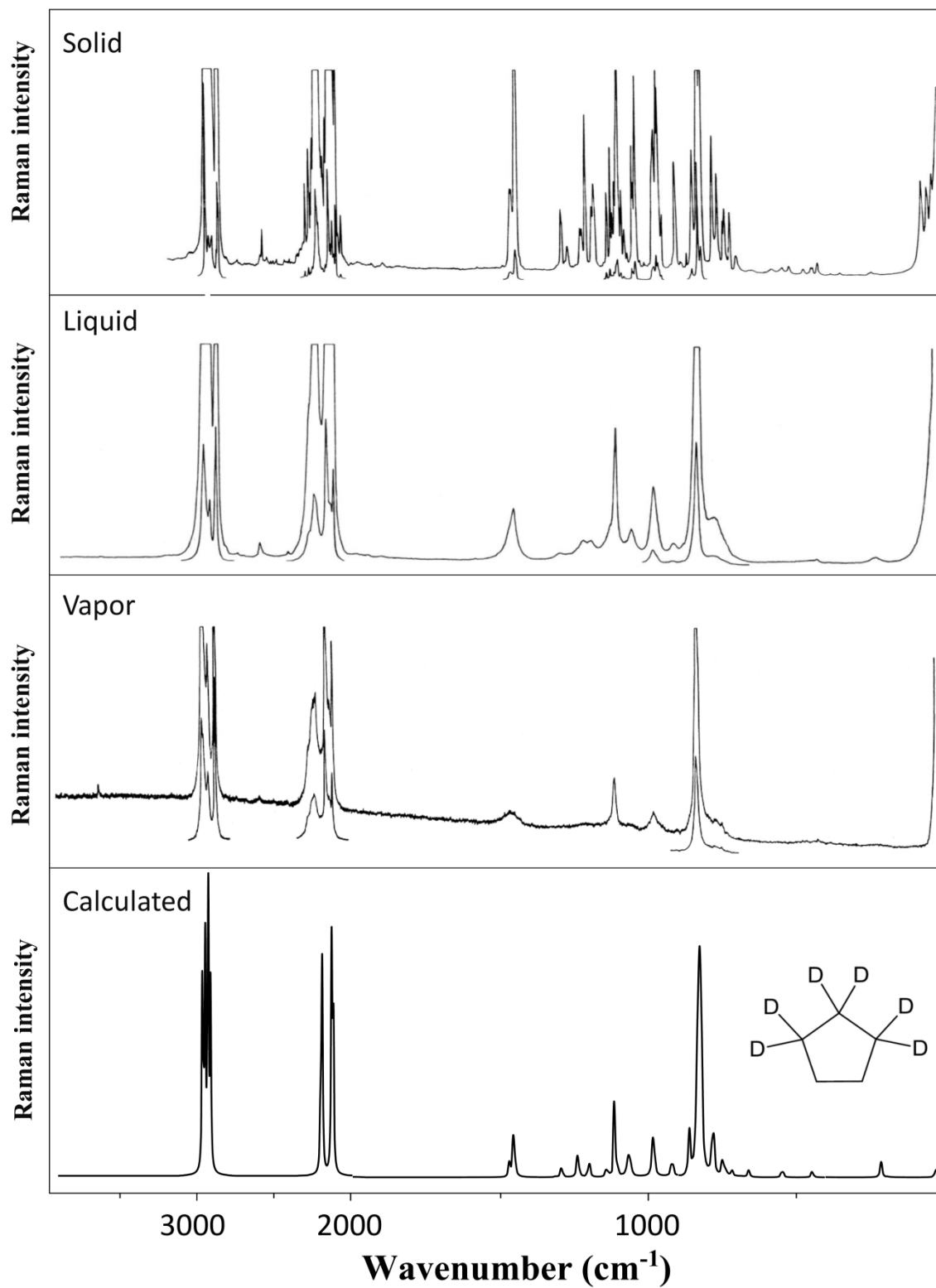
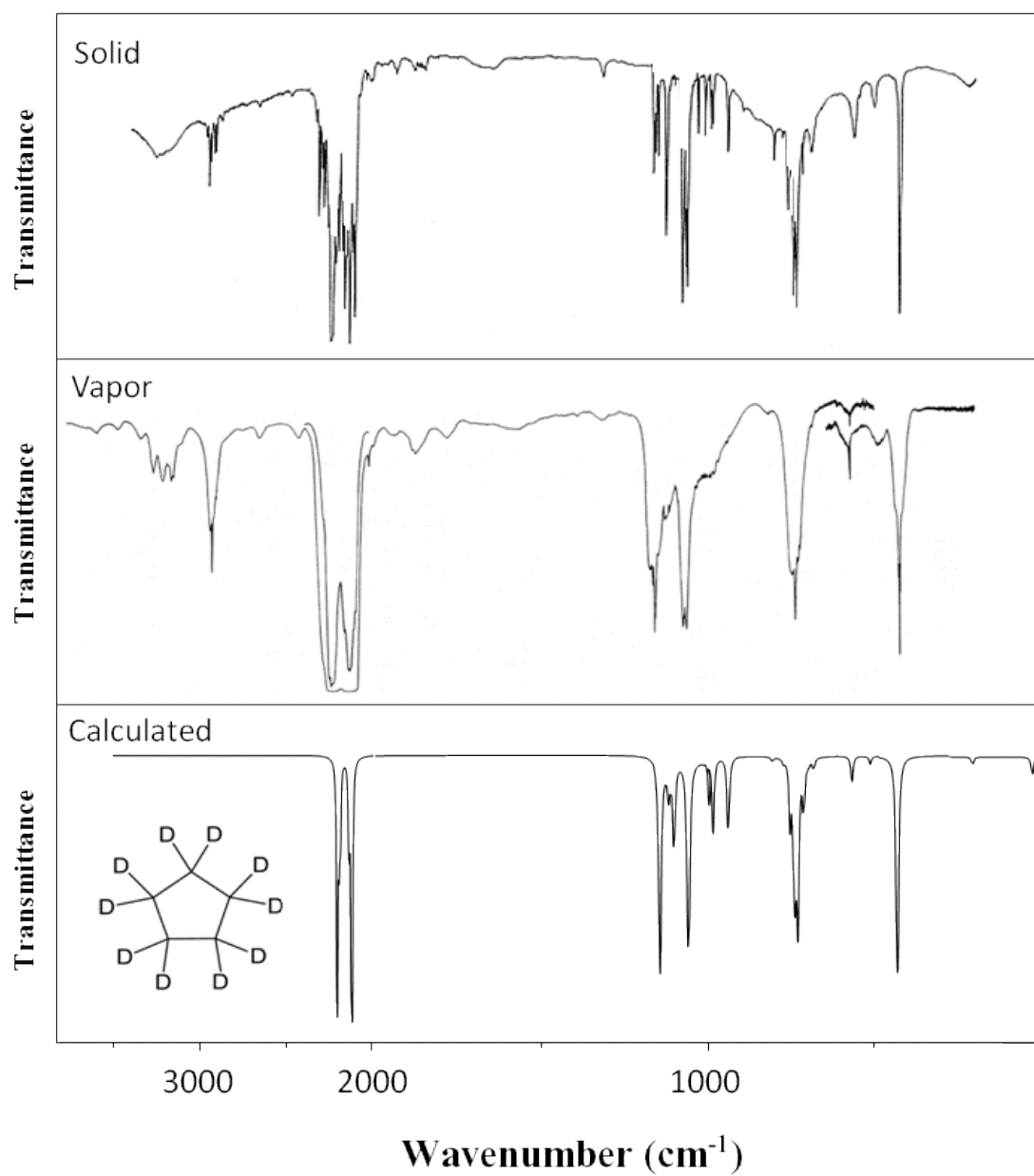


Fig. 51. Observed and calculated Raman spectra of cyclopentane-1,1,2,2,3,3-d<sub>6</sub>.



**Fig. 52.** Observed and calculated infrared spectra of cyclopentane-d<sub>10</sub>.



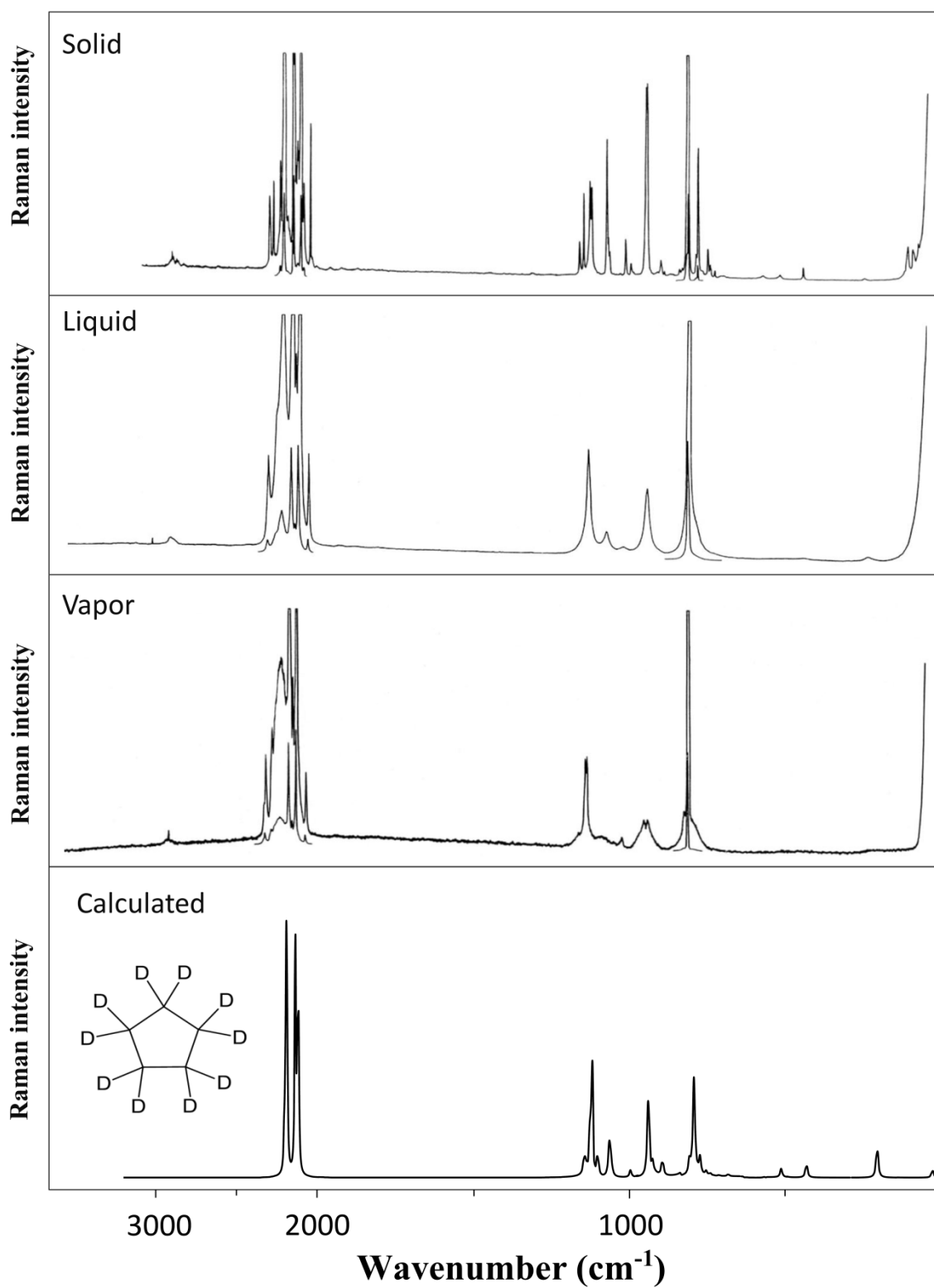


Fig. 53. Observed and calculated Raman spectra of cyclopentane-d<sub>10</sub>.

those from the  $C_2$  calculations are shown. As learned to expect from previous computations [58-61] the calculated spectra agree remarkably well with those observed, especially in their frequencies. Table 14 compares the observed and calculated spectra for cyclopentane and Table 15 does this for its  $d_{10}$  isotopomer. Table 16 presents the data for the  $1,1-d_2$  and  $1,1,2,2,3,3-d_6$  isotopomers and Table 17 shows the comparison for cyclopentane- $d_1$ . A more detailed listing of the observed infrared and Raman data for these molecules in vapor, liquid, and solid (frozen) phases can be found elsewhere [4]. For the  $d_1$ ,  $d_2$ , and  $d_6$  isotopomers the calculated frequency depends on where the deuteriums are substituted since both the twist and bent structures each have three different types of carbon atoms. For the bent form of the  $d_2$  isotopomer the two deuterium atoms can be attached to the carbon atom on the symmetry plane (carbon atom 1) or to a carbon atom next to it (carbon atom 2) or to a carbon atom farthest away (carbon atom 3). For the twist structure they can be on the carbon atom on the  $C_2$  axis (carbon atom 1) or to one of the other types of carbon atoms. If the computations are done with deuterium atoms other than on carbon atom 1, the  $C_s$  or  $C_2$  symmetry is lost and additional vibrational mixing is allowed. Similar considerations apply to the  $d_6$  isotopomer. This results in differences in the computed frequencies. Tables 18 and 19 list the calculated frequencies for the six isotopomeric forms of the  $d_2$  and  $d_6$  molecules along with the average values for each. The calculated frequency and intensity values listed in Table 16 presents the average values from Tables 18 and 19. Examination of Fig. 43 helps to understand that there are actually six different cyclopentane- $1,1-d_2$  or - $1,1,2,2,3,3-d_6$  configurations depending on where the deuteriums

**Table 14**  
Observed and calculated wavenumbers (cm<sup>-1</sup>) for cyclopentane.

	Observed <sup>a</sup>			Calculated C <sub>2</sub>		Calculated C <sub>s</sub>		Calculated D <sub>5h</sub>		Observed solid <sup>a</sup>	
	Freq.	Int. (IR, R)		Freq.	Int. (IR, R)	Freq.	Int. (IR, R)	Freq.	Int. (IR, R)	Freq.	Int. (IR, R)
A <sub>1</sub> ' v <sub>1</sub>	CH <sub>2</sub> sym. str.	2936	sh*, s	2930	(55, 51)	2929	(57, 53)	2943	(0, 100)	2933 <sup>c</sup>	s*, vs*
v <sub>2</sub>	CH <sub>2</sub> def.	1486	—, sh	1485	(3, 10)	1485	(4, 10)	1494	(0, 17)	1449	—, m*
v <sub>3</sub>	Ring breathing	886	—, s	869	(14, 100)	868	(14, 100)	847	(0,100)	882	—, vs*
A <sub>2</sub> ' v <sub>4</sub>	CH <sub>2</sub> wag (all i.p.)	1304	—, w*	1320	(1, 6)	1320	(0.9, 6)	1308	(0,0)	1304 <sup>c</sup>	m*, m*
E <sub>1</sub> ' v <sub>5</sub>	CH <sub>2</sub> sym. str.	2920	—, m*	2915	(20, 19)	2917	(13, 14)	2929	(85, 0)	2912 <sup>c</sup>	s*, —
		2907	sh*, s	2911	(27, 24)	2909	(38, 30)	2929	(85, 0)	2910 <sup>c</sup>	s*, —
v <sub>6</sub>	CH <sub>2</sub> def.	1462	s, m	1461	(100, 12)	1462	(100,13)	1473	(100, 0)	1460	vs*, —
		1462	s, m	1460	(71, 9)	1460	(72, 9)	1473	(100, 0)	1454	vs*, s*
v <sub>7</sub>	CH <sub>2</sub> wag	1316	m*, vw*	1333	(0.2, 0.4)	1333	(0.8, 0.6)	1338	(0.03, 0)	1316	s*, w*
		1316	m*, vw*	1333	(0.7, 0.5)	1332	(0.04,0.2)	1338	(0.03, 0)	1316	s*, w*
v <sub>8</sub>	Ring str.	896	s, w sh*	893	(48, 27)	893	(47,30)	903	(50, 0)	903	s*, s*
		881	ms*, sh	888	(52, 2)	886	(55, 2)	903	(50, 0)	897	s*, m*
E <sub>2</sub> ' v <sub>9</sub>	CH <sub>2</sub> sym. str.	2907	sh*, s	2903	(34, 6)	2904	(26, 3)	2918	(0, 9)	2902	—, m*
		2880	vs, s	2897	(16, 74)	2896	(17, 72)	2918	(0, 9)	2865 <sup>c</sup>	vs*, vs*
v <sub>10</sub>	CH <sub>2</sub> def.	1455	s*, —	1457	(93, 49)	1456	(94,49)	1456	(0, 38)	1446	vs*, m*
		1448	ms*, m	1451	(4, 68)	1451	(4, 69)	1456	(0, 38)	1437	w*, m*
v <sub>11</sub>	CH <sub>2</sub> wag	1295	m*, m*	1303	(15, 24)	1303	(15, 25)	1253	(0, 8)	1293	s*, m*
		1280	m*, w*	1297	(0.2, 1)	1297	(1, 0.1)	1253	(0, 8)	1279	m*, w*
v <sub>12</sub>	Ring	1030	w*, m	1032	(0.6, 23)	1033	(0.4, 23)	1056	(0, 10)	1043	w*, s*
		1022	w*, m*	1023	(0.1, 26)	1021	(0.1, 27)	1056	(0, 10)	1025	—, s*
v <sub>13</sub>	Ring bend	618	w, —	614	(2, 3)	613	(2, 3)	680	(0, 6)	616	w*, —
		546	m, —	546	(29, 1)	546	(29, 2)	680	(0, 6)	546	s*, —
A <sub>1</sub> '' v <sub>14</sub>	CH <sub>2</sub> twist	1207	w*, w*	1208	(10, 20)	1203	(12, 22)	1264	(0, 0)	1211 <sup>c</sup>	w*, —
A <sub>2</sub> '' v <sub>15</sub>	CH <sub>2</sub> antisym. str.	2965	vs, s	2972	(100, 20)	2972	(100, 20)	2978	(100, 0)	2953	vs*, —
v <sub>16</sub>	CH <sub>2</sub> rock	858	ms*, —	856	(18, 3)	855	(18, 4)	723	(83, 0)	859	s*, —
E <sub>1</sub> '' v <sub>17</sub>	CH <sub>2</sub> antisym. str.	2951	s*, s	2953	(15, 100)	2953	(15, 100)	2960	(0, 35)	2951	—, vs*
		2951	s*, s	2943	(39, 3)	2943	(41, 3)	2960	(0, 35)	2951 <sup>c</sup>	—, vs*
v <sub>18</sub>	CH <sub>2</sub> twist	1250	w, m*	1267	(21, 35)	1267	(20, 36)	1269	(0, 26)	1255 <sup>c</sup>	m, —
		1213	w*, w*	1221	(4, 3)	1223	(8, 5)	1269	(0, 26)	1211	w*, —
v <sub>19</sub>	CH <sub>2</sub> rock	817	w*, w*	812	(2, 2)	812	(2, 1)	763	(0, 0.2)	811 <sup>c</sup>	w*, —
		768	w, vvw	759	(15, 0.2)	760	(15, 0.3)	763	(0, 0.2)	776 <sup>c</sup>	w*, —
E <sub>2</sub> '' v <sub>20</sub>	CH <sub>2</sub> antisym. str.	2951	s*, s*	2957	(19, 51)	2957	(25, 42)	2932	(0, 0)	2965	—, vs*
		2951	s*, s*	2955	(30, 42)	2956	(23, 52)	2932	(0, 0)	2965	—, vs*
v <sub>21</sub>	CH <sub>2</sub> twist	1185	w*, w*	1192	(4, 4)	1194	(8, 0.4)	1201	(0, 0)	1185	w*, w*
		1167	—, w*	1162	(0.2, 17)	1162	(0.1, 18)	1201	(0, 0)	1159	m*, w*
v <sub>22</sub>	CH <sub>2</sub> rock	985	w*, w*	988	(12, 5)	989	(12, 5)	997	(0, 0)	984 <sup>c</sup>	s*, w*
		968	w*, —	959	(23, 1)	960	(23, 1)	997	(0, 0)	958 <sup>c</sup>	s*, w*
v <sub>23</sub>	CH <sub>2</sub> bend (o.p.)	273	—, vvw	258	(0.2, 0.6)	259	(0.2, 0.7)	197i	(0, 0)	—	—, —
		5 <sup>d</sup>	—, —	33	(0.3, 0.1)	17	(0.4, 0.1)	197i	(0, 0)	—	—, —

<sup>a</sup> Intensity, from vapor spectra unless indicated by \* for liquid or solid; s = strong, m = medium, v= very, sh = shoulder.

<sup>b</sup> Refs. [102,103].

<sup>c</sup> Reassigned.

<sup>d</sup> 2B where B = pseudorotational constant

Table 15

Observed and calculated wavenumbers ( $\text{cm}^{-1}$ ) for cyclopentane-d<sub>10</sub>.

			Observed <sup>a</sup>		Calculated C <sub>2</sub>		Calculated C <sub>s</sub>		Calculated D <sub>5h</sub>		Observed solid <sup>a</sup>	
			Freq.	Int. (IR, R)	Freq.	Int. (IR, R)	Freq.	Int. (IR, R)	Freq.	Int. (IR, R)	Freq.	Int. (IR, R)
A <sub>1</sub> '	v <sub>1</sub>	CD <sub>2</sub> sym. str.	2141	s*, s	2135	(30, 100)	2136	(29, 100)	2145	(0, 100)	2138	s*, ---
	v <sub>2</sub>	CD <sub>2</sub> def.	1130	w, m	1132	(26, 15)	1133	(22, 16)	1131	(0, 17)	1123	w*, m*
	v <sub>3</sub>	Ring breathing	805	w*, vs	793	(0.2, 100)	792	(0.4, 100)	777	(0, 100)	804	---, vs*
A <sub>2</sub> '	v <sub>4</sub>	CD <sub>2</sub> wag (all i.p.)	1018	w*, w	1036	(0.2, 0.001)	1036	(0.02, 0.001)	1043	(0, 0)	1025 <sup>c</sup>	m*, vw*
E <sub>1</sub> '	v <sub>5</sub>	CD <sub>2</sub> sym. str.	2120	vs, s	2123	(40, 16)	2124	(39, 10)	2130	(77, 0)	-----	---, ---
			2120	vs, s	2121	(36, 29)	2119	(41, 44)	2130	(77, 0)	-----	---, ---
v <sub>6</sub>	CD <sub>2</sub> def.	1167	s, ---	1160	(89, 2)	1159	(94, 2)	1149	(100, 0)	1158	w*, m*	
		1157	m*, vw	1157	(100, 0.7)	1157	(100, 0.8)	1149	(100, 0)	1153	s*, ---	
		1072	s, w*	1075	(57, 6)	1075	(58, 6)	1080	(50, 0)	1060	s*, ---	
		1072	s, w*	1074	(50, 3)	1073	(51, 2)	1080	(50, 0)	1057	vs*, ---	
v <sub>8</sub>	Ring str.	759	m*, ---	754	(31, 4)	754	(35, 5)	755	(38, 0)	758 <sup>c</sup>	s*, ---	
		737	s, w*	740	(72, 2)	734	(87, 1)	755	(38, 0)	740	s*, w*	
E <sub>2</sub> '	v <sub>9</sub>	CD <sub>2</sub> sym. str.	2109	s*, s*	2115	(32, 25)	2116	(29, 7)	2123	(0, 11)	2109 <sup>c</sup>	vs*, vs
			2109	s*, s*	2114	(35, 20)	2113	(35, 25)	2123	(0, 11)	2109 <sup>c</sup>	vs*, vs
v <sub>10</sub>	CD <sub>2</sub> def.	1135	---, m	1140	(4, 8)	1138	(11, 7)	1115	(0, 9)	1143 <sup>c</sup>	w*, s*	
		1120	s*, m*	1116	(73, 12)	1115	(77, 13)	1115	(0, 9)	1119 <sup>c</sup>	m*, m*	
v <sub>11</sub>	CD <sub>2</sub> wag	805	w*, vs	807	(3, 15)	808	(2, 16)	843	(0, 9)	790	w*, ---	
		775	w*, m*	773	(3, 17)	773	(2, 18)	843	(0, 9)	772 <sup>c</sup>	w*, s*	
v <sub>12</sub>	Ring	1080	---, w	1078	(0.2, 15)	1078	(0.1, 15)	1067	(0, 8)	1071	m*, s	
		1060	s, ---	1069	(84, 2)	1070	(88, 2)	1067	(0, 8)	1066	vs*, s*	
v <sub>13</sub>	Ring bend	515	w*, vw*	512	(5, 1)	511	(5, 1)	642	(0, 8)	505	w*, vw*	
		427	m, w*	430	(51, 0.7)	430	(52, 0.7)	642	(0, 8)	427	s*, ---	
A <sub>1</sub> "	v <sub>14</sub>	CD <sub>2</sub> twist	893	---, w*	894	(0.3, 4)	894	(0.2, 4)	894	(0, 0)	---	---, '---
A <sub>2</sub> "	v <sub>15</sub>	CD <sub>2</sub> antisym. str.	2240	vs, m*	2203	(100, 17)	2203	(100, 17)	2206	(100, 0)	2220	vs*, ---
			565	m*, vw*	567	(16, 0.1)	568	(17, 0.1)	522	(62, 0)	562 <sup>c</sup>	m*, vw*
E <sub>1</sub> "	v <sub>17</sub>	CD <sub>2</sub> antisym. str.	2220	s*, s	2193	(9, 42)	2193	(9, 38)	2196	(0, 38)	2213	vs*, s*
			2220	s*, s	2192	(17, 39)	2192	(17, 40)	2196	(0, 38)	2209	s*, s*
v <sub>18</sub>	CD <sub>2</sub> twist	946	---, m	940	(25, 29)	941	(31, 30)	939	(0, 20)	943 <sup>c</sup>	w*, s*	
		934	w*, m	938	(25, 29)	938	(21, 29)	939	(0, 20)	939 <sup>c</sup>	w*, s*	
v <sub>19</sub>	CD <sub>2</sub> rock	690	w*, ---	697	(3, 0.01)	697	(1, 0.01)	570	(0, 0.1)	699 <sup>c</sup>	w*, ---	
		690	w*, ---	682	(6, 2)	682	(6, 2)	570	(0, 0.1)	696	w*, ---	
E <sub>2</sub> "	v <sub>20</sub>	CD <sub>2</sub> antisym. str.	2164	m*, s	2185	(12, 50)	2185	(12, 49)	2180	(0, 0)	2151 <sup>c</sup>	m*, vs*
			2164	m*, s	2183	(17, 0.1)	2183	(17, 0.1)	2180	(0, 0)	2151 <sup>c</sup>	m*, vs*
v <sub>21</sub>	CD <sub>2</sub> twist	1005	w*, w*	1009	(28, 4)	1009	(28, 4)	979	(0, 0)	1007 <sup>c</sup>	w*, m*	
		988	w*, w*	985	(46, 0.7)	985	(49, 0.8)	979	(0, 0)	982 <sup>c</sup>	m*, vw*	
v <sub>22</sub>	CD <sub>2</sub> rock	737	s, w*	730	(94, 0.4)	734	(76, 0.9)	740	(0, 0)	733 <sup>c</sup>	vs*, ---	
		716	w*, w*	712	(27, 0.9)	712	(32, 0.9)	740	(0, 0)	718 <sup>c</sup>	vw*, ---	
v <sub>23</sub>	CD <sub>2</sub> bend (o.p.)	216	---, vw	204	(0.2, 0.4)	204	(0.2, 0.4)	155i	(0, 0)	---	---, ---	
		4 <sup>d</sup>	---, ---	26	(0.5, 0.04)	14	(0.5, 0)	155i	(0, 0)	---	---, ---	

<sup>a</sup> Intensity, from vapor spectra unless indicated by \* for liquid or solid; s = strong, m = medium, v = very, sh = shoulder.

<sup>b</sup> Refs. [102,103].

<sup>c</sup> Reassigned.

<sup>d</sup> 2B where B = pseudorotational constant.

**Table 16**

 Observed and calculated wavenumbers (cm<sup>-1</sup>) for cyclopentane-d<sub>2</sub> and cyclopentane -d<sub>6</sub>.

			cyclopentane-1,1-d <sub>2</sub>						cyclopentane-1, 1, 2, 2, 3, 3-d <sub>6</sub>					
			Observed <sup>a</sup>		Calculated <sup>b</sup>		Calculated C <sub>2v</sub>		Observed <sup>a</sup>		Calculated <sup>b</sup>		Calculated C <sub>2v</sub>	
			Freq.	Int. (IR, R)	Freq.	Int. (IR, R)	Freq.	Int. (IR, R)	Freq.	Int. (IR, R)	Freq.	Int. (IR, R)	Freq.	Int. (IR, R)
A <sub>1</sub> (A, A')	ν <sub>1</sub>	CH <sub>2</sub> sym. str. (i.p.)	2942	s*, s	2952	(29, 100)	2940	(17, 100)	2881	s, s	2906	(57, 100)	2934	(100, 100)
	ν <sub>2</sub>	CH <sub>2</sub> (CD <sub>2</sub> ) sym. str.	2883	—, s	2907	(46, 25)	2923	(43, 9)	2152	—, s	2130	(41, 92)	2139	(38, 67)
	ν <sub>3</sub>	CD <sub>2</sub> sym. str. (i.p.)	2127	ms, —	2122	(26, 29)	2131	(20, 14)	2100	s*, m	2115	(42, 33)	2124	(8, 12)
	ν <sub>4</sub>	CH <sub>2</sub> def.(i.p.)	1480	w*, sh	1480	(17, 17)	1489	(15, 17)	1462	m, m	1470	(64, 18)	1480	(99, 13)
	ν <sub>5</sub>	CH <sub>2</sub> (CD <sub>2</sub> ) def.(i.p.)	1468	m, —	1460	(100, 27)	1464	(46, 23)	1118	m*, w	1115	(53, 18)	1114	(17, 15)
	ν <sub>6</sub>	CH <sub>2</sub> wag (i.p.)	1333	m*, —	1331	(1, 0.4)	1337	(0.4, 0.02)	1305	vw, w*	1302	(3, 7)	1286	(2, 6)
	ν <sub>7</sub>	CH <sub>2</sub> (CD <sub>2</sub> ) wag (i.p.)	1238	w*, w*	1251	(12, 37)	1252	(0.1, 8)	1125	m*, m*	1127	(46, 14)	1130	(91, 4)
	ν <sub>8</sub>	CD <sub>2</sub> def.	1095	w*, m	1097	(53, 32)	1103	(39, 15)	1068	vw, m*	1068	(25, 13)	1072	(4, 15)
	ν <sub>9</sub>	Ring stretch	1035	w*, m	1022	(3, 27)	1050	(2, 7)	985	w, w	982	(19, 28)	1018	(16, 9)
	ν <sub>10</sub>	Ring stretch	897	m, s	888	(55, 22)	894	(43, 5)	760	—, w	767	(36, 7)	769	(43, 21)
	ν <sub>11</sub>	Ring breathing	874	w*, s	862	(6, 100)	831	(1, 100)	841	m, s	829	(11, 100)	811	(12, 100)
	ν <sub>12</sub>	Ring bending	515	w, w*	516	(28, 2)	663	(0.1, 7)	455	w, vw	461	(34, 1)	645	(0.04, 9)
A <sub>2</sub> (A, A'')	ν <sub>13</sub>	CH <sub>2</sub> antisym. str. (o.p.)	2960	s, s*	2956	(30, 61)	2960	(0, 44)	2935	sh*, s*	2959	(62, 100)	2940	(0, 24)
	ν <sub>14</sub>	CH <sub>2</sub> (CD <sub>2</sub> ) antisym. str. (o.p.)	—	—, —	2946	(44, 23)	2932	(0, 0)	2219	vs*, s*	2189	(16, 44)	2191	(0, 30)
	ν <sub>15</sub>	CH <sub>2</sub> twist (o.p.)	1238	w*, w*	1225	(7, 17)	1266	(0, 11)	1234	—, w*	1233	(2, 26)	1259	(0, 20)
	ν <sub>16</sub>	CH <sub>2</sub> (CD <sub>2</sub> ) twist (o.p.)	1173	—, w*	1179	(2, 17)	1223	(0, 6)	920	—, m*	921	(12, 17)	918	(0, 10)
	ν <sub>17</sub>	CH <sub>2</sub> rock (o.p.)	1066	m*, m*	1074	(7, 15)	1082	(0, 4)	1099	m*, m*	1093	(8, 2)	1079	(0, 1)
	ν <sub>18</sub>	CD <sub>2</sub> twist	849	w*, m*	842	(8, 13)	856	(0, 1)	780	w*, w	786	(10, 27)	772	(0, 0.02)
	ν <sub>19</sub>	CH <sub>2</sub> (CD <sub>2</sub> ) rock (o.p.)	755	—, w*	753	(7, 7)	731	(0, 1)	675	w*, —	708	(3, 4)	611	(0, 0.05)
	ν <sub>20</sub>	Radial ring mode	261	—, vw	244	(0.2, 1)	179i	(0.01, 0.03)	240	—, vw	222	(0.2, 1)	158i	(0.01, 0.01)
	B <sub>1</sub> (B, A'')	ν <sub>21</sub>	CH <sub>2</sub> sym. str. (o.p.)	2918	—, m*	2914	(36, 29)	2929	(100, 0)	2925	—, m	2919	(87, 85)	2921
ν <sub>22</sub>		CH <sub>2</sub> (CD <sub>2</sub> ) sym. str. (o.p.)	2875	s, s*	2899	(27, 73)	2918	(0, 12)	2135	s, s*	2120	(41, 29)	2128	(68, 3)
ν <sub>23</sub>		CH <sub>2</sub> def. (o.p.)	1464	m, m	1458	(71, 38)	1473	(100, 0)	1456	m, m	1456	(100, 60)	1461	(60, 35)
ν <sub>24</sub>		CH <sub>2</sub> (CD <sub>2</sub> ) def. (o.p.)	1458	m, m	1453	(42, 74)	1456	(0, 42)	1132	m, m*	1138	(29, 6)	1121	(100, 4)
ν <sub>25</sub>		CH <sub>2</sub> wag (o.p.)	1317	w*, —	1321	(2, 5)	1322	(0.1, 0.4)	—	—, —	1314	(3, 4)	1322	(2, 0.7)
ν <sub>26</sub>		CH <sub>2</sub> (CD <sub>2</sub> ) wag (o.p.)	1290	—, w*	1289	(6, 13)	1287	(0.1, 4)	1100	m*, m*	1105	(43, 6)	1098	(36, 0.04)
ν <sub>27</sub>		CD <sub>2</sub> wag (o.p.)	1135	w, w*	1127	(11, 5)	1110	(3, 0.6)	1060	w*, m*	1060	(31, 22)	1071	(21, 3)
ν <sub>28</sub>		Ring stretch	940	w*, vw	943	(11, 11)	996	(16, 9)	834	w*, m*	834	(17, 39)	872	(16, 9)
ν <sub>29</sub>		Ring stretch	830	w*, sh	827	(10, 31)	818	(29, 2)	755	m, w*	753	(37, 9)	803	(49, 2)
ν <sub>30</sub>		Ring bending	570	w, w*	594	(3, 3)	680	(0, 6)	572	w, w*	554	(5, 2)	669	(0.3, 8)

**Table 16** continued.

			cyclopentane-1,1-d <sub>2</sub>						cyclopentane-1, 1, 2, 2, 3, 3-d <sub>6</sub>					
			Observed <sup>a</sup>		Calculated <sup>b</sup>		Calculated C <sub>2v</sub>		Observed <sup>a</sup>		Calculated <sup>b</sup>		Calculated C <sub>2v</sub>	
			Freq.	Int. (IR, R)	Freq.	Int. (IR, R)	Freq.	Int. (IR, R)	Freq.	Int. (IR, R)	Freq.	Int. (IR, R)	Freq.	Int. (IR, R)
A <sub>1</sub> (A, A')	ν <sub>1</sub>	CH <sub>2</sub> sym. str. (i.p.)	2942	s*, s	2952	(29, 100)	2940	(17, 100)	2881	s, s	2906	(57, 100)	2934	(100, 100)
	ν <sub>2</sub>	CH <sub>2</sub> (CD <sub>2</sub> ) sym. str.	2883	---, s	2907	(46, 25)	2923	(43, 9)	2152	---, s	2130	(41, 92)	2139	(38, 67)
	ν <sub>3</sub>	CD <sub>2</sub> sym. str. (i.p.)	2127	ms, ---	2122	(26, 29)	2131	(20, 14)	2100	s*, m	2115	(42, 33)	2124	(8, 12)
	ν <sub>4</sub>	CH <sub>2</sub> def.(i.p.)	1480	w*, sh	1480	(17, 17)	1489	(15, 17)	1462	m, m	1470	(64, 18)	1480	(99, 13)
	ν <sub>5</sub>	CH <sub>2</sub> (CD <sub>2</sub> ) def.(i.p.)	1468	m, ---	1460	(100, 27)	1464	(46, 23)	1118	m*, w	1115	(53, 18)	1114	(17, 15)
	ν <sub>6</sub>	CH <sub>2</sub> wag (i.p.)	1333	m*, ---	1331	(1, 0.4)	1337	(0.4, 0.02)	1305	vw, w*	1302	(3, 7)	1286	(2, 6)
	ν <sub>7</sub>	CH <sub>2</sub> (CD <sub>2</sub> ) wag (i.p.)	1238	w*, w*	1251	(12, 37)	1252	(0.1, 8)	1125	m*, m*	1127	(46, 14)	1130	(91, 4)
	ν <sub>8</sub>	CD <sub>2</sub> def.	1095	w*, m	1097	(53, 32)	1103	(39, 15)	1068	vw, m*	1068	(25, 13)	1072	(4, 15)
	ν <sub>9</sub>	Ring stretch	1035	w*, m	1022	(3, 27)	1050	(2, 7)	985	w, w	982	(19, 28)	1018	(16, 9)

<sup>a</sup> Intensity, from vapor spectra unless indicated by \* for liquid or solid; s= strong, m=medium, w=weak, v= very, sh=shoulder.

<sup>b</sup> Wavenumbers and frequencies obtained by averaging all possible twisted and bent conformations. Tables 18 and 19 present details.

B3LYP calculations. Scaling factors: 0.985 below 1500 cm<sup>-1</sup>, 0.973 between 1500 and 2000 cm<sup>-1</sup> and 0.961 above 2000 cm<sup>-1</sup>

**Table 17**Wavenumbers ( $\text{cm}^{-1}$ ) for the vibrations of cyclopentane and cyclopentane- $\text{d}_1$ .

	Cyclopentane			Cyclopentane- $\text{d}_1$			
	Observed <sup>a</sup>		Calculated <sup>b</sup> Freq. Int. (IR, R)	Observed <sup>a</sup>		Calculated <sup>b</sup>	
	Freq.	Int. (IR, R)		Freq.	Int. (IR, R)	Freq.	Int. (IR, R)
CH <sub>2</sub> antisym. str.	2965	2972	(100, 20)	2960	s, s*	2969	(100, 29)
CH <sub>2</sub> antisym. str.	2951	2957	(22, 47)	2957	---, s	2956	(27, 57)
CH <sub>2</sub> antisym. str.	2951	2956	(27, 47)	2957	---, s	2954	(21, 100)
CH <sub>2</sub> antisym. str.	2951	2953	(15, 100)	2941	---, s	2949	(39, 47)
CH <sub>2</sub> antisym. str.	2951	2943	(40, 3)	2922	---, w	2936	(51, 34)
CH <sub>2</sub> sym. str.	2936	2929	(56, 52)	2919	---, m*	2922	(39, 38)
CH <sub>2</sub> sym. str.	2920	2917	(17, 17)	2907	m*, ---	2913	(31, 28)
CH <sub>2</sub> sym. str.	2907	2909	(32, 27)	2903	----, m*	2906	(34, 14)
<b>CH<sub>2</sub> sym. str. (CH str.)</b>	<b>2907</b>	<b>2904</b>	<b>(30, 5)</b>	<b>2878</b>	<b>s, s</b>	<b>2897</b>	<b>(20, 78)</b>
<b>CH<sub>2</sub> sym. str. (CD str.)</b>	<b>2880</b>	<b>2896</b>	<b>(16, 73)</b>	<b>2166</b>	<b>ms, m*</b>	<b>2156</b>	<b>(20, 24)</b>
CH <sub>2</sub> def.	1486	1485	(4, 10)	1477	sh*, sh*	1480	(16, 13)
CH <sub>2</sub> def.	1462	1462	(100, 13)	1456	ms, m*	1461	(100, 13)
CH <sub>2</sub> def.	1462	1460	(72, 9)	1448	sh*, m*	1457	(78, 38)
CH <sub>2</sub> def.	1455	1456	(94, 49)	1446	sh*, m*	1453	(45, 57)
<b>CH<sub>2</sub> def. (CD wag)</b>	<b>1448</b>	<b>1451</b>	<b>(4, 69)</b>	<b>1100</b>	<b>vw, w*</b>	<b>1100</b>	<b>(8, 11)</b>
<b>CH<sub>2</sub> wag (CH wag)</b>	<b>1316</b>	<b>1333</b>	<b>(0.5, 0.5)</b>	<b>1328</b>	<b>w*, vw*</b>	<b>1338</b>	<b>(26, 9)</b>
CH <sub>2</sub> wag	1316	1332	(0.4, 0.4)	-----	---, ---	1328	(8, 6)
<b>CH<sub>2</sub> wag (CH wag)</b>	<b>1304</b>	<b>1320</b>	<b>(1, 6)</b>	<b>1315</b>	<b>m, vw*</b>	<b>1322</b>	<b>(11, 6)</b>
CH <sub>2</sub> wag	1295	1303	(15, 25)	1301	m*, w*	1314	(12, 9)
CH <sub>2</sub> wag	1280	1297	(0.6, 0.6)	1285	w*, w*	1298	(12, 17)
CH <sub>2</sub> twist	1250	1267	(21, 36)	1272	w, w*	1277	(13, 21)
CH <sub>2</sub> twist	1213	1223	(6, 4)	1257	---, w*	1243	(11, 19)
CH <sub>2</sub> twist	1207	1203	(7, 21)	1219	---, w*	1209	(6, 16)
CH <sub>2</sub> twist	1185	1194	(6, 2)	1177	---, w*	1180	(9, 6)
CH <sub>2</sub> twist	1167	1162	(0.1, 17)	1160	vw, w*	1170	(3, 17)
Ring	1030	1033	(0.5, 23)	1030	---, w	1026	(1, 24)
Ring	1024	1021	(0.1, 26)	1020	w*, w	1004	(6, 18)
<b>CH<sub>2</sub> rock (CD wag)</b>	<b>985</b>	<b>989</b>	<b>(12, 5)</b>	<b>820</b>	<b>w, ---</b>	<b>818</b>	<b>(21, 6)</b>
CH <sub>2</sub> rock	968	960	(23, 1)	955	m*, vw	959	(25, 6)
Ring stretch	896	893	(47, 29)	925	w*, vw	918	(38, 9)
Ring breathing	886	868	(14, 100)	885	m*, s	867	(13, 100)
Ring stretch	881	886	(54, 2)	896	ms*, w*	888	(54, 16)
CH <sub>2</sub> rock	858	855	(18, 4)	839	w*, ---	845	(13, 8)
CH <sub>2</sub> rock	817	812	(2, 2)	763	w*, w*	759	(9, 4)
CH <sub>2</sub> rock	768	760	(15, 0.2)	-----	---, ---	721	(14, 2)
Ring bend	618	613	(2, 3)	604	w, w*	603	(2, 3)
Ring bend	546	546	(29, 1)	530	w, ---	529	(30, 1)
Radial ring mode	273	259	(0.2, 0.6)	268	---, w	249	(0.2, 0.6)
Pseudorotation	5 <sup>d</sup>	25	(0.4, 0.1)	5 <sup>d</sup>	---, ---	29	(0.4, 0.1)

<sup>a</sup> Intensity, from vapor spectra unless indicated by \* for liquid or solid; s=strong, m=medium, w=weak, v=very, sh=shoulder.

<sup>b</sup> Wavenumbers and frequencies obtained by averaging all possible twisted and bent conformations. Table 20 presents details.

<sup>c</sup> 2B where B = pseudorotational constant.

**Table 18**Calculated vibrational frequencies ( $\text{cm}^{-1}$ ) for conformers of cyclopentane-1,1-d<sub>2</sub>. Different positions of deuterium substitution.

Twist Conformer								Bent Conformer									
d <sub>2</sub> location				d <sub>2</sub> location				d <sub>2</sub> location				Average T. and B.					
Carbon 1		Carbon 2		Carbon 3		Average		Carbon 1		Carbon 2		Carbon 3		Average		Average T. and B.	
Freq.	Int. (IR, R)	Freq.	Int. (IR, R)	Freq.	Int. (IR, R)	Freq.	Int. (IR, R)	Freq.	Int. (IR, R)	Freq.	Int. (IR, R)	Freq.	Int. (IR, R)	Freq.	Int. (IR, R)	Freq.	Int. (IR, R)
2962	(100, 28)	2967	(100, 40)	2971	(100, 32)	2968	(100, 34)	2971	(100, 26)	2969	(100, 40)	2964	(100, 34)	2967	(100, 34)	2968	(100, 34)
2957	(23, 52)	2955	(37, 60)	2957	(24, 70)	2956	(29, 63)	2957	(31, 48)	2956	(29, 76)	2956	(34, 53)	2956	(31, 60)	2956	(30, 61)
2952	(29, 100)	2952	(39, 99)	2953	(20, 100)	2952	(29, 100)	2953	(5, 100)	2952	(35, 100)	2952	(36, 100)	2953	(29, 100)	2952	(29, 100)
2950	(78, 15)	2947	(37, 41)	2943	(37, 11)	2946	(45, 23)	2942	(47, 4)	2944	(22, 32)	2949	(66, 28)	2946	(44, 24)	2946	(44, 23)
2917	(40, 40)	2929	(67, 62)	2930	(54, 89)	2927	(56, 68)	2929	(52, 77)	2930	(74, 93)	2923	(48, 46)	2927	(60, 69)	2927	(58, 69)
2913	(51, 33)	2913	(33, 30)	2915	(32, 27)	2914	(36, 29)	2916	(16, 17)	2917	(27, 21)	2909	(58, 41)	2914	(36, 28)	2914	(36, 29)
2904	(44, 9)	2905	(57, 12)	2912	(39, 38)	2907	(47, 22)	2909	(53, 74)	2907	(49, 23)	2906	(38, 6)	2907	(46, 28)	2907	(46, 25)
2897	(19, 87)	2897	(21, 100)	2901	(35, 49)	2899	(27, 77)	2905	(31, 4)	2898	(29, 86)	2896	(22, 92)	2899	(27, 69)	2899	(27, 73)
2194	(16, 15)	2191	(19, 22)	2188	(19, 26)	2191	(19, 22)	2188	(19, 22)	2189	(20, 27)	2193	(18, 18)	2190	(19, 22)	2191	(19, 22)
2131	(28, 24)	2124	(28, 30)	2116	(24, 32)	2122	(26, 29)	2114	(24, 27)	2119	(26, 34)	2129	(29, 26)	2122	(26, 29)	2122	(26, 29)
1477	(5, 18)	1479	(18, 22)	1481	(20, 14)	1480	(16, 17)	1481	(16, 14)	1480	(26, 16)	1477	(11, 22)	1479	(18, 17)	1480	(17, 17)
1461	(100, 21)	1457	(100, 93)	1461	(100, 11)	1459	(100, 36)	1461	(100, 19)	1461	(100, 14)	1461	(100, 25)	1461	(100, 19)	1460	(100, 27)
1456	(93, 82)	1460	(77, 18)	1459	(76, 21)	1459	(80, 30)	1460	(63, 7)	1456	(47, 45)	1455	(72, 93)	1456	(61, 47)	1458	(71, 38)
1454	(41, 86)	1455	(39, 93)	1452	(11, 63)	1453	(28, 75)	1452	(4, 61)	1454	(68, 73)	1454	(77, 89)	1453	(56, 74)	1453	(42, 74)
1331	(0.1, 0.5)	1331	(1, 0.3)	1330	(0.05, 0.3)	1331	(1, 0.4)	1331	(0.3, 0.6)	1330	(1, 0.2)	1331	(1, 1)	1331	(1, 0.5)	1331	(1, 0.4)
1321	(2, 9)	1321	(1, 8)	1320	(2, 2)	1321	(2, 5)	1318	(1, 0.2)	1322	(2, 5)	1321	(2, 10)	1321	(2, 5)	1321	(2, 5)
1319	(2, 12)	1312	(4, 12)	1303	(4, 11)	1310	(4, 12)	1300	(7, 20)	1307	(5, 10)	1318	(3, 12)	1310	(5, 13)	1310	(4, 12)
1299	(10, 19)	1289	(6, 23)	1285	(4, 10)	1289	(6, 15)	1295	(1, 2)	1277	(2, 9)	1297	(10, 23)	1289	(5, 11)	1289	(6, 13)
1241	(15, 27)	1252	(13, 58)	1256	(9, 24)	1251	(12, 34)	1246	(7, 21)	1263	(15, 42)	1243	(13, 56)	1252	(12, 39)	1251	(12, 37)
1240	(12, 47)	1229	(10, 23)	1213	(1, 9)	1225	(6, 19)	1211	(1, 10)	1220	(4, 12)	1238	(16, 27)	1225	(8, 16)	1225	(7, 17)
1164	(5, 5)	1180	(6, 13)	1202	(1, 11)	1185	(4, 11)	1209	(0.03, 8)	1188	(5, 4)	1169	(6, 11)	1185	(4, 8)	1185	(4, 9)
1163	(2, 27)	1174	(0.6, 25)	1191	(3, 8)	1179	(2, 16)	1193	(1, 7)	1187	(2, 22)	1166	(2, 26)	1180	(2, 19)	1179	(2, 17)
1107	(9, 19)	1126	(9, 6)	1138	(15, 1)	1127	(11, 5)	1138	(14, 1)	1134	(13, 2)	1114	(5, 10)	1127	(10, 4)	1127	(11, 5)
1104	(17, 21)	1098	(53, 43)	1094	(65, 28)	1097	(50, 31)	1092	(59, 27)	1096	(68, 33)	1101	(40, 38)	1097	(55, 33)	1097	(53, 32)
1086	(12, 24)	1072	(2, 23)	1070	(10, 10)	1074	(7, 16)	1070	(10, 8)	1070	(6, 15)	1080	(4, 23)	1074	(6, 15)	1074	(7, 15)
1018	(2, 40)	1020	(3, 39)	1025	(3, 18)	1022	(3, 27)	1028	(1, 15)	1021	(4, 25)	1019	(3, 42)	1021	(3, 27)	1022	(3, 27)
968	(41, 29)	967	(32, 27)	967	(11, 9)	967	(25, 17)	962	(8, 7)	967	(19, 13)	967	(43, 32)	966	(26, 17)	967	(26, 17)
934	(6, 3)	940	(7, 12)	952	(16, 12)	943	(10, 10)	958	(15, 14)	944	(15, 13)	936	(5, 5)	944	(11, 11)	943	(11, 11)
898	(62, 34)	893	(56, 39)	879	(49, 8)	889	(54, 21)	876	(42, 3)	884	(56, 24)	897	(65, 41)	888	(56, 23)	888	(55, 22)



**Table 18** continued.

Twist Conformer								Bent Conformer									
d <sub>2</sub> location								d <sub>2</sub> location									
Carbon 1		Carbon 2		Carbon 3		Average		Carbon 1		Carbon 2		Carbon 3		Average		Average T. and B.	
Freq.	Int. (IR, R)	Freq.	Int. (IR, R)	Freq.	Int. (IR, R)	Freq.	Int. (IR, R)	Freq.	Int. (IR, R)	Freq.	Int. (IR, R)	Freq.	Int. (IR, R)	Freq.	Int. (IR, R)	Freq.	Int. (IR, R)
863	(6, 100)	862	(9, 100)	861	(1, 100)	862	(5, 100)	861	(1, 100)	861	(6, 100)	862	(9, 100)	861	(6, 100)	862	(6, 100)
857	(15, 6)	844	(12, 36)	833	(2, 4)	842	(9, 13)	829	(0.3, 2)	838	(5, 16)	853	(16, 19)	842	(8, 12)	842	(8, 13)
831	(4, 75)	838	(6, 59)	816	(14, 7)	828	(9, 32)	805	(19, 2)	831	(11, 18)	833	(6, 76)	827	(11, 29)	827	(10, 31)
806	(31, 7)	800	(39, 15)	783	(40, 4)	794	(38, 8)	787	(21, 6)	790	(50, 7)	804	(35, 14)	795	(37, 9)	795	(38, 8)
763	(0.1, 9)	747	(3, 6)	756	(12, 8)	754	(6, 8)	763	(19, 7)	742	(7, 5)	756	(1, 8)	752	(8, 6)	753	(7, 7)
648	(6, 0.3)	695	(11, 4)	732	(12, 2)	700	(10, 2)	730	(14, 2)	724	(11, 4)	663	(9, 2)	701	(11, 3)	701	(11, 3)
601	(2, 6)	590	(4, 5)	598	(2, 2)	595	(3, 4)	600	(1, 2)	590	(5, 3)	593	(2, 6)	593	(3, 3)	594	(3, 3)
540	(32, 2)	523	(29, 3)	501	(24, 1)	517	(27, 2)	497	(21, 1)	507	(28, 2)	533	(33, 3)	515	(28, 2)	516	(28, 2)
257	(0.2, 1)	248	(0.2, 1)	237	(0.2, 0.6)	246	(0.2, 1)	231	(0.1, 0.6)	238	(0.2, 1)	250	(0.2, 1)	241	(0.2, 1)	244	(0.2, 1)
31	(0.3, 0.03)	31	(0.3, 0.2)	32	(0.3, 0.1)	31	(0.3, 0.1)	27	(0.3, 0.1)	26	(0.4, 0.2)	25	(0.4, 0.1)	26	(0.4, 0.1)	29	(0.3, 0.1)

B3LYP calculations. Scaling factors: 0.985 below 1500 cm<sup>-1</sup>, 0.973 between 1500 and 2000 cm<sup>-1</sup> and 0.961 above 2000 cm<sup>-1</sup>

**Table 19**Calculated vibrational frequencies ( $\text{cm}^{-1}$ ) for conformers of cyclopentane-1, 1, 2, 2, 3, 3 - $\text{d}_6$ . Different positions of deuterium substitution.

Twist Conformer								Bent Conformer									
$\text{d}_6$ location								$\text{d}_6$ location									
Carbon 1		Carbon 2		Carbon 3		Average		Carbon 1		Carbon 2		Carbon 3		Average		Average T. and B.	
Freq.	Int. (IR, R)	Freq.	Int. (IR, R)	Freq.	Int. (IR, R)	Freq.	Int. (IR, R)	Freq.	Int. (IR, R)	Freq.	Int. (IR, R)	Freq.	Int. (IR, R)	Freq.	Int. (IR, R)	Freq.	Int. (IR, R)
2955	(84, 46)	2959	(100, 65)	2965	(100, 63)	2961	(100, 77)	2967	(99, 49)	2962	(100, 76)	2956	(97, 52)	2961	(100, 79)	2961	(100, 78)
2951	(78, 75)	2951	(85, 100)	2947	(33, 56)	2949	(64, 99)	2944	(8, 28)	2949	(65, 100)	2999	(90, 85)	2968	(62, 100)	2959	(62, 100)
2906	(100, 14)	2915	(80, 57)	2929	(78, 100)	2919	(86, 82)	2931	(100, 100)	2923	(66, 91)	2908	(100, 29)	2919	(88, 89)	2919	(87, 85)
2898	(27, 100)	2902	(63, 100)	2914	(61, 43)	2906	(57, 100)	2917	(53, 17)	2907	(67, 87)	2898	(45, 100)	2906	(57, 100)	2906	(57, 100)
2201	(72, 19)	2200	(76, 30)	2196	(62, 30)	2198	(71, 35)	2195	(61, 24)	2198	(67, 36)	2201	(81, 23)	2198	(72, 36)	2198	(72, 36)
2192	(5, 39)	2190	(13, 39)	2188	(24, 24)	2190	(16, 43)	2188	(23, 16)	2189	(21, 37)	2191	(7, 40)	2189	(16, 44)	2189	(16, 44)
2184	(9, 5)	2185	(18, 29)	2185	(20, 42)	2185	(18, 37)	2185	(20, 33)	2185	(19, 47)	2184	(13, 11)	2185	(17, 37)	2185	(17, 37)
2135	(40, 64)	2133	(48, 75)	2124	(33, 64)	2130	(41, 88)	2120	(25, 67)	2130	(41, 77)	2135	(48, 71)	2130	(40, 96)	2130	(41, 92)
2123	(48, 9)	2122	(39, 25)	2115	(36, 37)	2119	(41, 34)	2117	(44, 3)	2118	(35, 41)	2124	(44, 11)	2120	(41, 24)	2120	(41, 29)
2121	(30, 18)	2115	(46, 33)	2114	(40, 19)	2115	(41, 30)	2113	(35, 22)	2113	(44, 38)	2118	(43, 23)	2115	(42, 36)	2115	(42, 33)
1466	(36, 16)	1468	(43, 21)	1473	(100, 16)	1470	(62, 18)	1475	(100, 13)	1471	(64, 25)	1465	(40, 20)	1469	(64, 19)	1470	(64, 18)
1456	(100, 56)	1456	(100, 71)	1456	(72, 50)	1456	(100, 59)	1456	(39, 39)	1457	(100, 84)	1455	(100, 61)	1456	(100, 62)	1456	(100, 60)
1315	(4, 7)	1313	(4, 7)	1314	(2, 1)	1314	(4, 4)	1313	(2, 0, 6)	1314	(1, 2)	1316	(5, 8)	1315	(3, 4)	1314	(3, 4)
1311	(2, 1)	1312	(3, 6)	1290	(5, 10)	1303	(3, 7)	1277	(0.005, 6)	1304	(7, 16)	1311	(1, 2)	1302	(3, 7)	1302	(3, 7)
1225	(1, 22)	1227	(1, 28)	1243	(3, 25)	1233	(2, 25)	1253	(5, 24)	1232	(2, 36)	1225	(1, 24)	1233	(2, 27)	1233	(2, 26)
1197	(7, 17)	1199	(8, 21)	1202	(18, 15)	1200	(11, 18)	1205	(16, 11)	1200	(12, 25)	1198	(8, 19)	1200	(11, 19)	1200	(11, 18)
1129	(31, 6)	1136	(30, 7)	1146	(21, 6)	1138	(30, 6)	1147	(14, 4)	1140	(28, 9)	1130	(29, 6)	1138	(29, 7)	1138	(29, 6)
1121	(25, 22)	1121	(41, 18)	1136	(62, 4)	1127	(46, 13)	1135	(51, 3)	1130	(54, 10)	1121	(32, 25)	1127	(47, 14)	1127	(46, 14)
1110	(68, 7)	1118	(38, 22)	1117	(48, 18)	1116	(53, 17)	1115	(40, 17)	1117	(40, 30)	1111	(54, 11)	1115	(52, 18)	1115	(53, 18)
1105	(9, 4)	1104	(37, 6)	1105	(69, 7)	1105	(41, 6)	1108	(57, 3)	1102	(57, 12)	1105	(23, 4)	1105	(44, 6)	1105	(43, 6)
1104	(10, 4)	1094	(3, 3)	1086	(12, 1)	1093	(8, 2)	1085	(16, 0.1)	1088	(2, 3)	1101	(8, 3)	1093	(8, 2)	1093	(8, 2)
1064	(14, 3)	1068	(3, 10)	1071	(70, 20)	1069	(26, 13)	1073	(71, 16)	1068	(23, 22)	1066	(5, 8)	1068	(24, 14)	1068	(25, 13)
1060	(3, 28)	1060	(33, 29)	1060	(41, 13)	1060	(29, 29)	1059	(41, 11)	1061	(44, 27)	1059	(16, 26)	1060	(32, 22)	1060	(31, 22)
973	(20, 29)	982	(14, 33)	986	(20, 22)	982	(19, 27)	985	(35, 16)	986	(13, 38)	975	(17, 31)	982	(20, 29)	982	(19, 28)
967	(5, 15)	973	(17, 24)	983	(30, 26)	976	(19, 23)	983	(7, 24)	979	(30, 34)	969	(10, 18)	976	(18, 24)	976	(18, 23)
919	(6, 12)	923	(11, 18)	919	(15, 18)	921	(12, 16)	917	(10, 15)	923	(17, 26)	920	(6, 14)	921	(11, 18)	921	(12, 17)
863	(26, 2)	861	(26, 7)	862	(12, 14)	862	(24, 9)	863	(6, 12)	861	(21, 16)	861	(27, 3)	862	(24, 9)	862	(24, 9)
834	(10, 17)	829	(9, 54)	836	(32, 30)	833	(17, 35)	835	(35, 7)	835	(18, 98)	833	(9, 31)	834	(17, 44)	834	(17, 39)
832	(8, 100)	835	(11, 100)	825	(12, 100)	830	(11, 100)	826	(8, 100)	824	(11, 100)	833	(9, 100)	828	(11, 100)	829	(11, 100)

**Table 19** continued.

Twist Conformer								Bent Conformer									
d <sub>6</sub> location								d <sub>6</sub> location									
Carbon 1		Carbon 2		Carbon 3		Average		Carbon 1		Carbon 2		Carbon 3		Average		Average T. and B.	
Freq.	Int. (IR, R)	Freq.	Int. (IR, R)	Freq.	Int. (IR, R)	Freq.	Int. (IR, R)	Freq.	Int. (IR, R)	Freq.	Int. (IR, R)	Freq.	Int. (IR, R)	Freq.	Int. (IR, R)	Freq.	Int. (IR, R)
792	(9, 10)	791	(6, 39)	778	(18, 25)	786	(11, 26)	769	(4, 15)	786	(13, 50)	792	(4, 22)	785	(8, 28)	786	(10, 27)
788	(28, 4)	773	(27, 4)	752	(40, 13)	767	(33, 8)	761	(43, 13)	752	(38, 2)	785	(30, 7)	767	(38, 7)	767	(36, 7)
779	(17, 21)	757	(30, 10)	737	(60, 1)	753	(38, 9)	736	(41, 1)	745	(44, 11)	770	(23, 12)	753	(36, 9)	753	(37, 9)
731	(14, 6)	732	(19, 6)	734	(44, 1)	733	(26, 4)	733	(61, 1)	734	(22, 5)	731	(15, 6)	733	(27, 4)	733	(27, 4)
697	(0.04, 4)	709	(1, 7)	714	(7, 3)	709	(3, 4)	697	(8, 0.6)	718	(6, 7)	699	(0.3, 5)	706	(4, 4)	708	(3, 4)
596	(2, 0.3)	606	(10, 1)	668	(21, 1)	629	(11, 1)	690	(15, 2)	636	(18, 2)	594	(3, 0.2)	630	(11, 1)	630	(11, 1)
547	(2, 3)	568	(4, 3)	546	(5, 2)	555	(4, 2)	540	(6, 1)	556	(3, 3)	558	(6, 3)	554	(6, 2)	554	(5, 2)
492	(31, 1)	465	(27, 2)	445	(41, 1)	463	(34, 1)	441	(35, 1)	451	(33, 2)	479	(28, 1)	460	(34, 1)	461	(34, 1)
238	(0.2, 0.6)	229	(0.2, 1)	212	(0.2, 0.6)	224	(0.2, 0.6)	205	(0.1, 0.5)	217	(0.2, 1)	232	(0.2, 0.6)	220	(0.2, 1)	222	(0.2, 1)
28	(0.2, 0.03)	29	(0.3, 0.1)	29	(0.6, 0.2)	29	(0.4, 0.1)	26	(0.6, 0.2)	24	(0.5, 0.2)	22	(0.3, 0.03)	24	(0.4, 0.1)	26	(0.4, 0.1)

B3LYP calculations. Scaling factors: 0.985 below 1500 cm<sup>-1</sup>, 0.973 between 1500 and 2000 cm<sup>-1</sup> and 0.961 above 2000 cm<sup>-1</sup>

are substituted and whether the molecules are bent or twisted. It is rather remarkable that the average calculated frequencies for the bent and twist structures are virtually identical for either the  $d_2$  and  $d_6$  isotopomers even though for individual configurations the range of values can be significant. For frequencies above  $800\text{ cm}^{-1}$  all of the calculated values for the individual configurations are within  $10\text{ cm}^{-1}$  of the average values shown in Table 16. This is also true for all but three of the lower frequencies. The ring-twisting (radial mode) is calculated to be in the  $231$  to  $257\text{ cm}^{-1}$  range for the different configurations of the  $d_2$  isotopomer and  $205$  to  $238\text{ cm}^{-1}$  for the  $d_6$ . The lowest ring-bending mode is computed to be  $497$  to  $540\text{ cm}^{-1}$  for the  $d_2$  and  $441$  to  $492\text{ cm}^{-1}$  for the  $d_6$ , and the  $\text{CD}_2$  rocking mode is calculated to vary from  $648$  to  $732\text{ cm}^{-1}$  for the  $d_2$  and from  $596$  to  $668\text{ cm}^{-1}$  for the  $d_6$ . Since this vibration is quite anharmonic, as shown by Bauman in a previous work [98], the good agreement between computed and observed wavenumbers is somewhat surprising. For the totally anharmonic pseudorotational motion the computed value of  $25\text{ cm}^{-1}$  is considerably higher than the pseudorotational constant of  $2.5\text{ cm}^{-1}$ . These calculations, are carried out for rigid, fixed structures whereas the actual vapor-phase molecule is non-rigid and flopping rapidly between each of these different configurations. Thus the observed spectra do not show separate vibrational bands in the infrared and Raman spectra for the twist and bent conformations.

Examination of Fig. 43 shows that the  $d_1$  isotopomer can have six different bent configurations and five different twist forms. Table 20 lists the calculated vibrational frequencies for each of these configurations. The average of these is shown in Table 17

**Table 20**

Calculated vibrational frequencies ( $\text{cm}^{-1}$ ) for conformers of cyclopentane- $\text{d}_1$ . Different positions of deuterium substitution.

Planar		Twist Conformer											
		$\text{d}_1$ - location											
		Carbon 1		Carbon 2 (a)		Carbon 2 (b)		Carbon 3 (a)		Carbon 3 (b)		Average	
Freq.	Int. (IR, R)	Freq.	Int. (IR, R)	Freq.	Int. (IR, R)	Freq.	Int. (IR, R)	Freq.	Int. (IR, R)	Freq.	Int. (IR, R)	Freq.	Int. (IR, R)
2975	(100, 5)	2966	(100, 33)	2969	(100, 34)	2968	(100, 23)	2971	(100, 25)	2971	(100, 29)	2969	(100, 30)
2960	(0, 47)	2957	(21, 65)	2956	(35, 52)	2956	(36, 39)	2957	(24, 56)	2957	(17, 78)	2957	(26, 59)
2953	(7, 53)	2954	(26, 92)	2954	(33, 84)	2954	(5, 100)	2953	(16, 100)	2954	(22, 98)	2954	(21, 100)
2941	(8, 100)	2952	(42, 67)	2948	(26, 54)	2952	(51, 36)	2949	(45, 57)	2943	(33, 12)	2949	(39, 47)
2932	(0, 0)	2938	(44, 25)	2930	(62, 64)	2942	(53, 3)	2943	(45, 4)	2930	(47, 86)	2937	(50, 34)
2930	(46, 0.6)	2916	(21, 47)	2919	(16, 22)	2928	(57, 34)	2930	(66, 53)	2917	(55, 22)	2922	(43, 38)
2929	(96, 0)	2912	(40, 31)	2913	(31, 25)	2913	(28, 20)	2915	(23, 21)	2913	(13, 37)	2913	(27, 27)
2922	(17, 11)	2904	(36, 9)	2904	(39, 8)	2904	(43, 9)	2911	(34, 25)	2906	(28, 6)	2906	(36, 12)
2918	(0, 13)	2897	(16, 100)	2897	(17, 100)	2897	(20, 61)	2900	(32, 40)	2897	(13, 100)	2898	(19, 81)
2161	(15, 12)	2162	(18, 23)	2167	(20, 28)	2147	(21, 15)	2136	(21, 20)	2166	(20, 34)	2156	(20, 24)
1489	(13, 16)	1478	(4, 11)	1480	(16, 14)	1480	(16, 12)	1482	(19, 14)	1482	(17, 13)	1480	(16, 13)
1473	(100, 0)	1461	(100, 13)	1460	(77, 12)	1460	(78, 10)	1461	(100, 12)	1461	(100, 11)	1461	(100, 11)
1464	(49, 20)	1456	(93, 52)	1457	(100, 62)	1457	(100, 50)	1459	(75, 21)	1459	(76, 20)	1458	(97, 39)
1456	(0, 39)	1454	(42, 53)	1455	(41, 61)	1455	(42, 50)	1452	(11, 64)	1452	(11, 61)	1454	(32, 58)
1338	(5, 2)	1334	(14, 8)	1339	(32, 15)	1336	(15, 4)	1338	(29, 4)	1343	(36, 14)	1338	(28, 9)
1331	(32, 13)	1332	(7, 6)	1325	(14, 18)	1331	(11, 1)	1330	(5, 1)	1323	(3, 6)	1328	(9, 6)
1328	(0.08, 1)	1321	(14, 6)	1321	(8, 5)	1323	(17, 9)	1327	(9, 5)	1320	(6, 6)	1322	(12, 6)
1301	(0.02, 2)	1319	(2, 11)	1319	(7, 2)	1312	(8, 15)	1301	(4, 5)	1317	(33, 7)	1314	(12, 8)
1266	(0, 13)	1299	(12, 15)	1302	(18, 29)	1297	(1, 4)	1296	(17, 20)	1300	(7, 17)	1299	(12, 17)
1264	(0.7, 26)	1286	(9, 20)	1285	(6, 8)	1270	(25, 36)	1266	(17, 31)	1279	(8, 14)	1277	(14, 22)
1258	(0.003, 9)	1240	(17, 18)	1252	(13, 39)	1231	(7, 12)	1234	(3, 6)	1255	(9, 19)	1242	(11, 18)
1252	(0, 8)	1212	(8, 19)	1216	(8, 7)	1205	(6, 23)	1200	(5, 24)	1211	(1, 6)	1209	(6, 16)
1214	(0.05, 2)	1169	(5, 6)	1184	(3, 4)	1173	(15, 2)	1185	(12, 5)	1192	(11, 16)	1180	(10, 7)
1180	(2, 1)	1159	(1, 19)	1172	(2, 29)	1162	(1, 20)	1166	(3, 11)	1187	(3, 9)	1169	(2, 17)
1096	(1, 3)	1099	(1, 8)	1085	(1, 11)	1113	(10, 11)	1108	(26, 16)	1093	(0.3, 9)	1100	(9, 11)
1055	(0, 9)	1024	(0.4, 25)	1022	(1, 28)	1027	(1, 26)	1031	(1, 23)	1028	(0.6, 20)	1026	(1, 24)
1037	(0.9, 8)	1014	(5, 25)	1007	(3, 18)	1009	(8, 22)	1015	(4, 18)	977	(8, 8)	1004	(6, 18)
977	(2, 0.5)	949	(42, 3)	965	(27, 11)	951	(27, 1)	964	(18, 4)	970	(2, 14)	959	(25, 6)
940	(26, 1)	920	(24, 4)	928	(27, 11)	906	(46, 3)	893	(47, 19)	944	(35, 6)	918	(39, 9)
899	(50, 0.6)	892	(46, 29)	886	(47, 27)	891	(55, 23)	887	(55, 2)	884	(51, 6)	888	(56, 17)
843	(0.4, 100)	863	(19, 100)	866	(18, 100)	869	(10, 100)	869	(9, 100)	869	(7, 100)	867	(14, 100)
835	(20, 1)	857	(15, 4)	848	(11, 24)	856	(15, 7)	842	(9, 6)	825	(10, 4)	846	(13, 8)
746	(1, 8)	831	(13, 6)	811	(32, 10)	838	(12, 7)	825	(9, 3)	785	(36, 4)	818	(23, 6)
743	(33, 0.3)	781	(7, 4)	607	(6, 4)	783	(7, 2)	792	(4, 2)	760	(14, 10)	745	(9, 4)
686	(19, 3)	685	(8, 1)	707	(15, 5)	727	(12, 1)	746	(19, 0.4)	741	(10, 3)	721	(14, 2)
680	(0, 6)	606	(2, 4)	609	(2, 4)	592	(4, 3)	603	(3, 3)	607	(1, 2)	603	(2, 3)
649	(24, 3)	543	(30, 2)	540	(32, 2)	528	(28, 2)	509	(23, 1)	532	(29, 1)	530	(31, 1)
196i	(0, 0)	258	(0.2, 1)	253	(0.2, 1)	252	(0.2, 0.6)	246	(0.1, 0.6)	247	(0.2, 0.5)	251	(0.2, 0.6)
186i	(0.003, 0.01)	32	(0.3, 0.04)	32	(0.3, 0.1)	32	(0.3, 0.1)	32	(0.3, 0.1)	33	(0.3, 0.1)	32	(0.4, 0.1)



and compared to observed values as well as to cyclopentane vibrational frequencies. Notably, most of the frequencies are little changed from the undeuterated molecule since the substitution only directly affects results in the lowering of three vibrations (C-D stretch and two C-D wags).

Table 14 presents the data for the  $d_0$  and Table 15 for the  $d_{10}$  molecules which would have  $D_{5h}$  symmetry if the molecule were planar. Miller and Inskeep [101] recognized that cyclopentane is not planar but nonetheless attempted to make assignments based on  $D_{5h}$  symmetry. This was in the early days of vibrational spectroscopy and only a few assignments were done correctly. Moreover, the authors did not recognize that the E type modes, which are doubly degenerate for a planar structure would split significantly for the  $C_2$  or  $C_s$  conformation. In 1969 and 1972 studies by Schettino and Marzocchi [102,103] of cyclopentane- $d_0$  and  $d_{10}$  crystals, the authors recognized the importance of splitting but, as shown in Tables 14 and 15, many of their assignments needed to be corrected by this present work. Nonetheless, having their data available has helped to confirm the assignments for the  $d_0$  and  $d_{10}$  isotopomers.

A particularly difficult aspect in making the vibrational assignments in the past was the uncertainty in knowing how much the doubly degenerate E modes in  $D_{5h}$  symmetry would split when the molecule took on either its twist or bent conformation. The work of Schettino and Marzocchi [102,103] on the  $d_0$  and  $d_{10}$  crystals was helpful, even though their assignments were not always correct. The present day reliability of density functional theory calculations in predicting frequencies, however, proved to be

remarkably helpful, and it is amazing that the calculated splittings agreed very well with those observed for all isotopomers. It is also a bit surprising that both the  $C_2$  and  $C_s$  structure calculations yield almost exactly the same average vibrational frequencies.

Table 21 presents a summary of the observed and calculated ring vibrational frequencies for each of the isotopomers. There is of course considerable vibrational mixing between the ring and  $CH_2$  (or  $CD_2$ ) wagging, twisting, and rocking modes so these should not be considered to be purely ring stretching or bending modes. However, the examination of the individual motions shows these to primarily involve the motion of the ring atoms. As seen in Table 25 and as expected, each of the ring mode frequencies decreases with increased deuteration. The one exception to this involves the highest frequency pair of ring stretches for the  $d_{10}$  isotopomer where the observed bands are at 1080 and 1060  $cm^{-1}$ , even higher than the  $d_0$  values of 1030 and 1024  $cm^{-1}$ . This results from the interaction with lower frequency  $CD_2$  modes interacting and pushing these values higher.



**Table 21**  
Ring vibrations ( $\text{cm}^{-1}$ ) of cyclopentane and its isotopomers.

$d_0$			$d_1$			$d_2$			$d_6$			$d_{10}$		
Obs.	$C_2, C_s$	Planar	Obs.	$C_2, C_s$	Planar	Obs.	$C_2, C_s$	Planar	Obs.	$C_2, C_s$	Planar	Obs.	$C_2, C_s$	Planar
1030	1033	1056	1045	1026	1055	1035	1022	1050	985	982	1018	1080	1078	1067
1024	1021		1008	1004	1037	940	943	996	834	834	872	1060	1069	
896	893	903	925	918	940	897	888	894	755	753	803	759	754	755
881	886		895	888	899	830	827	818	760	767	769	739	732	
886	868	847	885	867	843	874	862	831	841	829	811	805	792	777
618	613	680	604	603	686	570	594	680	572	554	669	515	512	642
546	546		530	529	649	515	516	663	737	733	695	427	430	
273	259	197i	268	249	196i	261	244	196i	240	222	184i	216	204	155i
5	25		5	29	186i	—	29	179i	—	26	158i	4	20	

B3LYP calculations. Scaling factor: 0.985

## Conclusions

In this study ab initio computations have been used to calculate the structure of the two conformational forms of cyclopentane, and it has been confirmed that the energy difference between the two forms is very small, almost certainly less than  $10\text{ cm}^{-1}$ . These calculations also support the experimentally determined two-dimensional potential energy surface with a barrier to planarity of  $1808\text{ cm}^{-1}$  which has been previously reported [98]. In this present work the barrier that resulted was found to be  $1887\text{ cm}^{-1}$  according to CCSD/cc-pVTZ calculations and  $1944\text{ cm}^{-1}$  according to MP4/cc-pVTZ calculations.

The reported infrared and Raman spectra for vapor, liquid, and solid phases for cyclopentane and four of its deuterated isotopomers agree very well with the computed B3LYP/cc-pVTZ calculated spectra. Utilizing the extensive experimental data complemented by the theoretical calculations, the first full, meaningful assignment of this remarkable molecule has been achieved.

## CHAPTER VIII

## METHYLCYCLOPROPANE AND RELATED MOLECULES

**Introduction**

Internal rotors attached to several three-membered ring molecules have been studied. Ab initio (CCSD/cc-pVTZ and MP2/cc-pVTZ) calculations have been carried out to determine the energies of the conformations as well as barriers to interconversion. The molecules investigated are shown below.

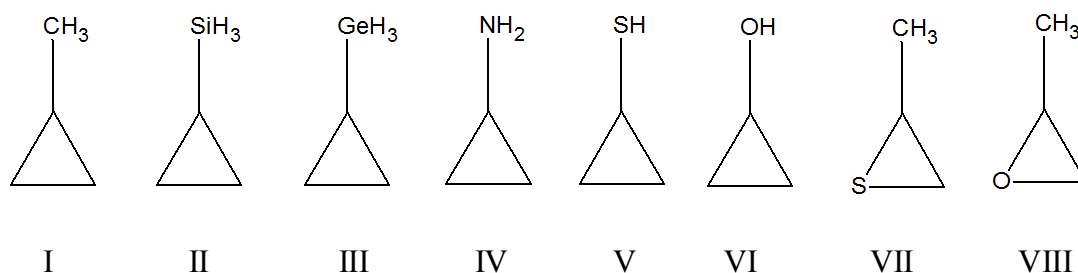
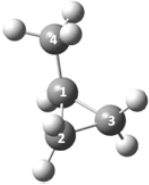
**Results and discussion**

Table 22 compares the experimentally determined barriers to internal rotation of methylcyclopropane (I), cyclopropylsilane (II), and cyclopropylgermane (III) [104-106] to the calculated (CCSD/cc-pVTZ and MP2/cc-pVTZ) barriers. The table also provides calculated data on bond distances changes and angles.

**Table 22**

Potential energy values and calculated geometrical parameters of the minimum energy conformations and barriers of methylcyclopropane, cyclopropylsilane and cyclopropylgermane.

	methylcyclopropane		cyclopropylsilane		cyclopropylgermane	
	minimum	barrier	minimum	barrier	minimum	barrier
Experimental energy (cm <sup>-1</sup> )	0	1060 <sup>a</sup>	0	694 <sup>b</sup>	0	474 <sup>c</sup>
CCSD/cc-pVTZ energy (cm <sup>-1</sup> )	0	987	0	616	0	472
MP2/cc-pVTZ energy (cm <sup>-1</sup> )	0	1030	0	662	0	517
< C <sub>2</sub> C <sub>1</sub> C <sub>3</sub> (degrees)	60.3	60.0	59.1	59.0	59.4	59.3
< C <sub>1</sub> C <sub>2</sub> C <sub>3</sub> (degrees)	59.9	60.0	60.4	60.5	60.3	60.3
< C <sub>1</sub> C <sub>3</sub> C <sub>2</sub> (degrees)	59.9	60.0	60.4	60.5	60.3	60.3
C <sub>1</sub> -C <sub>2</sub> (Å)	1.510	1.506	1.497	1.518	1.501	1.515
C <sub>1</sub> -C <sub>3</sub> (Å)	1.504	1.506	1.517	1.518	1.514	1.514
C <sub>2</sub> -C <sub>3</sub> (Å)	1.510	1.506	1.497	1.496	1.501	1.499
C <sub>1</sub> -C <sub>4</sub> , Si, Ge (Å)	1.508	1.521	1.858	1.873	1.926	1.935

<sup>a</sup> Ref. [104].

<sup>b</sup> Ref. [105].

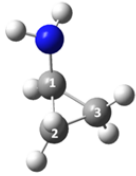
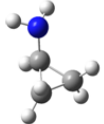
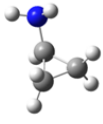
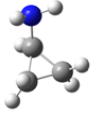
<sup>c</sup> Ref. [106].

Cyclopropylamine (IV) (Table 23 and Fig. 54) possesses two different barriers to interconversion. Kalasinsky et al. [107] reported the experimental barriers to internal rotation of this molecule to be  $1077 \pm 150 \text{ cm}^{-1}$  and  $1266 \pm 150 \text{ cm}^{-1}$  as compared to the calculated values in the present work of 956 and  $1507 \text{ cm}^{-1}$  (CCSD/cc-pVTZ), and 981 and  $1565 \text{ cm}^{-1}$  (MP2/cc-pVTZ).

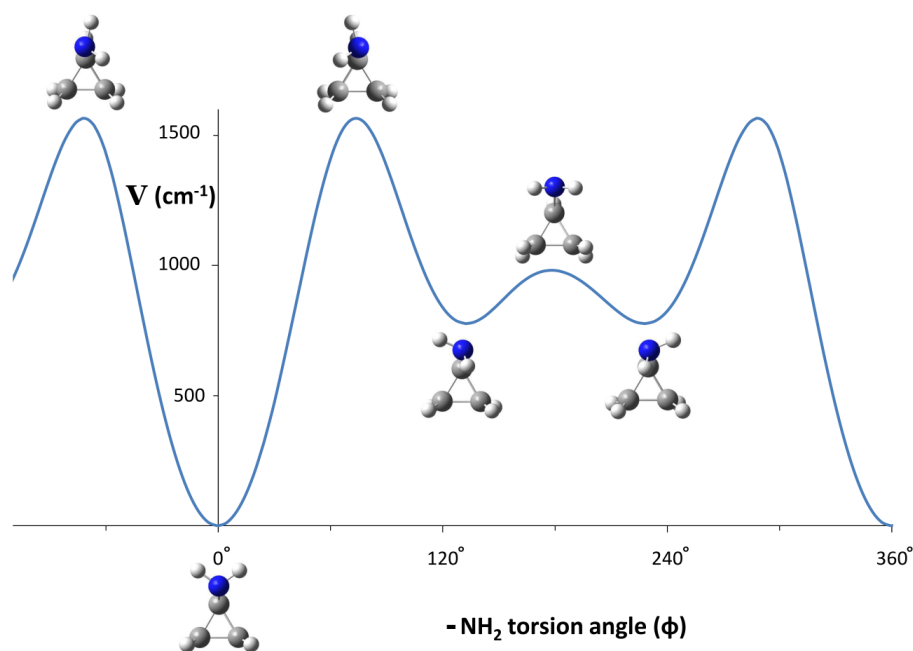
Cyclopropanethiol (V) (Table 24 and Fig. 55) and cyclopropanol (VI) (Table 25 and Fig. 56) also possess two different barriers to interconversion.

**Table 23**

Potential energy values and calculated geometrical parameters of the minimum energy conformations and barriers of cyclopropylamine.

	cyclopropylamine			
	minima		barriers	
				
Experimental energy (cm <sup>-1</sup> )	0	592 <sup>a</sup>	1077 <sup>a</sup>	1266 <sup>a</sup>
CCSD/cc-pVTZ energy (cm <sup>-1</sup> )	0	753	956	1507
MP2/cc-pVTZ energy (cm <sup>-1</sup> )	0	777	981	1565
< C <sub>2</sub> C <sub>1</sub> C <sub>3</sub> (degrees)	60.4	60.6	60.2	60.7
< C <sub>1</sub> C <sub>2</sub> C <sub>3</sub> (degrees)	59.8	59.2	59.9	59.7
< C <sub>1</sub> C <sub>3</sub> C <sub>2</sub> (degrees)	59.8	60.1	59.9	59.6
C <sub>1</sub> -C <sub>2</sub> (Å)	1.501	1.508	1.504	1.499
C <sub>1</sub> -C <sub>3</sub> (Å)	1.501	1.495	1.504	1.501
C <sub>2</sub> -C <sub>3</sub> (Å)	1.510	1.516	1.509	1.516
C <sub>1</sub> -N (Å)	1.442	1.444	1.444	1.454

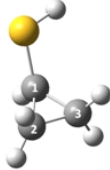
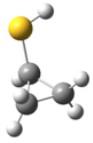
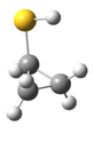
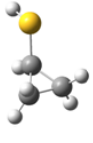
<sup>a</sup> Ref. [107].

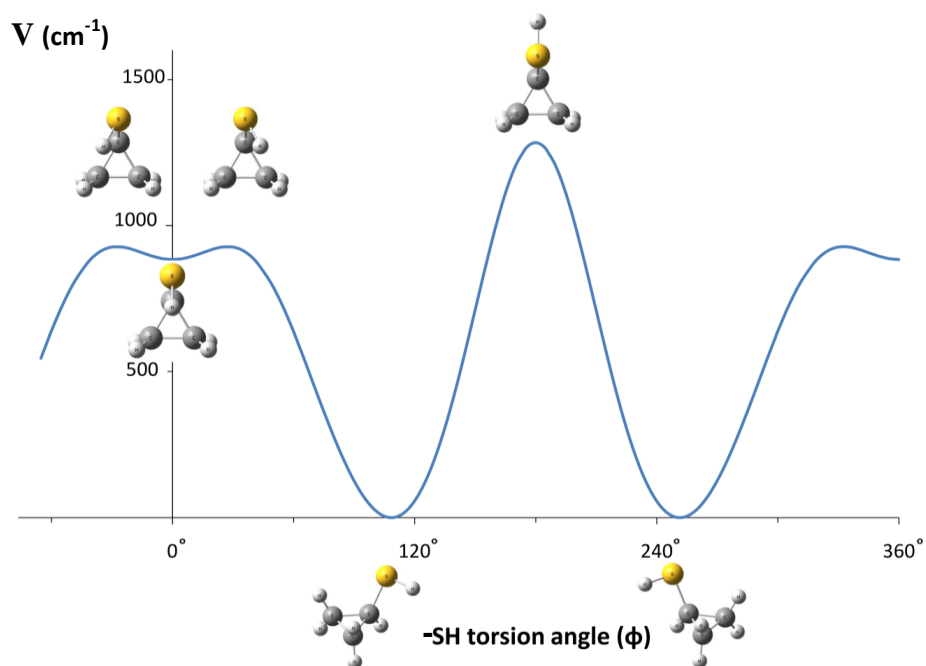


**Fig. 54.** Internal rotation potential energy function of cyclopropylamine. MP2/cc-pVTZ calculations.

**Table 24**

Potential energy values and calculated geometrical parameters of the minimum energy conformations and barriers of cyclopropanethiol.

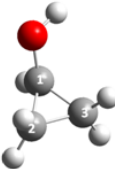
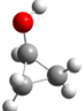
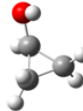
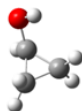
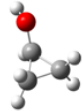
	cyclopropanethiol			
	minima		barriers	
				
Experimental energy (cm <sup>-1</sup> )	---	---	---	---
CCSD/cc-pVTZ energy (cm <sup>-1</sup> )	0	834	873	1189
MP2/cc-pVTZ energy (cm <sup>-1</sup> )	0	884	927	1284
< C <sub>2</sub> C <sub>1</sub> C <sub>3</sub> (degrees)	60.0	60.6	60.5	60.4
< C <sub>1</sub> C <sub>2</sub> C <sub>3</sub> (degrees)	60.0	59.7	59.7	59.8
< C <sub>1</sub> C <sub>3</sub> C <sub>2</sub> (degrees)	60.1	59.7	59.8	59.8
C <sub>1</sub> -C <sub>2</sub> (Å)	1.506	1.499	1.502	1.501
C <sub>1</sub> -C <sub>3</sub> (Å)	1.505	1.499	1.500	1.501
C <sub>2</sub> -C <sub>3</sub> (Å)	1.505	1.514	1.511	1.511
C <sub>1</sub> -S (Å)	1.791	1.799	1.801	1.807



**Fig. 55.** Internal rotation potential energy function of cyclopropanethiol. MP2/cc-pVTZ calculations.

**Table 25**

Potential energy values and calculated geometrical parameters of the minimum energy conformations and barriers of cyclopropanol.

	cyclopropanol			
	minima		barriers	
				
Experimental energy (cm <sup>-1</sup> )	---	---	---	---
CCSD/cc-pVTZ energy (cm <sup>-1</sup> )	0	758	765	842
MP2/cc-pVTZ energy (cm <sup>-1</sup> )	0	764	775	864
< C <sub>2</sub> C <sub>1</sub> C <sub>3</sub> (degrees)	60.9	61.2	61.1	61.1
< C <sub>1</sub> C <sub>2</sub> C <sub>3</sub> (degrees)	59.9	59.4	59.4	59.4
< C <sub>1</sub> C <sub>3</sub> C <sub>2</sub> (degrees)	59.2	59.4	59.5	59.4
C <sub>1</sub> -C <sub>2</sub> (Å)	1.490	1.496	1.498	1.494
C <sub>1</sub> -C <sub>3</sub> (Å)	1.501	1.496	1.495	1.494
C <sub>2</sub> -C <sub>3</sub> (Å)	1.516	1.523	1.521	1.520
C <sub>1</sub> -O (Å)	1.399	1.398	1.399	1.405

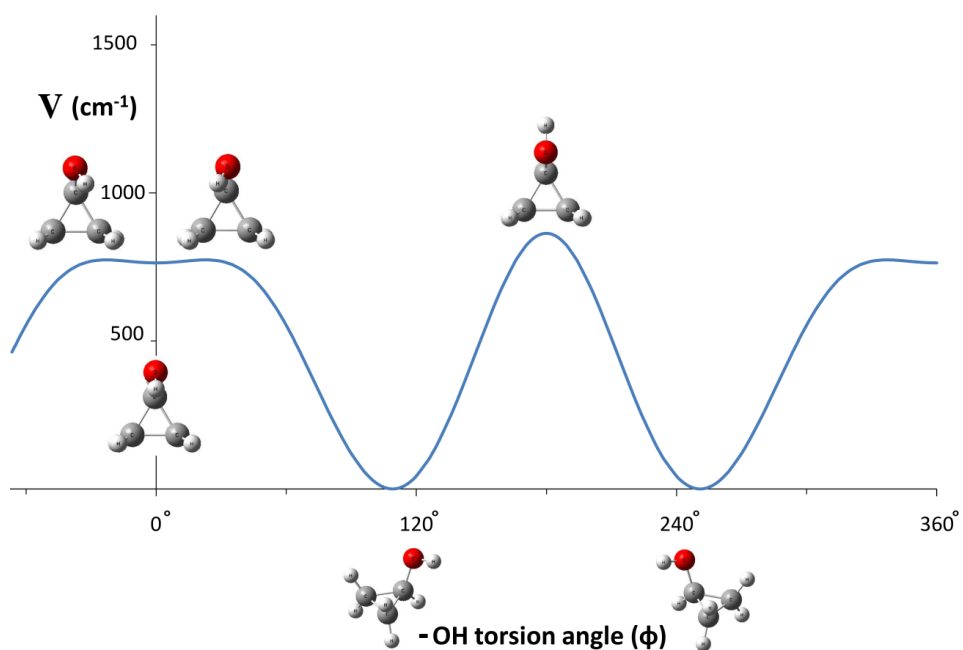


**Fig. 56.** Internal rotation potential energy function of cyclopropanol. MP2/cc-pVTZ calculations.

Fig. 57 shows the calculated transitions obtained from Raman vapor-phase spectra of methylcyclopropane [104]. The theoretical potential function based on MP2/cc-pVTZ calculations is in excellent agreement with the experimental potential function. The experimental potential function has the form:

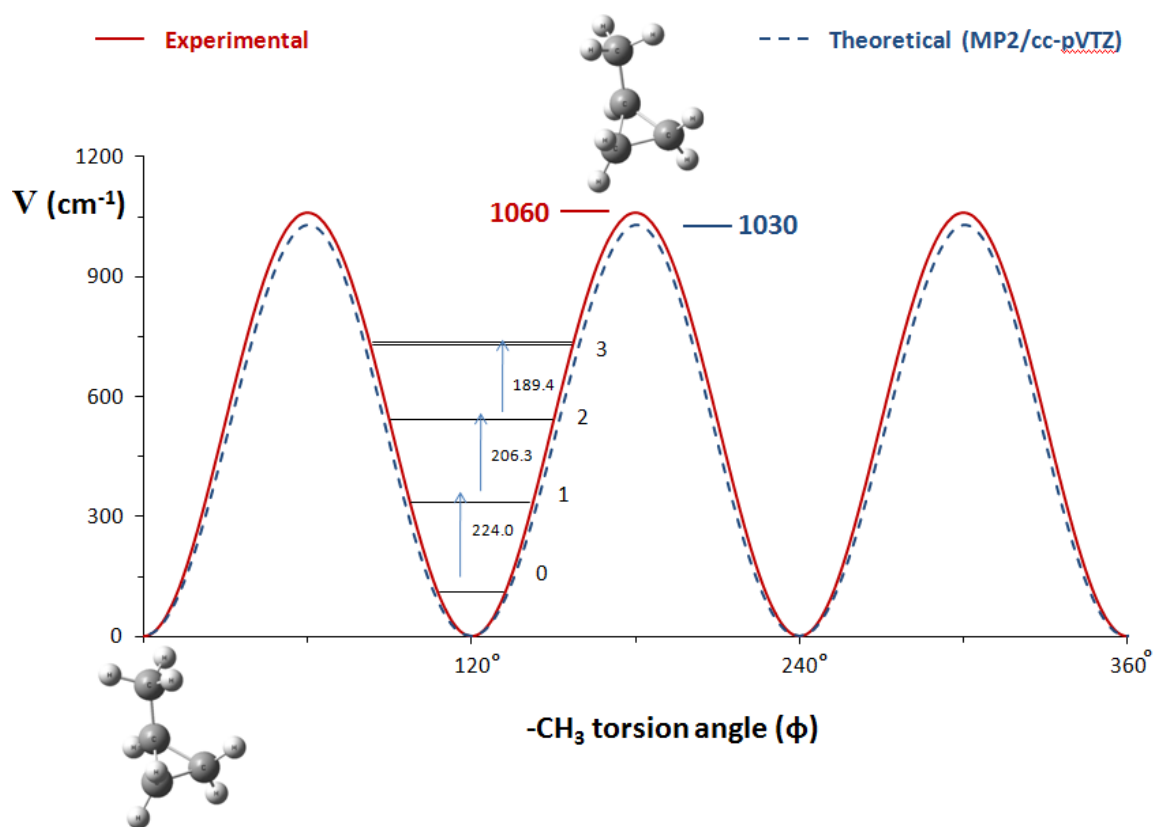
$$\frac{1}{2} V_3 (1 - \cos(\phi)) + \frac{1}{2} V_6 (1 - \cos(3\phi)) \quad (26)$$

where  $V_3 = 1060 \text{ cm}^{-1}$  and  $V_6 = 9 \text{ cm}^{-1}$  [104].

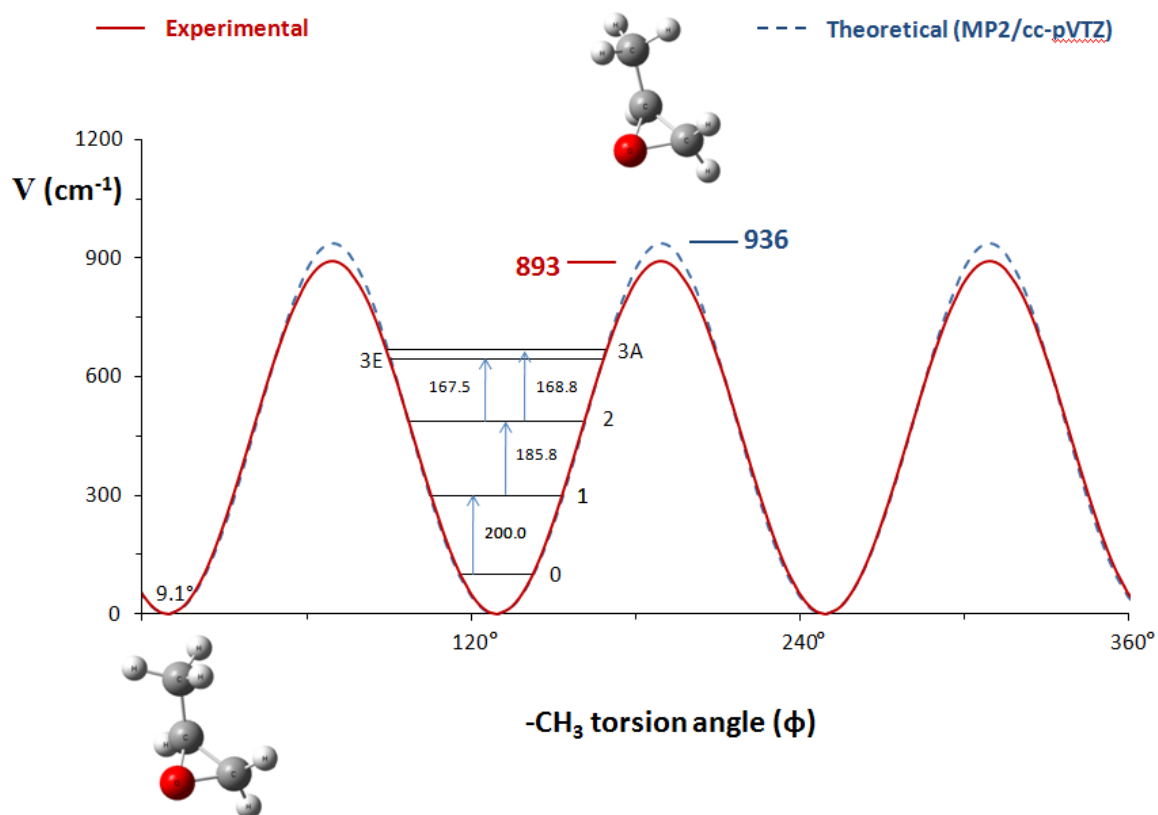
Fig. 58 presents a comparison between the experimental and calculated MP2/cc-pVTZ potential energy function of propylene oxide. The experimental potential function obtained from vapor-phase Raman spectra has the form of Eq. 26 and  $V_3 = 893 \text{ cm}^{-1}$  and  $V_6 = -7 \text{ cm}^{-1}$  [104].

Table 26 compares the experimentally determined barriers of internal rotation of propylene sulfide (VII) and propylene oxide (VIII) [104] with the barriers from CCSD/cc-pVTZ and MP2/cc-pVTZ calculations. Finally, Fig. 59 shows that the potential energy functions of propylene sulfide (VII) and propylene oxide (VIII) are only slightly different.





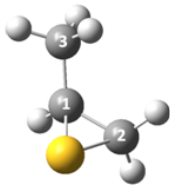
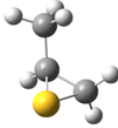
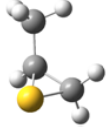
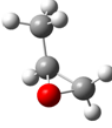
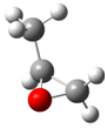
**Fig. 57.** Experimental and theoretical internal rotation potential energy functions of methylcyclopropane.



**Fig. 58.** Experimental and theoretical potential internal rotation energy functions of propylene oxide.

**Table 26**

Potential energy values and calculated geometrical parameters of the minimum energy conformations and barriers of propylene sulfide and propylene oxide.

	propylene sulfide		propylene oxide	
	minimum	barrier	minimum	barrier
				
Experimental energy (cm <sup>-1</sup> )	0	1148 <sup>a</sup>	0	893 <sup>a</sup>
CCSD/cc-pVTZ energy (cm <sup>-1</sup> )	0	1121	0	900
MP2/cc-pVTZ energy (cm <sup>-1</sup> )	0	1180	0	936
< O,SC <sub>1</sub> C <sub>3</sub> (degrees)	66.0	65.7	59.2	59.0
< C <sub>1</sub> O,SC <sub>2</sub> (degrees)	47.9	47.9	61.7	61.8
< C <sub>1</sub> C <sub>3</sub> O,S (degrees)	66.2	66.4	59.1	59.2
C <sub>1</sub> -C <sub>2</sub> (Å)	1.481	1.483	1.464	1.465
C <sub>1</sub> -O,S (Å)	1.827	1.831	1.426	1.429
O,S-C <sub>2</sub> (Å)	1.824	1.821	1.427	1.425
C <sub>1</sub> -C <sub>3</sub> (Å)	1.507	1.521	1.502	1.514

<sup>a</sup> Ref. [104].

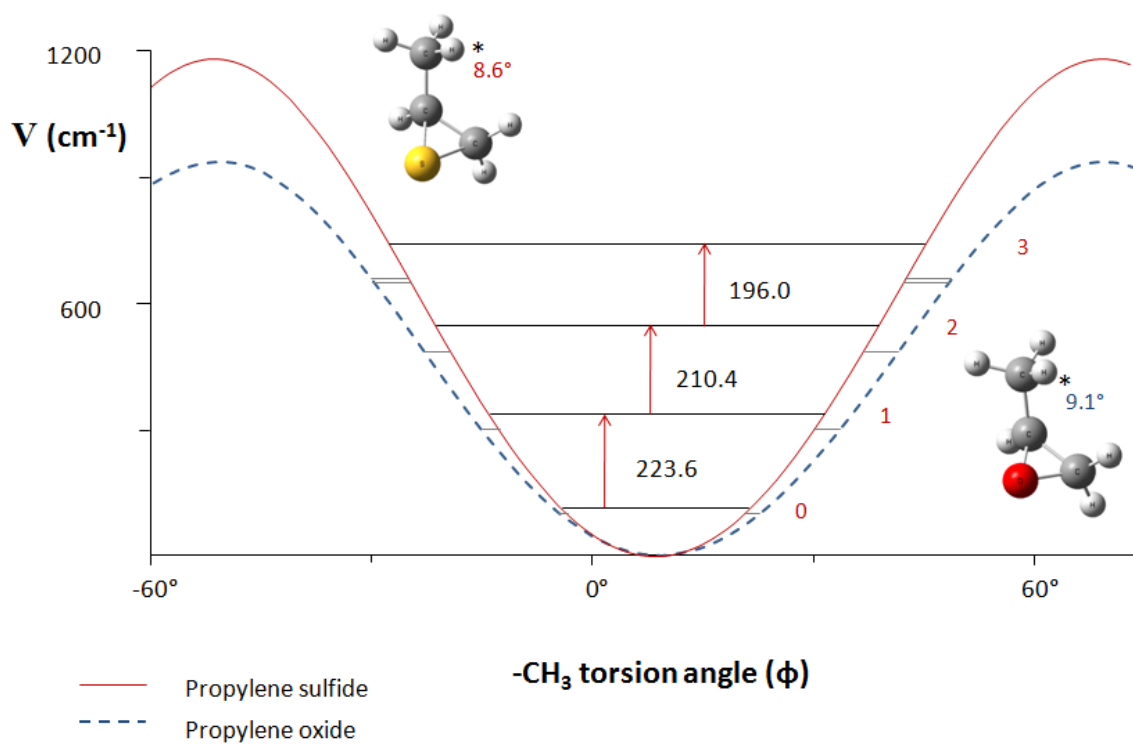
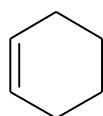


**Fig. 59.** Experimental internal rotation potential energy functions for propylene sulfide and propylene oxide.

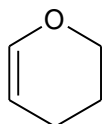
CHAPTER IX  
CYCLOHEXENE AND ITS OXYGEN ANALOGS

**Introduction**

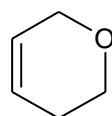
Approximately twenty years ago the low-frequency vibrations and the conformational dynamics of cyclohexene (CYH) and its oxygen analogs 2,3-dihydropyran (23DHP), 3,6-dihydro-2H-pyran (36DHP), 1,4-dioxene (14DOX), and 1,3-dioxene (13DOX) were investigated by Rivera-Gaines, Leibowitz and Tecklenburg in Laane's research group [5,6]. Previously, the far-infrared and Raman spectra of these molecules had been reported [7-10].



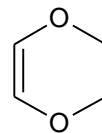
CYH



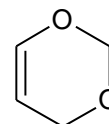
23DHP



36DHP



14DOX



13DOX

Using the vibrational data two-dimensional vibrational potential energy surfaces in terms of their ring-bending and ring-twisting vibrations were computed. Each of the molecules was found to be twisted with a high barrier to planarity. An intermediate energy bent structure was found to be a saddle point in the potential energy surface. These studies were complemented by molecular mechanics (MM2) calculations. Microwave [11-13] work on these systems had also been reported. In 1985 a more recent microwave study of 14DOX was also published [14].

In the present study high level ab initio calculations have been carried out to compute the structures of these molecules and to predict the energy differences between the twisted, bent, and planar structures. These were then compared to values from previous work. Density functional theory calculations were also carried out to compare the theoretical vibrational frequencies to the three lowest experimental frequencies. Previous theoretical calculations using various basis sets for cyclohexene [108,109] and the oxygen analogs [110,111] have been reported, and the results are compared to those.

### **Computations**

Initial MP2/3-11++g(d,p) computations of the twist and planar conformations were performed by Teresa Brito in some cases with the help of Kathleen McCann. In this work the geometrical parameters for the structure of each molecule and the rotational constants were calculated utilizing ab initio (MP2/cc-pVTZ) and density functional theory (B3LYP/cc-pVTZ) computations. The low-frequency vibrations were calculated using density functional theory (B3LYP/cc-pVTZ). The twisting barriers and barriers to interconversion along with the angles for the twisted and bent structures were calculated using ab initio (MP2/cc-pVTZ) computations. The scaling factor for the calculated (B3LYP/cc-pVTZ) Raman spectra for the molecules 23DHP and 14DOX were 0.984 for frequencies below  $1900\text{ cm}^{-1}$  and 0.961 for the frequencies above  $2750\text{ cm}^{-1}$ . The Gaussian 03 program [112] was used to carry out the ab initio and the density functional theory computations.

## Results and discussion

Fig. 60 shows the bond lengths and angles computed for the five different molecules using the MP2/cc-pVTZ computations. Table 27 compares the values to those reported from the microwave work. Assumed values from the microwave (MW) work [11-14] are shown in parentheses. For cyclohexene (CYH) the electron diffraction (ED) data [113] are also shown. The agreement can be seen to be very good. Table 28 compares the scaled vibrational frequencies from the density functional theory (B3LYP/cc-pVTZ) calculation for the ring-bending, ring-twisting, and double bond twisting vibrations to the experimental values. Table 29 compares the calculated rotational constants to those from the microwave studies [11-14]. Again the agreement is excellent, demonstrating that both the experimental and theoretical values have been well determined.

Previous work in Laane's research group [5,6] was focused on determining the two-dimensional vibrational potential energy surfaces (PESs) for these molecules in terms of their ring-bending and ring-twisting vibrations. These PESs predicted the energy differences between the twisted and planar structures along with the twisting angles for each molecule. The relative energy of the bent saddle points and the bending angles were also predicted. However, because the experimental data typically only extended to about  $1000\text{ cm}^{-1}$  above the ground state, the energies of the twisting barriers and the bent saddle points could only be obtained by extrapolation.

In this present work the structures and relative energies of the twisted, bent, and planar forms have been computed. The twisting and bending angles, as

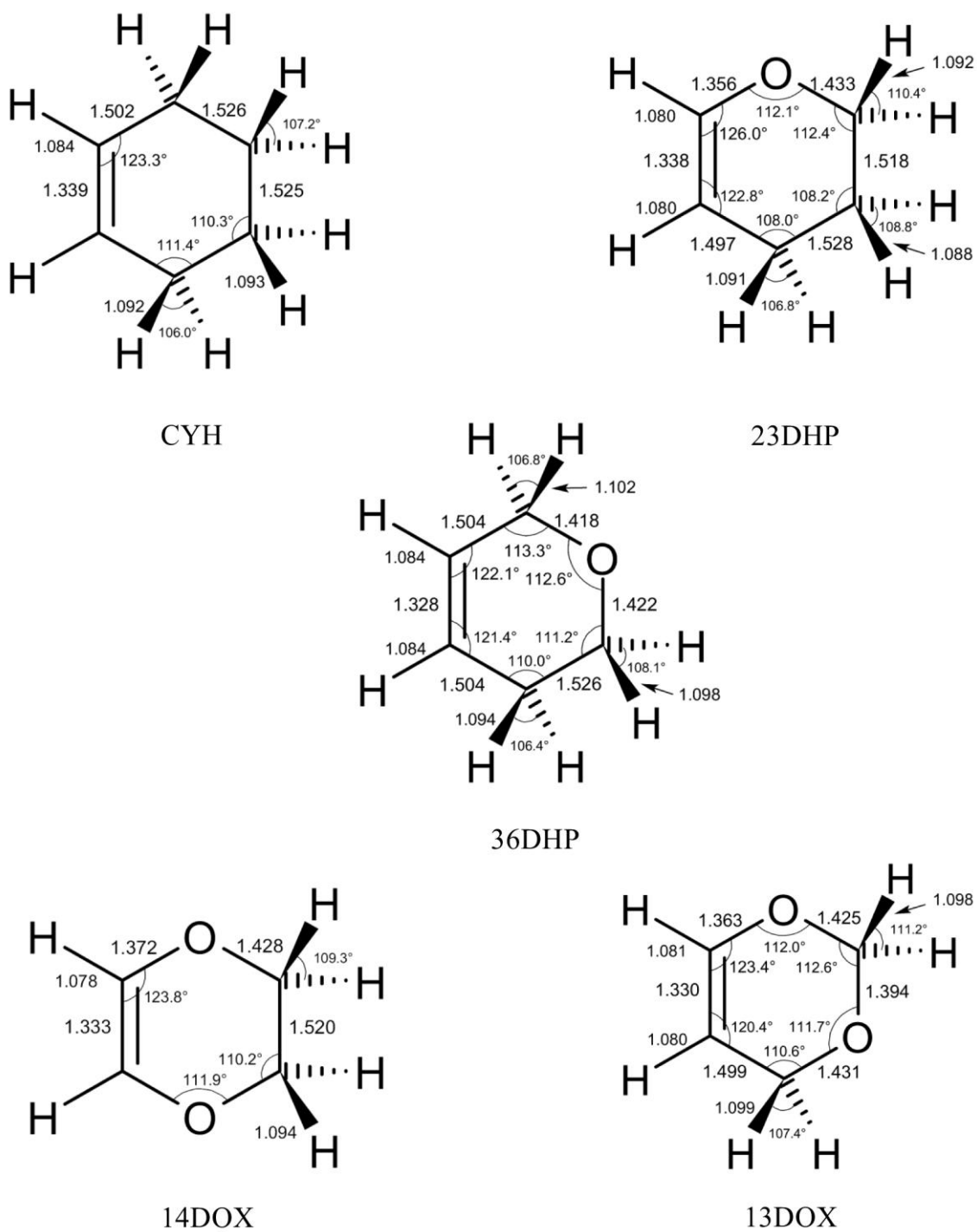


**Fig. 60.** Calculated structures for cyclohexene, 2,3-dihydropyran, 3,6-dihydropyran, 1,4-dioxene, and 1,3-dioxene.



**Table 27**Experimental and calculated<sup>a</sup> structural parameters<sup>b</sup> for cyclohexene and its oxygen analogs.

	CYH			23DHP		36DHP		14DOX		13DOX
	Obs. <sup>c</sup> ED	Obs. <sup>d</sup>	Calc.	Obs. <sup>e</sup> MW	Calc.	Obs. <sup>f</sup> MW	Calc.	Obs. <sup>g</sup> MW	Calc.	Calc.
C <sub>1</sub> =C <sub>6</sub>	1.334	(1.34)	1.339	(1.34)	1.338	1.338	1.328	1.338	1.333	1.33
=C <sub>1</sub> -C <sub>2</sub>	1.502	(1.51)	1.502	-----	-----	1.504	1.504	-----	-----	-----
=C <sub>1</sub> -O <sub>2</sub>	-----	-----	-----	(1.41)	1.356	-----	-----	1.403	1.372	1.363
C <sub>2</sub> -C <sub>3</sub>	1.515	(1.53)	1.526	-----	-----	-----	-----	-----	-----	-----
C <sub>2</sub> -O <sub>3</sub>	-----	-----	-----	-----	-----	1.426	1.418	-----	-----	-----
O <sub>2</sub> -C <sub>3</sub>	-----	-----	-----	(1.42)	1.433	-----	-----	1.400	1.428	1.425
C <sub>3</sub> -C <sub>4</sub>	1.537	(1.53)	1.525	1.52	1.518	-----	-----	1.523	1.52	-----
C <sub>3</sub> -O <sub>4</sub>	-----	-----	-----	-----	-----	-----	-----	-----	-----	1.394
O <sub>3</sub> -C <sub>4</sub>	-----	-----	-----	-----	-----	1.426	1.422	-----	-----	-----
C <sub>4</sub> -C <sub>5</sub>	1.515	(1.53)	1.526	(1.53)	1.528	1.524	1.526	-----	-----	-----
C <sub>4</sub> -O <sub>5</sub>	-----	-----	-----	-----	-----	-----	-----	1.400	1.428	-----
O <sub>4</sub> -C <sub>5</sub>	-----	-----	-----	-----	-----	-----	-----	-----	-----	1.431
C <sub>5</sub> -C <sub>6</sub> =	1.502	(1.51)	1.502	(1.51)	1.497	1.504	1.504	-----	-----	1.499
O <sub>5</sub> -C <sub>6</sub> =	-----	-----	-----	-----	-----	-----	-----	1.403	1.372	-----
=C <sub>1</sub> -H	-----	(1.09)	1.084	(1.09)	1.08	(1.09)	1.084	(1.09)	1.078	1.081
H-C <sub>6</sub> =	-----	(1.09)	1.084	(1.09)	1.08	(1.09)	1.084	(1.09)	1.078	1.08
C <sub>2</sub> -H <sub>a</sub> , p.	-----	(1.10)	1.095	-----	-----	(1.10)	1.102	-----	-----	-----
C <sub>2</sub> -H <sub>b</sub> , p.	-----	(1.10)	1.092	-----	-----	(1.10)	1.092	-----	-----	-----
C <sub>3</sub> -H <sub>a</sub> , p.	-----	(1.10)	1.09	(1.09)	1.092	-----	-----	(1.10)	1.089	1.098
C <sub>3</sub> -H <sub>b</sub> , p.	-----	(1.10)	1.093	(1.09)	1.088	-----	-----	(1.10)	1.094	1.086
C <sub>4</sub> -H <sub>a</sub> , p.	-----	(1.10)	1.093	(1.09)	1.088	(1.10)	1.098	(1.10)	1.094	-----
C <sub>4</sub> -H <sub>b</sub> , p.	-----	(1.10)	1.09	(1.09)	1.091	(1.10)	1.089	(1.10)	1.089	-----
C <sub>5</sub> -H <sub>a</sub> , p.	-----	(1.10)	1.092	(1.09)	1.091	(1.10)	1.094	-----	-----	1.099
C <sub>5</sub> -H <sub>b</sub> , p.	-----	(1.10)	1.095	(1.09)	1.088	(1.10)	1.095	-----	-----	1.091
<C <sub>6</sub> =C <sub>1</sub> -C <sub>2</sub>	123.4	123.3	123.3	-----	-----	122.2	122.1	-----	-----	-----
<C <sub>6</sub> =C <sub>1</sub> -O <sub>2</sub>	-----	-----	-----	(123.4)	126	-----	-----	123.4	123.8	123.4
<C <sub>1</sub> =C <sub>6</sub> -C <sub>5</sub>	123.4	123.3	123.3	(123.3)	122.8	121.5	121.4	-----	-----	120.4
<C <sub>1</sub> =C <sub>6</sub> -O <sub>5</sub>	-----	-----	-----	-----	-----	-----	-----	123.4	123.8	-----
<C <sub>1</sub> -C <sub>2</sub> -C <sub>3</sub>	111.9	111.6	111.4	-----	-----	-----	-----	-----	-----	-----
<C <sub>1</sub> -O <sub>2</sub> -C <sub>3</sub>	-----	-----	-----	(111.6)	112.1	-----	-----	110.3	111.9	112
<C <sub>1</sub> -C <sub>2</sub> -O <sub>3</sub>	-----	-----	-----	-----	-----	111.5	113.3	-----	-----	-----
<C <sub>6</sub> -C <sub>5</sub> -C <sub>4</sub>	111.9	111.6	111.4	(110.3)	108	109.7	110	-----	-----	-----
<C <sub>6</sub> -O <sub>5</sub> -C <sub>4</sub>	-----	-----	-----	-----	-----	-----	-----	110.3	111.9	-----
<C <sub>6</sub> -C <sub>5</sub> -O <sub>4</sub>	-----	-----	-----	-----	-----	-----	-----	-----	-----	110.6
<C <sub>2</sub> -C <sub>3</sub> -C <sub>4</sub>	110.9	110.3	110.3	-----	-----	-----	-----	-----	-----	-----
<C <sub>2</sub> -O <sub>3</sub> -C <sub>4</sub>	-----	-----	-----	-----	-----	110.8	112.6	-----	-----	-----
<O <sub>2</sub> -C <sub>3</sub> -C <sub>4</sub>	-----	-----	-----	-----	112.4	-----	-----	110.4	110.2	-----
<O <sub>2</sub> -C <sub>3</sub> -O <sub>4</sub>	-----	-----	-----	-----	-----	-----	-----	-----	-----	112.6
<C <sub>3</sub> -C <sub>4</sub> -C <sub>5</sub>	110.9	110.3	110.3	-----	108.2	-----	-----	-----	-----	-----
<O <sub>3</sub> -C <sub>4</sub> -C <sub>5</sub>	-----	-----	-----	-----	-----	111.5	111.2	-----	-----	-----
<C <sub>3</sub> -O <sub>4</sub> -C <sub>5</sub>	-----	-----	-----	-----	-----	-----	-----	-----	-----	111.7
<C <sub>3</sub> -C <sub>4</sub> -O <sub>5</sub>	-----	-----	-----	-----	-----	-----	-----	110.4	110.2	-----
<H-C <sub>2</sub> -H	-----	105.5	106	-----	-----	(109.5)	106.8	-----	-----	-----
<H-C <sub>3</sub> -H	-----	106.7	107.2	(109.0)	110.4	-----	-----	(109.5)	109.3	111.2
<H-C <sub>4</sub> -H	-----	106.7	107.2	(109.0)	108.8	(109.5)	108.1	(109.5)	109.3	-----
<H-C <sub>5</sub> -H	-----	105.5	106	(109.0)	106.8	(109.5)	106.4	-----	-----	107.4
τ	-----	30.1	31.4	30.5	32.1	31.5	33.5	29.9	31.2	34.9

<sup>a</sup> MP2/cc-pVTZ calculation. Assumed values in parentheses.<sup>b</sup> Distances in Å and angles in degrees; a.p., b.p. above and below skeletal plane.<sup>c</sup> Ref. [113].<sup>d</sup> Ref. [11].<sup>e</sup> Ref. [14].<sup>f</sup> Ref. [13].<sup>g</sup> Ref. [12].

**Table 28**

Low-frequency vibrations of cyclohexene and its oxygen analogs.

	Vibration frequencies (cm <sup>-1</sup> )					
	Bending		Twisting		D.B. Twisting	
	Obs. <sup>a</sup>	Calc. <sup>b</sup>	Obs. <sup>a</sup>	Calc. <sup>b</sup>	Obs. <sup>a</sup>	Calc. <sup>b</sup>
CYH	165.1	162	276.1	273	392.1	395
23DHP	177.2	178	286.1	274	427.9	445
36DHP	177.5	173	299.7	292	392.7	394
14DOX	191.4	194	297.1	294	465.1	479
13DOX	189.6	187	325.8	319	445.8	449

<sup>a</sup> Refs. [5,6].<sup>b</sup> B3LYP/cc-pVTZ calculation.**Table 29**

Rotational constants of cyclohexene and its oxygen analogs.

	Rotational constants (GHz)								
	A			B			C		
	Obs. <sup>a</sup>	Calc. <sup>b</sup>	Calc. <sup>c</sup>	Obs. <sup>a</sup>	Calc. <sup>b</sup>	Calc. <sup>c</sup>	Obs. <sup>a</sup>	Calc. <sup>b</sup>	Calc. <sup>c</sup>
		<i>(ab. initio)</i>	DFT		<i>(ab. initio)</i>	DFT		<i>(ab. initio)</i>	DFT
CYH	4.7392	4.7988	4.7425	4.5444	4.5780	4.5606	2.5624	2.5910	2.5574
23DHP	5.1982	5.2708	5.1862	4.7479	4.7642	4.7726	2.7109	2.7368	2.7045
36DHP	5.0852	5.1412	5.0847	4.8494	4.8801	4.8669	2.7125	2.7389	2.7064
14DOX	5.6977	5.784	5.676	4.9684	4.9687	5.0072	2.8652	2.8897	2.8655
13DOX		5.6749	5.5897		5.1129	5.1264		2.9067	2.8746

<sup>a</sup> Refs. [11-14].<sup>b</sup> MP2/cc-pVTZ calculation.<sup>c</sup> B3LYP/cc-pVTZ calculation.

defined before [5,6], are shown in Figure 61. Table 30 compares the values of the twist angle for the lowest energy structure obtained from the ab initio calculations here to the experimental microwave results [11-14], to the molecular mechanics (MM)

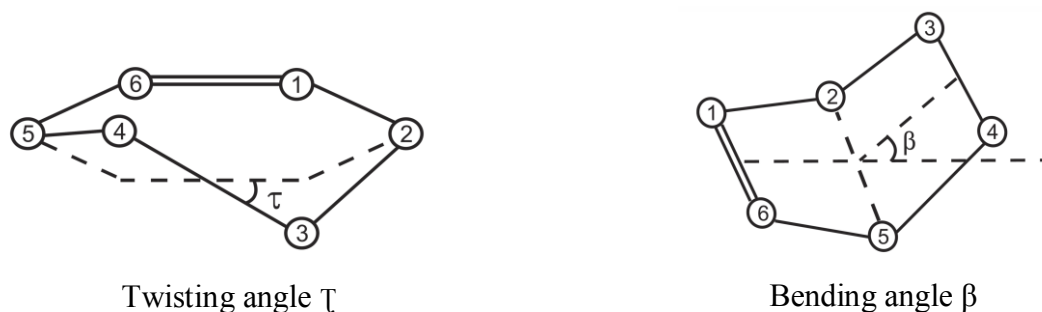


**Fig. 61.** Out of plane coordinates for the ring vibrations of cyclohexene.

**Table 30**

Bending and twisting angles of cyclohexene and oxygen analogs.

	Twisting angle				Bending angle	
	IR. <sup>a</sup>	MW	Calc. <sup>b</sup>	MM2. <sup>a</sup>	IR. <sup>a</sup>	Calc. <sup>b</sup>
CYH	39	30.1 <sup>c</sup>	31.4	30.4	60	50
23DHP	36.5	30.5 <sup>d</sup>	32.1	30.6	55	47
36DHP	38.2	31.5 <sup>e</sup>	33.5	33.6	53	48
14DOX	35.1	29.9 <sup>f</sup>	31.2	29.3	40	40
13DOX	37.8		34.9	30.9	48	47

<sup>a</sup> Refs. [5,6].

<sup>b</sup> MP2/cc-pVTZ calculation.

<sup>c</sup> Ref. [11].

<sup>d</sup> Ref. [14].

<sup>e</sup> Ref. [13].

<sup>f</sup> Ref. [12].

results, and also to the values from the PESs determined from the far-infrared data [5,6]. The table also compares the computed bending angles in this work for the saddle points to those predicted by the previously reported PESs. As can be seen, the twisting angle from this work and the microwave and MM2 values all agree by better than  $2^\circ$ . The microwave values tend to be slightly lower. This may be due to the fact that the microwave calculations required the assumption of some bond distances (see Table 27). Clearly the experimental rotational constants (Table 29) and theoretical values agree very well (better than 1%) so the difference in twist angles does not result from experimental uncertainties.

The poorest agreement for the twisting angles comes from the PESs determined from infrared data which are  $2.9^\circ$  to  $7.6^\circ$  higher than the theoretical ones. The worst case is cyclohexene itself. As mentioned before, the PESs were calculated based on somewhat limited data confined towards the low end of the potential surface. Hence, these are less reliable than the results presented here for systems where the data extend above the energy barriers [41,66]. The bottom line is that the results from this present work here provides the best values for the twisting angles calculated so far.

The bending angles for the saddle points in the PESs were also calculated in the present work and these are also shown in Table 30 where they are compared to values from the PESs determined from the infrared data. For 14DOX and 13DOX the agreement with the previous work is excellent and the bending angle ranges from  $40$  to  $48^\circ$ . For 36DHP the agreement is moderately good and for 23DHP only fairly good. Again the worst case is for cyclohexene. The computed values here are quite reliable

and it can be considered that the higher infrared values come from the approximations inherent in extrapolating the PESs to values above the experimental data.

Perhaps the most interesting results are shown in Table 31 where the energies for the twisted, bent, and planar structures are compared. The values from the infrared PESs are considerably higher than the results reported here, and again this to result would be due from the extrapolations carried out for the PESs. In other words, the ab initio results from this present work give the most reliable values so far even though they are considerably higher than the density functional theory values. The molecular mechanics results from the MM3 [111] model is shown on Table 31 and is compared to both the ab initio and infrared results.

**Table 31**  
Twisting barriers and barrier to interconversion.

	Twisting barrier (cm <sup>-1</sup> )				Barrier to interconversion (cm <sup>-1</sup> )			
	<i>Ab. initio</i> <sup>a</sup>	DFT <sup>a</sup>	MM3. <sup>b</sup>	IR. <sup>c</sup>	<i>Ab. initio</i> <sup>a</sup>	DFT <sup>a</sup>	MM3. <sup>b</sup>	IR. <sup>c</sup>
CYH	4105	3199		4700	1869	1914	2310	3600
23DHP	3675	2840	3320	4080	2609	2382	3130	3480
36DHP	3608	2738	3910	4130	2038	2041	2520	3540
14DOX	3989	3065	2900	4130	3459	2873	2900	3830
13DOX	3958	3005	4410	3500	2889	2608	3880	3120

<sup>a</sup> This work.

<sup>b</sup> Ref. [111].

<sup>c</sup> Ref. [6].

As an additional test to see how well the density functional theory (B3LYP/cc-pVTZ) calculations in this work do in predicting spectra the Raman spectrum of 23DHP and 14DOX has been calculated. Figures 62 and 63 compare these to those reported in

the literature [7]. As can be observed, the frequency agreement is excellent and the intensity agreement is good.

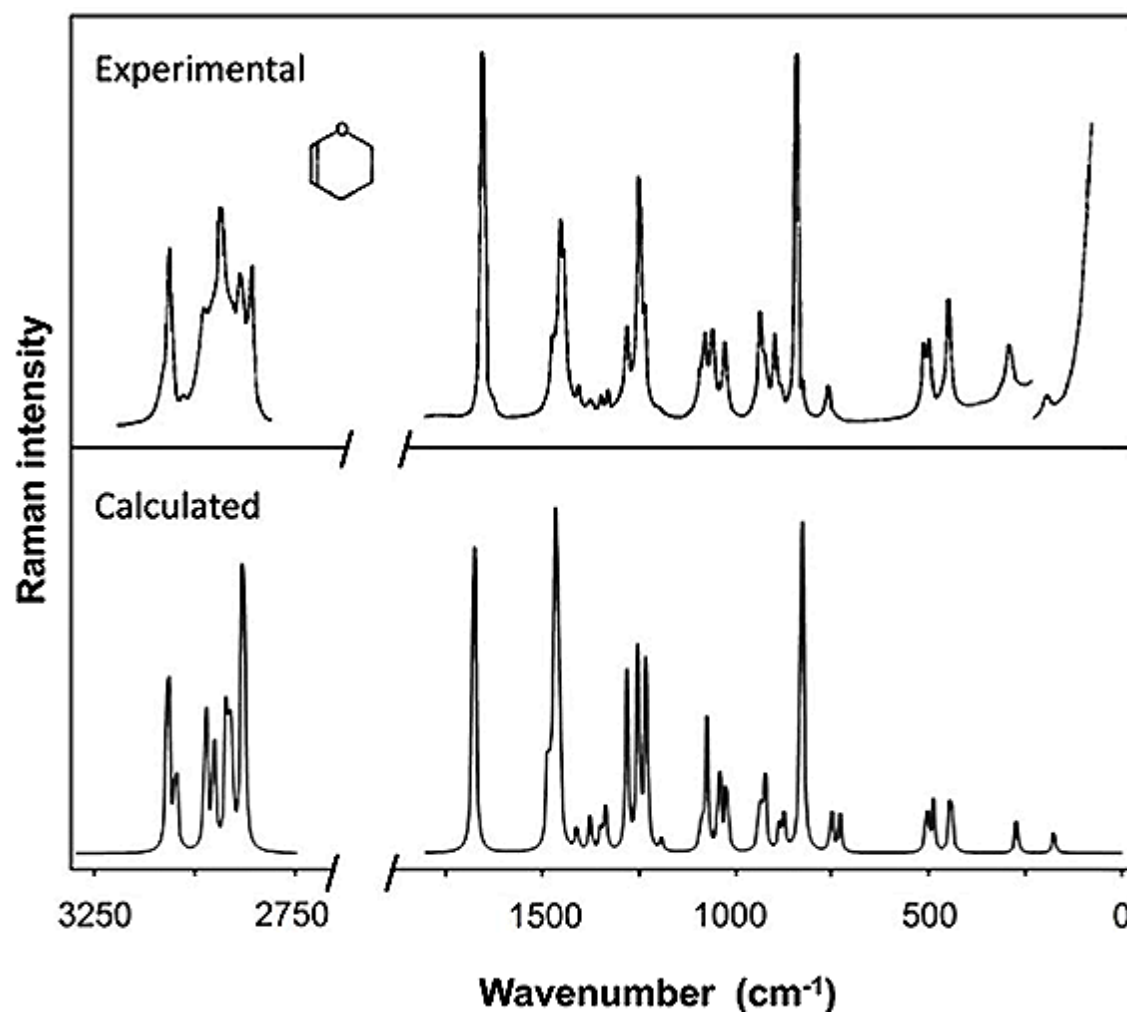


**Fig. 62.** Comparison of the experimental and calculated Raman spectra of 2,3-dihydroxyran.

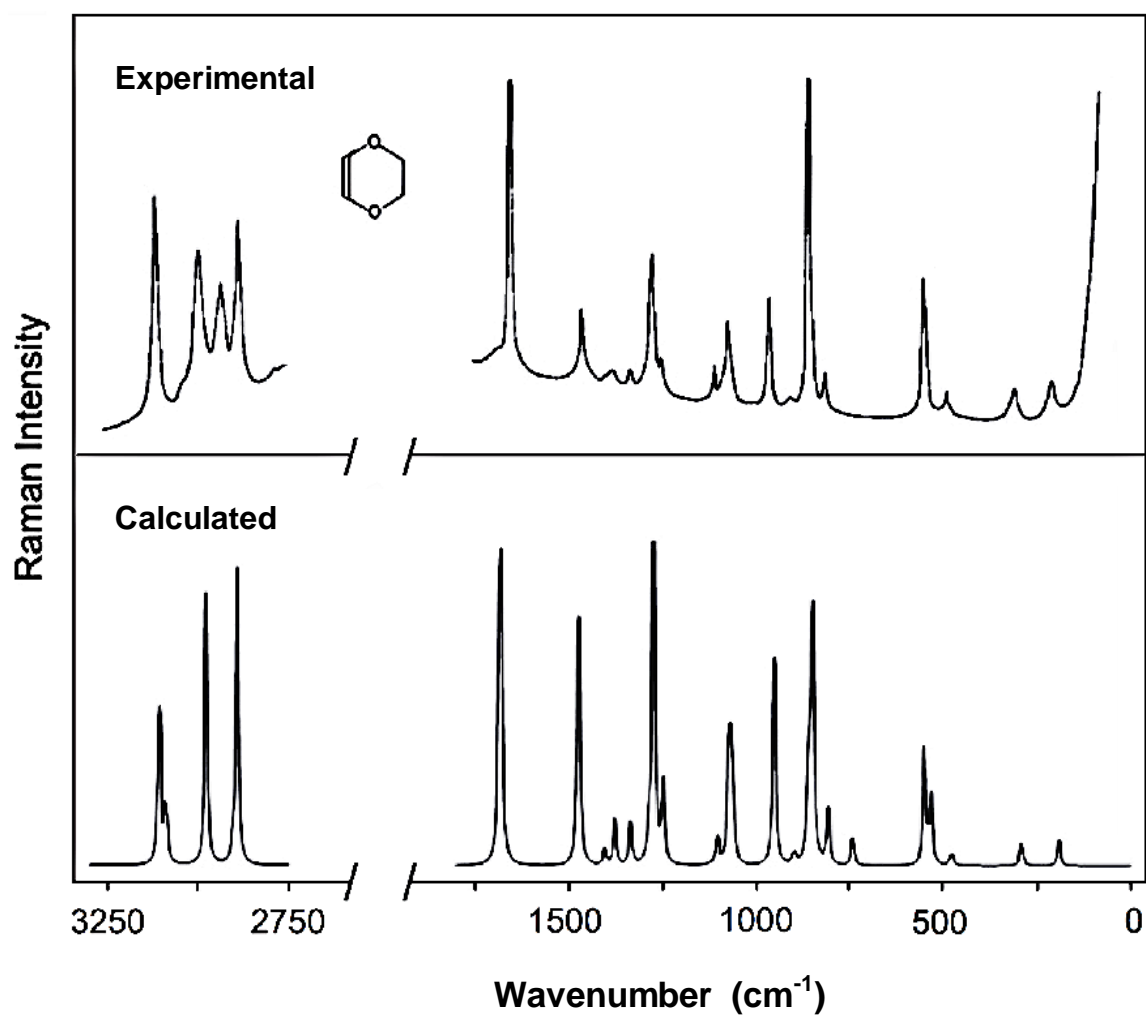


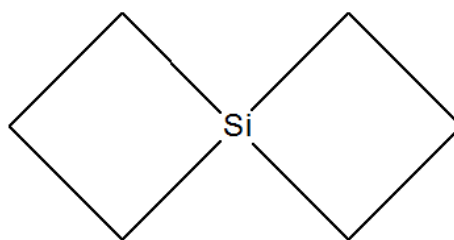
Fig. 63. Comparison of the experimental and calculated Raman spectra of 1,4-dioxene.

## CHAPTER X

## 4-SILASPIRO-(3,3)-HEPTANE

**Introduction**

4-Silaspiro(3,3)-heptane (SSH) is a molecule with two four-membered rings connected at a silicon atom. Cooke and Laane [114] previously concluded that this molecule has both rings puckered adopting a  $C_2$  symmetry based on infrared and Raman data.



SSH

Ab initio MP2/cc-pVTZ calculations have been carried out for this molecule to determine the lowest energy structure and to predict the relative energies of other configurations. The calculated energies for the structures where both rings were left to pucker freely were computed. The calculated energies for the structures where both rings were planar and where just one of the rings was planar were also computed, in addition to the energies for structures where one of the rings was forced to be



puckered to a certain angle. Undergraduate student Cross Medders performed the initial calculations on this molecule, and the work was completed in the present study.

## Results and discussion

According to MP2/cc-pVTZ calculations, SSH has both rings puckered with puckering angles (PA) of  $34^\circ$  and a puckering coordinate  $x_1 = x_2 = 0.17 \text{ \AA}$ . This is very similar to the angle for silacyclobutane of  $35^\circ$  [115]. Fig. 64 shows that the puckering angle  $PA_1 = PA_2 = PA$  and of the puckering coordinate  $x_1 = x_2$ . In addition to the puckering of the rings the two four-membered rings twist relative to each other so the two planes of the  $\text{SiC}_2$  groups in the rings are not perpendicular to each other. The twist angle is  $9.4^\circ$ . Fig. 65 shows the geometrical parameters and the twist angle of the molecule. Fig. 66 shows the calculated potential energy surface for this molecule in terms of the two rings puckering coordinates  $x_1$  and  $x_2$ . A topographical view of Fig. 66 is presented in Fig. 67, where the relative energy values for the barriers to ring inversion are indicated in  $\text{cm}^{-1}$ . Since the molecule has two rings that can freely pucker, the potential energy surface has four equivalent minima at  $x_1$  and  $x_2$  values of  $\pm 0.17 \text{ \AA}$  or  $\pm 34^\circ$ .

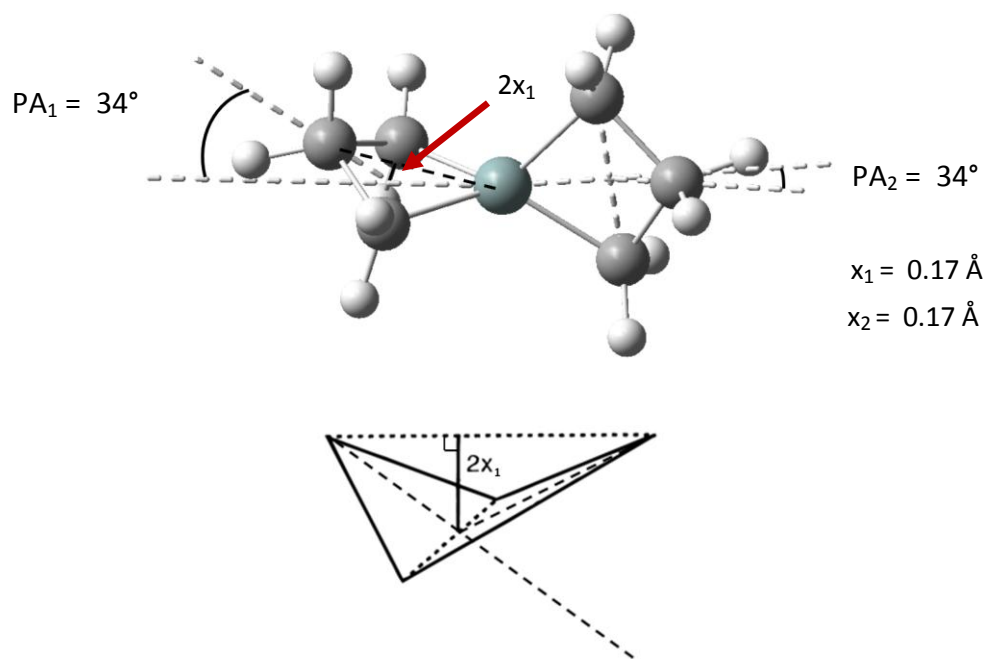


**Fig. 64.** Puckering angle and puckering coordinate of 4-silaspiro-(3,3)-heptane.

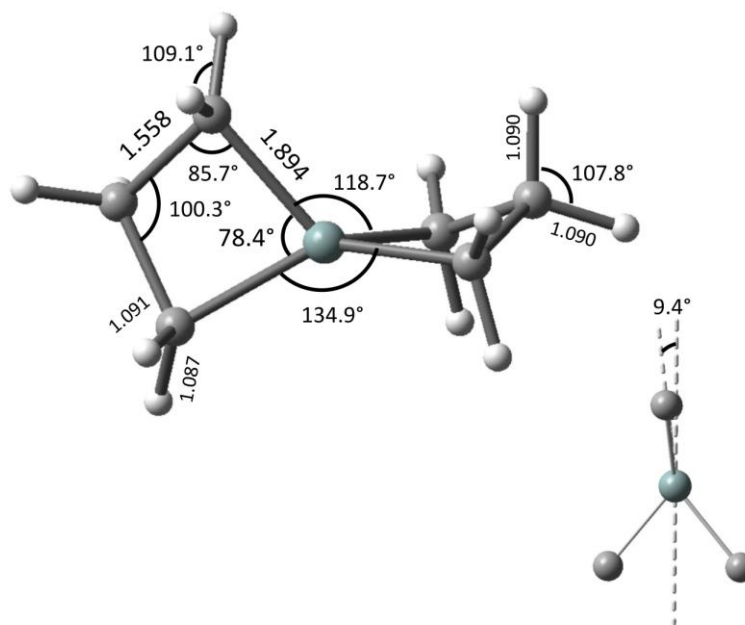


**Fig. 65.** Calculated structure of 4-silaspiro-(3,3)-heptane. MP2/cc-pVTZ calculation.

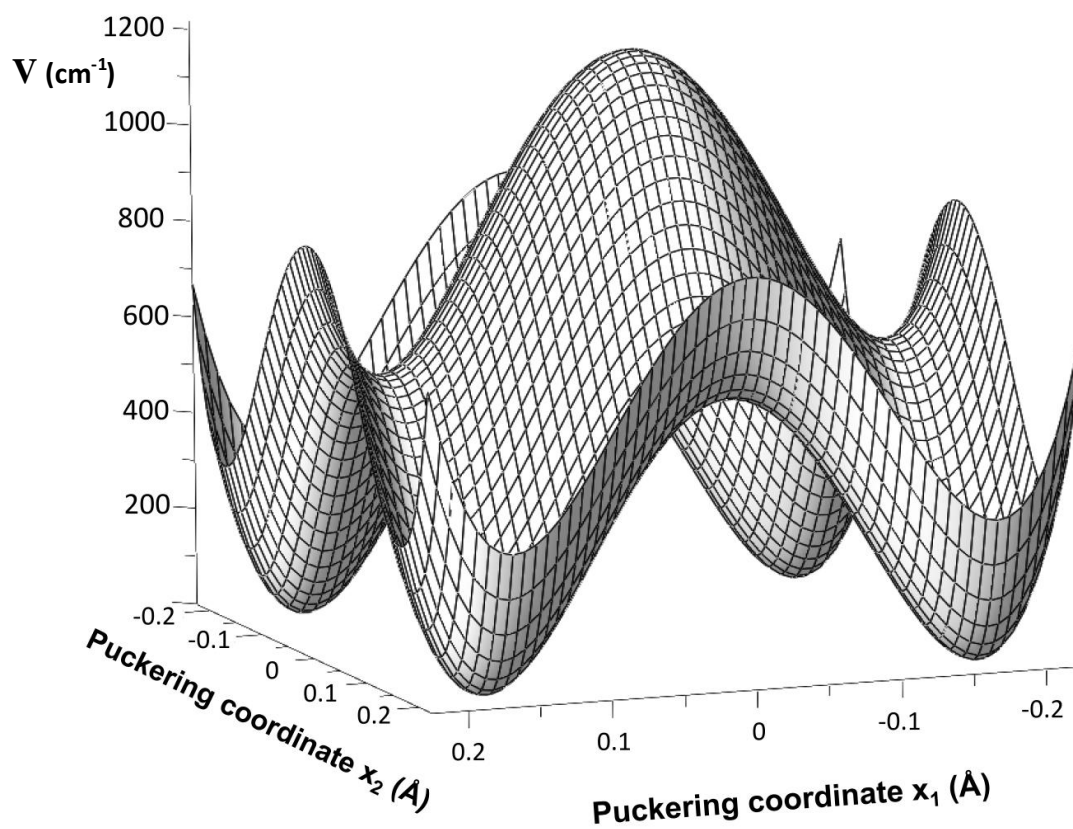


**Fig. 66.** Ring-puckering potential energy surface of 4-silaspiro-(3,3)heptane. MP2/cc-pVTZ calculations.

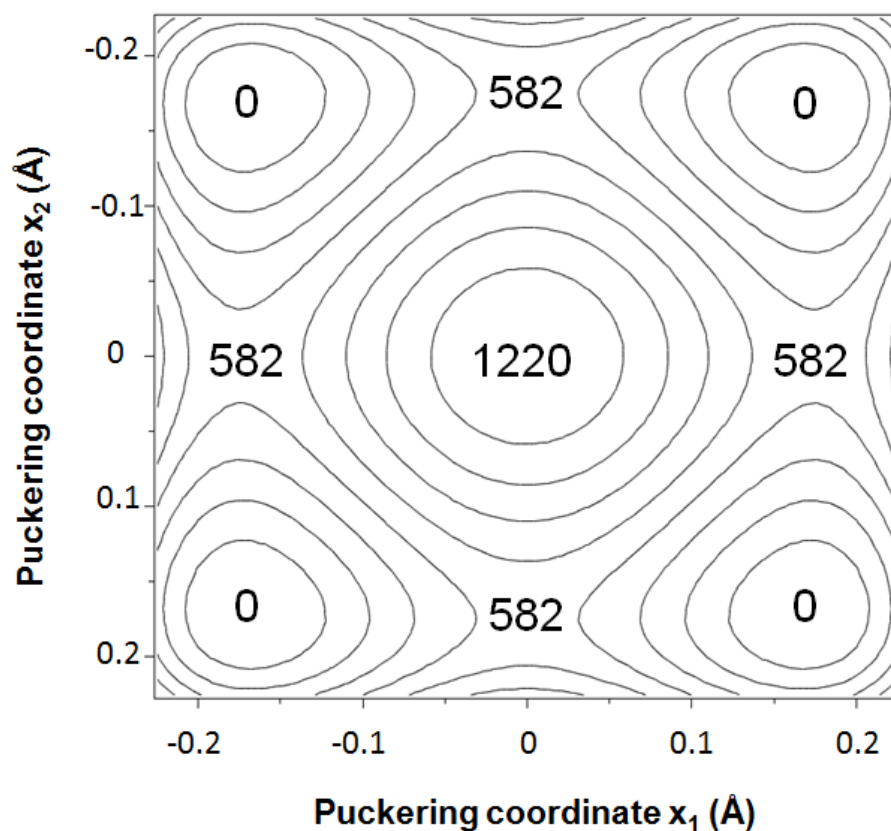


**Fig. 67.** Topographic view of the ring-puckering potential energy surface of 4-silaspiro-(3,3)-heptane. MP2/cc-pVTZ calculations.

Table 32 shows the values of the puckering coordinates  $x_1$  and  $x_2$  and the corresponding energy of different calculated structures of SSH that were taken into account to perform a statistical fitting. The equation obtained for the potential surface utilizing the Maple 14 mathematical program is

$$V (\text{cm}^{-1}) = 6.9 \times 10^5 (x_1^4 + x_2^4) - 4.2 \times 10^4 (x_1^2 + x_2^2) + 6.8 \times 10^4 x_1^2 x_2^2 + 1220.4 \quad (27)$$

The experimental vapor-phase infrared and Raman spectra previously reported by Cooke and Laane [15,114] were compared to the calculated (B3LYP/cc-pVTZ) spectra of this molecule, and vibrational assignments were made in the present study. The experimental spectra [15,114] are compared to the calculated results in Figs. 68 and 69 and in Table 33. There is an excellent agreement between the calculated and the experimental spectra.

No data have been reported as yet for the ring-puckering spectra, but the potential energy surface shown in Figs. 66 and 67 will allow the energy levels and spectral transitions to be calculated.

**Table 32**

Calculated potential energy, puckering angles and puckering coordinates of 4-silaspiro-(3,9)-heptane<sup>a</sup>.

Energy (cm <sup>-1</sup> )	0	0.7	582	1220	370	179
Puckering coordinates (Å)						
x <sub>1</sub>	0.175	0.175	0.179	0.000	0.179	0.177
x <sub>2</sub>	0.175	-0.173	0.001	0.000	0.170	0.114
Puckering angles (degrees)						
PA <sub>1</sub>	34.2	34.2	35.1	0.0	35.0	34.8
PA <sub>2</sub>	34.2	-33.9	0.0	0.0	14.9	22.4

<sup>a</sup> MP2/cc-pVTZ calculations.

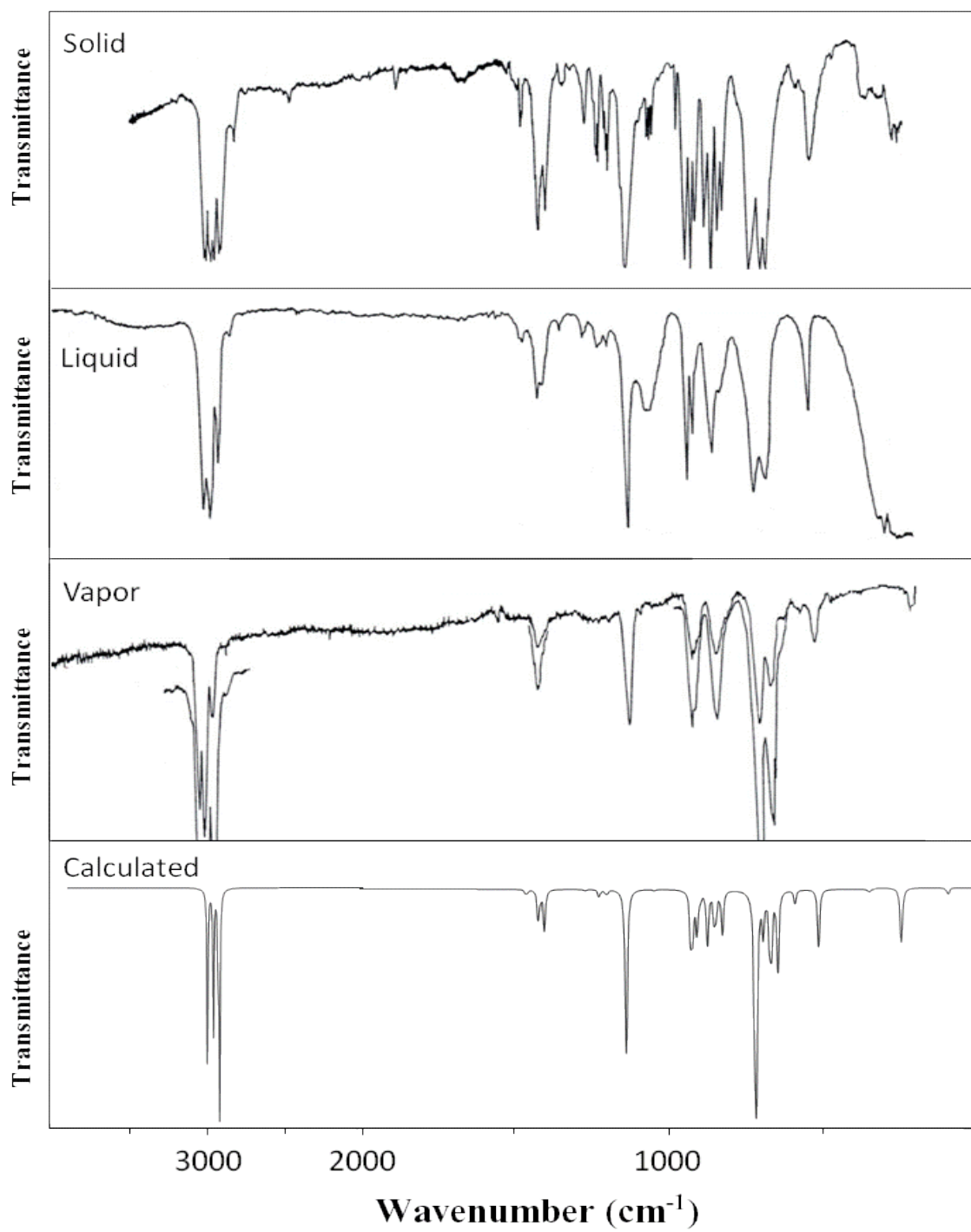


**Fig. 68.** Observed and calculated infrared spectra of 4-silaspiro-(3,3)-heptane.

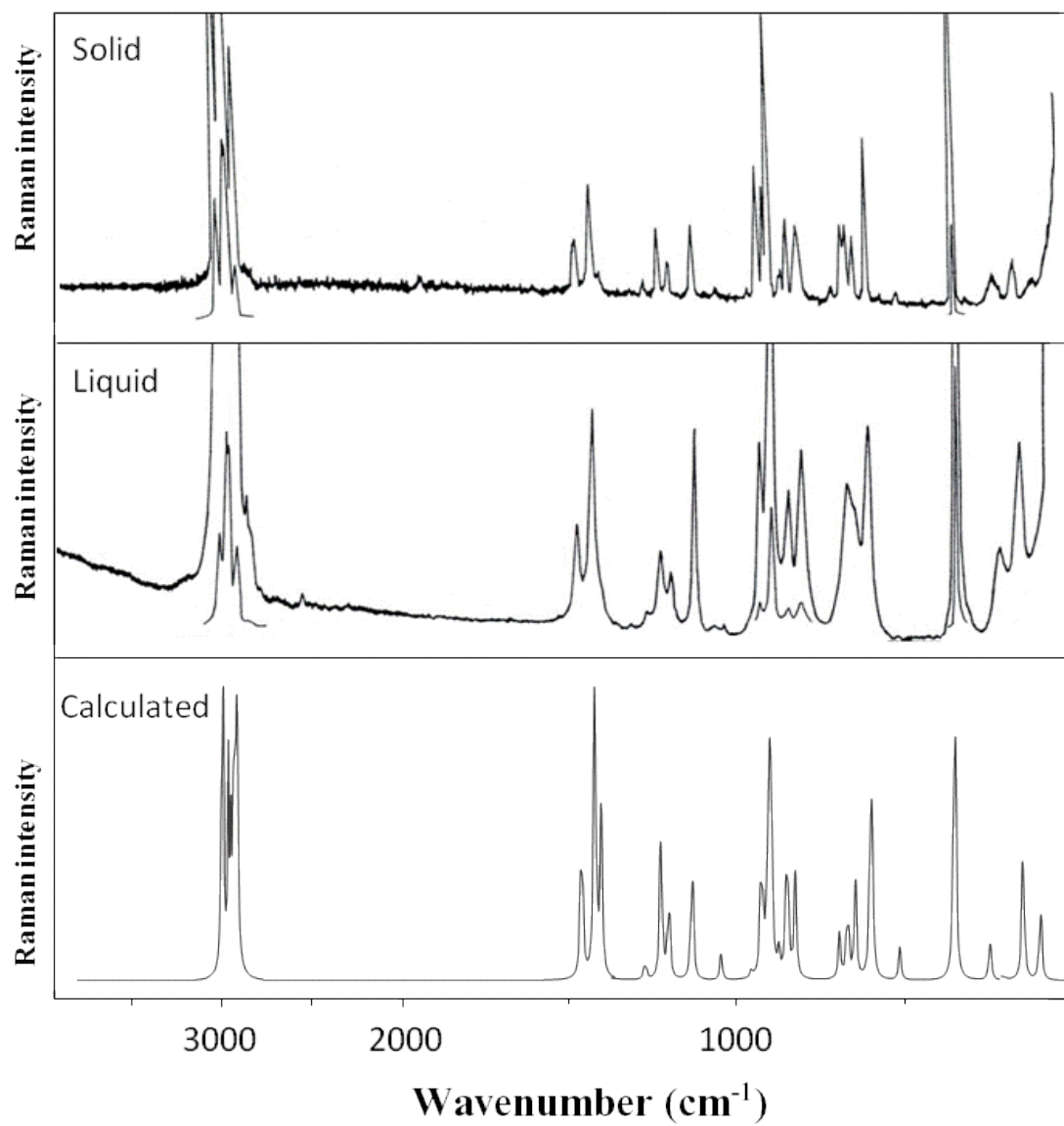


Fig. 69. Observed and calculated Raman spectra of 4-silaspiro-(3,3)-heptane.

**Table 33**  
Vibrational assignments of 4-silapero-(3,3)-heptane.

			C <sub>1</sub>		D <sub>2</sub> d			
			Obs.	Int (IR, R)	Calc. Freq.	Int (IR, R)	Calc. Freq.	Int (IR, R)
A <sub>1</sub>	v <sub>1</sub>	$\alpha$ -CH <sub>2</sub> symmetric stretch	2931	vs, vs*	2931	(13, 50)	2938	(0, 100)
	v <sub>2</sub>	$\beta$ -CH <sub>2</sub> symmetric stretch	2948	vs, ---	2920	(100, 13)	2921	(0, 23)
	v <sub>3</sub>	$\beta$ -CH <sub>2</sub> deformation	1451	w*, m*	1462	(1, 35)	1452	(0, 32)
	v <sub>4</sub>	$\alpha$ -CH <sub>2</sub> deformation	1420	m, ---	1423	(1, 51)	1430	(0, 65)
	v <sub>5</sub>	$\alpha$ -CH <sub>2</sub> wag	1115	---, m	1133	(1, 43)	1130	(0, 24)
	v <sub>6</sub>	Ring stretch	894	m*, s*	901	(4, 100)	873	(0, 91)
	v <sub>7</sub>	$\beta$ -CH <sub>2</sub> rock /Si-C symmetric stretch	808	m*, m*	827	(3, 32)	730	(0, 100)
	v <sub>8</sub>	Ring: Si-C symmetric stretch i.p.	360	m*, s*	354	(1, 97)	344	(0, 80)
A <sub>2</sub>	v <sub>9</sub>	$\alpha$ -CH <sub>2</sub> antisymmetric stretch	-----	---, ---	2998	(6, 7)	2974	(0, 0)
	v <sub>10</sub>	$\beta$ -CH <sub>2</sub> twist	1210	w*, m*	1225	(1, 22)	1235	(0, 0)
	v <sub>11</sub>	$\alpha$ -CH <sub>2</sub> twist	929	---, m*	929	(0.7, 2)	944	(0, 0)
	v <sub>12</sub>	Ring: deformation / $\alpha$ -CH <sub>2</sub> rock	527	s*, w*	517	(17, 10)	543	(0, 0)
B <sub>1</sub>	v <sub>13</sub>	$\alpha$ -CH <sub>2</sub> antisymmetric stretch	2986	vs*, ---	2999	(34, 48)	2975	(0, 41)
	v <sub>14</sub>	$\beta$ -CH <sub>2</sub> twist	1210	w*, m*	1226	(1, 32)	1237	(0, 32)
	v <sub>15</sub>	$\alpha$ -CH <sub>2</sub> twist	957	m*, ---	957	(0.1, 2)	969	(0, 0.3)
	v <sub>16</sub>	Ring: Si-C antisymmetric stretch/ $\alpha$ -CH <sub>2</sub> rock	670	m, m*	672	(33, 25)	653	(0, 9)
	v <sub>17</sub>	$\alpha$ -CH <sub>2</sub> rock	175	---, m*	150	(0.003, 8)	156	(0, 0.3)
B <sub>2</sub>	v <sub>18</sub>	$\alpha$ -CH <sub>2</sub> symmetric stretch	2864	s, s*	2931	(16, 38)	2938	(28, 0.0001)
	v <sub>19</sub>	$\beta$ -CH <sub>2</sub> symmetric stretch	2910	vs*, vs*	2920	(22, 100)	2921	(100, 5)
	v <sub>20</sub>	$\beta$ -CH <sub>2</sub> deformation	1451	w*, m*	1461	(1, 28)	1452	(2, 6)
	v <sub>21</sub>	$\alpha$ -CH <sub>2</sub> deformation	1420	m, ---	1422	(9, 64)	1429	(6, 60)
	v <sub>22</sub>	$\alpha$ -CH <sub>2</sub> wag	1120	m, ---	1139	(51, 1)	1133	(79, 0.02)
	v <sub>23</sub>	Ring stretch	908	ms*, m*	911	(13, 26)	592	(100, 1)
	v <sub>24</sub>	$\beta$ -CH <sub>2</sub> rock /Si-C symmetric stretch	820	w*, ---	828	(10, 0.7)	792	(54, 3)
	v <sub>25</sub>	$\alpha$ -CH <sub>2</sub> rock/Si-C symmetric stretch	540	m, ---	594	(4, 3)	886	(12, 27)
E	v <sub>26</sub>	$\alpha$ -CH <sub>2</sub> antisymmetric stretch	2978	vs, ---	2999	(45, 27)	2983	(51, 10)
			2978	vs, ---	2999	(18, 52)	2983	(51, 10)
	v <sub>27</sub>	$\beta$ -CH <sub>2</sub> antisymmetric stretch	2960	vs*, s*	2961	(8, 93)	2952	(1, 5)
			2960	vs*, s*	2961	(73, 15)	2952	(1, 5)
	v <sub>28</sub>	$\alpha$ -CH <sub>2</sub> symmetric stretch	2864	s, s*	2929	(24, 62)	2933	(44, 3)
			2864	s, s*	2929	(5, 23)	2933	(44, 3)
	v <sub>29</sub>	$\alpha$ -CH <sub>2</sub> deformation	1410	m*, m*	1420	(7, 43)	1420	(14, 6)
			1410	m*, m*	1419	(5, 17)	1420	(14, 6)
	v <sub>30</sub>	$\beta$ -CH <sub>2</sub> wag	1260	w*, w*	1272	(0.3, 7)	1268	(4, 5)
			1260	w*, w*	1271	(0.2, 0.2)	1268	(4, 5)
	v <sub>31</sub>	$\alpha$ -CH <sub>2</sub> twist	1185	w*, m*	1203	(1, 14)	1188	(2, 9)
1185			w*, m*	1202	(0.6, 16)	1188	(2, 9)	



**Table 33** continued.

	Obs.	Int (IR, R)	C <sub>1</sub>		D <sub>2d</sub>	
			Calc. Freq.	Int (IR, R)	Calc. Freq.	Int (IR, R)
<b>E</b> v <sub>32</sub> α-CH <sub>2</sub> wag	1043	w*, ---	1047	(0.2, 5)	1093	(0.5, 0.5)
	1043	w*, ---	1047	(0.2, 4)	1093	(0.5, 0.5)
v <sub>33</sub> Ring: C-C antisymmetric stretch	928	s*, m*	928	(14, 33)	934	(15, 12)
	924	m, ---	927	(14, 10)	934	(15, 12)
v <sub>34</sub> β-CH <sub>2</sub> rock	863	m*, m*	876	(16, 8)	838	(46, 0.05)
	848	m, m*	852	(16, 52)	838	(46, 0.05)
v <sub>35</sub> Ring: Si-C sym. str. and α-CH <sub>2</sub> rock/ α,β-CH <sub>2</sub> rock α-CH <sub>2</sub> rock/ α,β-CH <sub>2</sub> rock	711	s, ---	720	(100, 0.2)	706	(38, 4)
	684	s*, m*	696	(12, 14)	706	(38, 4)
v <sub>36</sub> Ring: Si-C antisymmetric stretch and α-CH <sub>2</sub> rock	654	w, w*	649	(24, 29)	623	(15, 22)
	614	---, m*	603	(0.004, 75)	623	(15, 22)
v <sub>37</sub> α-CH <sub>2</sub> rock	236	s*, w*	250	(1, 7)	174	(3, 5)
	225	m*, w*	247	(3, 5)	174	(3, 5)

B3LYP calculations. Scaling factors: 0.985 below 1500 cm<sup>-1</sup>, 0.973 between 1500 and 2000 cm<sup>-1</sup> and 0.961 above 2000 cm<sup>-1</sup>

## CHAPTER XI

### CONCLUSIONS

Spectroscopic studies have been performed and theoretical calculations have been carried out on cyclic and bicyclic molecules in order to determine the structures and relative energies of their conformations and to predict and compare their theoretical infrared and Raman spectra to the experimental ones.

Infrared and Raman spectroscopy have been utilized to investigate the conformations of the cyclic alcohols, 3-cyclopenten-1-ol, 2-cyclopenten-1-ol, 2-cyclohexen-1-ol, and the cyclic amines, 3-cyclopenten-1-amine, 2-aminoindan, 2-cyclopenten-1-amine, 1-aminoindan, and 2-hydroxytetralin. All these molecules are capable of possessing intramolecular  $\pi$ -type hydrogen bonding. Ab initio (CCSD/cc-pVTZ and MP2/cc-pVTZ) and density functional theory (B3LYP/cc-pVTZ) computations have been carried out to complement the experimental work.

It has been shown in this work that the unusual intramolecular  $\pi$ -type hydrogen bond lowers the energy of cyclic molecules and that these conformers can be identified spectroscopically. Both the experimental spectra and the ab initio calculations show that the alcohols studied in this work can exist in several different conformations.

It was found that the 3-cyclopenten-1-ol molecule can exist in four different conformational forms, one of which has an unusual weak intramolecular  $\pi$ -type hydrogen bonding between the hydroxyl hydrogen and the C=C double bond. The four conformers can interconvert through the ring-puckering vibration and the internal

rotation of the -OH group on the five-membered ring. The energy barriers to interconversion between the conformers range from 720 to 1390  $\text{cm}^{-1}$  (8.6 to 16.6 kJ/mol). The conformer of 3-cyclopenten-1-ol with the intramolecular  $\pi$ -type hydrogen bond is its lowest energy form and is 401 to 564  $\text{cm}^{-1}$  (4.8 to 6.8 kJ/mol) lower in energy than the other three conformers.

The vapor-phase infrared and Raman spectra of 3-cyclopenten-1-ol have been collected at temperatures ranging from 25° to 257°C, and also in the liquid phase at room temperature. The hydrogen-bonded conformer is calculated to be more than 47% abundant at these temperatures. The O-H stretching band for the conformer with the weak intramolecular  $\pi$ -type hydrogen bond was observed at 3623.4  $\text{cm}^{-1}$  whereas the conformers without hydrogen bonding have higher frequency bands at 3655.4, 3659, and 3637.6  $\text{cm}^{-1}$ . The wavenumber difference between the conformers of lowest energy implies that the O-H stretching force constant is reduced by about 2% due to the hydrogen bonding. The C=C stretching frequencies for these two conformers are 1607.3 and 1620.7  $\text{cm}^{-1}$ , respectively, implying that this stretching force constant is also reduced by about 2% due to the hydrogen bonds. Nonetheless, the intramolecular hydrogen bonding is large enough to give the conformer with the hydrogen of the -OH group directed towards the middle of the C=C bond sufficiently lower energy to make it the dominant species.

Each cyclic alcohol has only one hydrogen atom attached to the electronegative oxygen atom and thus can have only one conformer of lowest energy and that is the one with the intramolecular  $\pi$ -type hydrogen bond. This is true for 3-cyclopenten-1-ol,

2-cyclopenten-1-ol and 2-cyclohexen-1-ol. These three molecules have the lowest energy forms at energies 72 to 564  $\text{cm}^{-1}$  (0.9 - 6.7 kJ/mol) lower than those of the other conformers. Because cyclic amines have two hydrogen atoms attached to the electronegative nitrogen atom, they have more than one conformer with an intramolecular  $\pi$ -type hydrogen bond. Thus 2-cyclopenten-1-amine has four conformations with intramolecular  $\pi$ -type hydrogen bonds. These have an energies 221 - 409  $\text{cm}^{-1}$  (2.6 - 4.9 kJ/mol) lower than the other two conformers without intramolecular hydrogen bonds. 3-Cyclopenten-1-amine and 2-aminoindan have two conformers, each with an intramolecular  $\pi$ -type hydrogen bond. These are 278 to 336  $\text{cm}^{-1}$  (3.3 - 4.0 kJ/mol) lower in energy than the other conformers. 1-Aminoindan, which possesses an aromatic ring has five conformations with intramolecular  $\pi$ -type hydrogen bonds. These five conformers are 343 to 629  $\text{cm}^{-1}$  (4.1 - 7.5 kJ/mol) lower in energy than the conformer without an intramolecular  $\pi$ -type hydrogen bond.

The five-membered cyclic molecules 3-cyclopentene-1-amine, 2-cyclopenten-1-ol, 2-cyclopenten-1-amine, and five-membered cyclic molecules attached to an aromatic ring (2-aminoindan and 1-aminoindan) pucker to maximize the intramolecular  $\pi$ -type hydrogen bonding interaction. The calculated puckering angles of the conformations of lowest energy of 3-cyclopenten-1-ol, 3-cyclopentene-1-amine and 2-cyclopenten-1-amine are 28°, 29° and 25° respectively.

The six-membered cyclic molecule 2-cyclohexen-1-ol and the six-membered ring attached to an aromatic ring 2-hydroxytetralin twist to maximize the formation of the intramolecular  $\pi$ -type hydrogen bonding. The calculated twisting angle of

2-cyclohexen-1-ol is  $30^\circ$  whereas the calculated twisting angle of 2-hydroxytetralin is  $29^\circ$ .

The infrared and Raman spectra of vapor, liquid, and solid state cyclopentane and its  $d_1$ , 1,1- $d_2$ , 1,1,2,2,3,3- $d_6$ , and  $d_{10}$  isotopomers have been analyzed. Ab initio (CCSD/cc-pVTZ and MP2/cc-pVTZ) and density functional theory (B3LYP/cc-pVTZ) computations were carried out. The CCSD/cc-pVTZ computations confirm that the two conformational forms of cyclopentane are the twist ( $C_2$ ) and bent ( $C_s$ ) structures and that they differ by less than  $10 \text{ cm}^{-1}$  (0.1 kJ/mol). The calculated bending angle for the  $C_s$  form is  $41.5^\circ$  and the dihedral angle of twisting is  $43.2^\circ$  for the  $C_2$  form. Moreover, the ab initio CCSD/cc-pVTZ calculations determine a barrier to planarity of  $1887 \text{ cm}^{-1}$ , in excellent agreement with the experimental value of  $1808 \text{ cm}^{-1}$ . A complete and reliable vibrational assignment for each of the isotopomers has been achieved comparing previously collected infrared and Raman spectra with B3LYP/cc-pVTZ computations.

Ab initio (CCSD/cc-pVTZ and MP2/cc-pVTZ) calculations have been carried out for methylcyclopropane, cyclopropylsilane, cyclopropylgermane, cyclopropylamine, cyclopropanethiol and cyclopropanol. The structure and the potential energy function for internal rotation was calculated for each of these molecules and compared to experimental results previously determined from infrared and Raman spectra. The calculated barrier to internal rotation and the experimental results were in excellent agreement. Typical barriers to internal rotation were in the  $470$  to  $1500 \text{ cm}^{-1}$  (5.6 to 17.9 kJ/mol) range.

Ab initio (CCSD/cc-pVTZ and MP2/cc-pVTZ), and density functional theory (B3LYP/cc-pVTZ) computations have been carried out for cyclohexene and its oxygen analogs 2,3-dihydropyran, 3,6-dihydro-2H-pyran, 1,4-dioxene and 1,3-dioxene. Each of the molecules was found to be twisted with a high barrier to planarity. The bent configurations represent saddle points in two-dimensional surfaces. The structures, relative energies, and frequencies for the lowest energy vibrations of the twisted, bent, and planar forms were calculated and compared to experimental results. The calculated results agree very well with previously reported microwave data, but the compared computed barriers differ somewhat to those based on low-frequency infrared data.

Ab initio (MP2/cc-pVTZ) and density functional theory (B3LYP/cc-pVTZ) calculations were carried out on 4-silaspiro-(3,3)-heptane (SSH) in order to calculate its molecular structure and vibrational spectra. This molecule possesses two four-membered rings joined to a central silicon atom, and a two-dimensional ring-puckering potential surface (PES) with four equivalent minima. Both rings of SSH are puckered with dihedral angles of  $34^\circ$ . The ab initio calculated barrier to planarity of each ring is  $582\text{ cm}^{-1}$  while the molecular structure with both rings is  $1220\text{ cm}^{-1}$  higher in energy. The calculated infrared and Raman spectra were also compared to those previously published. The agreement is excellent.

## REFERENCES

- [1] J. M. Bakke, L. H. Bjerkeseeth, *J. Mol. Struct.* 470, (1998) 247.
- [2] A. A. Al-Saadi, Ph.D. Dissertation, Texas A&M University, College Station, 2006.
- [3] E. Kilpatrick, K. S. Pitzer, R. Spitzer, *J. Am. Chem. Soc.* 69 (1947) 2483.
- [4] L. E. Bauman, Ph.D. Dissertation, Texas A&M University, College Station, 1977.
- [5] V.E. Rivera-Gaines, S.J. Leibowitz, J. Laane, *J. Am. Chem. Soc.* 113 (1991) 9735.
- [6] M.M.J. Tecklenburg, J. Laane, *J. Am. Chem. Soc.* 111 (1989) 6920.
- [7] R.C. Lord, T.C. Rounds, T. Ueda, *J. Chem. Phys.* 57 (1972) 2572.
- [8] J.R. Durig, R.O. Carter, L.A. Carreira, *J. Chem. Phys.* 60 (1974) 3098.
- [9] T.L. Smithson, H. Wieser, *J. Chem. Phys.* 72 (1980) 2340.
- [10] E.A. Dixon, G.S.S. King, T.L. Smithson, H. Wieser, *J. Mol. Struct.* 71 (1981) 97.
- [11] L.H. Scharpen, J.E. Wollrab, D.P. Ames, *J. Chem. Phys.* 49 (1968) 2368.
- [12] J.A. Wells, T.B. Malloy, *J. Chem. Phys.* 60 (1974) 2132.
- [13] J.A. Wells, T.B. Malloy, *J. Chem. Phys.* 60 (1974) 3987.
- [14] J.C. Lopez, J.L. Alonso, *Z. Z. Naturforsch.* 40a (1985) 913.
- [15] J. M. Cooke, Ph.D. Dissertation, Texas A&M University, College Station, 1979.
- [16] R. L. Flurry, *Quantum Theory: An Introduction*, Prentice-Hall Inc., Englewood

- Cliffs, NJ, 1983.
- [17] R. L. Liboff, *Introductory Quantum Mechanics*, Third Edition, Addison-Wesley, Reading, MA, 1998.
- [18] J. Simons, J. Nichols, *Quantum Mechanics in Chemistry*, Oxford University Press, New York, 1997.
- [19] C. Møller, M. S. Plesset, *Physical Review*, 46 (1934) 618.
- [20] Æ. Frisch, M. J. Frisch, G. W. Trucks, *Gaussian 03 User's Reference*, Gaussian Inc., Carnegie, PA, 2003.
- [21] A. G. Császár, W. D. Allen, Y. Yamaguchi, H. F. Schaefer III, in P. Jensen, P. R. Bunker (Eds.), *Ab initio determination of accurate ground electronic state potential energy hypersurfaces for small molecules*, *Computational Molecular Spectroscopy*, John Wiley and Sons, Chichester, England, 2000, Chapter 2.
- [22] J. Čížek, *J. Chem. Phys.*, 45 (1966) 4256.
- [23] J. B. Foresman, Æ. Frisch, *Exploring Chemistry with Electronic Structure Methods*, Second Edition, Gaussian Inc., Pittsburgh, PA, 1996.
- [24] G. D. Purvis III, R. J. Barlett, *J. Chem. Phys.*, 76 (1982) 1910.
- [25] P.W. Atkins, R.S. Friedman, *Molecular Quantum Mechanics*, Third Edition, Oxford University Press, New York, 1997.
- [26] P.J. Stephens, F.J. Devlin, C. F. Chabalowski, M. J. Frisch, *J. Phys. Chem.*, 98 (1994) 11623.
- [27] A. D. Becke, *J. Chem. Phys.* 98 (1993) 5648.
- [28] W. Koch, M. C. Holthausen, *A Chemist's Guide to Density Functional Theory*,



Second Edition, Wiley-VCH, Weinheim, Germany, 2000.

- [29] A. D. Becke, *Phys. Rev. A* 38 (1988) 3098.
- [30] J. P. Perdew, Y. Wang, *Phys. Rev. B* 45 (1992) 13244.
- [31] A. D. Becke, *J. Chem. Phys.* 98 (1993) 1372.
- [32] L. A. Curtiss, K. Raghavachan, G. W. Trucks, J. A. Pople, *J. Chem. Phys.* 94 (1991) 7221.
- [33] C. Lee, W. Yang, R. Parr, *Phys. Rev. B* 37 (1988) 785.
- [34] S.H. Vosko, L. Wilk, M. Nusair, *Can. J. Phys.* 58 (1980) 1200.
- [35] T. H. Dunning Jr., *J. Chem. Phys.* 90 (1989) 1007.
- [36] K. Haller, W.-Y. Chiang, A. del Rosario, J. Laane, *J. Mol. Struct.* 379 (1996) 19.
- [37] J. Laane, K. Jaller, S. Sakurai, K. Morris, D. Autrey, Z. Arp, W. Y. Chiang, A. Combs, *J. Mol. Struct.* 650 (2003) 57.
- [38] F. A. Carey, R. J. Sunberg, *Advanced Organic Chemistry, Part A: Structure and Mechanisms*, Kluwer Academic, Olenum Publishers, New York, 2000.
- [39] H. Beyer, W. Walter, *Handbook of Organic Chemistry*, Prentice Hall, Stuttgart, Germany, 1991.
- [40] J. McMurry, *Organic Chemistry*, Wadsworth Inc., Pacific Grove, California, 1992.
- [41] J. Laane, *J. Phys. Chem. A* 104 (2000) 7715.
- [42] G. R. Desiraju, T. Steiner, *The Weak Hydrogen Bond in Structural Chemistry and Biology*, Oxford University Press, New York, 1999.

- [43] S. Grabowski, *Challenges and Advances in Computational Chemistry and Physics*, Vol. 3, *Hydrogen Bonding-New Insights*, Springer, Dordrecht, The Netherlands, 2006.
- [44] O. R. Wulf, U. Liddel, S. B. Hendricks, *J. Am. Chem. Soc.* 58 (1936) 2287.
- [45] G. Gilli, P. Gilli, *The Nature of the Hydrogen Bond: Outline of a Comprehensive Hydrogen Bond Theory*, Oxford University Press, New York, 2009.
- [46] L. Pejov, M. Solimannejad, V. Stefov, *Chem. Phys.* 323 (2006) 259.
- [47] R. Karaminkov, S. Chervenkov, H. Neusser, *J. Phys. Chem. Chem. Phys.* 10 (2008) 2852.
- [48] Y. Honkawa, Y. Inokuchi, K. Ohashi, N. Nishi, H. Sekiya, *Chem. Phys. Lett.* 376 (2003) 244.
- [49] P. R. Schleyer, D. S. Trifan, R. Bacskai, *J. Am. Chem. Soc.* 80 (1958) 6691.
- [50] M. Oki, H. Iwamura, *Bull. Chem. Soc.* 32 (1959), 567.
- [51] J. F. Bacon, J. H. van der Maas, *Spectrochim. Acta* 44A (1988) 1215.
- [52] J. M. Bakke, A. M. Schie, T. Skjente, *Acta Chem. Scand.* B40 (1986) 703.
- [53] E. F. Healy, J. D. Lewis, A. B. Minniear, *Tetrahedron Lett.* 35 (1994) 6647.
- [54] A. Al-Saadi, M. Wagner, J. Laane, *J. Phys. Chem. A* 110 (2006) 12292.
- [55] A. A. Al-Saadi, E. J. Ocola, J. Laane, *J. Phys. Chem. A* 114 (2010) 7453.
- [56] E. J. Ocola, A. A. Al-Saadi, J. Laane, *J. Phys. Chem. A* 114 (2010) 7457.
- [57] M. J. Frisch, G. W. Trucks, H. B. Schlegel, G. E. Scuseria, M. A. Robb, J. R. Cheeseman, G. Scalmani, V. Barone, B. Mennucci, G. A. Petersson,

H. Nakatsuji, M. Caricato, X. Li, H. P. Hratchian, A. F. Izmaylov, J. Bloino, G. Zheng, J. Sonnenberg, L. M. Hada, M. Ehara, K. Toyota, R. Fukuda, J. Hasegawa, M. Ishida, T. Nakajima, Y. Honda, O. Kitao, H. Nakai, T. Vreven, J. A. Montgomery Jr., J. E. Peralta, F. Ogliaro, M. Bearpark, J. J. Heyd, E. Brothers, K. N. Kudin, V. N. Staroverov, R. Kobayashi, J. Normand, K. Raghavachari, A. Rendell, J. C. Burant, S. S. Iyengar, J. Tomasi, M. Cossi, N. Rega, N. J. Millam, M. Klene, J. E. Knox, J. B. Cross, V. Bakken, C. Adamo, J. Jaramillo, R. Gomperts, R. E. tratmann, O. Yazyev, A. J. Austin, R. Cammi, C. Pomelli, J. W. Ochterski, R. L. Martin, K. Morokuma, V. G. Zakrzewski, G. A. Voth, P. Salvador, J. J. Dannenberg, S. Dapprich, A. D. Daniels, Ö. Farkas, J. B. Foresman, J. V. Ortiz, J. Cioslowski, D. J. Fox, Gaussian 09, Revision A.02, Gaussian, Inc., Wallingford, CT, 2009.

- [58] J. Yang, K. McCann, J. Laane, *J. Mol. Struct.* 695-696 (2004), 339.
- [59] J. Yang, J. Choo, O. Kwon, J. Laane, *Spectrochim. Acta Part A* 68 (2007) 1170.
- [60] D. Autrey, J. Yang, J. Laane, *J. Mol. Struct.* 661-662 (2003) 23.
- [61] A. A. Al-Saadi, J. Laane, *J. Mol. Struct.* 830 (2007) 46.
- [62] D. Autrey, J. Choo, J. Laane, *J. Phys. Chem. A* 105 (2001) 10230.
- [63] R. B. Moffett, *Org. Synth. Coll.* 4 (1963) 238.
- [64] J. K. Crandall, D. B. Banks, R. A. Colyer, R. J. Watkins, J. P. J. Arrington, *Org. Chem.* 33 (1968) 423.
- [65] K. McCann, M. Wagner, A. Guerra, P. Coronado, J. R. Villarreal, J. Choo, S.

- Kim, J. Laane, *J. Chem. Phys.* 131 (2009) 044302/1-9.
- [66] J. Laane, in J. Laane (Ed.), *Vibrational Potential Energy Surfaces in Electronic Excited States*, *Frontiers of Molecular Spectroscopy*, Elsevier Publishing, Amsterdam, 2009, Chapter 4.
- [67] M. Z. M. Rishard, M. Wagner, J. Choo, J. Laane, *J. Phys. Chem. A* 113 (2009) 7753.
- [68] A. A. Al-Saadi, J. Laane, *Organometallics*, 27 (2008) 3435.
- [69] A. A. Al-Saadi, J. Laane, *Spectrochim. Acta Part A* 71A (2008) 326.
- [70] M. Z. M. Rishard, R. M. Irwin, J. Laane, *J. Phys. Chem. A* 111 (2007) 825.
- [71] A. A. Al-Saadi, J. Laane, *J. Phys. Chem. A* 111 (2007) 3302.
- [72] C. Mlynek, H. Hopf, J. Yang, J. Laane, *J. Mol. Struct.* 742 (2005) 161.
- [73] D. Autrey, N. Meinander, J. Laane, *J. Phys. Chem. A* 108 (2004) 409.
- [74] J. Choo, S. Kim, S. Drucker, J. Laane, *J. Phys. Chem. A* 107 (2003) 10655.
- [75] AGUI, Semichem, Inc.
- [76] H. Iga, T. Isozaki, T. Suzuki, T. Ichimura, *J. Phys. Chem. A* 111 (2007) 5981.
- [77] J. M. Bakke, A. M. Shie, T. Skjetne, *Acta Chemica Scandinavica*, B40 (1986) 703.
- [78] K. Le Barbu-Debus, F. Lahmani, A. Zehnacker-Rentien, N. Guchhait, *Phys. Chem. Chem. Phys.* 8 (2006) 1001.
- [79] T. Isozaki, H. Iga, T. Suzuki, T. Ichimura, *J. Chem. Phys.* 126 (2007) 214304-1.
- [80] T. Isozaki, Y-I. T., T. Suzuki, T. Ichimura, *Chem. Phys. Letters*, 495 (2010) 175.
- [81] K. S. Pitzer, W. E. Donath, *J. Am. Chem. Soc.* 81 (1959) 3213.

- [82] W. J. Lafferty, D. W. Robinson, R. V. St. Louis, J. W. Russell, H. L. Strauss, J. Chem. Phys. 42 (1965) 2915.
- [83] B. G. Engerholm, A. C. Luntz, W. D. Gwinn, D. O. Harris, J. Chem. Phys. 50 (1969) 2446.
- [84] J. A. Greenhouse, H. L. Strauss, J. Chem. Phys. 50 (1969) 124.
- [85] J. R. Durig, D. W. Wertz, J. Chem. Phys. 49 (1968) 679.
- [86] L. A. Carreira, G. J. Jiang, W. B. Person, J. N. Willis, J. Chem. Phys. 56 (1972) 1440.
- [87] J. Laane, J. Chem. Phys. 50 (1969) 1946.
- [88] D. W. Wertz, J. Chem. Phys. 51 (1969) 2133.
- [89] W. H. Green, A. B. Harvey, J. A. Greenhouse, J. Chem. Phys. 54 (1971) 850.
- [90] L. Carreira, R. C. Lord, J. Chem. Phys. 51 (1969) 3225.
- [91] J. R. Durig, J. N. Willis, J. Chem. Phys. 52 (1970) 6108.
- [92] J. B. Lewis, T. B. Malloy Jr., T. H. Chao, J. Laane, J. Mol. Struct. 12 (1972) 427.
- [93] L. F. Colegrove, J. C. Wells, J. Laane, J. Chem. Phys. 93 (1990) 6291.
- [94] J. Choo, J. Laane, J. Chem. Phys. 101 (1994) 2772.
- [95] S. Leibowitz, J. Laane, J. Chem. Phys. 101 (1994) 2740.
- [96] J. Laane, *Vibr. Spectra and Struct.* 1 (1972) 25.
- [97] H. L. Strauss, *Ann. Rev. Phys. Chem.* 34 (1983) 301.
- [98] L. E. Bauman, J. Laane, *J. Phys. Chem.* 92 (1988) 1040.
- [99] T. H. Chao, J. Laane, *J. Mol. Spectrosc.* 70 (1978) 357.
- [100] E. J. Ocola, L. E. Bauman, J. Laane, *J. Phys. Chem. A.* 115 (2011) 6531.

- [101] F. A. Miller, R. G. Inskeep, *J. Chem. Phys.* 18 (1950) 1519.
- [102] V. Schettino, P. Marzocchi, *J. Chem. Phys.* 57 (1972) 4225.
- [103] V. Schettino, P. Marzocchi, *J. Chem. Phys.* 51 (1969) 5264.
- [104] J. R. Villareal, J. Laane, *J. Chem. Phys.* 62 (1975) 303.
- [105] J. Laane, E.M. Nour, M. akkouri, *J. Mol. Spec.* 102 (1983) 368.
- [106] M. B. Kelly, J. Laane, M. Dakkouri, *J. Mol. Spec.* 137 (1989) 82
- [107] V. F. Kalasinsky, D. E. Powers, W. C. Harris, *J. Phys. Chem.* 83 (1979) 506.
- [108] S.V. Shishkina, O. Shinshkin, J. Leszczynski, *Chem. Phys. Lett.* 354 (2002) 428.
- [109] S.V. Shishkina, O. Shinshkin, S.M. Desenko, J. Leszczynski, *J. Phys. Chem. A.* 111 (2007) 2368.
- [110] J. Choo, S.-N. Lee, K.-H. Lee, *Bull. Korean Chem. Soc.* 17 (1996) 7.
- [111] F. Freeman, C. Lee, W.J. Hehre, H.N. Po, *J. Comp. Chem.* 18 (1997) 1392.
- [112] M. J. Frisch, G. W. Trucks, H. B. Schlegel, G. E. Scuseria, M. A. Robb, J. R. Cheeseman, J. A. Montgomery Jr., T. Vreven, K. N. Kudin, J. C. Burant, J. M. Millam, S. S. Iyengar, J. Tomasi, V. Barone, B. Mennucci, B. M. Cossi, G. Scalmani, N. Rega, G. A. Petersson, H. Nakatsuji, M. Hada, M. Ehara, K. Toyota, R. Fukuda, J. Hasegawa, M. Ishida, T. Nakajima, Y. Honda, O. Kitao, H. Nakai, M. Klene, X. Li, J. E. Knox, H.P. Hratchian, J. B. Cross, V. Bakken, C. Adamo, J. Jaramillo, R. Gomperts, R. E. Stratmann, O. Yazyev, A. J. Austin, R. Cammi, C. Pomelli, J. W. Ochterski, P. Y. Ayala, K. Morokuma, G. A. Voth, P. Salvador, J. J. Dannenberg, V. G. Zakrzewski,

S. Dapprich, A. D. Daniels, M. C. Strain, O. Farkas, D. K. Malick,  
A. D. Rabuck, K. Raghavachari, J. B. Foresman, J. V. Ortiz, Q. Cui,  
A. G. Baboul, S. Clifford, J. Cioslowski, B. B. Stefanov, G. Liu, A. Liashenko,  
P. Piskorz, I. Komaromi, R. L. Martin, D. J. Fox, T. Keith, M. A. Al-Laham,  
C. Y. Peng, A. Nanayakkara, M. Challacombe, P. M. W. Gill, B. Johnson,  
W. Chen, M. W. Wong, C. Gonzalez, J. A. Pople, Gaussian 03, Revision  
C.02, Gaussian, Inc., Wallingford, CT, 2004.

[113] H.J. Geise, H.R. Buys, *Rec. Trav. Chim. Pays-Bays* 89 (1970) 1147.

[114] J. M. Cooke, J. Laane, *Spectrochimica Acta*, 42 A (1986) 335.

[115] A. Al-Saadi, J. Laane, *Organometallics*, 27 (2008) 3435.

## VITA

Name: Esther Juliana Ocola

Address: Department of Chemistry, Texas A&M University  
College Station, TX 77842-3012

Email Address: [eocola@mail.chem.tamu.edu](mailto:eocola@mail.chem.tamu.edu)

Education: B.S., Chemistry, Universidad Nacional de Ingeniería, Perú, 1990  
M.S., Chemistry, Cornell University, 2002